DSE - Minimum Fly-By-Wire Trainer

Perform the preliminary design of a FBW light training aircraft with minimum direct operating costs

N.O. Abuter Grebe	4169395	L.J. van Horssen	4139178
N. Barfknecht	4150198	W. Jousma	4144368
A.J. van den Berg	4019016	F.G.J. Rijks	4084713
M.J. van den Broek	4140575	D. de Vries	4132033
J. van den Elshout	4165063		

Final Report

Design Synthesis Exercise

TU Delft Delft University of Technology

Aerospace Engineering

June 24, 2014

Preface

In light of finalizing the Bachelors degree at Delft University of Technology, nine Aerospace Engineering students have performed a preliminary design study for a Fly-By-Wire (FBW) trainer aircraft with minimum direct operating cost (DOC). In this final report, the latest results are presented. A baseline aircraft configuration is presented, with the effect of different FBW configurations on this baseline aircraft and in particular the effects on the DOC.

The motivation for this study is the high accident rate in general aviation, which costs quite some lives. Most of these accidents are caused by pilot error and are related to infrequent flying due to the high costs of flying. A FBW trainer offers the opportunity to incorporate Flight Envelope Protection (FEP), preventing the pilot from stepping outside the operational limits of the aircraft. This will increase the safety in general aviation.

This design synthesis exercise (DSE) was performed over a course of ten weeks, by nine Bachelor students at the faculty of Aerospace Engineering at Delft University of Technology. The project was supervised by dr. Steven Hulshoff, ir. Olaf Stroosma and dr. ir. Axelle Viré.

The group would like to thank their supervisors for their valuable feedback throughout the design process. We would also like to thank ir. Ferdinand Postema for information on certification procedures, especially those that were met for the university's Cessna Citation II. Finally, we would like to thank dr. ir. Clark Borst for information on the SAFAR project and on FBW systems in general. Fm

SUMMARY

During the last 10 weeks, the preliminary design of a minimum fly-by-wire trainer aircraft was performed. This section provides an overview of the design process as a whole.

Roskam's preliminary design methods were used as a baseline during the course of this project. The applicable steps from Roskam's books were implemented into one MATLAB tool. First of all, the market was analyzed and the size was determined. It was found that the market is not favorable at the moment, but it is anticipated that the market will recover at one point. The final design is a conventional high wing aircraft with fixed landing gear. This configuration was preferred to maximize market acceptance and minimize development risk and cost.

After choosing this configuration, the aircraft was designed in more detail. This was split up into different disciplines: structures, stability & control, aerodynamics, fly-by-wire, performance, and aircraft systems. In the structures department, the wing box, the fuselage and the landing gear were designed. As prerequisite, a V-n diagram was constructed and a materials trade-off was performed. It was decided to use 7075-T6 aluminum for the wing box and fuselage due to the good specific strength and stiffness properties, and to ease manufacturing, reducing cost. It was possible to design steel landing gear with minimum maintenance and light weight. The static and dynamic stability were analyzed, which gave input to sizing the stability and control surfaces. It was determined that the surface areas of the horizontal and vertical tail should be 1.96 m^2 and 0.68 m^2 respectively. Furthermore the chord ratios of the elevator, rudder and aileron were sized to be 0.358, 0.328, and 0.196 respectively. The dynamic behavior of the aircraft was found to be acceptable for all modes; The phugoid proved to be the most critical. The first step in the aerodynamics part was selecting an airfoil; For the main wing the NACA 3416 was finally selected. Thereafter the lift and drag polars of the aircraft were constructed and the pitch moment was found. All three were found to be satisfactory.

For the fly-by-wire system, different options were worked out. These options were using a full FBW system, a FBW system with mechanical back-up, and one full FBW system with graceful degradation. It was concluded that the option with mechanical back-up seemed the most feasible as it imposes the least development and certification risk. Thereafter the flight envelope protection options were determined. The different options were full authority, limited authority and auto-throttle. There is no clear winner, as it depends on the type of FBW system used. The last part of the FBW system was looking into options for auto-land. No feasible options were uncovered at this moment, however a precision approach can be achieved with a SBAS receiver.

The performance part was mainly a way to validate if the design meets the requirements set at the start of the design. This was done by analyzing stall, take-off, climb, landing and speed characteristics, and comparing the results to the requirements. The take-off distance and landing distance turned out to be 340 m and 317 m respectively where they were required to be 500 m and 400 m. The rate of climb and climb gradient were 1605 ft/min and 0.3459 respectively where it was required that they should be 800 ft/min and 0.0833. A payload-range diagram and flight envelope were created using the performance results. The fuel system, cockpit instrumentation, avionics, propulsion and electrical system were sized. The most important conclusions were:

- All the fuel would fit in the wing;
- An off-the-shelf glass cockpit and avionics would be used;
- Rotax 912s as engine;
- The electrical systems needs to deal with peak loads of 670.5 W;
- The battery has to produce enough power to deal with the peak load.

Following from all of the design steps, a final design was created where the MTOW turned out to be 637 kg. Further aircraft design process was analyzed and divided into five phases, being finish preliminary design, engineer detailed design, perform testing, manufacturing and develop product support. The main actions for each phase were identified. Then the cost of the project development and direct operating cost were estimated. The Eastlake model was used for the development cost, which led to the minimum amount of aircraft that need to be sold per year to break even. This was done for the 6 different variations of control system. The control system which led to the least amount of aicraft that need to be sold, is the mechanical back-up with 12 aircraft per year. Also the market share that is needed to break even is presented, for both a good and a bad market.

For the direct operating cost, a model was made using different components. The main contributors are fuel, maintenance and insurance. So to minimize the direct operating cost, the specific fuel consumption, required maintenance and insurance should be minimized. It was found that the direct operating cost decreases when graceful degradation is added. The DOC was determined to be between 65-67 euros/hr for private use and 47-49 euros/hr for flight schools.

The main risk during further project development lies in certification of the aircraft using a FBW system. During a requirement compliance check, it was found that this design meets all critical requirements. During a RAMS analysis, the reliablity was determined to be sufficient, the availability was satisfactory, the maintainability was simple for this configuration and the safety is increased due to the use of FBW.

List of Symbols

Symbol	Unit	Description
α_h	[rad]	Horizontal tail angle of attack
$\bar{\gamma}$	[-]	Average access thrust over weight ratio
$\bar{a}$	[m s^{-3}]	Average decceleration
$\bar{c}$	[m]	Mean chord
$\bar{w}$	[lbs ft^{-2}]	Maximum average control surface loading
$\bar{x_{ac}}$	[-]	Normalized x-position of aerodynamic center to LEMAC
$\bar{x_{cg}}$	[-]	Normalized x-position of center of gravity to LEMAC
β	[rad]	Sideslip angle
δ	[rad]	control surface deflection
δ	[mm]	Deflection
Δn	[-]	Factor depending on pilot technique
δ_r	[rad]	Rudder Deflection
ΔC_L	[-]	Change in lift coefficient
$\dot{P}$	[rad s^{-2}]	Roll rate derivative
ϵ_w	[rad]	Wing twist angle
η	[-]	Actuator efficiency
η_{rudder_i}	[-]	Lower rudder position as percentage of vertical tail halfspan
η_{rudder_o}	[-]	Upper rudder position as percentage of vertical tail halfspan
η_{i_a}	[-]	distance of aileron to centerline as percentage of halfspan
η_{i_a}	[-]	Inner aileron position as percentage of wing halfspan
η_{o_a}	[-]	Outer aileron position as percentage of wing halfspan
η_p	[-]	Propulsive efficiency
γ	[-]	Ratio of specific heats
γ_{LOF}	[-]	Access thrust over weight at liftoff
λ	[-]	Taper Ratio Wing
$\Lambda_{c/4}$	[rad]	Quarter chord sweep
Λ_h	[rad]	Horizontal tail sweep angle
λ_h	[-]	Horizontal tail taper ratio
Λ_v	[rad]	Vertical tail sweep angle
λ_v	[-]	Vertical tail taper ratio
λ_w	[-]	Wing taper ratio
(L/D)	[-]	Lift over drag ratio
(T/W)	[-]	Thrust over weight ratio
(W/P)	[N W^{-1}]	Power loading
(W/S)	[N m^{-2}]	Wing loading
μ	[Pa s]	Dynamic viscosity of air
μ'	[-]	Friction coefficient
μ_g	[-]	Wheel-ground rolling friction coefficient
ν	[-]	Poisson ratio
ω	[rad s^{-1}]	Deflection rate
ϕ	[-]	Relative humidity
ϕ	[deg]	Twist angle
ϕ_1	[rad]	Bank angle at which steady state roll rate is reached
ρ	[kg m^{-3}]	Density of air
ρ	[kg m^{-3}]	Density
ρ^*_w	[kg m^{-3}]	Saturated water vapor density
ρ_0	[kg m^{-3}]	Density of air at sea-level
ρ_h	[kg m^{-3}]	Density of humid air
ρ_w	[kg m^{-3}]	Actual water vapor density
σ	[-]	Density ratio
σ_c	[N mm^{-2}]	Compressive Stress
$\sigma_{cr,E}$	[N mm^{-2}]	Euler column buckling stress
σ_{cr}	[N mn^{-2}]	Critical Stress
σ_m	[N mm^{-2}]	Von Mises Stres
τ	[-]	Control surface angle of attack effectiveness parameter
τ	[N mm^{-2}]	Shear stress
θ	[deg]	Deflection angle
θ_{fc}	[rad]	Fuselage clearance angle

Symbol	Unit	Description
a	[m s^{-1}]	Speed of sound
A	[-]	Aspect ratio
a	[rad^{-1}]	Wing lift gradient
A	[mm^2]	Enclosed area
a_{vt}	[rad^{-1}]	Vertical tail lift gradient
a_0	[m s^{-1}]	Speed of sound at sea level
AR	[-]	Aspect ratio
AR_h	[-]	Horizontal tail aspect ratio
AR_v	[-]	Aspect ratio vertical tail
b	[m]	Wing span
B_r	[m^2]	Boom Area
b_r	[m]	Span of rudder
b_{sk}	[mm]	Stringer spacing
b_v	[m]	Span of vertical tail
b_h	[m]	Span of horizontal tail
c	[m]	Chord length
c_a	[m]	Chord length, aileron
c_c	[m]	Chord length, control surface
$Cd_{C_l=1.2}$	[-]	Drag coefficient at C_l = 1.2
Cd_{cruise}	[-]	Cruise drag coefficient
C_{D_0}	[-]	Zero-lift drag coefficient
C_D	[-]	Drag coefficient
c_f/c	[-]	Ratio of flap chord to tip chord
C_{h_α}	[rad^{-1}]	Hinge moment coefficient derivative with angle of attack
C_{h_δ}	[rad^{-1}]	Hinge moment coefficient derivative control surface deflection
C_h	[-]	Hinge moment coefficient
c_h	[m]	Root chord of horizontal tail
C_{h0}	[-]	Zero deflection hinge moment coefficient
$C_{L_{\alpha_h}}$	[rad^{-1}]	Horizontal tail lift gradient
$C_{L_{\alpha_v}}$	[rad^{-1}]	Vertical tail lift gradient
$C_{L_{\alpha_{wf}}}, C_{L_{\alpha_W}}$	[rad^{-1}]	Wing lift gradient
$C_{l_{\delta_a}}$	[rad^{-1}]	Aileron roll control derivative
$C_{l_{design}}$	[-]	Design lift coefficient
$C_{L_{max,flap}}$	[-]	Maximum lift coefficient with full flaps
$C_{L_{max_{clean}}}$	[-]	Maximum lift coefficient, clean configuration
$C_{L_{max_{land}}}$	[-]	Maximum lift coefficient, landing configuration
$C_{L_{max_{TO}}}$	[-]	Maximum lift coefficient, take-off configuration
$C_{L_{max}}$	[-]	Maximum lift coefficient
C_L	[-]	Lift coefficient
$C_{m_{\delta_e}}$	[rad^{-1}]	Horizontal tail lift gradient
C_M	[-]	Pitching moment coefficient
$C_{n_{\beta_{wf}}}$	[rad^{-1}]	Weathervane stability for wing and fuselage
C_{n_β}	[rad^{-1}]	Weathervane stability coeffcient
C_{n_β}	[rad^{-1}]	Yaw moment coefficient derivative with angle of attack
$C_{n_{\delta_r}}$	[rad^{-1}]	Yaw moment coefficient derivative with rudder deflection
$C_{n_{\delta_r}}$	[rad^{-1}]	Rudder effectiveness
C_{n0}	[-]	Yaw moment coefficient zero deflection, zero sideslip
C_r	[m]	Wing root chord
c_r	[m]	Chord length of rudder
c_v	[m]	Root chord of vertical tail
c_v	[m]	Chord length of vertical tail
c_w	[m]	chord length main wing
c_w	[m]	Chord length, wing
C_{y_β}	[rad^{-1}]	Side force coefficient per rad sideslip
$C_{y_{\delta_r}}$	[rad^{-1}]	Side force coefficient per rad sideslip
cg_w	[m]	Wing center of gravity location
CGR	[-]	Climb gradient
D	[N]	Drag
$d\epsilon/d\alpha$	[-]	Downwash gradient at horizontal tail
d_c	[m]	Distance from aircraft center of gravity to aircraft center of side area in x-direction
D_p	[m]	Propeller diameter
E	[s]	Endurance
e	[-]	Oswald efficiency factor
E	[N mm^{-2}]	Modulus of elasticity

Symbol	Unit	Description
f	[-]	Ratio take-off to landing weight
$F_{diameter}$	[m]	Fuselage diameter
F_{height}	[m]	Fuselage height
F_{length}	[m]	Fuselage length
$f_{replaced}$	[-]	Fraction of trainer aircraft replaced per year
f_{TO}	[-]	Obstacle height
$f_{training}$	[-]	Fraction of total flight hours spend on training
F_w	[N]	Aircraft side force
g	[m s^{-2}]	Gravitational acceleration
G	[N mm^{-2}]	Shear modulus
g_0	[m s^{-2}]	Sea level gravitational acceleration
h	[m]	Altitude
$h_{aircraft}$	[hr]	Average amount of flight hours per trainer aircraft
h_L	[m]	Landing obstacle height
h_{PL}	[hr]	Average hours required to obtain a pilot license
h_{SL}	[hr]	Average hours required to obtain a student licence
h_{TO}	[m]	Takeoff obstacle height
h_{total}	[hr]	Average amount of training hours in the US per year
I	[A]	Current
i_w	[rad]	Wing incidence angle
I_{xx}	[mm^4]	Area moment of inertia about the x-axis
I_{xz}	[mm^4]	Product of inertia
I_{yy}	[mm^4]	Area moment of inertia about the y-axis
I_{zz}	[kgm^2]	Mass Moment of inertia around Yaw-Axis
I_{zz}	[mm^4]	Area moment of inertia about the z-axis
k	[-]	Induced drag factor
k_{TP}	[-]	Conversion factor from thrust to power
L	[K]	Temperature lapse rate
L	[N]	Lift
L	[m]	Section length
L/D	[-]	Lift to drag ratio
m	[kg]	mass
M_{air}	[g mol^{-1}]	Molar mass of air
M_H	[Nm]	Hinge moments
M_{S_0}	[-]	Sea level stall Mach number
M_S	[-]	Stall Mach number
M_w	[g mol^{-1}]	Molar mass of water
M_x	[Nm]	Moment around the x-axis
M_y	[Nm]	Moment around the y-axis
M_z	[Nm]	Moment around the z-axis
n	[-]	Load factor
n_{air}	[mol]	Amount of air molecules
$n_{aircraft}$	[-]	Total trainer fleet size
$n_{newaircraft}$	[-]	Average amount of aircraft replaced each year
n_{tot}	[mol]	Total number of molecules
n_w	[mol]	Amount of water molecules
P	[W]	Power
p	[Pa]	Pressure
p_0	[Pa]	Sea level pressure
P_a	[hp]	Power available
P_{av}, P_{avg}	[W]	Average power
P_{cont}	[W]	Continuous power required
P_{peak}	[W]	Peak power required
P_r	[W]	Power required
P_{ss}	[rad s^{-1}]	Steady state roll rate
P_{TO}	[hp]	Takeoff power
q_b	[N mm^{-1}]	Basic open section shear flow
q_s	[N m^{-1}]	Shear flow
q_{s0}	[N mm^{-1}]	Closing shear flow
q_t	[N mm^{-1}]	Torsional shear flow
q_{tot}	[N mm^{-1}]	Total shear flow
R	[m]	Range
R	[J kg^{-1} K^{-1}]	Specific gas constant of air
RC	[m s^{-1}]	Rate of climb
S	[m^2]	Wing area
S_a	[m^2]	Surface area of aileron

Symbol	Unit	Description
s_{air}	[m]	Distance of air segment at landing
S_c	[m^2]	Surface area of control surface
S_h	[m^2]	Horizontal tail surface area
$s_L, s_{landing}$	[m]	Landing distance
s_{LG}	[m]	Distance of ground segment at landing
S_r	[m^2]	Surface area of rudder
S_s	[m^2]	Side body surface of aircraft
$s_{take-off}, s_{TO}$	[m]	Take-off distance
S_v, S_{vt}	[m^2]	Vertical tail surface area
S_{wf}	[m^2]	Fuselage wetted area
S_x	[N]	Shear force in x-direction
S_z	[N]	Shear force in z-direction
T	[K]	Temperature
T	[N]	Thrust
t	[mm]	Material thickness
t/c	[-]	Airfoil thickness-to-chord ratio
T_0	[K]	Temperature at sea level
$t_{rot_{\Delta\delta_e}}$	[s]	Time to rotate control surface over 1 degree
t_{rot}	[s]	Time to rotate control surface over full range of motion
t_{sk}	[mm]	Skin thickness
t_{ss}	[s]	Time required to reach steady state roll rate
TOP	[N^2 m^{-2} W^{-1}]	Take-off parameter
U	[V]	Voltage
U	[m s^{-1}]	Velocity component along the x_B axis
V	[m^3]	Volume
V	[m s^{-1}]	Velocity
V_3	[m s^{-1}]	Decision speed
V_A	[m s^{-1}]	Approach speed
V_C	[m s^{-1}]	Design cruise speed
V_{cruise}	[m s^{-1}]	Cruise speed
V_{max}	[m s^{-1}]	Maximum velocity
$V_{s_{TO}}$	[m s^{-1}]	Takeoff stall speed
V_{S_0}	[m s^{-1}]	Stall speed at sea level
V_{S_L}	[m s^{-1}]	Landing stall speed
V_S	[m s^{-1}]	Stall speed
V_S	[m s^{-1}]	Stall speed
V_{TD}	[m s^{-1}]	Touchdown speed
V_{wf}	[m^3]	Wing fuel volume
V_x	[N]	Shear force in x-direction
V_y	[N]	Shear force in y-direction
V_z	[N]	Shear force in z-direction
W	[N]	Weight
W	[m s^{-1}]	Velocity component along the z_B axis
W/S	[N m^{-2}]	Wing loading
W_E	[kg]	Aircraft empty weight
W_f	[kg]	Fuel weight
W_{pl}	[kg]	Payload weight
W_{tfo}	[kg]	Weight of trapped fuels and oils
W_{TO}	[N]	Takeoff weight
x_{ac_a}	[m]	Aerodynamic center location in x-direction
x_{cg}	[m]	Center of gravity location in x-direction
x_h	[m]	Horizontal tail location, x-direction
x_v	[m]	Vertical tail location, x-direction
z_h	[m]	Horizontal tail location, z-direction

List of Abbreviations

Abbreviation	Description
AHRS	Attitude and Heading Reference System
AKI	Anti-Knock Index
AMOI	Area Moment of Inertia
APU	Auxiliary Power Unit
AR	Aspect Ratio
c.g.	Center of Gravity
CAD	Computer Aided Design
CFD	Computational Fluid Dynamics
CFIT	Controlled Flight into Terrain
CFRP	Carbon Fibre Reinforced Polymer
CGR	Climb Gradient
CS	Certification Specifications
DOC	Direct Operating Cost
DSE	Design Synthesis Excercise
FAR	Federal Aviation Regulations
FBW	Fly-By-Wire
FCC	Flight Control Computers
FCS	Flight Control System
FEM	Finite Element Method
FEP	Flight Envelope Protection
GA	General Aviation
GBAS	Ground-Based Augmentation System
GD	Graceful Degradation
GNSS	Global Navigation Satellite System
GPS	Global Positioning System
GRP	Glass Reinforced Plastic
IFR	Instrument Flight Rules
ILS	Instrument Landing System
ISA	International Standard Atmosphere
MAC	Mean Aerodynamic Chord
MLS	Microwave Landing System
MMOI	Mass Moment of Inertia
MTBF	Mean Time Between Failure
MTOW	Maximum Take-Off Weight
NACA	National Advisory Committee for Aeronautics
OEW	Operative Empty Weight
p.d.	Preliminary Design
PL	Private License
PPL	Private Pilot License
RAMS	Reliability Availability Maintainability Safety
RC	Rate of Climb
RON	Research Octane Number
SAFAR	Small Aircraft Future Avionics Architecture
SAS	Stability Augmentation System
SBAS	Satellite-Based Augmentation System
SFC	Specific Fuel Consumption
SL	Student License
TBO	Time Between Overhaul
VAT	Value-Added Tax
VFR	Visual Flight Rules
VGSL	Visually-Guided Landing System

LIST OF FIGURES

List of Tables

CONTENTS

1 INTRODUCTION

A big issue in general aviation is the fact that a lot of pilots fly infrequently due to financial restrictions. This lack of practice may then lead to inadequate responses in difficult flying conditions, potentially with fatal consequences. Furthermore, airspace becomes crowded as the aviation industry grows. Especially in Europe, this induces the need for a smarter air traffic management system based more on digital than on analogue communications. [58] Current general aviation aircraft are not yet sufficiently equipped to function within such systems. In addition to the problems for general aviation, commercial aviation will come to face a pilot shortage in the near future. [59] A solution should be found to sustain the growing demands for air transport.

Currently, the cost of FBW systems is a major drawback to the development of fully fly-by-wire operated light aircraft. The SAFAR project aims to develop the state of FBW technology to the point of practical application. Aurora flight sciences has fitted a DA-42 with FBW and autoland and Diamond Aircraft is planning on introducing FBW options on some of their aircraft within the near future. None of them feature full FBW operations without mechanical back-up.

Objective: To perform the preliminary design of a FBW light training aircraft with minimum direct operating costs.

Within this report, a preliminary design study is performed for a light trainer aircraft featuring a fly-by-wire system. The incorporation of fly-by-wire systems into light aircraft will increase their usability in future airspace environments, ensuring general aviation remains possible. The aircraft will tackle the safety issues within general aviation using flight envelope protection and optional autoland functionality. A FBW trainer aircraft will also allow for more cost-efficient training of commercial airline pilots for the larger FBW aircraft.

This design will aim to provide the benefits of FBW in safety to the light aircraft market, whilst minimizing operating costs to compensate for the inherently higher costs of FBW systems over the conventional mechanical options.

The starting point for the aircraft design is an analysis of the opportunities and development of the aircraft market as described in Chapter 2. The process of designing the aircraft starts of in Chapter 3 with a definition of the design approach for this minimum FBW trainer.

The first element of design is the description and illustration of the aircraft configuration as provided in Chapter 4. Using this configuration, the structure is analyzed and designed for optimum performance in Chapter 5. Chapter 6 then continues with a discussion of the aerodynamic properties of the aircraft.

Subsequently, the stability and controllability of the aircraft are analysed as discussed in Chapter 7. Following this analysis, the FBW control system options are elaborated upon in Chapter 8. This leads up to an analysis of flight performance, which is described in Chapter 9.

The major subsystems of the aircraft and their connections are discussed and sized in Chapter 10. From the different elements of systems, structural design and aerodynamics, an overview of the integrated design is then provided in Chapter 11. Chapter 12 describes the basics of operations and logistics for the aircraft.

The steps to be taken in future project development beyond this preliminary design study are determined and summarised in Chapter 13. This is followed by an analysis of the aircraft cost in Chapter 14 and a technical risk assessment for project development and aircraft operations in Chapter 15. Finally, in Chapter 16, the design is checked for compliance with the requirements and, in Chapter 17, the aircraft is analyzed for reliability, availability, maintenance and safety.

Chapter 18 then concludes the report and discusses recommendations for future work and research towards development of this aircraft.

2
MARKET ANALYSIS

To be able to derive proper requirements for the design and to make sure that the minimum fly-by wire aircraft will be successful in the general aviation market it is important to perform a detailed market analysis. The aircraft design is aimed at flight schools which require a safe and affordable aircraft to train their students. A secondary market opportunity lies in the private owners who want a safe aircraft. In this chapter it is investigated what the size of the primary market is. The main question is: how many FBW trainers can be sold to flight schools each year?

In order to answer this question first the general aviation market for trainer aircraft is analyzed in Section 2.1. This is be done by analyzing the amount of aircraft required for the US market and extrapolating the result to the global market. In Section 2.2 the current market for trainer aircraft is discussed. This is done by identifying competitors and examining their sales over the last decade. In Section 2.3 these aircraft are analyzed for their operating and initial unit cost. From that financial requirements can be derived to ensure the development of a competitive product.

2.1 GENERAL AVIATION MARKET

In this section the amount of aircraft required for training is estimated. This is done by estimating the amount of aircraft required in the USA and extrapolating these results.

The estimation of trainer aircraft in the USA will be based on the number of Pilot Licenses issued. With that number the amount of training hours is estimated. Then the fleet size is estimated based on the amount of training hours. The market size is estimated from the fleet size.

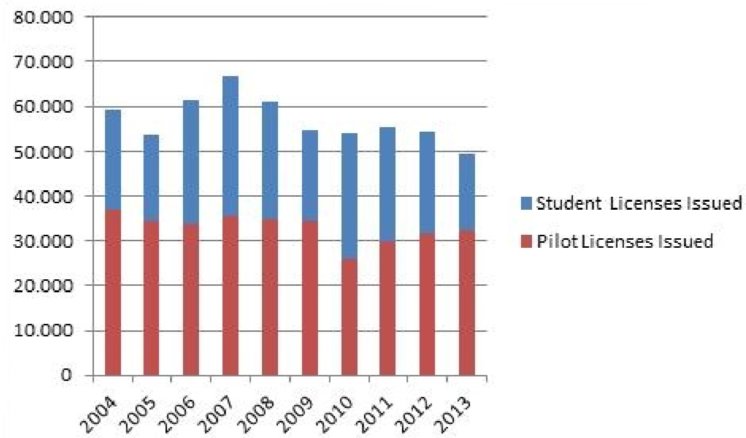

Figure 2.1: Number of student certificates issued each year [1]

The pilot licenses (PL) and student licenses (SL) issued in the USA are depicted in Figure 2.1. It can be seen that the amount of certificates obtained has slightly decreased over the last ten years. This decrease starts from 2008 which is also the beginning of the current economic crisis. After the crisis it is expected these numbers will recover to the values before the crisis.

In this market analysis is assumed that the amount of PL and SL issued is constant to the average of the last ten years. This is a conservative guess, since this data is affected by the economic crisis.

The average amount of student pilot licenses issued is approximately 57,000 per year. The average pilot spends 35 flight hours to obtain this license. Another 25 to 35 hours is needed to obtain a PPL. The average amount of Pilot Licenses issued each year is 33,000. This number includes private, commercial and transport licenses.

With these numbers, the amount of training hours can be estimated using Equation (2.1). It is assumed that everyone who obtained a pilot license already has a student license. This is represented in the value of h_{PL}, which is 30 hours. Another assumption is that, on average, everyone who gets a pilot license flies 65 hours in a single piston aircraft. With these assumptions it follows that 1.83 million flight hours are spent on training purposes in the USA alone.

$$h_{total} = n_{SL} \cdot h_{SL} + n_{PL} \cdot h_{PL} \tag{2.1}$$

Now the fleet size can be estimated. A trainer aircraft flies a thousand hours per year on average [60]. It is assumed that 70 to 90% of these hours is used for training. The other 10 to 30% accounts for rentals. This number is a conservative guess and more research has to be done to determine the exact ratio between rentals and training. With these values the number of aircraft required can be calculated using Equation (2.2).

$$n_{aircraft} = \frac{h_{total}}{h_{aircraft} \cdot f_{training}} \tag{2.2}$$

With the current fleet size known, now the question becomes how many aircraft can be sold. Unfortunately, the fleet size does not grow. The fleet size will grow with -0.1%per year over the next 20 years [2], so it essentially stays constant. This means the number of aircraft sold is equal to the number of aircraft retiring

So how many trainer aircraft retire each year? For the market in general the numbers are very bad. From Figure 2.2 it becomes apparent that only 1.5% of the GA fleet is replaced per year. During the crisis this even dropped to 0.5%.

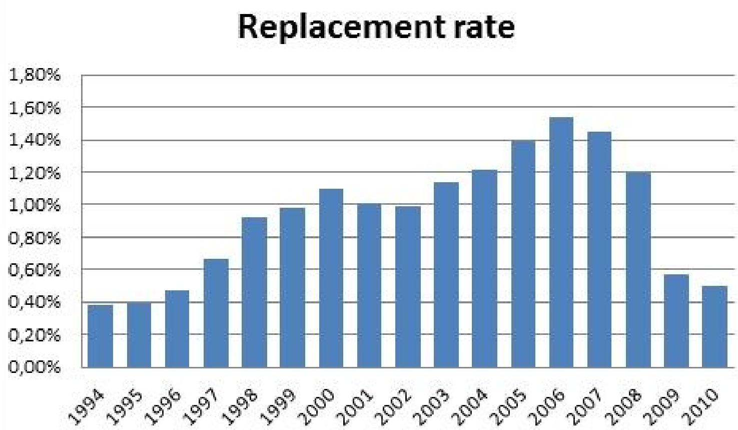

Figure 2.2: Replacement rate of GA fleet per year [2]

Fortunately flight schools appear to replace their fleet more often. Not many flight schools publish the date of manufacture of their aircraft, but the registration numbers of their aircraft can be looked up. By doing this it was discovered that flight schools barely have any aircraft over forty years of age. Therefore the assumption is made that a flight school replaces its fleet once every 40 years. This corresponds to a replacement rate of 2.5%. With this number the market size in the USA can be calculated by using Equation (2.3).

$$n_{newaircraft} = n_{aircraft} \cdot f_{replaced} \tag{2.3}$$

Note that this market size does not take into account the state of the economy. It is just the average market size. When this aircraft will enter the market after the crisis, the market will probably be even bigger. As can be seen from Figure 2.2, the market size can vary by 300% within a few years. Therefore the market might grow bigger than the current average. Since the aircraft will preferably enter the market when the economy is healthy again, it is reasonable to assume an above average market. Therefore a market size of 1.0 to 1.7 times the average market size is assumed.

Finally the result from the US market must be extrapolated to the global market. This extrapolation will be based on the GA fleet size worldwide and in the US. The global GA fleet size is approximately twice the size of the US GA fleet size. [2] Therefore it will be assumed that the market is twice as big as well.

With all the values above, the market size can be calculated. Since a few variables are not exactly known, but specified as a range, the worst case scenario and best case scenario are calculated. Putting in the values as specified in this section leads to a market size of 84 to 272 aircraft sold per year. When taking the 25% and 75% values as upper and lower limits, the size of the primary market becomes 124 to 219 aircraft per year.

2.2 Current Aviation Market

The overall US single piston engine aircraft sales are depicted in Figure 2.3. It can be seen that the market sales after the financial crisis between the years 2009-2013 are still only about one third of the sales in the pre-crisis period of 2004-2008. Leading to the conclusion that this particular market is still in a deep crisis. Cause is the fact that USA and particular the US job market still have not recovered from the financial crisis. Private owners are directly driving the piston engine sales. Since the overall outlook for the US job market is only moderate, a fast recovery cannot be expected in the near future [61].

Overall sales data for European manufactured single piston engine aircraft are available in the period between 2011 and 2013. Sales average around 220 aircraft a year in this period. Press releases for Grob Aircraft AG and Diamond Aircraft Industries show that both companies had difficulties to survive the financial crisis and were only able to maintain operation with massive lay-offs and new investors [62, 63].

For the market analysis comparable aircraft were selected. Following selection criteria lead to a list of aircraft shown in Table 2.2.

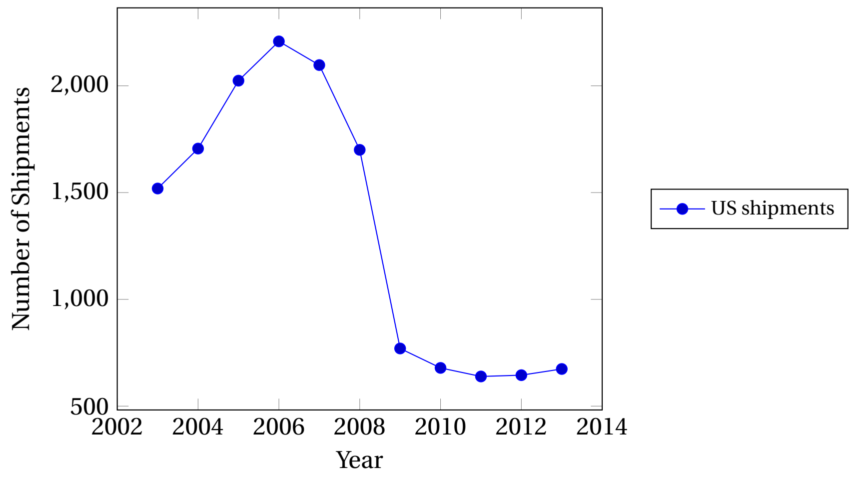

Figure 2.3: US single piston engine aircraft shipments between 2003 and 2013 [2]

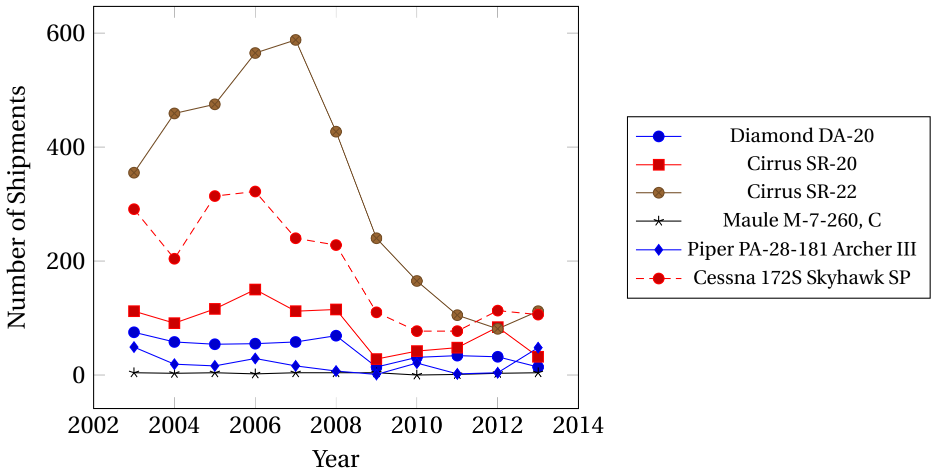

Figure 2.4: Shipments per model [2]

- Aircraft from established manufacturers
- Lower/Lowest series aircraft of the respective manufacturer
- Still in production
- Maximum of 5 seats
- Single piston engine

Sales of some of the reference aircraft are shown in Table 2.1. The same drop in sales around the years 2008/2009 is observed as shown in Figure 2.3. Especially the sales of the Diamond DA-20, which is very similar to the aircraft that has to be developed, have not recovered but even dropped during the year 2013 to 14 shipments. The sales of the four-seat aircraft depend largely on the aircraft. While the sales of the Cessna 172S and the Cirrus SR22 are stable, the sales of the Cirrus SR20 decreased.

It has to be concluded that the market outlook for a two-seat training aircraft is negative at the present time. Therefore it is advised to wait to develop this aircraft until the market starts recovering.

Table 2.1: Shipment of General Aviation Aircraft [2]

Year	Diamond DA-20	Cirrus SR-20	Cirrus SR-22	Maule M-7-260, C	Piper PA-28-181 Archer III	Cessna 172S Skyhawk SP	Total
2003	75	112	355	4	49	291	886
2004	58	91	459	3	19	204	833
2005	54	116	475	4	16	314	979
2006	55	150	565	2	29	322	1123
2007	58	112	588	4	16	240	1018
2008	69	115	427	4	7	228	850
2009	14	28	240	4	1	110	397
2010	31	42	165	0	21	77	336
2011	34	48	105	1	2	77	267
2012	32	84	81	3	4	113	317
2013	14	32	112	4	48	106	316
Total	494	930	3572	33	212	2082	7323

2.3 Cost Analysis

The cost analysis consists out of two parts, the analyses of the initial purchasing cost of the aircraft which have to be paid once at the beginning and the operating cost which occur during the lifetime of the aircraft. The first one will impact the resources needed at the start while the second influences the cost of each individual flight.

In Table 2.2 the previous presented reference aircraft are shown with data on their unit cost, engines, propellers and performance indicators. Both the engines and propellers have a TBO, time before overhaul, which indicates the time after which the part has to be sent back to the manufacturer for a complete overhaul. By inspecting the table one can see that these cost are usually one third of the cost of a new part. Where necessary prices were converted from dollar to Euro with the exchange rate from the 28th of April 2014 [36].

Table 2.2: Reference aircraft data for cost analysis [8–36]

Aircraft	Diamond DA20-A1	Diamond DA20-C1	Grob G115E	Grob G120A	Cirrus SR20 G3	Cirrus SR22 G5	Maule MT-7-260	Piper Archer	Cessna 172S Skyhawk
Price starts at (€)	122920	135360	288000	?	251928	346968	165837	243853	208440
Engine	Rotax 912 S3	Continental IO-240-B3B	Lycoming AEIO-360-B1F/B	Lycoming AEIO-540-D4D5	Continental IO-360-ES	Continental IO-550-N	Lycoming IO-540-V4A5	Lycoming-0-360-A4M	Lycoming IO-360-L2A
Engine TBO (h/yr)	2000/15	2200/12	1600/6	1400/6	2200/12	2200/12	2000/12	2000/12	2000/12
Engine overhaul cost (€)	7000	11952	12802.32	16380	16840.8	19411.92	19637.28	11769.12	12802.32
Engine Price (Europe)	21700	21434	39849	54223	26019	27739	48490	32070	36966
Propeller	Hoffmann HO-V352F/170FQ	Sensenich W69EK7	Hoffmann HO-V 343 K-V/183 GY	Hartzell HC-C3YR-1RF/F7663R	Hartzell P/N PHC-J3YF-1MF/F7392-1	Hartzell PHC-J3Y(1)F-1N/N7605(C)(B)	Hartzell HC-C2YR-1BF/F8477D-6	Sensenich 76EM8S14-0-62	McCauley 1A170E/JHA7660
Propeller Cost (€)	5665	1047.6	12966	12549.6	12257.28	23692.32	10663.2	3326.4	?
Propeller TBO (h)/(yr)	1500	?	?	2400/6	2400/6	2400/6	2400/6	?	2000/6
Propeller overhaul cost (€)	2190	?	?	2412	2145.6	3312	1944	?	?
Fuel	RON 95/AKI 91/100LL Avgas	100/100 LL	100/100 LL	100/100 LL	100/100 LL	100/100 LL	100/100 LL	100/100 LL	100/100 LL
Fuel consumption (75% Power)	18.5	30	41.64	71.92	48.55	61.11	56.78	36.72	33.31
Fuel cost (incl. VAT, €)	1.82	2.92	2.92	2.92	2.92	2.92	2.92	2.92	2.92
Fuel Cost per hour (€/h)	33.73	87.60	121.59	210.01	141.77	178.44	165.80	107.22	97.27
OEW (kg)	510	529	685	960	943	1009	769	776	744
MTOW (kg)	750	800 (750)	990	1490	1383	1542	1134	1157	1157
Useful Payload (kg)	240	271 (221)	305	530	440	533	365	381	416
Max Range (km)	927	1013	1129	1537	1453	1500	1118	967	1125
Crew+Pax	2	2	2	2	5	5	5	4	4
Cruise Speed (km/h)	215	219	278	307	306	339	264	237	230

2.3.1 Unit Cost

Looking at Table 2.2, the base unit price of each reference aircraft can be found. For the two-seat Diamond DA20 it ranges between €122,920 and €135,360 depending on which model is chosen. All of the four-seaters are more expensive and range between €200,000 to €350,000. This is due to an increase in weight which requires a bigger engine and propeller. Additionally four-seater aircraft are used also for cross country travelling besides flight training. Due to this fact they offer a wide range of extras to make the aircraft more comfortable.

All of the reference aircraft except the Diamond DA20-A1 use either a Continental or Lycoming engine. These engines originate back to the 50's and 60's but received upgrades over the years and therefore can be still competitive. Further they have proven their design and reliability during the years of operation. However from the Rotax 912S it can be seen that new engine can reach these levels as well. The engine costs make up a big fraction of the overall aircraft cost.

From Table 2.2 becomes obvious that the price scales with the engine displacement and therefore engine power. For example an engine with a displacement of 360 cubic inches averages at approximately €35,000. Whereas the Continental IO-240-B3B with its 240 cubic inch displacement costs only around €21,500. Thus to bring down the purchasing cost of the aircraft the smallest engine has to be used which still can satisfy the performance requirements.

Another major part of the aircraft costs is determined by the use of the propeller. Factors that influence this part will be the material and the number of blades. In Table 2.2 it can be seen that the DA20-C1 has a very cheap, wooden, two-bladed Sensenich propeller. When comparing it to the composite, three-bladed Hartzell propeller on the Cirrus SR22 there is a difference of around €22,500. The medium-priced propellers are usually made from aluminum.

The performance and payload requirements of the aircraft are similar to the Diamond DA20. The unit cost however of the aircraft design is going to be higher compared to the DA20 due to the fly-by-wire system that will be incorporated. It will require some amount of redundancy leading to a higher number of actuators, sensors and computers. Further the development and certification cost of the fly-by wire system are going to increase the price of the aircraft until the break even point is reached. Another feature that is going to increase the price of the aircraft is the exchangeable auto-land system which is going to contain additional sensors and communication equipment. On the other side not one system is required per aircraft. Flight schools can invest in a couple of aircraft but only buy one auto-land system which can be utilized in any of these aircraft on a demand basis.

From the unit price of the reference aircraft is becomes apparent that the unit price of the aircraft should lie between the price of a Diamond DA20 and a Cessna 172.

2.3.2 Operating Cost

The operating cost can be split up into several categories: fuel cost per hour, oil cost per hour, the engine overhaul and the propeller overhaul, inspection and insurance cost. Further costs are going to arise for general repairs, like exchanging a bearing on a control surface. To keep the cost analysis simple only the fuel cost per hour, the engine overhaul cost and the propeller overhaul cost were determined.

The fuel cost per hour depends on the fuel consumption and the type of fuel consumed of each engine. The overhaul costs and time before overhaul for the engines and propellers are defined by the respective manufacturers. Overhaul has to be performed on a 'what is reached first basis'. meaning that the overhaul either has to be performed after the operation hours or after the specified years. However a TBO of for example 2000 hours does not mean that the engine will reach this lifetime without maintenance. Sometimes it becomes necessary to perform an overhaul even before the official TBO has been reached.

In Table 2.2 the data on the fuel consumption of each engine can be found. What immediately stands out is the fact that the Diamond DA20-A1 does not use Avgas 100/100 LL but is able to use automotive fuel (RON 95/AKI 91) which will save on operating costs enormously. The price of Avgas was €2.92 per liter at Teuge Airport on the 03.04.2014, while the average Dutch price of automotive fuel was around €1.82 per liter on 28.04.2014. So having an engine which runs on automotive fuel is an important step in minimizing the operating costs.

The overhaul times and costs are taken from the manufacturer's manuals. The TBO for the engines varies anywhere between 1,400 and 2,200 flying hours or 6 to 15 years, whichever comes first. The longer the TBO is, the longer the engine will last according to the manufacturer. Overhauling the engine also varies per model from close to €7,000 up to almost €20000, making it a cheaper option than replacing the entire engine. The same principle applies to overhauling the propellers. The TBO varies between 1,500-2,400 hours or about six years. The overhaul cost for the propellers is between about €2,000 to €3,000, again the composite propeller on the SR22 being the most expensive one.

2.4 Conclusion

Based on the findings from the market and cost analysis some recommendations can be derived. First the market for single engine piston aircraft is rather small at the moment and a lot of companies are competing against each other. At the present time there does not seem to be any profitable market for two-seat trainer aircraft as can be deduced from the low sales of the DA20. This is supported by the fact that the DA20 is an aircraft which has in comparison with its market competitors a significantly lower unit and operating cost.

Therefore it is advised to wait until the market recovers from the current economic crisis. This will give a market size of around 160 aircraft per year. Whether this market is big enough to make any profit will depend on the price and DOC of the minimum FBW trainer. This will be determined in Chapter 14.

3
DESIGN APPROACH

The purpose of this chapter is to discuss the design approach for the second phase of the preliminary design of a minimum FBW trainer. The first phase has been discussed in [64]. This chapter is structured as follows: Section 3.1 gives the functional flow diagram, with the functions for which the aircraft is designed. In Section 3.2, verification & validation is discussed. Then, in Section 3.3 the approach to sustainability is discussed. Section 3.4 gives a brief overview of the design approach, Section 3.5 describes the design steps of the second preliminary design sequence, Section 3.6 presents and discusses the N2-chart governing preliminary design (p.d.) sequence II.

3.1 FUNCTIONAL FLOW DIAGRAM

A functional flow diagram has been made based on the functional break-down. The full functional flow diagram and functional break-down can be found in Appendix A. Zoomed-in parts of the functional flow diagram are discussed in the following sections.

3.1.1 PRE-FLIGHT INSPECTION

When one zooms-in on the pre-flight inspection, the functional flow for this part can be found in Figure 3.1.

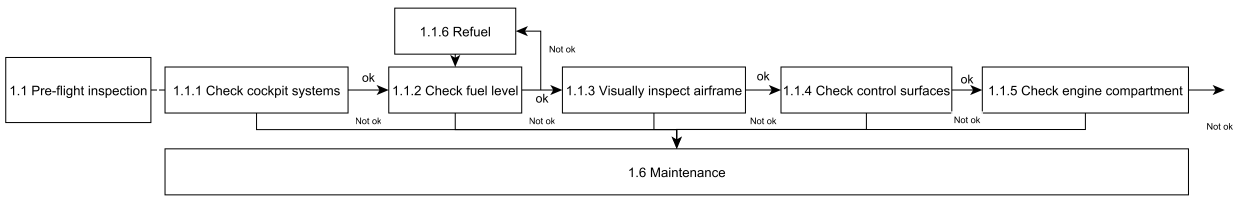

Figure 3.1: Functional flow diagram of pre-flight inspection

Before every flight, the pilot should check/inspect the cockpit systems, airframe, control surfaces and the engine compartment. When something is found to be out of order, for example, oil drips are found in the engine compartment, the aircraft should be sent in for maintenance.

Next to maintenance related inspections, the pilot should inspect the fuel level. When this fuel level is not enough to perform the planned training, the aircraft should be refueled.

3.1.2 TAXI

When the aircraft has passed the pre-flight inspection, the taxi operations can be initiated. The functional flow diagram of taxi operations can be found in Figure 3.2.

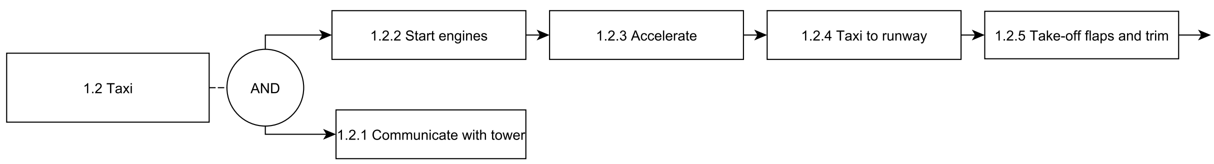

Figure 3.2: Functional flow diagram of taxi

The pilot has to establish communication with the tower and start the engine of the aircraft. After that, the aircraft has to accelerate and taxi to the runway. The pilot initiates take-off flaps and trims the aircraft in order to be able to rotate later during take-off.

3.1.3 TAKE-OFF

Following the taxi operations, the aircraft is ready to start take-off. The take-off functional flow diagram can be found in Figure 3.3.

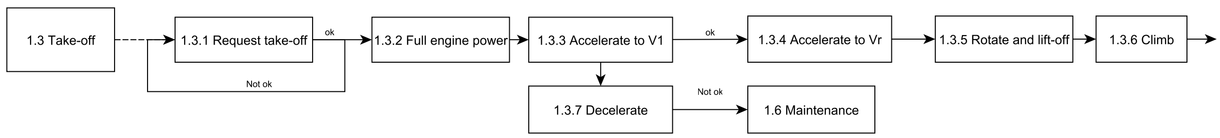

Figure 3.3: Functional flow diagram of take-off

The pilot has to request the take-off. When take-off permission is not granted, the pilot has to wait and try again or follow orders from the tower.

When take-off permission is granted, full engine power has to be applied and the aircraft has to accelerate. If the decision speed (V_1) is not reached in time, the take-off should be aborted and the cause of the low acceleration has to be found during maintenance. If the decision speed is reached in time, the aircraft should accelerate further to rotation speed and then rotate and lift off. The climb is then initiated.

3.1.4 Training

At the moment the aircraft has reached the desired altitude, the planned training can be started. The functional flow of the different flight training profiles can be found in Figure 3.4.

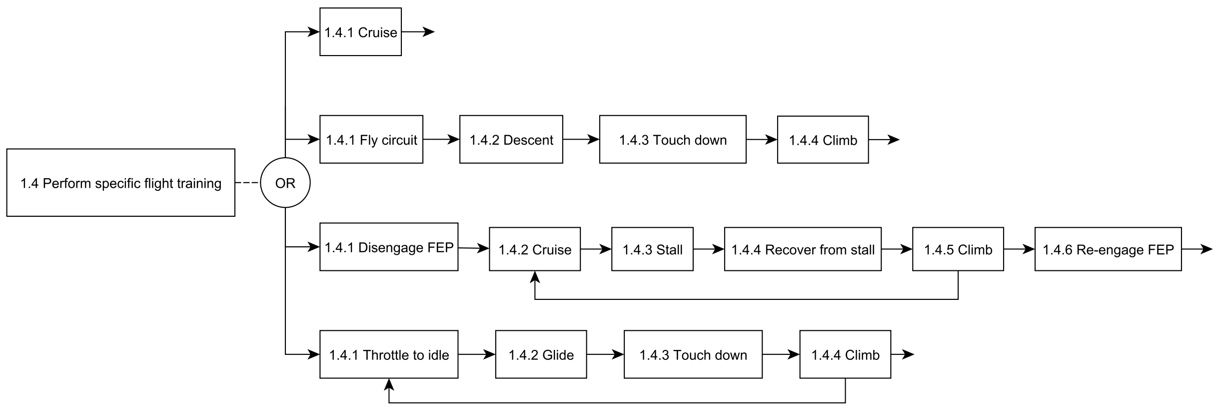

Figure 3.4: Functional flow diagram of specific training profiles

The first training profile that has been shown in the functional flow diagram is the cross-country flight. This simply consists of a cruise flight.

The second profile shown in the functional flow diagram is the standard circuit pattern This includes flying a circuit, descent, touchdown and followed by a climb back up for the next circuit. This means that the pilot does a couple of go-around maneuvers in this training profile.

The third profile shown is the stall training profile. As the aircraft includes flight envelope protection (FEP), which does not allow stall, the FEP first has to be disengaged. Subsequently, the pilot cruises, stalls the aircraft, recovers from stall and climbs again. Before the landing is initiated, it is highly advisable to re-engage the FEP.

The last training profile is simulated engine failure. In this training, the engine setting is changed to idle power. The pilot is now obligated to glide the aircraft towards an airport (while protected by FEP). When the aircraft touches down, a go-around will be initiated and the aircraft will climb again.

3.1.5 Land

After the specific flight training, the landing has to be initiated. The functional flow diagram of the landing can be found in Figure 3.5.

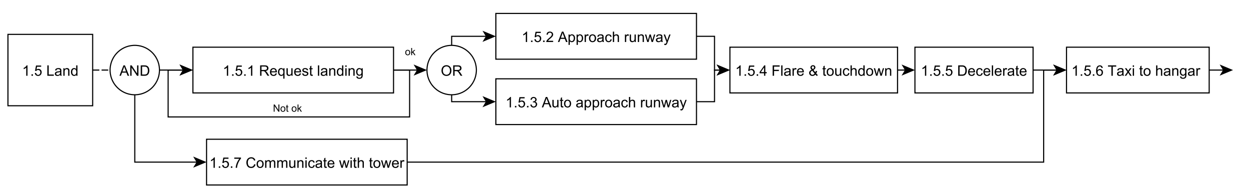

Figure 3.5: Functional flow diagram of landing

The pilot first has to request permission to land. When permission is not granted, he either has to hold or diverge to another airport as instructed by the tower.

When landing permission is granted, the pilot has to fly the approach to the airfield. If he is not capable of doing it himself, the auto approach function can be used.

When the approach is done, the flare and touchdown are performed and the aircraft decelerates to taxi speed. Finally, the aircraft is taxied back to the hangar.

3.1.6 Debrief

The debrief can be initiated when the student pilot arrives at the hangar. The functional flow of the debrief can be found in Figure 3.6.

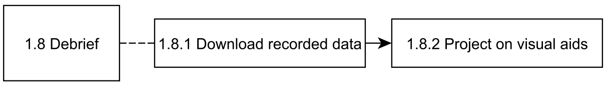

Figure 3.6: Functional flow diagram of debrief

First, the recorded data has to be downloaded from the flight computer, for example using a laptop. The data can then be displayed using visual tools. In this way, the student can receive valuable feedback. The instructor can show him, for example, when he reached the boundaries of the flight envelope and how to prevent that in the future.

3.1.7 Maintenance

Every 50 or 100 flight fours, the aircraft goes into maintenance. A more elaborate description of maintenance can be found in Chapter 17. However, a basic version of maintenance procedures can be found in Figure 3.7.

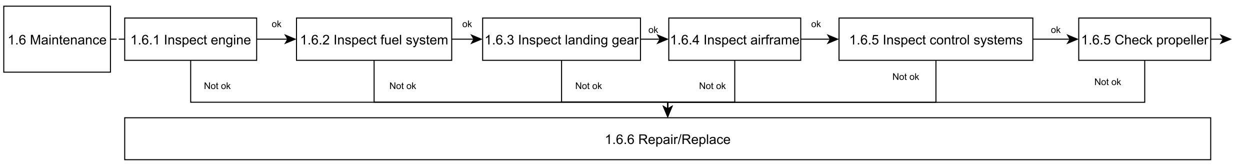

Figure 3.7: Functional flow diagram of maintenance

During maintenance the engine, fuel system, landing gear, airframe, control systems and propeller have to be inspected. Failed or damaged parts are then either repaired or replaced.

3.2 Verification and Validation Procedures

In Figure 3.8 the validation and verification procedure is broken down into its components [3]. Firstly, on the left side of the diagram, the requirements are defined , moving from general mission requirements over system requirements to subsystem requirements. On the right side of the diagram, the systems are designed and then merged step by step starting with the subsystems design, followed by system design and ending with a design capable of performing the mission, elaborated upon in Section 3.2.2.

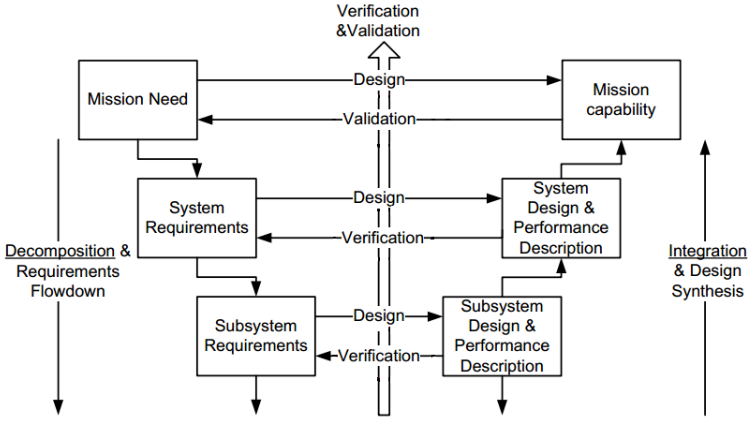

Figure 3.8: V-model for Verification and Validation [3]

3.2.1 Decomposition and Requirements Flowdown

Starting from the given mission requirements, the system and subsystems requirements were developed based on the VALID rule [3]. For each component there were some limiting requirements, which needed to be identified and taken into account in the design steps. All requirements were validated upon definition and collected centrally.

3.2.2 Integration and Design Synthesis

Subsystem Design

The aircraft features many subsystems and design elements, namely the landing gear, wingbox, fuselage, control system, aerodynamics, stability and control, fuel system, cockpit instrumentation, avionics and electrical power.

Each subsystem is verified and validated during development, and it is designed based on the developed requirements. For the systems incorporated into the MATLAB iteration procedure, this verification is performed whilst writing the software.

System Design and Mission capability

Once the system design is finished, the product needs to be verified. The mission requirements which were defined in the baseline report [50] are compared to the obtained design results in Chapter 16.

3.2.3 Verification and Validation

The design solution is verified with the defined requirements and validated with stakeholder requirements; based on this analysis, all of them show compliance with the requirements. Nevertheless, uncertainty remains regarding the certification of the system.

All results from computational models and handmade calculations were compared with standard literature and reference data. These procedures are explained in each corresponding chapter. The performed tasks are sufficient at this stage of the preliminary design, and it is recommended to continue these procedures in the following design stages applying the guidelines provided in the documents DO 178-C.

3.2.4 Internal Quality Checks

At the start and end of each day, a briefing and debriefing meeting is conducted. In the briefing, the general progress is discussed and everybody presents their current work and when they expect it to be finished. In the debriefing, every member communicates how much he progressed and if he can meet his deadline. When a member ran into a problem, he first consulted with a colleague which could help him with the problem. If both team members could not get to a solution, the whole group was consulted.

Not only the feasibility of the final results, but also the results of the individual design steps were checked with reference aircraft on feasibility, preferably by a team member not involved in the design of that part. In order to verify the requirements, it is recommended to use CFD-simulations to check the results.

Lastly major design decisions, which influence the total design where first discussed within the group. This way it was made sure everyone knew what which major decision have been made.

3.3 Sustainability

Sustainability plays an important role in aircraft development. This section first discusses sustainability on a social and economic level and then describes the influence and considerations in design of environmental sustainability.

3.3.1 Social and Economic Sustainability

The general aviation (GA) market is a tough market. Flying has never been cheap, fuel prices continue to rise and the current economic crisis has its impact as well.

general aviation is also confronted with high accident rates. The rate of fatal accidents is 50 times higher compared to commercial aviation. 80% of these accident have pilot related causes. 64.3% of these pilot related causes are due to personal error. Another 22.1% is caused by insufficient training.

Figure 3.9 provides an overview of causes for instructional aircraft accidents. The four most common causal factors are: failure to maintain directional control, failure to maintain airspeed, inadequate supervision and stall/spin. These numbers are unacceptable and can be reduced when using FBW technology already applied in the aviation industry. By removing these accident sources, this technology can reduce the accident rate by at least 50%.

In order to give GA a sustainable future, a new generation of aircraft is needed. These aircraft must provide safety using FBW technology while keeping flying affordable by minimizing purchase cost and direct operating costs.

The minimum-FBW trainer which is developed will be part of this new generation. Safety will be provided by including FBW technology. With this technology it is possible to mitigate the causal factors mentioned above. Pilot errors will no longer be fatal, but corrected by the FBW system. This will decrease the accident rate by at least 50%.

The minimum FBW trainer will also be optimized for low DOC. The main contributors to DOC are fuel cost and insurance. The fuel consumption will be minimized by optimizing for minimum weight and maximum aerodynamic performance and time will be devoted to select a fuel efficient engine. On the long term insurance rates will probably drop as well. This will be due to lower accident rates. Insurance companies have to turn out less money and reduce the insurance rates. This makes the minimum FBW trainer not only a safe aircraft, but also an affordable one.

3.3.2 Environmental Sustainability

An important aspect of sustainability is the environmental impact of the aircraft. The biggest impact on the environment comes from the fuel of the aircraft.

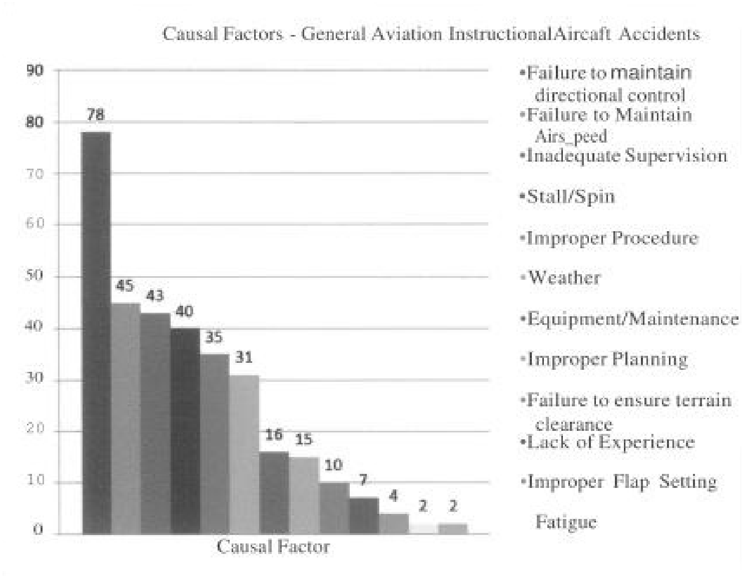

Figure 3.9: Frequency of reported causal factors in general aviation instructional loss of control accidents [4]

The impact of fuel on the environment depends on two things. First the type of fuel. In general aviation Euro 95 and Avgas are used. The biggest difference between these two is that Avgas contains lead. This is a toxic material. Long term exposure to small concentrations damages the central nervous system and several other systems in your body [65].

At this moment Avgas is a major contributor to the lead emission in the USA. A lead free version of Avgas still has to pass certification and will not be compatible with all current engines [66]. Euro 95 on the other hand is lead free. Therefore an engine which runs on Euro 95 will be selected.

The impact on the environment also depends on the amount of fuel burnt. The less fuel burnt, the lower the impact on environment. Therefore time and resources will be attributed to find ways to reduce the fuel consumption of the aircraft by optimizing the aircraft for minimum weight and high aerodynamic performance. Additionally, time is devoted to the selection of a fuel efficient engine.

Other contributors to the environmental impact of an aircraft are manufacturing and recyclability of the aircraft. During manufacturing the use of environmentally friendly manufacturing techniques are important. The amount of waste material has to be minimized and reused when possible.

In this feasibility study not much time will be devoted to manufacturing, so at this point it is not possible to go into detail about sustainability during manufacturing. It is recommended to do this in later stages of the design.

At the end of the operational lifetime the aircraft must be dismantled. It is preferable that large parts of the aircraft can be recycled. This reduces the environmental impact of the aircraft. Therefore recyclability will play a role in material selection. Special attention is paid to the airframe material and the selection of the batteries.

The airframe is important since it accounts for approximately half of the aircraft empty weight. The batteries are important since most battery types contain toxic materials which are hard to recycle.

The airframe generally consists of composites or aluminium. Composites are the lightest option and reduce the overall weight and fuel consumption of the aircraft. However, composites are more expensive since it makes manufacturing relatively labour intensive. Another disadvantage is the absence of an (environmentally friendly) recycling technique. Aluminum on the other hand is easily recyclable using only five percent of the energy required to acquire it from bauxite [67]. This makes aluminium probably the most sustainable solution. The trade-off between these materials is made in Section 5.1.

Selection of the batteries also largely influences the sustainability of the aircraft. Large battery packages can add a significant amount of weight to the aircraft and some kind of batteries contain all kind of toxic materials. Recyclability is also an issue. A good pick is probably Li-ion batteries. These batteries have a high energy density and are recyclable. However, these batteries have a failure rate of 10^{-7} [68]. Therefore these batteries can not be crucial for the aircraft. A trade-off on battery selection is done in Section 10.6.3.

3.4 Overview

In the preceding report (Ref. [64]) the execution of the first phase of the preliminary design of a minimum FBW trainer was described. Roskam's method for the preliminary design of aircraft [39, 52–57, 69] was chosen to be used for that purpose. Part II of Roskam's eight books citeroskamII contains the step plan that governs the entire preliminary design process. It is broken up into two isolated phases referred to as p.d. sequence I and II. These phases roughly correspond to first applying Class I methods in sequence I and then Class II methods in sequence II.

The preliminary design process of a minimum FBW trainer was continued following steps of p.d. sequence II (steps 17-36). The steps can be divided into four specialist categories being: aerodynamics, flight performance and mechanics, structural design and production aspects, and systems design and layout. To improve the detail and quality of the design and analysis the group was divided into groups corresponding to these specialisms.

3.5 Preliminary Design Sequence II

The purpose of this section is to describe the steps of p.d. sequence II specifically for the purpose of designing a minimum FBW trainer. The reader is taken through the preliminary design sequence from Roskam step by step. However, due to time constraints these steps are not followed to the letter. For example, the amount of CAD drawings made in this project is lower than Roskam suggests.

Step 17

Step 17 is dedicated to systems design and layout. It takes as input the CAD drawings from p.d. sequence I and any requirements and constraints that influence the design and layout of all important systems. Ref. [39] contains a detailed description of all aircraft systems and includes methods to design and layout them. This step can be broken up into three substeps to be executed in order. First all major systems of the aircraft shall be listed. Then a so called 'ghost' view shall be prepared for each system in full CAD showing their arrangement and routing through the aircraft. Finally, by analyzing a combined ghost view including all systems, the systems shall be deconflicted and a final ghost view of all the systems in the aircraft shall be prepared in full CAD.

Note that for this specific design case, the design of a minimum FBW trainer, the fly-by-wire system shall also be designed. Since FBW is an important driver in this project extra effort shall be put into working out this system in as much detail as possible. Ghost views of the FBW system shall show all different subsystems, their location and arrangement in the aircraft and routing of the connections between them. Extra care shall also be put into effectively separating the redundant copies for safety aspects. Note that separation shall also be shown for all other redundant systems.

In Table 3.1 the input and output of this step is tabulated.

Table 3.1: In- and output of step 17

Input	**Output**
CAD drawings from p.d. sequence I	Ghost views of each major system
Constraints/requirements on systems	Combined ghost view of all systems

Step 18

Step 18 is dedicated to systems design and layout as well. Again it takes the CAD drawings from p.d. sequence I. Furthermore it takes as input all requirements and constraints that influence the design and layout of the landing gear system, including tires, strut design, retraction scheme and disposition of the landing gear. Chapter 2 of Ref. [39] contains descriptions of all possibilities and contains methods to size and design the landing gear system. This step shall result in choosing the landing gear tires to be used and corresponding performance data (loads, deflections, shock absorption), a detailed description of the landing gear struts (CAD drawings, load calculations, shock absorption), schematic drawings showing the retraction scheme if applicable, a detailed description of the ground performance (turn radii, steering systems, braking systems) and a detailed description of the landing gear configuration and layout (CAD drawings and three-views, load calculations).

In Table 3.2 the input and output of this step is tabulated.

Table 3.2: In- and output of step 18

Input	**Output**
CAD drawings from p.d. sequence I	Detailed description of tires to be used
Constraints/requirements on landing gear system	Detailed description of landing gear struts
	Detailed description of retraction scheme (if applicable)
	Detailed description of ground performance
	Detailed description of landing gear configuration and layout

Step 19

Step 19 is the first of a set of 5 steps that are dedicated to the structural design and layout of the entire aircraft. This step takes the CAD drawings from p.d. sequence I. Chapter 7 of Ref. [54] contains a step-by-step method to be executed in this step. The output of this step is a CAD drawing of the structural design and layout of the entire aircraft. It also serves as a basis for structural weight estimations to be performed at a later stage.

In Table 3.3 the input and output of this step is tabulated.

Table 3.3: In- and output of step 19

Input	Output
CAD drawings from p.d. sequence I	CAD drawings of structural design and layout

STEP 20

The goal of step 20 is to construct the V-n diagram for the aircraft. Section 4.2 of Ref. [55] contains a step-by-step method to achieve that. It takes as input any requirements and constraints that influence the V-n diagram. Furthermore it takes as input all parameters from p.d. sequence I that influence the V-n diagram.

In Table 3.4 the input and output of this step is tabulated.

Table 3.4: In- and output of step 20

Input	Output
Constraints/requirements of influence	V-n diagram of the aircraft
Parameters of influence from p.d. sequence I	

STEP 21

In step 21 a Class II weight and balance analysis shall be performed. This step takes the three-views of p.d. sequence I as input, as well as the V-n diagram that was constructed in step 20. The structural design and layout that was developed in step 19 should be used as input for estimating the weight of the structure of the aircraft. Chapters 4 through 8 of Ref. [55] describe how this problem should be approached. Chapter 4 specifically contains a step-by-step method to this purpose. This step will yield the c.g. range and the moments and products of inertia of the aircraft.

In Table 3.5 the input and output of this step is tabulated.

Table 3.5: In- and output of step 21

Input	Output
Three-views from p.d. sequence I	c.g. ranges of the aircraft
V-n diagram of step 20	Moments of inertia of the aircraft
Structural design and layout from step 19	Products of inertia of the aircraft

STEP 22

Step 22 involves analyzing the results obtained in step 21 and drawing conclusions on the structural design and layout as it has been developed. This analysis and these conclusions shall be documented.

STEP 23

Step 23 is the final step of the set of 5 dedicated to structural analysis and design of the aircraft. It involves redrawing the three-view from p.d. sequence I following the changes made in these steps. At this point it is necessary to feed these changes back to step 17 if the changes have an impact on the aircraft systems. If the changes have little or no impact on the systems, but they do have an impact on the structural design and layout they shall be fed back to step 19. Otherwise, if the changes do not or only marginally influence both the systems and the structure, no iterations need to be performed.

STEP 24

Step 24 is dedicated to flight mechanics. More specifically, this step involves performing a Class II stability and control analysis of the aircraft. It takes the three-view of the aircraft, as it is at the end of the iterations as described in step 23, as an input. Ref. [57] contains all the methods for this step. In this step all stability and control derivatives of the aircraft will be calculated. Furthermore the gain of any required SAS-loops (Stability Augmentation System) shall be sized and the stick force versus speed and versus load factor slopes shall be determined for aircraft with reversible flight controls. For the latter, it shall be such that these slopes obey certification requirements. Deliverables of this step include documentation of all calculations and results for the stability and control derivatives, SAS-loop gain sizing and stick force slopes as well as trim diagrams for both powered and gliding flight, description of the take-off rotation analysis, and description of the roll performance, description of control during final approach and on the runway under the influence of crosswind, description of the open loop dynamic handling of the aircraft. Finally, using all information obtained until this point, the actuators shall be designed for all size and rate requirements. This process and its results shall also be documented.

At this point the three-view resulting from step 23 and iterations shall be updated again. The new three-view shall be fed back to step 17, step 19 and/or back into the start of this step depending on the impact of the changes. The whole process as described from the step into which the three-view is fed back onward, including step 24, shall be executed again, including any inner iterations. If, after working through this whole process, arriving once more at this point, new changes to the three-view again have impact on any of the preceding design steps, more iterations shall be considered.

In Table 3.6 the input and output of this step is tabulated.

Table 3.6: In- and output of step 24

Input	**Output**
Three-views resulting from step 23	Trim diagram for powered and gliding flight
Constraints/requirements of influence	All stability and control derivatives
	Final sizes of stabilizing and control surfaces
	Roll performance characteristics

Step 25

Step 25 is dedicated to aerodynamics. More specifically the drag polars from p.d. sequence I shall be recomputed in this step using Class II methods [53]. This is done by means of component build-up methods. A detailed description of this process is presented in chapter 4 of Ref. [56]. The tail and surface sizes of step 23 shall be used as input, not the resulting tail geometry and sizes that result from step 24. Furthermore the geometry of the aircraft as it was designed until this point is an input to this step as well. This step results in updated drag polars that more closely resemble the aircraft.

In Table 3.7 the input and output of this step is tabulated.

Table 3.7: In- and output of step 25

Input	**Output**
Tail and surface sizes from step 23	Drag polars
Three-views from step 23	

Step 26

Step 26 is the first of a set of three steps dedicated to the power and performance of the aircraft. In this step the installed power and/or thrust of the propulsion system shall be analyzed [53]. A method for these computations is described in detail in Ref. [56], chapter 6. This step will result in obtaining the characteristics and capabilities of the propulsion system.

In Table 3.8 the input and output of this step is tabulated.

Table 3.8: In- and output of step 26

Input	**Output**
	Installed power and/or trust characteristics

Step 27

Step 27 involves reinvestigating all requirements with respect to performance. As a start the requirements listed in Ref. [64] shall be reviewed and filtered for requirements on performance. Finally the ones that are critical shall be identified and reported on.

In Table 3.9 the input and output of this step is tabulated.

Table 3.9: In- and output of step 27

Input	**Output**
	Performance requirements

Step 28

Step 28 is the last of the set of three steps dedicated to analyzing the performance of the aircraft. In this step the performance capabilities of the aircraft that are critical shall be computed. The drag polars of step 25 and the engine characteristics of step 26 shall be used as input for these calculations. The computed performance capabilities shall then be compared to the results of step 27. If they obey to the requirements the design process can be continued beyond step 29. If they do not, iterations shall be needed. The methods necessary for these calculations are described in Ref. [57], Chapter 5.

In Table 3.10 the input and output of this step is tabulated.

Table 3.10: In- and output of step 28

Input	Output
Drag polars from step 25 Installed power and/or trust characteristics from step 26 Performance requirements from step 27	Judgment of compliance with requirements

STEP 29

Step 29 is dedicated to iteration of the design. More specifically the whole process as described until this point, that is, steps 17 through 28, including interim iterations as required, shall be repeated until all requirements are met and the solution is converged. The configuration shall be adjusted if necessary.

In Table 3.11 the input and output of this step is tabulated.

Table 3.11: In- and output of step 29

Input	Output
Results of steps 17-28	Refined design

STEP 30

From this point on no further design iterations are required. With other words, the sequence of steps 30 through 36 is a linear process. Step 30 itself is the first of a set of three dedicated to refining the aircraft geometry, both inner and outer, and all the aircraft's systems in detail. This step specifically involves finalizing the three-view of the aircraft and tabulating all the essential airplane geometry parameters [53].

In Table 3.12 the input and output of this step is tabulated.

Table 3.12: In- and output of step 30

Input	Output
Results of steps 1-29	Finalized three-views Detailed geometric parameters

STEP 31

Step 31 involves finalizing the inboard profiles of the aircraft [53].

In Table 3.13 the input and output of this step is tabulated.

Table 3.13: In- and output of step 31

Input	Output
Results of steps 1-29	Finalized inboard profiles

STEP 32

Step 32 is similar to step 17. All essential aircraft systems shall be defined in a preliminary layout drawing. In particular it shall be shown in detail how the primary and secondary flight control system is layed out. It shall be clearly shown that the systems are deconflicted and that they are shielded from potential hazards and obstacles. This shall be backed up by clear documentation on this matter.

In Table 3.14 the input and output of this step is tabulated.

Table 3.14: In- and output of step 32

Input	Output
Results of steps 1-29	Preliminary layout drawings of all systems Clear documentation proofing adequate layout

STEP 33

Step 33 is the first of a set of three dedicated to structural, manufacturing and maintenance design. This step in particular involves going back to the work done in step 19, where the structural arrangement of the aircraft was defined. The geometry of the aircraft may have changed in steps 20-32, affecting the structural arrangement. It shall be checked if the arrangement of step 19 is still valid and if it is not, it shall be adjusted. This step has the same outputs as step 19.

In Table 3.15 the input and output of this step is tabulated.

Table 3.15: In- and output of step 33

Input	Output
CAD drawings resulting from all preceding steps	Defined CAD drawings of structural design and layout

STEP 34

Step 34 involves preparing a preliminary manufacturing breakdown [53].

In Table 3.16 the input and output of this step is tabulated.

Table 3.16: In- and output of step 34

Input	Output
Results from all preceding steps	Preliminary manufacturing breakdown

STEP 35

Step 35 involves making a study of maintenance and accessibility requirements. For this case a schematic showing all essential access requirements for inspection and for maintenance is needed [53]. It shall be ensured that the structural arrangement from step 33 is compatible with these. Furthermore a schematic showing that the engine and APU (if applicable) can be easily inspected and removed shall be prepared. This study shall be clearly reported on.

In Table 3.17 the input and output of this step is tabulated.

Table 3.17: In- and output of step 35

Input	Output
Results from all preceding steps	Report proofing maintainability and accessibility

STEP 36

Step 36 is the final step of the p.d. sequence II. It involves performing a preliminary cost analysis of the aircraft [53]. Methods do perform this analysis are described in Ref. [69].

In Table 3.18 the input and output of this step is tabulated.

Table 3.18: In- and output of step 36

Input	Output
Results from all preceding steps	Cost estimation for the aircraft

STEP 37

Step 37 is not defined as a numbered step in Ref. [53]. For the purpose of clarity it is assigned a number in this report. This step involves documenting all the work done in p.d. sequence I and II in detail.

In Table 3.19 the input and output of this step is tabulated.

Table 3.19: In- and output of step 37

Input	Output
Results from all preceding steps	Final report describing work done and design

3.6 N2 CHART

Figure 3.10 shows the N2-chart of p.d. sequence II. Note that only the output originating from p.d. sequence I is specifically indicated, since for all other outputs the complete result of the outputting step is expected by the receiving step.

As can be easily identified from the N2-chart there are two iterations present. The interim one being the feedback from step 23 to either step 17 or 19 and the main one being the feedback from step 29 to step 17. Depending on the course of the design process, these iterations shall be repeated multiple times to arrive at a valid and converged final result.

3.7 DEVELOPMENT OF THE MATLAB TOOL

All the calculations from the books are done in MATLAB. This results in a MATLAB program which contains all the steps from design sequence I and II. In these design sequences, the aircraft is designed, its performance is calculated and it is checked whether requirements are met.

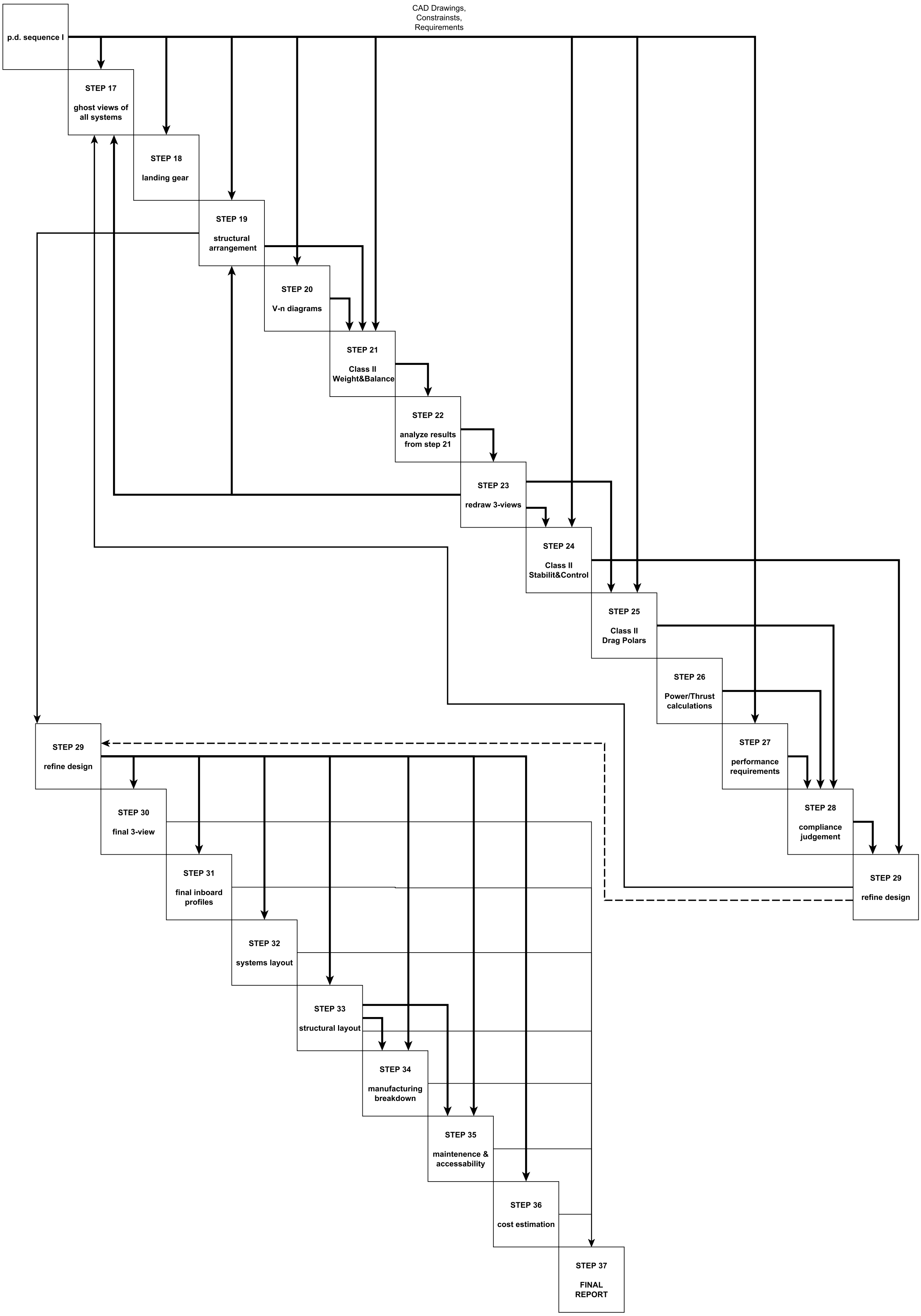

Figure 3.10: N2-chart of p.d. sequence II

In order to run the program, more than 100 input variables are needed. These variables are specified in an input file. Most of these variables can not be varied or hardly influence the design, but some have major consequences. The most critical input variables are: Payload Weight, Aspect ratio and Specific Fuel Consumption.

The Payload Weight is the most important value in the aircraft design. It has the biggest influence on the take-off weight which directly influences wing area and power requirements. In order to maximize performance, payload weight has to be minimized while still meeting requirements.

The requirements on payload is two pilots for dual training, and one pilot for maximum range. In order to meet these requirements, a payload weight of 145 kg is selected. With this weight the useful load becomes 218 kg. With this useful load it is possible to fly 562 km and loiter for 45 minutes with two 80 kg persons.

The second most important parameter is the Aspect Ratio of the wing. In order to increase aerodynamic performance, the aspect ratio has to be as high as possible. Since the Aspect Ratio is one of the first parameters to be fixed, this optimization is based on reference aircraft only. The average AR of reference aircraft is 7.6 an the maximum values are between 10 and 11 with one out lier at 12.9 [50]. Therefore it was decided to fix the AR at 10. This is close to the maximum AR on the market, but still feasable.

The third important parameter is the Specific Fuel Consumption (SFC). This parameters says something about the efficiency of the engine. The lower this value, the lower the fuel weight required which reduces weight and DOC. SFC depends solely on the engine selection. Therefore an efficient engine should be selected.

With these and other input parameters specified, the MATLAB code runs the Design Sequence I and II. Both Design sequences iterate themselves for empennage sizing and Lift over Drag. When these values do not change anymore, the aircraft design is finished. The last part of the program checks whether the design meets the requirements. For every requirement this is written to the screen.

Both design sequences are based on Roskam, but some changes were made to design sequence II in order to incorporate FBW. The FBW systems changes the weight, power and costs budget. The incorporation of the FBW weight in the MATLAB tool is described in Section 11.2 and the incorporation of the power budget is described in Section 10.6. The cost analysis is not a part of Design Sequence II and is therefore not included in the program.

4
AIRCRAFT LAYOUT

The purpose of this chapter is to present and discuss the layout of the final design. First dimensioned drawings of the aircraft will be presented in Section 4.1. These will then be discussed and the major design decisions that lead to this final layout will be justified in Section 4.2.

4.1 DIMENSIONED DRAWINGS

Figures 4.1 to 4.4 contain the top, side, front and isometric views of the aircraft

4.2 DESIGN CHOICES

The mayor layout design decisions that have been made are the following:

- Conventional configuration;
- High wing;
- Conventional tailplane;
- Tricycle landing gear configuration;
- Non-retractable landing gear;
- Nose mounted tractor propeller; and
- Side-by-side seating of the pilots.

A section is dedicated to each of these decisions.

CONVENTIONAL CONFIGURATION

A conventional configuration was chosen over a non-conventional design to minimize the development and operational risk. Furthermore it was argued that a conventional design was preferable for the main mission of this aircraft, namely, ab initio flight training. Since non-conventional aircraft are very rarely used by private pilots it is not logical to design an aircraft meant for training them in a non-conventional manner. This argument thus clearly focuses on market acceptance, which is greatly improved by choosing a conventional design over a non-conventional one. To summarize: a conventional configuration was chosen to minimize risk and maximize market acceptance.

HIGH WING

A high wing configuration was chosen over a mid or low wing to increase pilot visibility. For the purpose of flight training, where VFR are dominant, this adds value. Furthermore a high wing configuration was preferred over a mid wing to decrease the size of the fuselage, since the mid wing would have to be places behind the pilots. This decreases the parasite drag and weight of the aircraft, which in turn increases fuel efficiency and decreases cost. The high wing configuration was preferred over the low wing because a high wing makes the aircraft easier to be embarked and disembarked by the pilots. This adds value, considering many pilots in training are of age. Finally, a high wing configuration is inherently more laterally stable than a mid or a low wing configuration. This is favorable for new pilots, since it reduces the operational risk and improves the flight quality. In conclusion, the argument for choosing a high wing configuration is one that focuses on improving visibility, reducing the cost, increasing market acceptance, and improving the stability of the aircraft.

CONVENTIONAL TAILPANE

A conventional tailplane was chosen over a cruciform, T-tail, or other non-conventional tailplane to reduce the development risk. It can be argued that a conventional tailplane also yields a lower structural weight than other tailplanes, since the horizontal stabilizer and the vertical fin can both be mounted directly on the fuselage. A fin mounted horizontal stabilizer introduces extra loads and moments on the vertical fin, which increases its structural weight and complexity. Due to these extra loads and moments the aircraft will need more maintenance. Choosing a conventional tail thus reduces the direct operating cost.

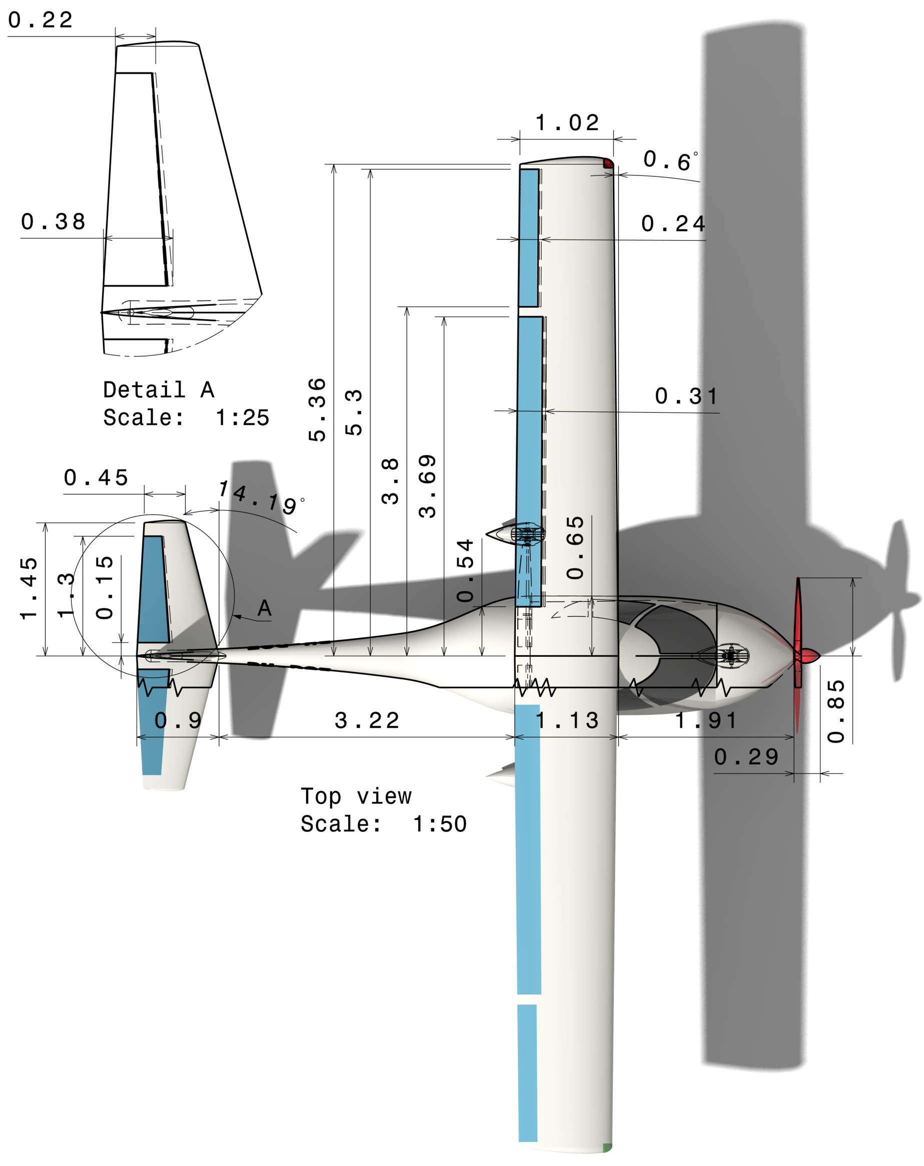

Figure 4.1: Dimensioned top view of the aircraft

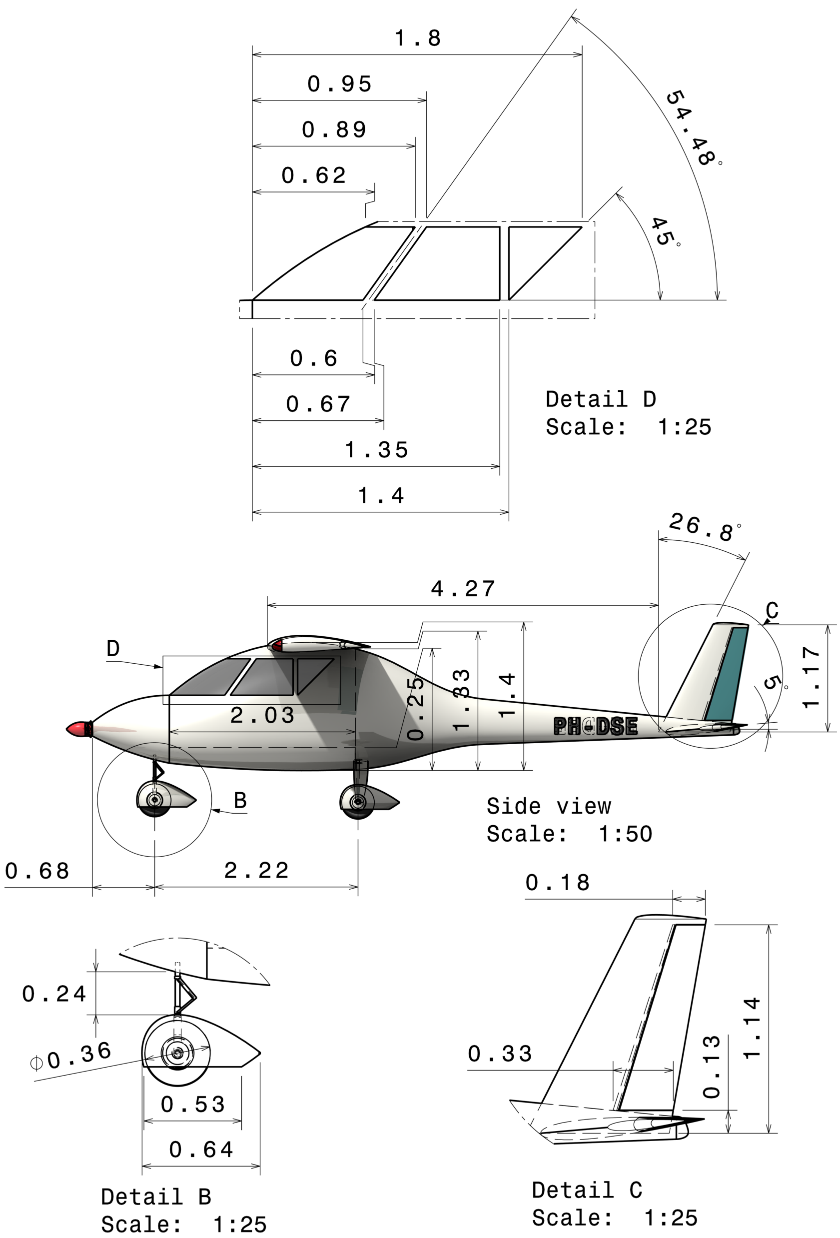

Figure 4.2: Dimensioned side view of the aircraft

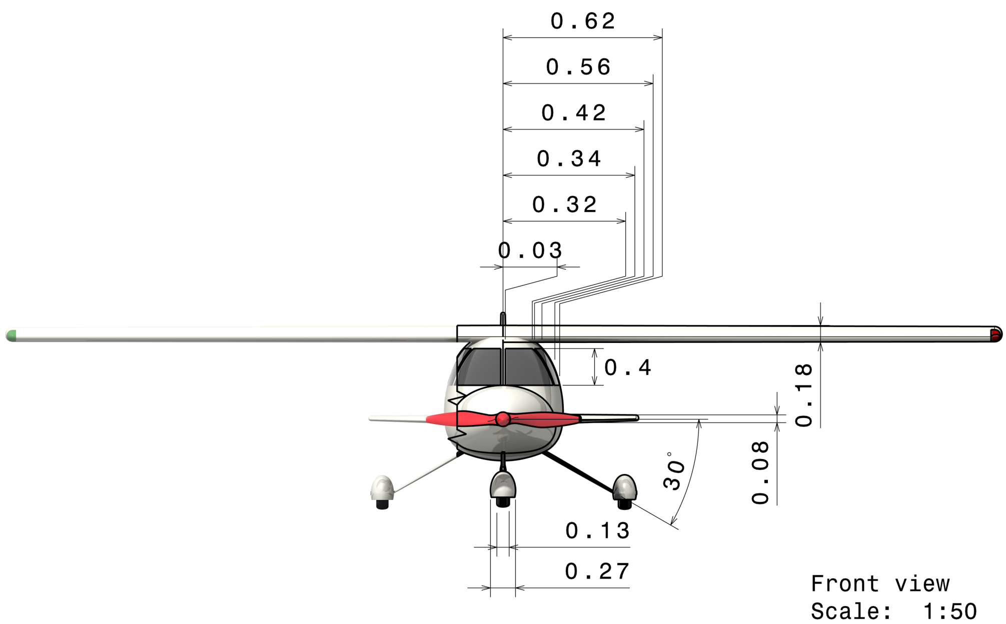

Figure 4.3: Dimensioned front view of the aircraft

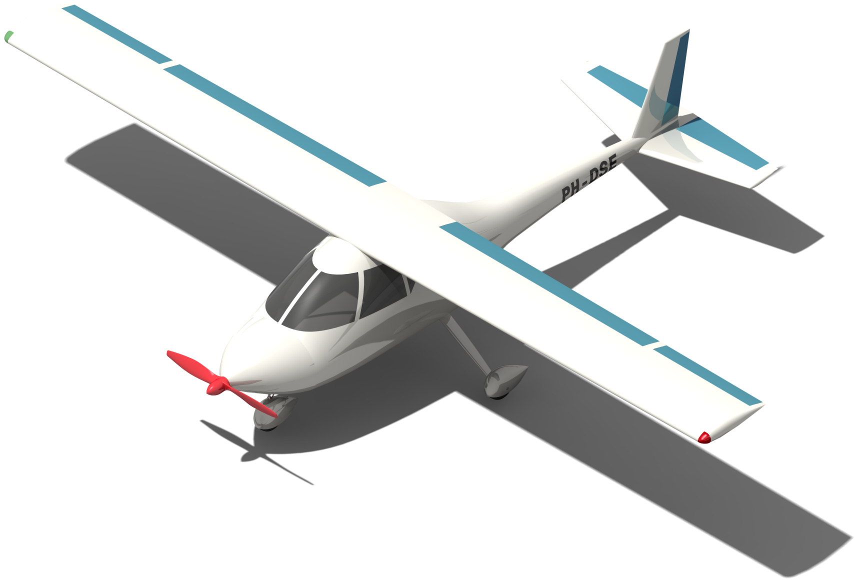

Figure 4.4: Isometric view of the aircraft

Tricycle Landing Gear Configuration

A tricycle landing gear configuration was chosen over a tail dragger to increase pilot visibility during ground operations. Most ab initio flight training in the current market is performed using tricycle gear aircraft. To be able to fit into this market the decision to go for such a configuration was one that was easily made.

Non-Retractable Landing Gear

The decision to use non-retractable landing gear was one that was easily made and is also easy to justify. Non-retractable landing gear has a lower complexity than retractable landing gear. This makes non-retractable landing gear less expensive and less demanding for maintenance, leading to lower purchase and direct operating cost. Furthermore ab initio flight training does not include retractable landing gear, so this is a feature that is not preferred from a market acceptance perspective. Using non-retractable landing gear has only a minor disadvantage compared to retractable landing gear in terms of parasite drag, since this aircraft will be flying at low airspeeds.

Nose-Mounted Tractor Propeller

The argument for mounting the propeller on the nose of the aircraft is twofold. Firstly there is more room in the nosecone than there is in the tailcone, since the latter will be where the tailplane is mounted. Secondly it is conventional to have a nose mounted propeller in one engine, general aviation aircraft. For the main mission of this aircraft this improves market acceptance.

Side-by-Side Seating of the Pilots

It was decided to seat the pilots side-by-side and not behind each other to fit the aircraft within the market for trainer aircraft. During flight training the trainer and the student will need to be communicating thoroughly. It is simpler for the trainer to explain operations to the student and for the student to ask questions to the trainer if they can point directly at the instruments and controls. It was therefore a logical choice to seat the pilots next to each other.

5 STRUCTURES

The structural design of the aircraft is essential to the flight performance. The aircraft should be safe to fly, whilst being lightweight to minimize drag and consequentially minimizing operating cost. Thus, structure should be designed to provide adequate performance at minimum weight.

This chapter discusses the structural arrangement of the aircraft. It will start with the selection of the material for construction in Section 5.1. This is followed by a determination of the required flight load factors in Section 5.2. The analysis and design of the wingbox structure is then discussed in Section 5.4, the fuselage design is illustrated in Section 5.5. Landing gear sizing and design is done in Section 5.6 and finally, manufacturing is considered in Section 5.7.

5.1 MATERIALS

A basic element of structural design is the choice of materials. For aircraft design, lightweight construction with high stiffness and strength is required. A good material forms a proper basis for such a design.

Several parameters need to be considered for an aircraft material, some of which are compared in Table 5.1. For example, the material strength, stiffness and toughness to withstand the loads applied. Resistance to fatigue is required as loads vary in magnitude in different flight elements. Material density with respect to the material properties should also be considered for lightweight construction. Resistance to corrosion plays a role as the aircraft is subjected to the environmental influence. For minimizing total cost of the aircraft, material cost and the cost of manufacturing should be evaluated.[70] Finally, the sustainability of the material used is determined by the production and end-of-life recycling possibilities.

Metals are a conventional choice for use in aircraft design. The are isotropic materials, featuring good strength and stifness properties and manufacturability.

The conventional choice is for aluminum. It is usually alloyed because of the softness of pure aluminum. Aluminum alloys have varying properties, but in general provide good stiffness for a rather low material density. They have good strength properties as well but they do suffer from deterioration due to fatigue. Aluminum is an affordable material and has good properties for manufacturing, thus reducing cost. This is further enhanced by the years of experience working with aluminum in the aircraft industry, which means a lot of knowledge is available. [70]

Common alloys in aircraft use are the 2024-T3 and 7075-T6. The 2000-series alloys have optimum properties similar to mild steel, but feature poor corrosion resistance when unprotected from the elements. The 7000-series are heat-treatable aluminum alloys with very high strength. [71]

Steel alloys are also sometimes used in aircraft structures. Steels can provide very high strengths and good stiffness. The strength of steel does degrade due to fatigue, but there is a fatigue limit, below which the material will never degrade. However, due to its relatively high material density, steel is generally only used for small components with varying loads and high strength requirements. [70]

If cost were not a concern, titanium would be a good material to choose for aircraft design. It features high specific properties and a distinct limit to fatigue degradation. Furthermore, it has good corrosion resistance. Titanium is rather expensive and more difficult to manufacture. Primary material costs and fabrication costs are approximately seven times that for aluminum or steel. [70]

A widely used titanium base alloy is the C-110M (Ti-8Mn) alloy, which is used for parts of the primary aircraft structure and aircraft skin. [71]

In recent years, the use of composite constructions has advanced and become more widespread. Composites generally consist of strong fibres, such as glass (GRP) or carbon fibre (CFRP), fixed in a plastic or epoxy resin matrix. These fibres have a very high tensile strength, but because the fibres are the basis for the strength of the composite, the material is anisotropic. This does allow for specific material design in line with major loads in tension. Compressive loads are less well taken, but the lay-up can be designed to take shear loads. The fibres giving the composite its strength are much less prone to fatigue than metals.

A problem composites is that they are brittle and strength is compromised by impact damage. Furthermore, there is a problem with inspection and repair. Composite may fail without showing visual cues to failure. The design and construction of composites is more complex and requires manual fabrication, inducing higher cost.

Design using composites does allow for constructions not possible using metals due to the flexibility of the fibres before setting in the matrix. A carbon fibre composite could be made three times stiffer than a glass fibre composite and two times stiffer than an aluminum alloy - for the same weight. [70]

Finally, for sustainability, aluminum provides good options for end-of-life recycling at rather low energy cost, whereas this is more costly for steel and titanium. Recycling carbon and glass composites is impractical and sustainable, recyclable composites are not yet acceptable for aircraft use.

For the wingbox and fuselage design, the 7075-T6 aluminum is chosen. This is because of the good specific strength and stiffness properties for aluminum. Additionally, the material and manufacturing cost of aluminum are low compared to the other materials. The requirements on the structural performance with respect to weight do not demand the step to a composite construction.

Table 5.1: Material properties [37, 38]

	AL7075-T6	AL2024-T3	Ti-8Mn	AlSl 4130	GRP (UD)	CFRP (UD)	
ρ	2810	2780	4730	785	1900	1600	[kg/m^3]
E	71.7	72.4	115	205	40	135	[Gpa]
G	26.9	27	43.2	80	4	5	[Gpa]
σ_u	572	440	900	670	1000	1500	[Mpa]
σ_y	503	345	810	435			[Mpa]

5.2 V-n Diagram

In order to design the structural layout of the aircraft, one of the main parameters that should be known is the maximum load factor that will be encountered. This can be done using a V-n diagram, in which the maximum allowable load factor for each airspeed are given.

5.2.1 V-speeds

In the V-n diagram some of these airspeeds are defined, since they are important in the operation of an aircraft. These airspeeds are:

- Design Maneuvering Speed (V_a)
- Design Cruise Speed (V_c)
- Design Dive Speed (V_d)
- Stall Speed in clean configuration ($V_{S_{clean}}$)
- Stall Speed in with flaps deployed ($V_{S_{flaps}}$)
- Maximum Flap Extended Speed ($V_{f_{max}}$)
- Design Landing Speed (V_L)

Design Maneuvering Speed (V_a)

To determine the design maneuvering speed, Equation (5.1) is used.

$$nW = \frac{1}{2}\rho V^2 SC_L \tag{5.1}$$

Where the load factor (n) is 4.4, which is the minimum positive limit maneuvering load factor, for utility category aircraft, according to CS 23.337. The wing loading (W/S) is a design point and the lift coefficient C_L follows from the aerodynamic design. Finally the density is determined according to the International Standard Atmosphere (ISA). All these values lead to the minimum design maneuvering speed of the aircraft.

Design Cruise Speed (V_c)

The cruise speed is a value that can be chosen for the design. The minimum requirement for the cruise speed however is 90 knots. This cruise speed might be too low though, according to CS 23.335, which states that the minimum cruise speed (in knots) should be higher than $33\sqrt{\frac{W}{S}}$, with W/S in lbs/ft^2. During the design of the V-n diagram, it is checked whether or not the requirement of CS 23.335 is met, if not, the cruise speed will be set to the minimum cruise speed.

Design Dive Speed (V_a)

The design dive speed is the absolute maximum airspeed the aircraft is allowed to have. The dive speed may not be less than $1.25V_c$, but also not less than $1.5V_{c_{min}}$ for utility category aircraft according to CS 23.335.

Stall Speed in clean configuration ($V_{S_{clean}}$)

The stall speed at +1g is also calculated using Equation (5.1). Setting the load factor to 1, and C_L to the lift coefficient in clean configuration the stall speed can be determined.

STALL SPEED IN WITH FLAPS DEPLOYED ($V_{S_{flaps}}$)
The stall speed with flaps deployed is calculated in the same manner as the stall speed in clean configuration. The only difference is that the lift coefficient is now the lift coefficient with flaps deployed.

MAXIMUM FLAP EXTENDED SPEED ($V_{f_{max}}$)
The maximum flap extended speed is restricted by three requirements. First of all, flight with flaps extended should be able to withstand a positive load factor of 2g. Furthermore $V_{f_{max}}$, should be larger than 1.4 times $V_{S_{clean}}$ and 1.8 times larger than $V_{S_{flaps}}$. Whichever is greater of these three requirements is the maximum flap extended speed.

DESIGN LANDING SPEED (V_L)
According to FAR 23.73, the landing speed should be atleast 1.3 times the minimum stall speed. Where the minimum stall speed is the stall speed with flaps deployed. The calculated landing speed is used in Chapter 9, to check whether or not it meets the requirement of the maximum landing distance of 400 m over a 50 ft obstacle. If not the case, then the stall speed should be reduced.

5.2.2 GUST LOADS
Another major part for load factors is the gust load. For utility category aircraft the gust loads on V_c and V_d should be evaluated. At cruise speed up and down gusts of 50 feet per second (i.e. 15.24 m/s) and at dive speed up and down gusts of 25 fps (i.e. 7.62 m/s) must be considered according to CS23.333. A so-called V_B must be also be evaluated for commuter category aircraft, however the trainer aircraft is a utility category aircraft, so V_B does not have to be considered. The gust load can be determined using Equation (5.2), from CS 23.341.

$$n = 1 \pm \frac{k_g \rho_o U_{de} V a}{2(W/S)} \tag{5.2}$$

Where the gust alleviation factor (k_g) is determined using Equation (5.3)

$$k_g = \frac{0.88\mu_g}{5.3 + \mu_g} \tag{5.3}$$

And the aeroplane mass ratio (μ_g) is calculated with Equation (5.4)

$$\mu_g = \frac{2(W/S)}{\rho \bar{C} a g} \tag{5.4}$$

The variables used in Equations (5.2) to (5.4), according to CS 23.341 are:

- U_{de} = Derived gust velocity at certain airspeed [m/s]
- ρ_0 = Density of air at sea-level [kg/m^3]
- ρ = Density of air at considered altitude [kg/m^3]
- W/S = Wing loading in the particular case [N/m^2]
- $\bar{C}$ = Mean geometric chord [m]
- g = Acceleration due to gravity [m/s^2]
- V = Aircraft equivalent speed [m/s]
- a = Wing lift curve slope [rad^{-1}]

5.3 LOAD FACTORS
The limit maneuvering loads and gust loads are combined together in the V-n diagram. The V-n diagrams are depended on the wing loading and the density. For the wing loading, the wing loading at maximum take-off weight is taken. This gives the highest speeds, and thus will also give the highest load factor due to gusts, according to Equation (5.2). For the density two extremes are taken into account. The first V-n diagram is made for sea-level as in Figure 5.1a. The other extreme is on cruise altitude as in Figure 5.1b. From these V-n diagrams the maximum and minimum load factor can be read.

5.4 WINGBOX ANALYSIS AND DESIGN
This section discusses the structural analysis and design of the wingbox for the aircraft. The wingbox is the main structural element of the wing, designed to bear the applied loads. For iteration in the complete aircraft design, the complete wing weight from statistical analysis is used. This analysis is used to come to an initial design of the wingbox construction. It is compared to the statistical values for design validation and feasibility for actual use.

This section will first describe the loads applied to the wing and the design load cases in Section 5.4.1. Then the methods for determining normal and shear stresses and critical values are discussed in Section 5.4.2. The design of the tool for numerical analysis is illustrated in Section 5.4.3. This is followed by a discussion of the design iteration process in Section 5.4.4 and a summary of the finalized design in Section 5.4.5. Some recommendations for further development are then made in Section 5.4.6.

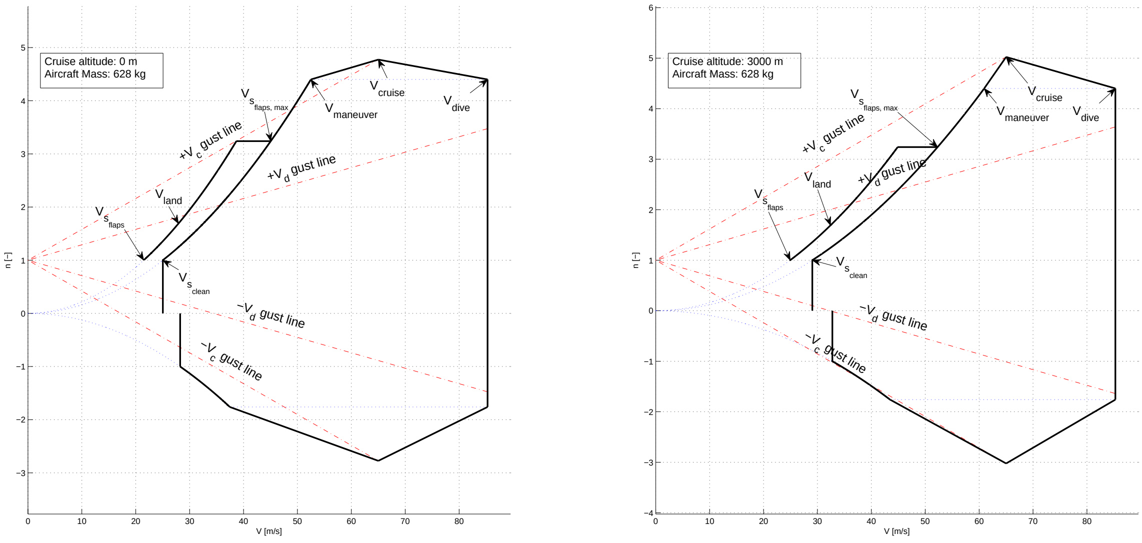

(a) V-n Diagram at sea-level

(b) V-n Diagram at a height of 3000 meter

Figure 5.1: V-n diagrams with flight envelope limits

5.4.1 LOADS

The wingbox needs to be designed to support all the loads that may be applied to the wing. The limits of load factors and velocities have been specified in the Vn-diagram in Figure 5.1b. The wingbox is designed to be able to sustain both the positive and negative extremes of the loading diagram; a maximum load factor of 4.5 and a minimum load factor of -2.5 at the corresponding velocity.

The total lift force is taken equal to the MTOW multiplied with the load factor and the lift distribution is taken linearly related to local chord length. The drag is related to the lift via Equation (5.5) and Equation (5.6). The air density, ρ, is assumed to be 1.225 kg/m^3, the ISA sea-level value. The zero-lift drag coefficient, $C_{D,0}$, the aspect ratio, A, and the Oswald factor, e, come from the aerodynamic design.

$$C_D = C_{D,0} + \frac{C_L^2}{\pi A e} \tag{5.5}$$

$$D = C_D \frac{1}{2}\rho V^2 S \qquad , \qquad L = C_L \frac{1}{2}\rho V^2 S \tag{5.6}$$

Fuel is stored in the wing and thus provides a distributed loading opposite to the lift force. The same goes for the wingbox weight distribution.

The wingbox load distributions are illustrated for the positive case in Figure 5.2 and for the negative load factor in Figure 5.3. The shear distributions over the wingbox are integrated to determine the moment distribution. The torsional moment distribution is provided in Figure 5.4 for both positive and negative load cases.

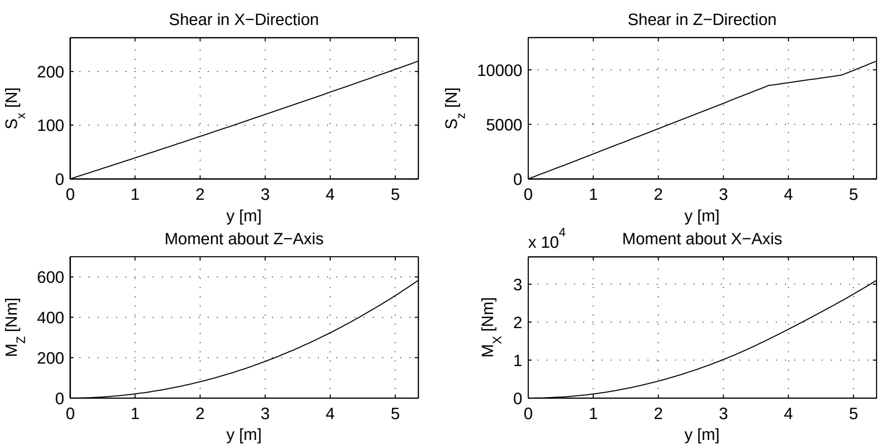

Figure 5.2: Wing loading diagrams, shear and moment distributions, n = 4.4

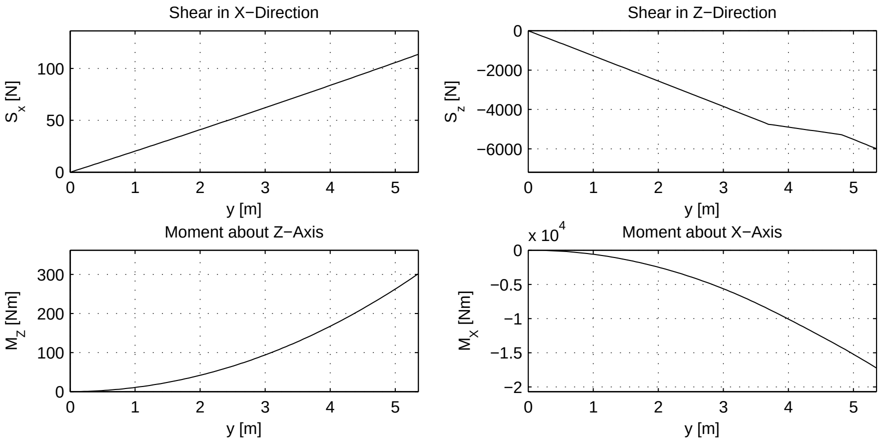

Figure 5.3: Wing loading diagrams, shear and moment distributions, n = -2.5

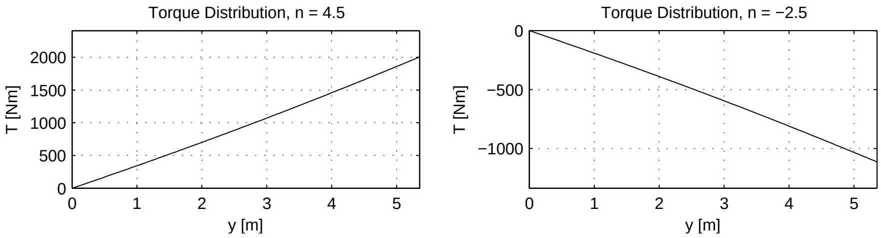

Figure 5.4: Torsional moment distribution over the wingspan

5.4.2 Wingbox Analysis Methods

This section describes the theory used for the determination of stresses and deformations in the wingbox. Starting with a geometrical definition, followed by the methods for stresses due to bending and shear, including the critical failure criteria for design. Finally, aeroelasticity is briefly considered.

Geometry

The axis system for wing box analysis starts at the left wing tip centroid, with the z-axis pointing downwards and the x-axis forwards in flight direction. The y-axis points from the tip towards the root.

For analysis, the wingbox is divided into a number of sections. The local x-axis and z-axis have their origin at the cross section centroid. For every cross section, the moments of inertia about both axes and the product of inertia are computed.

Bending

The moments generated by the shear loads applied on the wing induce normal stresses in the skins and spars. These stresses are computed using the standard equation for bending of beams given in Equation (5.7) [70]. For upward bending, the top panel is loaded in compression and the bottom panel in tension, for downward bending - negative load factors - the bottom panel is loaded in compression and the top panel in tension.

$$\sigma = \frac{M_x z}{I_{xx}} + \frac{M_z x}{I_{zz}} \tag{5.7}$$

Due to the compressive loads that may be applied to the top and bottom panels, they are checked for buckling using Equation (5.8). t_{sk} is the skin thickness, b_{sk} is the spacing between stringers. The critical stress for Euler column buckling of the stringers is calculated with Equation (5.9). [70]

$$\sigma_{cr} = \frac{4\pi^2 E}{12(1-\nu)^2}\left(\frac{t_{sk}}{b_{sk}}\right)^2 \tag{5.8}$$

$$\sigma_{cr,E} = \frac{\pi^2 EI}{LA} \tag{5.9}$$

Besides the stresses, the tip deflection is checked by summing the effect of deflection from the root to the tip. The section deflection length and angle are computed using Equation (5.10) [70]. These are then combined over the wingspan to compute the tip deflection.

$$\delta = \frac{ML^2}{2EI} \quad , \quad \theta = \frac{ML^2}{EI} \tag{5.10}$$

Shear Stresses

The shear stresses resulting from torsion and the applied shear loading are also computed for the wingbox. Equation (5.11) shows that the total shear flow, q_{tot}, is built up from the basic open section shear flow, q_b, the closing shear flow, q_{s0}, and the shear flow due to torsion q_t [70].

$$q_{tot} = q_b + q_{s0} + q_t \tag{5.11}$$

The basic shear flow distribution for each section is computed using Equation (5.12) [70].

$$q_b = -\left(\frac{I_{xx}S_x - I_{xz}S_z}{I_{xx}I_{zz} - I_{xz}^2}\right)\int_0^s tx\,ds - \left(\frac{I_{zz}S_z - I_{xz}S_x}{I_{xx}I_{zz} - I_{xz}^2}\right)\int_0^s tz\,ds \tag{5.12}$$

The closing shear flow for each section is determined using 5.13 [70].

$$q_{s0} = \frac{\oint \frac{q_b}{t} ds}{\oint \frac{1}{t} ds} \tag{5.13}$$

Finally, the shear flow due to torsion, resulting from shear load offset from the shear centre, is computed with Equation (5.14) [70]. The shear centre location is assumed to be at the centroid of the cross section for determination of the applied torque due to lift offset.

$$q_t = \frac{T}{2A} \tag{5.14}$$

The shear stresses can be calculated from the shear flow by dividing by the panel thickness, as in Equation (5.15) [70].

$$\tau = \frac{q_{tot}}{t} \tag{5.15}$$

The angle of twist of each section is computed using Equation (5.16) [70]. These are summed for the total tip twist angle.

$$\phi = \frac{1}{2AG} \cdot \oint \frac{q_{tot}}{t} ds \tag{5.16}$$

Von Mises

To analyse the combined load from the normal stresses and the shear stress, the Von Mises yield stress is determined using Equation (5.17). The stress distribution over the wingbox is shown in Figure 5.8. The Von Mises stress should be compared to the material yield stress to check for yielding under the combined loading.

$$\sigma_m = \sqrt{\sigma^2 + 3\tau^2} \tag{5.17}$$

Static Aeroelastic

The effects of aeroelasticity are briefly considered. The torsional divergence speed is computed using 5.18 [70]. It is much higher than the speeds defined within the flight envelope and therefore not driving the design. The effects of control reversal and flutter are not considered for also being primarily high speed effects.

$$V_D = \sqrt{\frac{\pi^2 GJ}{2\rho e c^2 s^2 C_{L\alpha}}} \tag{5.18}$$

$$J = \frac{T}{G\frac{d\phi}{dy}} \approx \frac{T}{G\frac{\phi}{y}} \tag{5.19}$$

5.4.3 Analysis Tool

All stress and deflection calculations for the wingbox are performed using a purpose-built MATLAB tool. The tool divides the wingbox into a number of spanwise sections and divides the top and bottom panel as well. By division into a large number of small sections, higher accuracy is achieved.

The spanwise sections are assumed to have a constant cross-section, neglecting the effects of taper. The geometry is varied across the different sections to improve accuracy of the geometrical model. The wing is assumed unswept because of the sweep angle is very small. The properties of the material are assumed homogeneous and isotropic and the cross section is assumed not to warp due to shear or bending. For the computation of drag, the sea-level air density is assumed.

The diagram in Figure 5.5 illustrates the working of the program and the relation between program elements. It starts off of an initial definition of the wingbox geometry. For this geometry, the stress distributions are computed. These stresses are then compared to the calculated critical stresses for buckling and the material yield stress. Parameters can then be modified to achieve a design which is optimized for weight and capable of taking the applied loads.

The buckling stresses in the panel under compression and the spars loaded in shear proved to be the critical parameters for design. Therefore, the structure was designed not to buckle within the specified flight envelope. Buckling starts in the elastic regime and does not cause immediate failure; a slightly buckled structure is still capable of carrying loads. It is thus assumed that the wingbox designed not to buckle at the extreme flight envelope load factors shall be able to sustain these load with an additional safety factor of 1.5 without failure, as required by the CS-23 regulations [40].

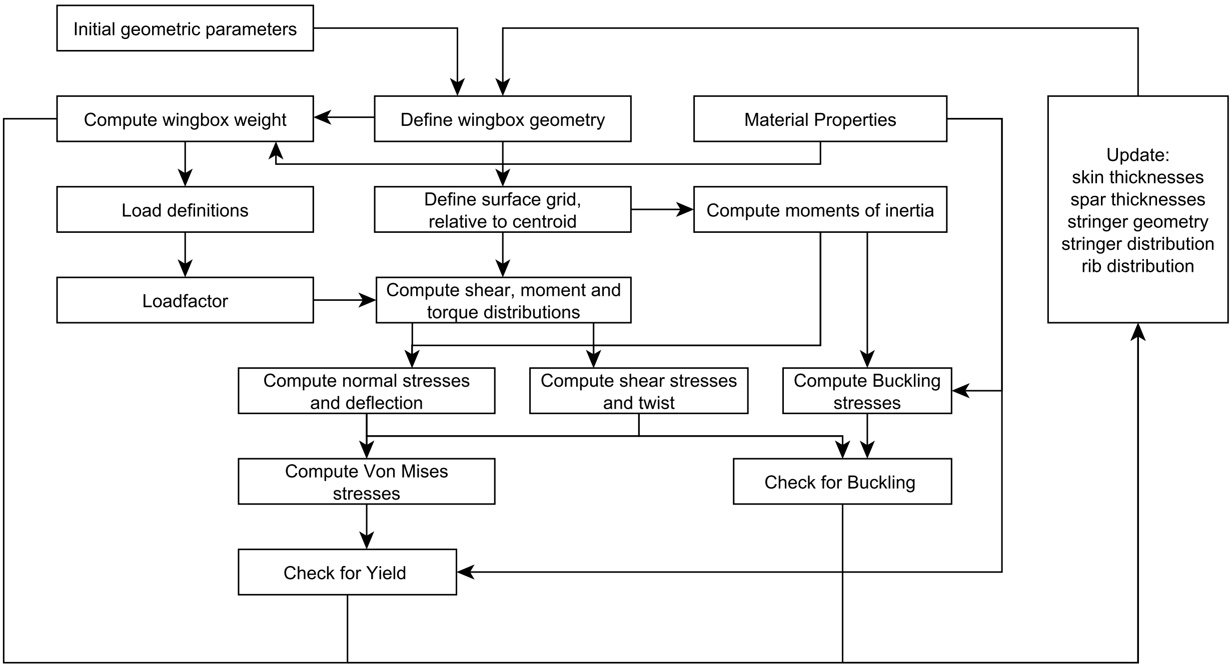

Figure 5.5: Block diagram for the numerical wingbox analysis tool

TOOL VERIFICATION

The analysis tool is verified by comparing the different elements with manual, analytical calculations for simple configurations. Error values were found to be within 1% deviation, which means the tool is a sufficiently accurate representation of the analytical methods.

5.4.4 DESIGN ITERATION & SENSITIVITY

The design was optimised by manual iteration. Increasing and decreasing parameters systematically from a baseline level showed that a design with a small skin thickness and more stringers lead to an optimum design. The skin thickness was chosen to be 0.6 mm, which followed from the iterative process.

Figure 5.6 illustrates the variation of wingbox weight for different skin thicknesses. The numbers of stringers in the different sections were changed to a minimum to maintain a structurally sound wingbox every iteration. This is the same way in which the other design parameters of the wingbox were iterated.

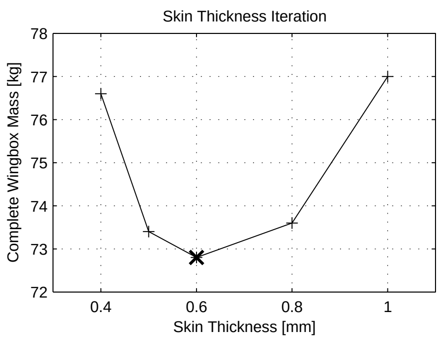

Figure 5.6: Wingbox mass variation as skin thickness is varied

For further design iterations, a sensitivity analysis was performed. For this preliminary design, the aspect ratio was fixed at 10, a lower aspect ratio at the same wing area and MTOW results in a lighter wingbox, a higher aspect ratio leads to a heavier wingbox. The same goes for the wingbox weight related to the MTOW. A heavier aircraft requires a heavier wing structure.

The results of this sensitivity analysis are plotted in the two graphs in Figure 5.7.

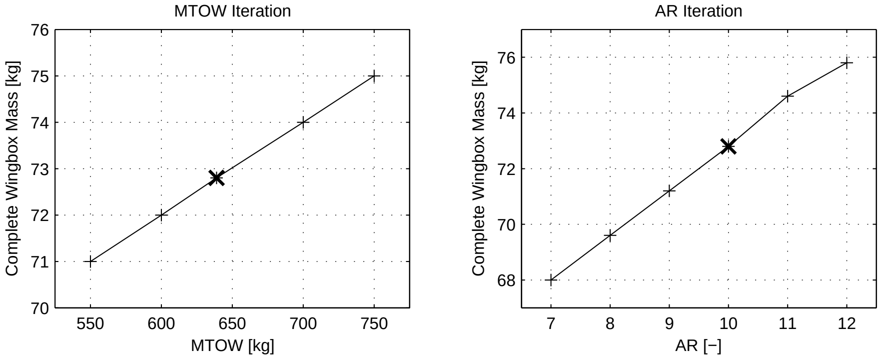

Figure 5.7: MTOW and AR variation effect on complete wingbox mass

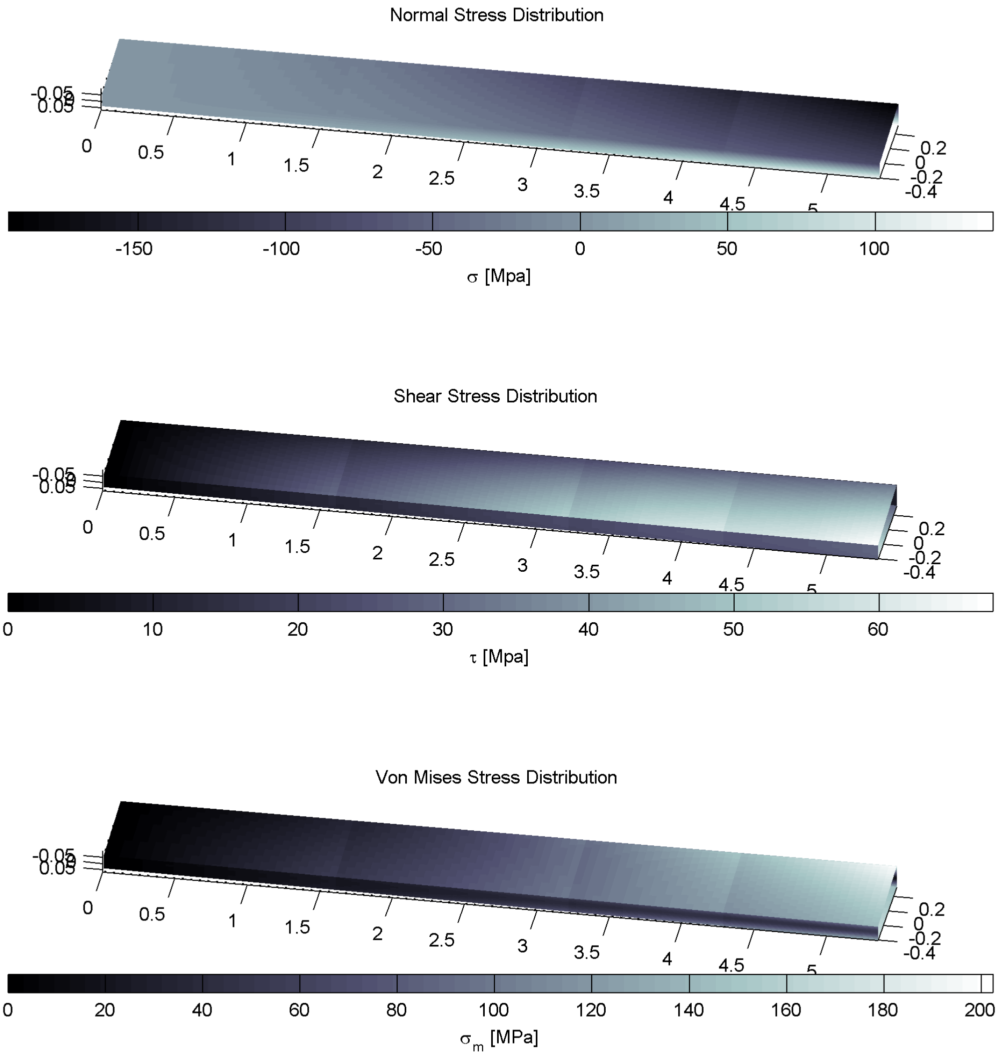

Figure 5.8: The normal, shear and Von Mises stress distributions over the wingbox surface, n = 4.4

5.4.5 Final Wingbox Design

The process of design iteration has lead to a finalized definition of the wingbox. Table 5.2 lists the geometrical wingbox parameters. The wingbox component mass distribution is provided in Table 5.3. The critical stresses for design of the wingbox are summarised in Table 5.4. The stress distributions are illustrated in Figure 5.8.

The wingbox is divided into four sections from tip to root with varying numbers of stringers. The transitions between sections are at 30%, 60% and 80% of the wingspan from the tip towards the root. The number of stringers increases towards the root on both top and bottom panels because of the increasing compressive stress, induced by the increasing bending moment.

The ribs are taken at a constant pitch for simplicity and located such that the stringers would not fail due to column buckling.

The spar thicknesses are constant throughout the span and such that they do not buckle due to the shear load applied.

Table 5.2: Wingbox Geometry

Skin Thickness	0.6	[mm]
Front Spar Thickness	2.0	[mm]
Aft Spar Thickness	1.4	[mm]
Wingbox Start	10	[%c]
Wingbox End	75	[%c]
Height Front	15	[%c]
Height Aft	10	[%c]
Rib Thickness	0.8	[mm]
Number of Ribs	12	[-]
Rib Spacing	0.5	[m]
Stringer Area	30	[mm^2]
Number of stringers:		
Top, Root Section	30	[-]
Top, Section three	25	[-]
Top, Section Two	20	[-]
Top, Tip Section	12	[-]
Bottom, Root Section	20	[-]
Bottom, Section three	17	[-]
Bottom, Section Two	13	[-]
Bottom, Tip Section	8	[-]

Table 5.3: Wingbox Mass

Skin	32.8	[kg]
Spar	14.2	[kg]
Stringers	30.1	[kg]
Ribs	2.6	[kg]
Complete Wingbox	72.8	[kg]

Table 5.4: Wingbox Stresses

n_{max} = 4.5	σ_c	σ_{cr}	
Top, Root Section	192.1	198.5	[MPa]
Top, Section three	141.3	141.8	[MPa]
Top, Section Two	90.3	92.6	[MPa]
Top, Tip Section	26.4	33.1	[MPa]
	τ_{max}	τ_{cr}	
Front Spar	64.3	67.7	[MPa]
Aft Spar	67.7	74.7	[MPa]
n_{min} = -2.5	σ_c	σ_{cr}	
Bottom, Root Section	77.7	85.2	[MPa]
Bottom, Section three	56.5	63.0	[MPa]
Bottom, Section Two	36.0	37.0	[MPa]
Bottom, Tip Section	10.6	13.4	[MPa]
	n_{max} = 4.5	n_{min} = -2.5	
Maximum, Tension	139.7	108.5	[MPa]
Minimum, Compression	194.1	77.7	[MPa]
Maximum, Shear	67.8	37.6	[MPa]
Maximum, Von Mises	202.3	113.0	[MPa]
Tip Deflection	13.4	7.5	[mm]
Tip Twist Angle	2.6	1.4	[deg]

5.4.6 RECOMMENDATIONS

The wingbox design was optimised as far as was possible for this preliminary design. Further improvements and weight reductions would be possible with more advanced optimisation. For example, with the inclusion of cut-outs or evaluating other design options. Analysis using more advanced Finite Element Methods would allow for more complex, but more efficient, structural elements to be evaluated.

Another possibility for weight reduction would be a strutted design. It was not evaluated for this preliminary design study because of time constraints and complexity. If struts were to be fitted, the influence on the aerodynamic design needs to be considered as well to determine whether the weight saving outweighs the additional interference drag on the aircraft.

5.5 FUSELAGE

Fuselages can be made with different structure types, namely: spaceframe, semi-monocoque, monocoque. The trainer aircraft will use a semi-monocoque structure, since this is nowadays the most used structure in aircraft [64]. The reason to chose a semi-monocoque, is that the development risk for the trainer aircraft is already significant, due to the incorporation of the FBW system.

WEIGHT DISTRIBUTION

Before being able to calculate any shear force the weight distribution should be known. This weight distribution was first determined using the class II weight estimation. When subsystems where preliminary designed an updated, more precise, weight could be estimated. This new weight was then used in the weight distribution. Most of these weights are assumed to be distributed loads, while others are assumed to be point loads. A special case is the fuselage weight. For the distribution of the fuselage weight, the fuselage was divided into 102 cross-section. The relative area of the cross-section w.r.t. the sum of all the cross-sections was looked at. Then this number was multiplied with the total weight of the fuselage to get a weight distribution. In formula form it described as Equation (5.20). The total weight distribution is given in Table 11.3. Note that the c.g. has been calculated, with the weight of the fuselage divided into the cross-sections.

$$W_i = \frac{\sum_{i=1}^{102} \left(A_i \cdot M_{fuselage}\right)}{\sum_{i=1}^{102} \left(A_i\right)} \tag{5.20}$$

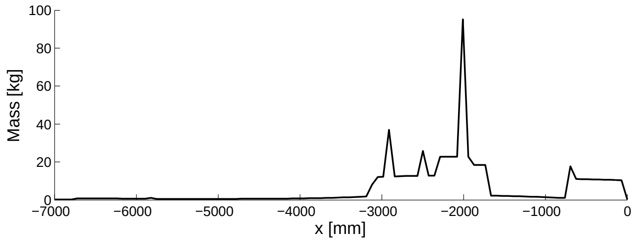

Figure 5.9: Mass Distribution along the x-direction

In Figure 5.9 it can be seen that a lot of mass is located around the wing and payload. The tail on the other hand is relatively light and in the nose, a lot of weight is introduced by the engine.

5.5.1 Loads

Before designing the structure first the loading's on the aircraft should be determined. These consists of shear forces in all three directions (i.e. x,y,z) and the moments around those axis. The reference system that is used, is as in Figure 5.10

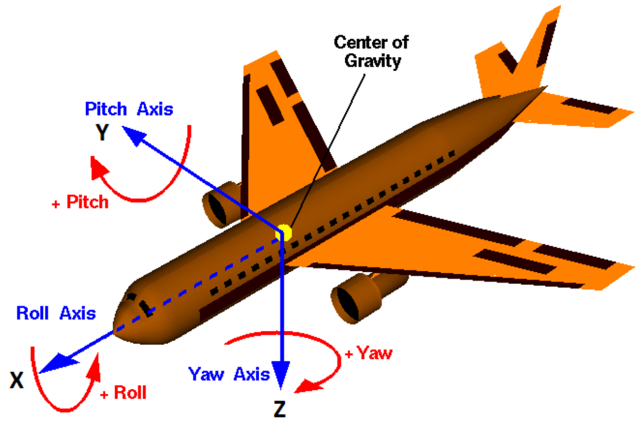

Figure 5.10: Body Axes [5]

Shear Force in x-direction

The contributors to the shear force in x-direction are mainly the thrust force and the drag due to the wing. The drag due to the fuselage, horizontal tail and vertical tail are neglected for the shear force in x-direction. The maximum shear force in x-direction is when the aircraft is accelerating and not when it is in static flight. Therefore a standard static approach, for determining the shear force, cannot be used because the forces are not in equilibrium. This problem can be solved by using an accelerating coordinate system [72]. Assuming a rigid body structure, the translational and angular acceleration can be determined. The acceleration of each mass particle can then be determined, knowing the translational and angular acceleration around the center of gravity (c.g.). Knowing the acceleration of each mass particle, the fictitious d'Alembert forces can be determined. This method is also known as inertia relief. For the fuselage, the cross-sections are the mass particles "particles". Applying the inertia relief method, a shear force diagram in x-direction can be constructed, as in Figure 5.11.

Shear Force in y-direction

The shear force in y-direction, is determined by calculating the force due to a rudder deflection and on top of that a gust load, which is defined by CS 23.443. Normally also the side wind at the side body surface could be determined, for this preliminary design however, this is neglected. The force due to the rudder deflection is calculated using Equation (5.21)

$$F_y = \frac{1}{2}\rho V^2 S_r \delta_r a_{vt} \tag{5.21}$$

The force due to a gust load on the vertical fin, according to CS 23.443, is described in Equation (5.22).

$$L_{vt} = \frac{\rho_0 K_{gt} U_{de} V a_{vt} S_{vt}}{2} \tag{5.22}$$

In Equations (5.21) and (5.22) the variables are:

- U_{de} = Derived gust velocity at certain airspeed [m/s]
- ρ_0 = Density of air at sea-level [kg/m^3]
- ρ = Density of air at considered altitude [kg/m^3]
- V = Aircraft equivalent speed [m/s]
- S_r = Area of the rudder [m^2]
- S_{vt} = Area of the vertical tail [m^2]
- δ_r = Rudder deflection [rad]
- a_{vt} = lift curve slope of the vertical tail [rad^{-1}]
- k_{gt} = Gust Alleviation Factor [-], as in Equation (5.3)

Just as the shear force in x-direction, for the shear force in y-direction, inertia relief had to be used. This is because a force on the vertical tail will rotate and translate the aircraft, so it is not a static problem anymore. One main difference with the shear-force in x-direction though, is that now an angular acceleration is induced, where in x-direction only translational acceleration was used. To determine the angular acceleration around the c.g. the mass moment of inertia (MMOI) around the yaw-axis must be determined. This was done using Equation (5.23). The mass contributions of the fuselage on the MMOI where calculated for the 102 cross-sections, however the contributions of the mass in y-direction cannot be assumed to be zero. The main contributor for the MMOI due to mass in y-direction is the main wing. The c.g. at one wing is approximately 45% of the half span of the wing, according to the wingbox design. Furthermore the weight of one wing is half the weight of the total wing. At this moment it is assumed that the MMOI due to the horizontal tail and due to the fuselage in y-direction is zero. In Section 5.5.8 this assumption will be checked for.

$$I_{zz} = \sum_{i=1}^{102} m_i x_i^2 + \sum_{i=1}^{2} m_i y_i^2 \tag{5.23}$$

Now the angular acceleration and translational acceleration can be calculated. Using inertia relief, the shear force diagram in y-direction can be constructed as in Figure 5.11.

SHEAR FORCE IN Z-DIRECTION

Last but not least is the shear force in z-direction. The main contributors for this shear force are lift due to the wing, lift due to the horizontal tail surface and the weight of the aircraft. For the shear force in z-direction, it is assumed that the aircraft flies in a steady, symmetric flight but with a load factor of 4.8. To get to the shear force distribution, it was assumed that the aircraft was hinged at the c.g. of the wing and also at the c.g. of the horizontal tail. This leads to 2 unknowns, for which there are two equations: moments equal to zero and force equal to zero. The weight distribution has been taken from Section 5.5. Solving this statics problem, the shear force diagram in z-direction was obtained, as in Figure 5.11.

MOMENT AROUND THE X-AXIS

The major contribution of the moment around the x-axis are the torque of the engine and the force on the rudder. Combining these two torques together allow for the construction of a moment diagram around the x-axis. Normally an asymmetrical loading also causes a torque; for example, in a turning flight. For this preliminary design however these asymmetrical loading's are neglected. These leads to a constant moment around the x-axis, along the x-axis. Which is shown in Figure 5.11.

MOMENT AROUND THE Y-AXIS

The moment around the y-axis is caused by the shear forces in z-direction. To determine the moment around the y-axis the shear force in z-direction is integrated along x-direction, as in Equation (5.24). This leads to the moment diagram as in Figure 5.11

$$M_y(x) = \int V_z(x) dx \tag{5.24}$$

MOMENT AROUND THE Z-AXIS

Similarly to the moment around the y-axis, the moment around the z-axis can be determined (i.e. yaw-axis). This leads to Figure 5.11

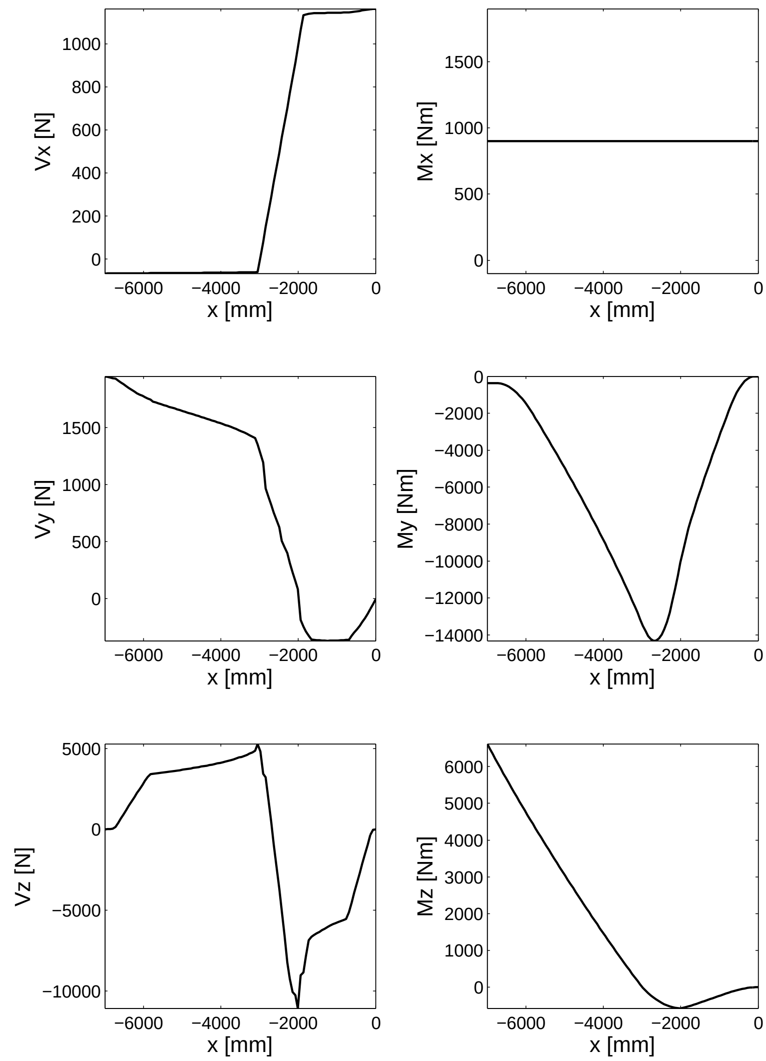

Figure 5.11: Loadings on the Fuselage

5.5.2 Geometry

In most commercial airliners the fuselage has a circular shape, because these fuselages have to be pressurized. In general aviation however, the geometry of the fuselage can have a lot more variety. Since the trainer aircraft is not a nice circle, the assumption of a circular cross-section would probably lead to too large errors. Therefore the fuselage structure was not assumed circular, but was imported from 3D drawings. Around the perimeter of the aircraft the stringers have been equally divided. This is done for the preliminary design, which may be later optimized. The reason why this is done, is that not all load cases are looked at. At this moment the force at the rudder due to maximum deflection and gust are taken into account. Furthermore an accelerating flight and a static flight have been looked at. In the life of the aircraft a lot more loading cases should be considered, such as asymmetrical flights, stall spin, but also ground loads should be considered. Up till this point, these flight conditions were neglected and therefore the fuselage cannot be fully optimized yet. The stringers in the fuselage in the analysis tool vary linearly from the nose to the tail. It is however very impractical to design such stringers. In a later stage of the design, it might be designed with a discrete distribution. For the preliminary analysis however, it gives a solid solution. In a later stage of the design, a more detailed structure and structural analysis can be made. Furthermore for the structural integrity of the fuselage there are 12 frames placed around the perimeter of the fuselage. For this preliminary design the 12 frames are equally dived over the fuselage. In a later design, these frames should be placed more precisely, so it could be used; for example, for the attachment of the wing. Having 12 frames and a fuselage length of 7000 mm, the average distance between two frames is approx. 580 mm. For this preliminary design the average distance is used for calculation, where it is needed; for example, in the calculation of the column buckling of the stringers.

5.5.3 Normal Stress

For the fuselage a method called structural idealization is used [70]. With structure idealization the stringers are assumed to circular booms with a certain area. The booms will only take the normal stress, and the skin in between the booms only take the shear stresses. Furthermore structure idealization assumes that the shear stress in the skin is constant, which is allowed because the length of the skin between booms is short. A typical lay-out of a cross-section, using structural idealization is as in Figure 5.12 More information about structural idealization can be found in: Aircraft Structures for Engineering Students, by T.H.G. Megson, chapter 20 [70].

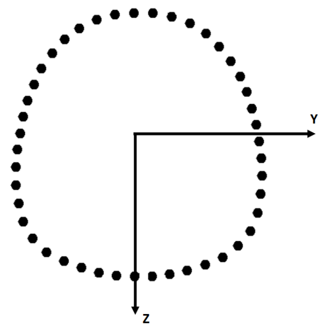

Figure 5.12: Example of a cross-section at a fuselage

After the structure idealization the fuselage can be analyzed at each cross-section. For the normal stress Equation (5.7) is used, but then in the y-z plane instead of the x-z plane. Additional to Equation (5.7) an extra term must be added to this equation. Since in the fuselage there is a shear force in x-direction, that shear force, divided by the sum of all the booms, introduces an stress per boom added on top of the normal stress due to bending. The results of this calculation can be seen in Figure 5.13.

The result at first might seem to be not so logical, since the bending moments around the y-axis are relatively large around $x = -2800$ [mm] relatively to the nose, but the normal stresses at this location are relatively low. This is mainly due to the fact that the bending moment is divided by the area moment of inertia to calculate the normal stress. The area moment of inertia is relatively large around $x = -2800$ [mm] relatively to the nose, especially compared to the area moment of inertia in the tail. For the failure mode, the normal stress will be combined with the shear stress, to create the Von Mises stress. For column buckling of the stringer however it is interesting to look at the normal stress. The column buckling for the stringers is described in Equation (5.9). One of the parameters which is not known is the area moment of inertia of the booms at each cross-section. This is because there is no decision made on which kind shape from the stringers will be used. There the area moment of inertia will be determined as function of the area of a stringer. For this preliminary design it is assumed to have a L-shaped beam as in Figure 5.13a.
To set up the relation between the cross-sectional area and the area moment of inertia, the from Table 5.5 data has been used for the L-shaped cross-section. From this data a quadratic regression was found, the relation between the cross-sectional area and the area moment of inertia can be found in Figure 5.13b

Table 5.5: Relation between area and area moment of inertia

a [mm]	b [mm]	t_1 [mm]	t_2 [mm]	Area [mm^2]	I_{xx} [mm^4]	I_{yy} [mm^4]
12	12	1	1	23	319	319
24	24	2	2	92	5096	5096
36	36	3	3	207	25800	25800

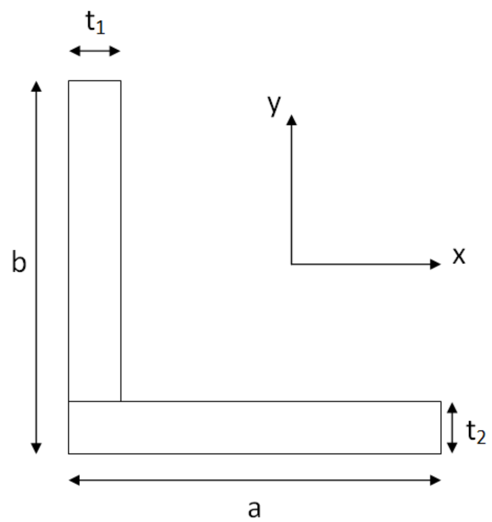

(a) L-shaped Stringer

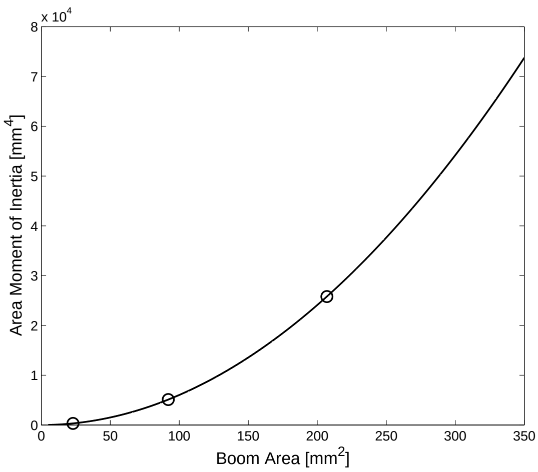

(b) Relation between the area and the area moment of inertia

The other unknown parameter is the Young's modulus, for the material which will be used for the fuselage, this is 71.7 GPa. The lowest calculated column buckling stress is now 1.2056e+05 MPa. The stresses will not even come close to this value, so column buckling will not occur. At this moment, this value is very large. In a later design this value could be reduced. One could increase the distance between the circumference frames, or reduce the cross-sectional area of the stringers.

5.5.4 Shear Stress

Due to the structure idealization, the shear stress between booms is assumed to be constant. Therefore Equations (5.12) and (5.13) can be simplified. The shear stress due to the shear stresses can be calculated using Equation (5.25) [70].

$$q_s = -\left(\frac{S_x I_{xx} - S_y I_{xy}}{I_{xx} I_{yy} - I_{xy}^2}\right) \sum_{i=1}^{n} B_r y_r - \left(\frac{S_y I_{yy} - S_x I_{xy}}{I_{xx} I_{yy} - I_{xy}^2}\right) \sum_{i=1}^{n} B_r x_r + q_{s,0} \tag{5.25}$$

Since the shear flow between booms in constant, the term $q_{S,0}$ can be calculated using Equation (5.26). Where the enclose area is the cross-sectional area of the fuselage. The areas $A_{i,i+1}$ are the area subtended by the skin panels 12, 23, 34 etc. Which has been calculated using the area of a polygon which is spanned between the: centroid, boom i and boom i + 1.

$$q_{s,0} = \frac{\sum_{i=1}^{n} A_{i,i+1} \cdot q_{b_{i,i+1}}}{A_{encl}} \tag{5.26}$$

The shear flow due to moment around the x-axis can be calculated using Equation (5.14). At each cross-section the shear flow between all the booms is calculated. When the this is done for all the cross-sections, the shear flow distribution can be draw, as in Figure 5.13

5.5.5 Von Mises Stress

To check for yield and skin buckling of the fuselage, the Von Mises stress must be calculated. This is done using Equation (5.17). The distribution of the Von Mises stress can then be constructed, as in Figure 5.13

5.5.6 Buckling

One of the main structural failures of the fuselage is skin buckling. To calculate the critical skin buckling stress, Equation (5.8), was used. The critical stress was also analyzed for the whole fuselage. Although in this analysis the bottom of the fuselage is not in compression, it is still checked for buckling. This is done because on the ground the bottom of the fuselage will be in compression and the top will be in tension. The difference between the critical buckling stress and the von mises stress can be seen in Figure 5.14. The minimum difference between the critical skin buckling stress and the Von Mises stress is 1.0 MPa. Note that in Figure 5.14 the difference between the critical skin buckling stress and Von Mises stress can be higher than 50 MPa at the nose and the tail. The scale on the plot, however is decreased to get a more detailed plot of the difference at the most important point. That is the area between -1000 and -3000 mm. The difference between the critical skin buckling and Von Mises at the tail can go up to 2300 MPa. The skin buckling is however to the critical design parameter at the tail. At the tail, yielding of the material is the major critical failure.

5.5.7 Analysis Tool

For the fuselage design a numerical analysis tool has been made. It imports the shape of the fuselage from CATIA, through an .iges file. Other parameters such as the load factor and the engine horsepower are taken from an excel file with import variables. The last input are the load cases needed to determine the moments and shear forces. When the moments and shear forces are known, the normal and shear stresses can be determined. From these stresses the Von Mises stress can be determined. Having all these stresses, it is investigated if the structure fails/ buckles. Finally the weight of the fuselage is outputted and inputted in the mass distribution, and the whole program is ran again. A graphical overview of the numerical fuselage analysis tool is Figure 5.15.

5.5.8 Tool Verification and Validation

To ensure that the fuselage analysis tool produces correct values, verification and validation procedures have to be performed. First of all for one cross-section a hand calculation was made. This showed, that the errors where smaller than 1.5%, which is close enough for this stage of the design. Furthermore a unit check for all the formula's have been performed.

For validation some of the values where checked, with values from Roskam. The fuselage weight of the Cessna 152 was estimated to be 105 kg [55]. The fuselage weight of the trainer aircraft, from the analysis tool is 90.4 kg. This difference is not too large, considering this is only a preliminary design. No detailed optimization has been done. Furthermore in this preliminary design, cut-outs in fuselage, have not been taken into account, which increases the weight.

The MMOI around the yaw-axis of the Cessna 172 is 2666 kg m^2, the MMOI of the trainer aircraft from the fuselage analysis tool is 2469 kg m^2. However the MMOI due to the horizontal tail was neglected, so the MMOI seems realistic.

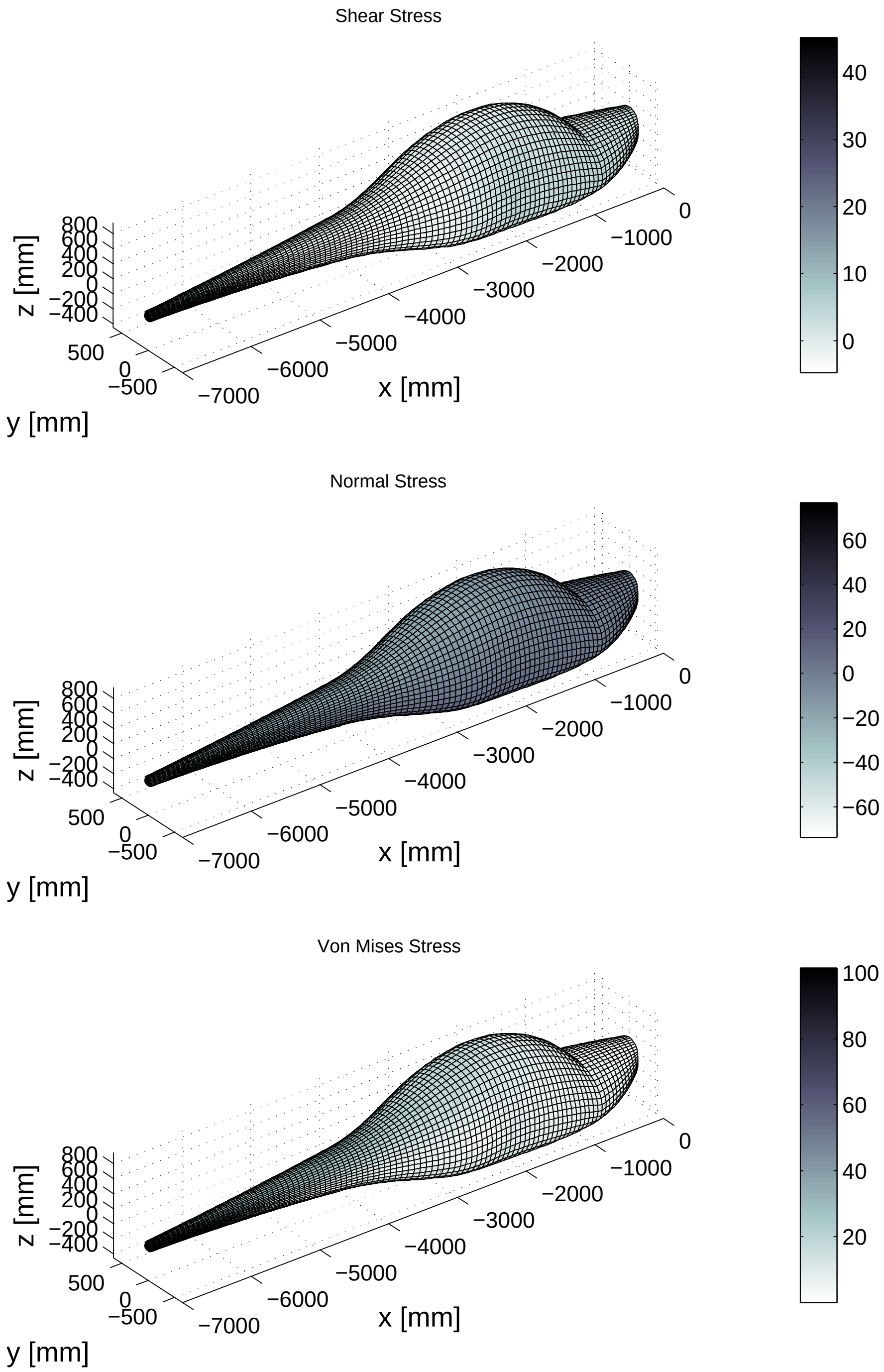

Figure 5.13: Stress Distriubtions along the Fuselage [Mpa]

5.5.9 Final Fuselage Design

The final design of the aircraft consists of 48 stringers, along the the whole fuselage. The cross-sectional areas of the stringers vary linearly from 40 mm^2 to 60 mm^2. The skin thickness is 0.8 mm and there are 12 circumference frames equally divided over the fuselage, with a cross-sectional area of 50 mm^2. The maximum Von Mises stress is 1.56 times higher than the fatigue strength of the chosen material. Which is aluminum 7075-T6, which has a fatigue strength of 159 MPa at 500 million cycles completely reversed stress [73]. The minimum difference between skin buckling and Von Mises stress is 1.1 MPa, it is assumed though that buckling does not necessarily lead to failure of the fuselage.

The total design of the aircraft can be found in Table 5.6

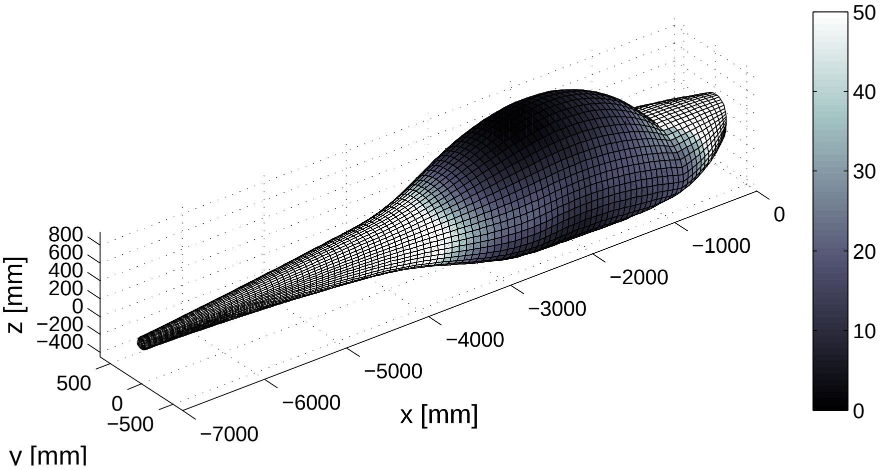

Figure 5.14: Difference between σ_{cr} for skin buckling and σ_m. [Mpa]

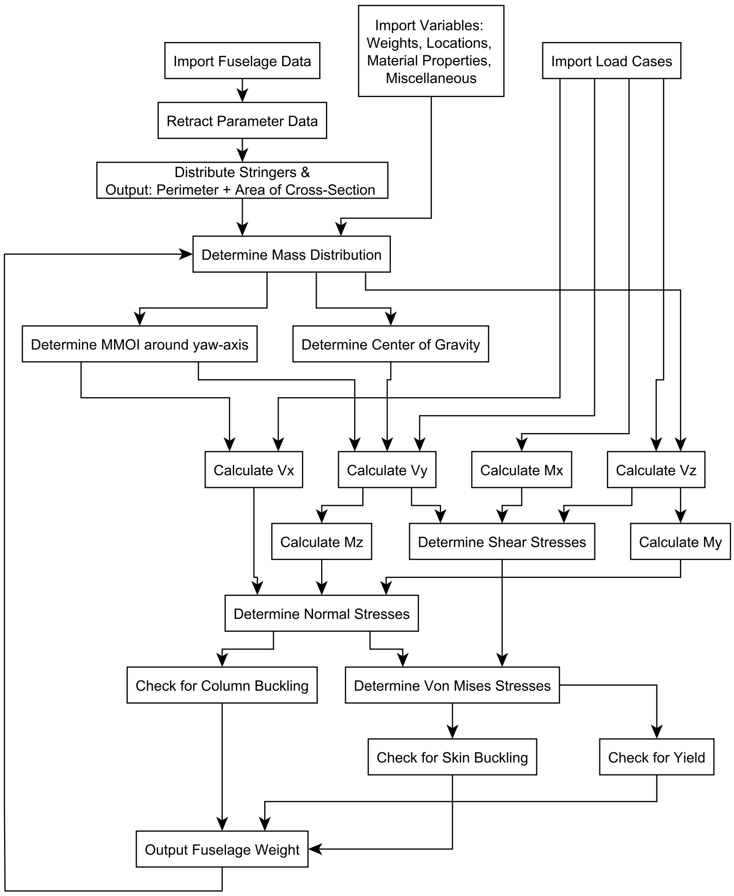

Figure 5.15: Block Diagram for the numerical fuselage analysis tool

Table 5.6: Final Design of Fuselage

Number of Stringers	48	-
Number of Frames	12	-
Skin Thickness	0.8	mm
Cross-Sectional Area Stringer (at nose)	40	mm^2
Cross-Sectional Area Stringer (at rear)	60	mm^2
Cross-Sectional Area Frames	50	mm^2
Distance between Frames	580	mm
Maximum Normal Stress	77	Mpa
Minimum Normal Stress	-74	Mpa
Maximum Shear Stress	45	Mpa
Minimum Shear Stress	-4.7	Mpa
Maximum Von Mises	101.7	Mpa
Minimum Column Buckling Stress	12056	Mpa
Minimum Difference between skin buckling and Von Mises	1.1	Mpa
Mass of the Stringers	48.8	kg
Mass of the Frames	37.6	kg
Mass of the Skin	4.0	kg
Total Mass	90.4	kg

5.5.10 Recommendations

The values which have now been found for the fuselage design are merely a preliminary design. Further research has to be done with major cut-outs in the fuselage; for example, at the windows. Around these cut-outs the extra reinforcements have to be made. Furthermore a better optimization can be done in a subsequent design stage; for example, in this design 48 stringers where used in the complete aircraft. This is however not necessarily the case, in the tail maybe less stringers can be used, because skin-buckling is not really a problem in the tail at this moment. Another problem is that 48 stringers, with a cross-section area of 60 mm^2 will most likely not fit in the tail. Therefore a more detailed study has to be made on the stringers. This preliminary design however, indicates is approximately needed in the aircraft. The last thing that has not been considered yet in the fuselage design is the bulkhead behind the engine. This will also increase the weight of the complete aircraft.

5.6 Landing Gear

In this section the preliminary design of the landing gear is discussed. First in Section 5.6.1 the requirements imposed by the CS-23 regulations and operational usage are discussed and determined. The tire selection is performed in Section 5.6.2. After that the rear landing gear is sized in Section 5.6.3 followed by the nose landing gear in Section 5.6.4. Other components needed for the landing gear like brakes, rims etc are discussed in Section 5.6.5. The section is concluded with a summary in Section 5.6.6 and recommendations for future steps in Section 5.6.7.

The landing gear has a tricycle non retractable layout. This decision was already made in [64]. Reasons can be found in the following list:

- Favorable for PPL training
- Good visibility over the nose during ground operation
- Good steering characteristics
- Level floor while on the ground
- Good stability against ground loops

These advantages are assumed to outweigh the disadvantage of increased drag and therefore higher fuel consumption.

The design of the landing gear was part of the MATLAB loop explained in Chapter 3. Thus the weight and aircraft characteristics used in this section belong to the last iteration made with the MATLAB program.

5.6.1 Requirements

In this part the requirements for the landing gear design are discussed. Requirements for the landing gear are either set by the operational capability of the aircraft or the CS-23 requirements which have to be fulfilled. Due to the role as a trainer aircraft a durable and simple landing gear option is needed. Further the aircraft has to be able to operate also under difficult airfield conditions since it cannot be assumed that all flight schools have access to a tarmac airfield. Roskam gives some indication on the required tire pressure to allow for operation under different airfield conditions. They are shown in Table 5.7.

Table 5.7: Recommended Tire Pressure for Various Surfaces [39]

Surface	Max Allowable Pressure ($kg\ cm^{-2}$)	Tire Pressure (psi)
Wet, boggy grass	1.8-2.5	25-35
Hard desert sand	2.1-3.2	30-45
Hard grass	2.8-4.2	40-60

The CS23 regulations have been analyzed for requirements that influence the design of the landing gear. The found requirements are tabulated in Table 5.8. These regulations differ in terms of how much they drive the design. Therefore they were examined on the design influence and it was chosen that only CS23.473 is used for the initial design of the landing gear. This selection is highlighted in Table 5.8.

Table 5.8: Relevant CS23 requirements for landing gear design [40]

.471	.485	.723	.731
.473	.493	.725	.733
.479	.497	.726	.735
.481	.499	.727	.745
.483			

From that the following requirements for the preliminary design can be derived:

- The aircraft shall be able to perform landing, take-off and taxiing on wet grass airfields.
- The landing gear shall comply to the regulations in CS23.473(d) and (g).

5.6.2 TIRE SELECTION

Tire selection was done according to the method given in Roskam [39]. First the weight distribution in static conditions was determined. Since the center of gravity position was not known yet the assumption was made that 10% of the weight is carried by the nose landing gear and 90% equally distributed by the main landing gear. This assumption is valid according to Roskam.

$$W_{\text{nose}} = 63.68\,\text{kg} = 140.39\,\text{lbs} \qquad W_{\text{main}} = 286.58\,\text{kg} = 631.80\,\text{lbs} \tag{5.27}$$

An extensive resource of reference tire data is given in [41]. When examining this list it became clear that only Type III tires are available in the required size range. A short extract of this list, with the most suitable tires, is given in Table 5.9.

Table 5.9: Goodyear Type III Tire Data [41]

Size	Ply Rating	Rated speed (mph)	Rated load (lbs)	Rated inflation (psi)	Maximum braking load (lbs)	Maximum bottoming load (lbs)	Part No	Weight (lbs)
5.00-4	6	120	1200	55	1740	3200	504C61-2	4.3
5.00-5	4	120	800	31	1160	2200	505C41-4	4.9
5.00-5	6	120	1285	50	1860	3500	505C61-8	4.9
5.00-5	10	120	2150	88	3120	5800	505C01-2	5.7
6.00-6	4	120	1150	29	1670	3100	606C41-6	8.8

By examining this table it becomes clear that all tires meet the load requirement calculated above. In terms of weight the five inch tires are the most suitable ones. The ply rating has an influence on the weight and the maximum allowable load. Five inch tires with a ply rating of six and ten can carry considerable more weight than those with a ply rating of four. But they also have a higher operating pressure. Since it was decided that the aircraft should also be able to use grass airfields with an unfavorable ground tires with a ply rating over 4 are not suitable. However dependent on the airfield surface also a more durable tire with a ply rating of six can be used without a weight penalty.

The selected 5.00-5 4 ply tire has to be checked against two more requirements. First the rated speed must not be exceeded and second during landing with the maximum inertia factor the maximum bottom load must not be exceeded. To check the speed requirement Roskam provides two formulas for calculating the maximum encountered speed during landing and take off.

$$V_{\text{tire/max}} = 1.2V_{S_L} = 1.2 \cdot 28.2 = 25.92\,\text{m/s} \tag{5.28}$$

$$V_{\text{tire/max}} = 1.2V_{S_{TO}} = 1.1 \cdot 23.6 = 25.96\,\text{m/s} \tag{5.29}$$

As one can see these speed are far below the maximum allowable speed of 120 mph. CS23.473 defines the maximum inertia factor as 2.67. Assuming that the aircraft touches down without the nose landing gear at this load factor the maximum encountered load becomes 1901 lbs per main tire which is below the limit of 2200 lbs. For the nose landing gear the static load has to multiplied by a factor of 1.45 to determine the maximum dynamic load [39].

$$P_{\text{dyn}} = 1.45 \cdot P_{\text{static}} = 1.45 \cdot 140.39 = 203.57\,\text{lbs} \tag{5.30}$$

As one can see also this load is below the maximum load of 2200 lbs. Therefore the same tire can be used for the nose wheel as well.

A sanity check was performed to compare the tire selection with tires used on aircraft with comparable size. For this the Diamond DA-20 was selected with a maximum take of weight of 750 kg. [28] shows that this aircraft uses 5.00-5 tires. Thus it can be concluded that a reasonable tire choice has been made.

5.6.3 REAR LANDING GEAR

In this subsection the design of the rear landing gear is discussed. First in Section 5.6.3 the possible design options for the rear landing gear are discussed. The preliminary strut sizing is performed in Section 5.6.3.

DESIGN OPTIONS

The different design options for a general aviation landing gear are given in Figure 5.16. First the spring leaf landing gear is discussed in Section 5.6.3 followed by the spring tube landing gear in Section 5.6.3. The third option namely the push-pull rod landing gear is treated in Section 5.6.3. Materials which can be used for the landing gear are discussed in Section 5.6.3. Finally it is decided in Section 5.6.3 which concepts have to be further analyzed.

Spring Leaf Main component of a spring leaf landing gear is as the name says a leaf spring. Directly attached to this spring are the tires. Thus it has the function of introducing the landing loads into the fuselage and at the same time to provide the necessary stiffness. Advantages of spring leafs are their easy production and low cost. But due to their flat rectangular shape with usually a constant thickness they are quite heavy. Sometimes they are laminated with multiple layers at certain locations to provide a constant stress distribution along the spring. Damping is done by tire scrub that is the friction of the tires with the ground during deflection of the landing gear.

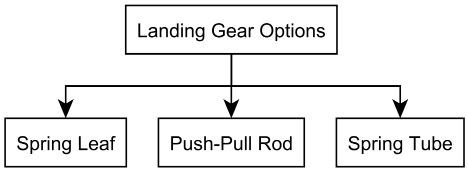

Figure 5.16: Design Option Tree for Rear Landing Gear

Spring Tube A spring tube is similar to a spring leaf landing gear. It also has the function of providing a certain stiffness along with the load introduction into the fuselage. Difference is that a spring tube has a round shape. Often they are tapered to provide a better stress distribution along the strut. They are more difficult to produce than spring leaf landing gears but offer weight advantages. Damping of the landing gear is produced by tire scrub.

Push-Pull Rod A push-pull rod landing gear separates the function of load introduction and stiffness. The function of the rods is to introduce the load into the fuselage whereas the stiffness is achieved by a separate spring or bungee ropes. Additional dampers can provide improved damping to prevent the aircraft from jumping during hard landings. Advantages are the lack of the expensive spring landing gears. Further stiffness can be changed by only exchanging the spring, whereas a spring tube or leaf landing gear requires a complete redesign. However a push-pull rod landing gear requires a more complicated mechanism and requires more maintenance.

Materials For the design of the landing gear three materials were considered: aluminum, steel and titanium. Composite landing gears were not considered because they are substantially more difficult to analyze and were therefore out of the scope for this preliminary design.

For aluminum the 7075-T6 alloy was chosen because it offers a high yield and ultimate strength in comparison with other alloys and is easily available. More advanced alloys like AL-LI alloys which offer a lower density together with a yield strength of up to 690 MPa were not considered because no data were available on price and availability [74]. For titanium the grade 5 alloy was chosen because it is the most commonly used alloy and offers excellent properties. The steel alloy used for design was chosen to be 60SiCrV7 due its excellent properties and readily available data. 60SiCrV7 is a steel which is used in automotive applications and is therefore quite common. The properties of the materials are summarized in Section 5.6.3.

Table 5.10: Material options for landing gear [42]

Material	E-mod [GPa]	σ_y [MPa]	σ_{ult} [MPa]	Density [kg m^{-3}]
AL 7075-T6	71.7	503	572	2810
TI Grade 5	114	910	1000	4450
ST 60SiCrV7	210	1650	1950	7430

As can be seen steel offers by far the highest yield strength but also has a high stiffness which is unfavorable in this application. Aluminum offers a low stiffness but also a low yield strength. Titanium seems to have the best properties due its stiffness close to the one of aluminum but the very high yield strength. However titanium is notorious for its price and the difficulty to machine it.

Trade-off Due to the whole design philosophy of the project to create a robust and easy to maintain aircraft it was decided to drop the push-pull rod landing gear layout. Higher production cost related with the spring tube/leaf landing gears are assumed to be justified with lower DOC. To be able make a final concept choice a MATLAB tool has been created for sizing and weight estimation.

Strut Sizing

In this sub section the approach used for the rear landing gear strut sizing is discussed. Following simplifying assumptions have been made:

- Energy of aircraft during maximum descent velocity is solely absorbed by main landing gear
- Load radius of tire can be subtracted from required landing gear deflection
- Tires have the same stiffness as main landing gear
- Fatigue is neglected
- Stress concentrations are neglected
- Constant shear force across cross-section
- No safety factor is applied during preliminary designs

First the energy that has to be absorbed by the main landing gear has to be calculated. According to CS23.473 it was determined that the maximum descent velocity is 2.47 ms^{-1}. With an aircraft weight of 636.84 kg one obtains a kinetic energy of 1942 J. By discretising the two landing gears as springs one can calculate the required deflection and stiffness with the following two equations

$$E = \frac{1}{2} k s_{\max}^2 \qquad a = \frac{k \cdot s_{\max}}{m} \tag{5.31}$$

Substitute the energy, the weight of the aircraft and the maximum inertia load factor and solving both equations yields a spring stiffness of $k = 71600\,\mathrm{Nm}^{-1}$ and a maximum required deflection of $s = 0.233\,\mathrm{m}$. Thus each landing gear leg needs a stiffness of $k = 35800\,\mathrm{Nm}^{-1}$.

With a peak inertia load factor of 2.67 one obtains a peak load per landing gear leg of 8340 N. As one can see in the following picture this load can be decomposed in a part acting along the axis of the landing gear leg and in a part acting orthogonal to it.

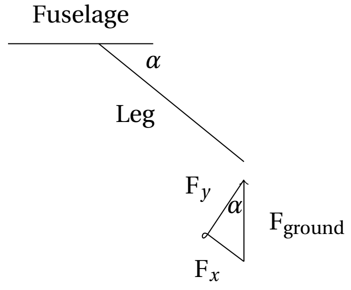

Figure 5.17: Landing gear geometry

The ground force can be decomposed as follows

$$F_x = F_{\text{ground}} \sin(\alpha) \qquad F_y = F_{\text{ground}} \cos(\alpha) \tag{5.32}$$

Determination of α was done by examining the three view of a Cessna 152, a value of 30° was found. This value was used for the preliminary design of the landing gear. Thus the forces acting along the landing gear axis and orthogonal to it are $F_x = 4170$ N and $F_y = 7223$ N respectively.

The calculation of the landing gear deflection is done by a semi analytical approach. First the beam is discretised into a number of section with length L. For every section the acting moment due to F_y is calculated. By looking at Figure 5.18 one realizes that the deflection of a particular section is the sum of the displacement of the previous section, the displacement due to the moment acting on the section and the displacement due to the slope of the beam of the previous section [75].

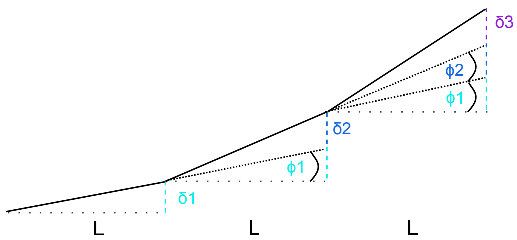

Figure 5.18: Sign convention for vertical displacement of landing gear legs

This expressed in a formula yields

$$\delta_{tot} = \underbrace{(\delta_1 + \cancel{\phi_0 * L})}_{\text{disp. 1st section}} + \underbrace{(\delta_2 + (\cancel{\phi_0} + \phi_1) * L)}_{\text{disp. 2nd section}} + \ldots + \underbrace{(\delta_n + \left(\sum_{i=1}^{n-1} \phi_i\right) * L)}_{\text{disp. nth section}} \tag{5.33}$$

Where the δ_i and ϕ_i are given by

$$\delta_i = \frac{M_i L_i^2}{2EI_i} \qquad \phi_i = \frac{M_i L_i}{EI_i} \tag{5.34}$$

From the tip displacement the spring stiffness can be calculated by Equation (5.35)

$$k = \frac{P}{\delta_{\text{tip}}} \tag{5.35}$$

Stress for every section in the landing gear was calculated by using the 'Flexure Formula'

$$\sigma_i = \frac{M_i y_i}{I_i} \tag{5.36}$$

This method was implemented in MATLAB which was then used for the landing gear sizing. A flow diagram of this script is given in Figure 5.19.

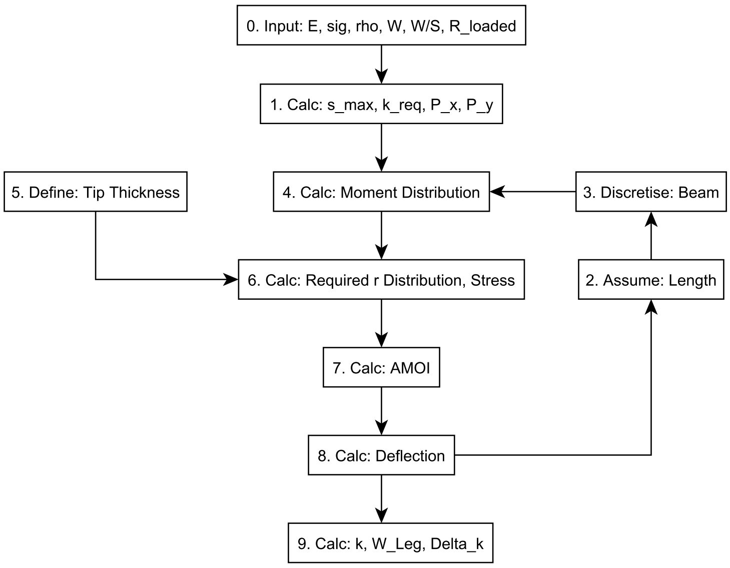

Figure 5.19: Landing Gear Design Flow Chart

Step 0 Define input parameters as variables.

Step 1 From the input parameters the required stiffness, required maximum deflection and forces along the axial and lateral direction are computed.

Step 2 Assume a landing gear leg length. With the landing gear length the stiffness of the spring can be influenced.

Step 3 Discretise the beam into sections with constant width L. 1000 sections were chosen which was the outcome of a grid convergence study for a rectangular beam of constant cross section.

Step 4 Calculate the moment distribution along the landing gear leg for every cross-section.

Step 5 Assume a start thickness, that is the thickness of the landing gear at the tip. A minimum thickness is required at that point because some space for the axle attachment is needed. 1 cm for steel, aluminum and titanium was assumed. For the spring leaf a start thickness and width was set.

Step 6 Determine the required thickness of the landing gear leg to meet 'Von-Mises-yield criterion', invoke tip thickness.

Step 7 Compute the area moment of inertia for every cross section along the landing gear leg.

Step 8 Calculate landing gear leg deflection and increase length if required.

Step 9 Calculate the weight of a landing gear leg along with its stiffness. On top of that the achieved stiffness is compared with the required stiffness.

Spring Tube Designs Results of the spring tube design are given in Table 5.11.

Table 5.11: Spring tube landing gear designs

Material	k [Nm^{-1}]	W [kg]	L [m]
Aluminum	156.0	5.86	1.151
Steel	157.42	4.53	0.863
Titanium	120.53	4.59	0.951

It was possible with all three materials to design a landing gear which meets the requirements. As one can see by inspection from Table 5.11 the steel and titanium version almost have the same weight. The aluminum version, however, has a significant weight disadvantage especially because this 1.3 kg additional weight is going to double since two legs are required. It also has to be noted that the aluminum landing gear is around 20 cm longer than the other two. Al three landing gear designs are stiffer softer as specified by the requirements. However this offset of stiffness is negligible small in comparison with the $k = 35800\,\mathrm{Nm}^{-1}$ required, especially for the preliminary design.

Table 5.12: Spring leaf landing gear designs

Material	k [Nm^{-1}]	W [kg]	L [m]
Titanium	321	18.43	1.24

Spring Leaf Designs A design for a spring leaf landing gear was done which is shown in Table 5.12. As one can see it meets the requirements but is almost 3.5 times heavier than the titanium landing gear in Table 5.11. It was therefore decided to abandon this design since the possible cost savings during production cannot justify this severe weight penalty.

Hollow Spring Tube Designs The third design approach was to design a landing gear which has a tubular cross section but is hollow instead of the solid one described in the paragraph above. The specification of this design are given in Table 5.13 as can be seen it was possible to reduce the weight for the titanium and steel version by almost 1 kg whereas a weight advantage of 0.5 kg was achieved for the aluminum version. Also in this design the landing gear was slightly stiffer than required. Producing a hollow strut leads to higher production cost especially drilling a hole with a large length to diameter ratio is problematic. One suitable production method is gun drilling which is used for this kind of application [76].

Table 5.13: Hollow spring tube landing gear designs

Material	k [Nm^{-1}]	W [kg]	L [m]
Aluminum	152.8	5.31	1.154
Titanium	157.3	3.90	0.955
Steel	44.48	3.53	0.871

Trade Off Based on the three designs presented above it can be concluded that the spring lead layout is not suitable for this application. Whether a hollow or solid strut should be used is dependent on the production cost. However gun drilling is used for a long time and therefore a proven production method which should not introduce major cost penalties. It is therefore decided to use a hollow landing gear design. Further the hydraulic lines of the brakes can be stores in the strut which leads to a neater design. Steel is selected as the material since it is cheaper, allows for shorter landing gear legs which is beneficial for drag and reduces the aircraft weight significantly.

5.6.4 Nose Gear

In this section the initial design of the nose landing gear is discussed. A nose landing gear for general aviation aircraft usually consists of the following components:

- Wheel
- Strut
- Shock absorber
- Shimmy damper
- Steering mechanism
- Retraction mechanism (in this case not needed)

The wheel selection was done in Section 5.6.2. For the preliminary nose gear design it was decided to perform a less elaborate analysis than in comparison with the main landing gear. This decision was made because of the non-existence of different design options. All nose landing gears for general aviation have on the preliminary level a very similar layout, off course big differences exist in the detail but these are not significant for this design stage.

For the nose gear strut a diameter of 2 cm is assumed with a hole size of 1 cm. This seems reasonable, especially by considering the results from Section 5.6.3. The length of the nose gear strut is the same as the height of the rear landing gear which is 60.8 cm. This ensures a level aircraft during ground operations. The expected nose gear load was already specified in Section 5.6.2. A sanity check was performed by using the Euler buckling formula (one end fixed, the other free to move), by using the same steel as for the main landing gear a buckling load of 20491 N was obtained. This is far below the expected nose gear load. For a more elaborate design the nose landing gear has to be checked against bending loads which occur due to wheel drag and obstacles as well as the stiffness and its effects on vibrations induced by the ground surface.

Shock absorption is usually achieved by means of an oleo strut. An oleo strut is a shock absorber of two telescoping struts. The upper part is called the cylinder and the lower part piston. Both parts form a chamber which contains a gas and oil. For the gas the most common choices are air or nitrogen. When a load is applied to the lower part that is the piston the air gets compressed and provides stiffness. Further there is a plate with an orifice in this arrangement. When the piston is pushed upwards, the oil gets forced through the orifice and by that the oleo strut performs damping action. Damping capability is important, since bouncing of the aircraft on the ground has to be prevented. The oleo strut length can be approximated by the following formula [39]:

$$E = \frac{1}{2} m_{\text{front}} v_l^2 = P_{\text{dyn}} \cdot s_{\text{oleo}} \tag{5.37}$$

The force of an oleo shock absorber is, in contrast with springs, can be assumed to be constant with deflection [39]. Solving this equation yields to an oleo strut length of 11 cm. This oleo is small enough to be in line with the nose landing gear strut. Therefore weight of the nose landing gear strut and the oleo together is assumed to be

$$W_{\text{strut+oleo}} = L\pi(r_{out}^2 - r_{in}^2)\rho_{\text{steel}} = 1\,\text{kg} \tag{5.38}$$

Shimmy is the rotational oscillatory movement of the nose landing gear around its steering axis. This oscillation is usually triggered by some kind of ground obstacle and can cause severe nose gear damage up to the point where it detaches from the fuselage. To compensate for this effect shimmy dampers are used. Since this aircraft is expected to operate on rough ground like grass a shimmy damper is incorporated in the nose gear assembly. Weight estimation was performed by looking at shimmy dampers of aircraft with comparable size. The weight is given in Table 5.14

Steering during taxiing on the ground can be done by either differential braking or a steering wheel. A combination of both is possible as well. For the design of this aircraft improved steering capability is desired since a lot of taxiing has to be performed during flight training.

5.6.5 Other Rear Landing Gear Components

Apart from a properly sized landing gear strut other components like rims, brakes and axles are required. In the case of a general aviation aircraft these components are standard products produced by certain aircraft suppliers. In Table 5.14 the remaining required components are listed. The listed components give a good indication in terms of cost and weight. If exactly these components are going to be used has to be determined in a later design stage.

Table 5.14: Aircraft landing gear aftermarket products [41, 43–45]

Manufacturer	Part No	Description	Static Load Rating [lbs]	Weight [kg]	Price [$]	Amount
Grove Aircraft	51-201 51-1M	Rear rim with brake	800	2.54	779.00	2
Grove Aircraft	5013	Rear axle	1250	0.42	44.00	2
Grove Aircraft	59-2M	Nose rim	800	1.09	319.00	1

Manufacturer	Part No	Description	Weight [kg]	Price [$]	Amount
LORD	SE1051-2	Shimmy	0.472	849.00	1
Cessna Aircraft	0942200	Nose wheel fairing	1.157	?	1
Cessna Aircraft	0941200	Rear wheel fairing	1.697	?	2
Goodyear	505C41-4	Nose gear tire	2.205	?	1
Goodyear	505C41-4	Main gear tire	2.205	?	2

Front axles are not produced by 'Grove Aircraft' but due to the same axle diameter it is assumed that the weight of a front axle is 0.42 kg as well. Other components like master cylinder, hydraulic lines, fluid and brake pedal were not included. Brake pedal and master cylinder is counted towards fixed equipment in the weight budget. Hydraulic lines, brake fluid, bolts, nuts and wheel pants are accounted for by a contingency of 15%.

5.6.6 Summary

Design driving requirements of the landing gear were analyzed. It was chosen to use a tricycle non retractable landing gear. A MATLAB tool was created to perform a trade off between different spring strut/leaf landing gear options. It was decided to use a steel tapered hollow strut main landing gear. Design of the nose landing gear was mainly derived by inspection of reference aircraft an no thorough stress analyses was performed, but from main landing gear sizing it was possible to proof the feasibility of the design. The weight of the landing gear components is summarized in Table 5.16. A drawing of the landing gear can be found in Table 5.16.The radii of the main landing gear strut along its length are given in Table 5.15.

5.6.7 Recommendations

After the preliminary layout of the landing gear several further steps have to be performed. First the remaining CS-23 regulations have to be taken into account for the landing gear design. For both the main and the nose landing gear a vibrational analysis should be performed. This enables to find the eigenfrequency of the landing gear and cross check it with the expected loads during take-off, landing and taxiing. An example vibrational analysis can be found in

Table 5.15: Radii of main landing strut

Length Strut (% Length)	0	10	20	30	40	50	60	70	80	90	100
Radius (cm)	1.00	1.00	1.06	1.19	1.29	1.38	1.46	1.53	1.59	1.65	1.71

Table 5.16: Weight of landing gear

Component	Weight [kg]
Main landing gear struts	7.06
Nose landing gear strut	1.00
Aftermarket products	19.07
Total	27.13
With contingency	31.25

[77]. For the main landing gear the fuselage integration has to be designed carefully due to the high induced bending moments. Further analyses could include the use of FEM software for code validation and design optimization. Another field of interest is fatigue analysis, for the preliminary design the assumption was made that it is negligible, in a more elaborate analysis this assumption should be validated. The steering mechanism and the oleo/shimmy integration need to be engineered with care. Last but not least a production plan has to made which should take into account the advanced geometry of the main landing gear with the aim of reducing production cost.

5.7 Production Plan

In this section a preliminary production plan of the aircraft is presented. A schematic overview is given in Figure 5.20. This flow diagram show the production plan on an assembly level. Parallel activities are positioned above each other on the same horizontal position.

First 4 separate sub-assemblies are produced these are the fuselage structure, the wing, the empennage and the landing gear assembly. The aluminum fuselage structure functions as the main part which all other parts get attached to in the assembly process. The wing assembly contains the wing box, the ailerons and flaps with its control mechanisms together with part of the aircraft's electrical and fuel system. These parts can all be assembled parallel to each other. The wing assembly is then put together like 'Lego bricks'. The same philosophy applies for the empennage and landing gear assembly. The empennage contains the tail structure and the rudder and elevator control surfaces and its control mechanisms. The landing gear system is composed from the landing gear struts, wheels, tires, brakes and other components.

In the integration phase the fuselage, wing, empennage and landing gear assembly are put together. From this point onwards the remaining components can be integrated. These include the avionics, the reamining electrical system, flight controls and brake hydraulics. Sequential to this part, the engine integration can be performed. Finally furnishing can be installed, the aircraft can get painted and the final tests before delivery can be performed.

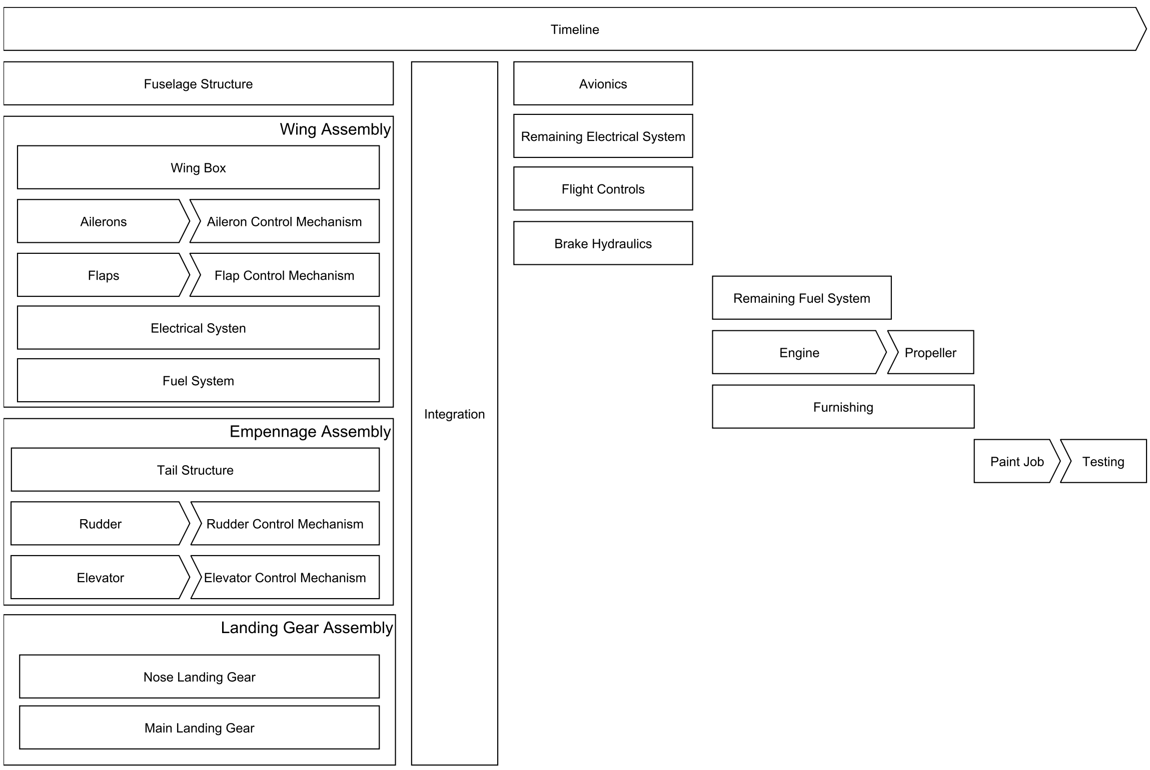

Figure 5.20: Production plan

6
AERODYNAMICS

The aerodynamic characteristics of the aircraft will be discussed in this chapter. First an (preliminary) airfoil selection will be done, then the aerodynamics tool will be discussed, after that the results will be presented and discussed and at last recommendations for future work will be provided.

6.1 AIRFOIL SELECTION

In this section, the airfoil selection will be performed. First the selection criteria will be discussed. Than a first selection will be made and last one airfoil will be selected.

6.1.1 CRITERIA AND WEIGHTS

MAXIMUM LIFT COEFFICIENT ($C_{l_{max}}$)

The maximum lift coefficient of the airfoil greatly influences the maximum lift which can be achieved from the three dimensional wing. Therefore, a high $C_{l_{max}}$ is preferable, such that it allows for simple high lift devices, as complex high lift devices imply a higher structural weight and a higher cost. A relative weight of two has been given to this criterion.

THICKNESS RATIO (t/c)

The thickness ratio of the airfoil is an important shape parameter, which determines the space available in the wing to store things; for example, fuel and actuators. In this stage the full layout of the FBW system is not known yet. This can influence the needed storage space in the wing (due to actuators). Therefore, for now the actuators are assumed to be located inside the wing. Next to the storage space, a high thickness ratio is also preferable for structural reasons, as it increases the moment of area. A relative weight of three has been given to this criterion.

PITCHING MOMENT COEFFICIENT (C_m)

As a high value for C_m of the airfoil implies a high value for the pitching moment of the three dimensional wing, a low C_m is preferable. High values of C_m require higher trim forces and therefore trim drag. A relative weight of two has been given to this criterion.

CRUISE AND CLIMB DRAG COEFFICIENT ($C_{d_{cruise}}$ & $C_{d_{CL=1.2}}$)

Both cruise and higher lift conditions are important to a trainer aircraft. Therefore the drag coefficient in both cruise and a higher lift condition are considered (in this case $C_l = 1.2$). A relative weight of one has been assigned to the drag coefficient in cruise condition and 1.5 for the drag coefficient in higher lift conditions.

STALL BEHAVIOR

Assuming that even though flight envelope protection is available during flight, stall training has to be performed so the stall behavior of the aircraft is important. A sudden loss of lift is harder to recover from than a gradual loss of lift. Next to that, the consequences of overshoot of the stall protection part in the flight envelope protection will be less when a gradual loss of lift occurs. A relative weight of one has been assigned to this criterion.

6.1.2 FIRST SELECTION

The first selection of the airfoils is based on the design lift coefficient. The design lift coefficient can be calculated with Equation (6.1). A suitable airfoil follows when the value of C_l is equal to $C_{l_{design}}$. The factor 1.1 in front of the equation accounts for loss of lift due to trim and the difference between two and three dimensional wing.

$$C_{l_{design}} = 1.1\left(\frac{W}{S}\frac{2}{\rho V_{cruise}^2}\right) \tag{6.1}$$

Using the already determined values of $\frac{W}{S}$, ρ and V_{cruise}, a $C_{l_{design}}$ equal to 0.3931 can be found. Four airfoils have been selected with a $C_{l_{design}}$ around 0.4: NACA 3416, NACA 63-415, Eppler 540 and Eppler 545.

Table 6.1: Airfoil Trade-off matrix

Parameter [weight]	NACA 3416	NACA 63-415	Eppler 540	Eppler 545
$C_{l_{max}}$	0	-	-	-
t/c	0	-	+	+
C_m	0	-	+	0
$C_{d_{cruise}}$	0	+	+	0
$C_{d_{C_l=1.2}}$	0	-	-	-
Stall behaviour	0	-	-	-
Total	**0**	**-9.5**	**-0.5**	**-2.5**

6.1.3 Trade-off Matrix

The four selected airfoils have been analyzed using XFLR5, at a Reynolds number of around $3 \cdot 10^6$ and a machnumber of 0.15 (cruise condition). The lift, drag and pitching moment results of the four airfoils are presented in Appendix B. The results of the trade-off are presented in Table 6.1.

As can be concluded from Table 6.1, the airfoil selected for further analysis will be NACA 3416.

6.2 Aerodynamics Tool

In order to estimate the aerodynamic behavior of the aircraft, a model had to be created. The used method and the verification and validation of the model will be discussed in this section.

6.2.1 Method

In general the Class II method for estimating aerodynamic behavior from Roskam has been used.

Lift

The Class II method for estimating lift coefficients can be found in [56] Chapter 8. As these methods are published around 1985, more modern techniques can be substituted for some parts. For all steps which involve analysis for a two dimensional wing, XFLR5 has been used.

The first two characteristics of the three dimensional wing follow from the airfoil. These are the zero lift angle of attack and the angle of attack till which the curve is linear.

Next to that the slope of the curve in the linear part of the C_L range has to be calculated. This consists of the slope of the wing (including an interference correction with the fuselage) and the slope of the horizontal tail. These are combined into a slope for the whole aircraft with Equation (6.2) together with (semi-)empirical estimations for parameters as $\left(\frac{V_h}{V}\right)^2$ and $\frac{d\epsilon}{d\alpha}$.

$$\left(C_{L_\alpha}\right)_{aircraft} = \left(C_{L_\alpha}\right)_{wing-fuselage} + \left(C_{L_\alpha}\right)_{tail} \frac{S_h}{S} \left(\frac{V_h}{V}\right)^2 \left(1 - \frac{d\epsilon}{d\alpha}\right) \tag{6.2}$$

The stall angle has been found with the method proposed in section 8.1.3.4 of Roskam book VI [56]. This method needs the maximum lift coefficient of the two dimensional wing, evaluated at the Reyenolds number of both the root and the tip. Next to that the span wise lift distribution is needed. This can be obtained from the MATLAB program TORNADO [78]. This program has been adapted to output the lift distribution for multiple angles of attack. The maximum two dimensional lift coefficient has been assumed to be linear between root and tip. At at certain angle of attack, line will be tangent to the span wise distribution. At this angle of attack stall begins. Using numerical integration, the maximum lift coefficient has been found.

The changes of the lift coefficient due to high lift devices have been calculated by using the methods proposed by Roskam in Chapter 8. The program computes the needed flap deflection for the initially sized flaps, when flaps have to be increased, a warning will be shown to the user.

The code architecture for the lift prediction has can be found in Figure 6.1.

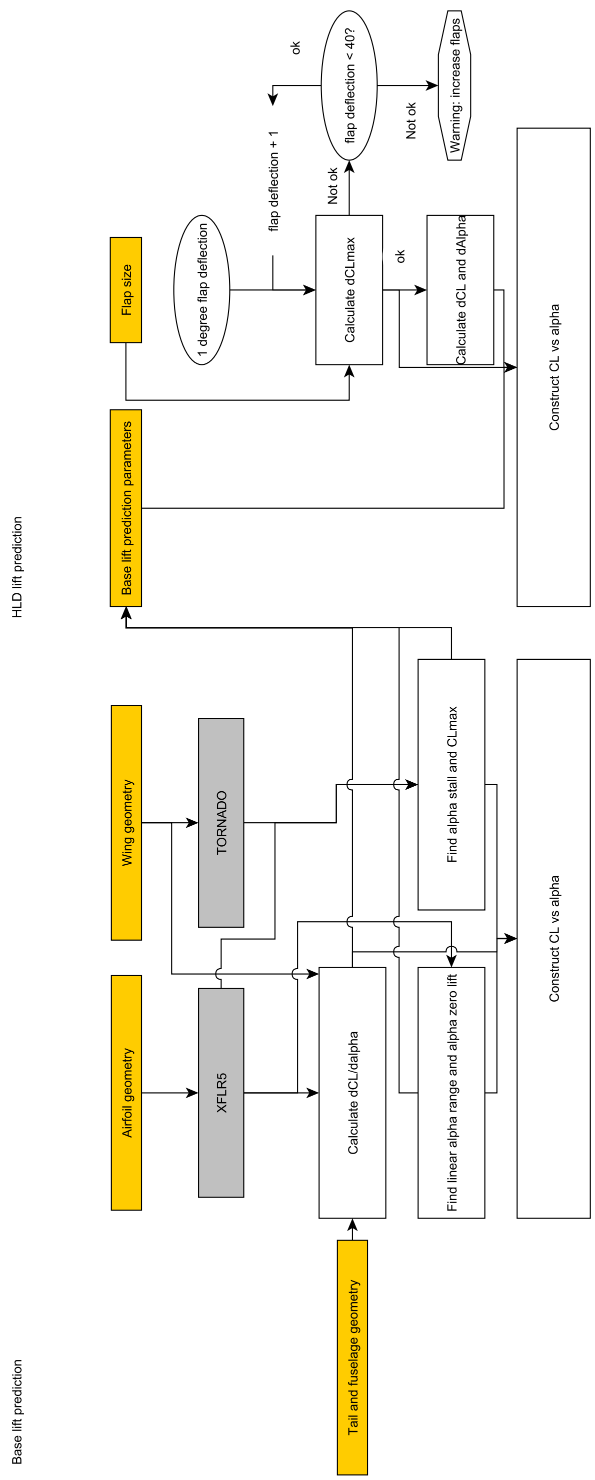

Figure 6.1: Lift prediction code architecture

DRAG

The drag coefficient estimation of Roskam consists of parasite drag induced drag. Due to problems with the methods used for induced drag, the drag has been estimated assuming a parabolic shape of the curve as seen in Equation (6.3).

$$C_D = C_{D_0} + \frac{C_L^2}{\pi A R e} \tag{6.3}$$

However, during verification, it turned out the Oswald efficiency was ridiculous and the method for estimating the Oswald efficiency has been replaced by the method explained in [79].

The value of C_{D_0} includes the contributions of the wing, fuselage, vertical/horizontal tail, windshield and landing gear. For take-off and landing condition, a correction has been added in order to contribute for the increased parasite drag due to flaps. A correction have been added to account for trim drag.

The code architecture for predicting drag can be found in Figure 6.2.

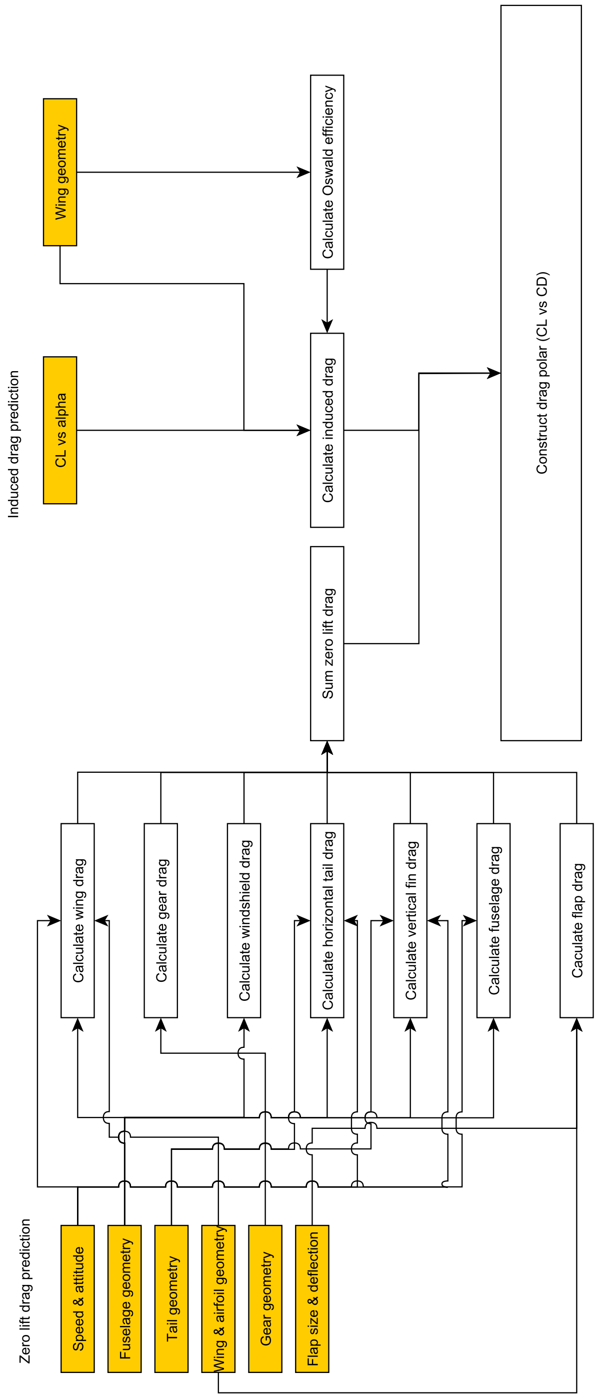

Figure 6.2: Drag prediction code architecture

PITCH MOMENT

The pitching moment calculations are limited to the zero lift pitching moment coefficient. This consists of the contribution of the wing and the contribution of the fuselage. The contribution of the wing has been estimated using the zero lift pitching moment of the two dimensional wing, found from XFLR5. The slope of the pitching moment follows from Equation (6.4).

$$\frac{dC_M}{dC_L} = \frac{x_{cg} - x_{ac}}{MAC} \tag{6.4}$$

Changes in zero lift pitching moment, of the airfoil are found using statistical data from Roskam. This has been turned into a three dimensional wing using the same method as before, except adding the difference in two dimensional pitching moment.

The code architecture for the pitching moment can be found in Figure 6.3.

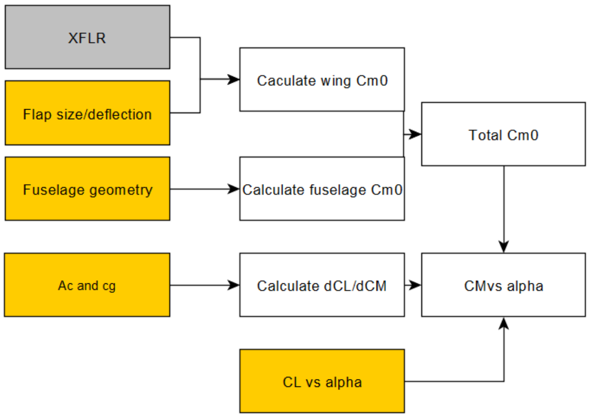

Figure 6.3: Pitch prediction code architecture

6.2.2 Verification & Validation

Verification

Verification has been done continuously during programming of the tool. This was necessary in order to check the digitization of all the figures with empirical data. Verification mainly has been done on checking whether the code produces the same results as when it will be done by hand. This gave no errors until the induced drag has been checked.

The induced drag did not seem to give a proper fit. Due to time constraints, the methods for calculating all the different contributions of the drag have been removed and a quadratic relation with the aircraft's lift has been assumed. A new problem was introduced by this adjustment: Roskam's method estimated a Oswald efficiency bigger than 1. This is not possible, therefore another method has been implemented which has been described in [79].

Validation

Validation has been performed by analyzing the data of the Cessna 172. Not all the aerodynamic characteristics of the Cessna 172 are known, but some can actually be compared to the code. The parameters which are compared are the parasite drag coefficient ($C_{D,0}$), Oswald efficiency (e) and flap deflection needed for landing conditions (δ_f). The results of the validation are summarized in Table 6.2.

Table 6.2: Validation parameters/data

Parameter	Data	Code output	Difference
e	0.75	0.8045	7.30%
$C_{D,0}$	0.0319	0.0305	4.60%
δ_f [deg]	40	43	7.50%

From this table it seems that the code slightly underestimates the drag coefficients. This discrepancies probably introduced due to the use of (semi-)empirical methods, which are unlikely to have a perfect fit with reality.

As lift to drag ratios from this analysis tool will be used in further analysis and in iterations of the design sequence, one should be careful while verifying requirements; for example, when range requirements are "just verified" an the lift to drag ratio is lower in reality, the requirement changes into "not verified".

6.2.3 Sensitivity

In order to get a view on how the aerodynamics of the aircraft can be optimized, a sensitivity analysis has to be performed. Due to time constraints, this will be limited to the drag coefficient of aircraft. Assuming the fuselage

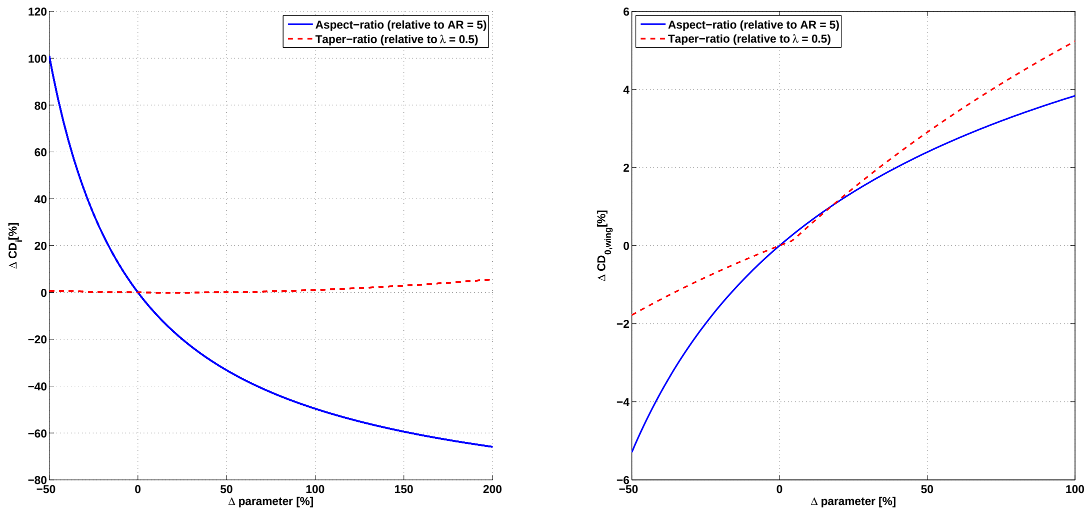

(a) Sensitivity of induced drag

(b) Sensitivity of parasite drag

Figure 6.4: Drag coefficient sensitivity

geometry is fixed, the effect of changing the wing plan-form is analyzed. This is done by varying the taper and aspect ratio of the wing. Next to that, the influence of weight on dimensional drag will be discussed.
From Figure 6.4a can be found that the induced drag is very sensitive when changing aspect-ratio and relatively insensitive when changing taper-ratio.
From Figure 6.4b can be found that the parasite drag is equally sensitive when changing taper and aspect ratio. However, the relative changes in parasite drag are still quite insensitive when compared with the changes in induced drag form the aspect ratio.

Next to this, a simple analysis of the influence of the weight on the (dimensional) drag can be analyzed.

$$D = 0.5\rho V^2 S C_D = 0.5\rho V^2 C_D \left(\frac{W}{S}\right)^{-1} W \tag{6.5}$$

From Equation (6.5) can be found that drag increases linearly with weight, assuming that the drag coefficient, velocity, density and the design point stay the same.

6.3 Results

The results of both lift an drag will be discussed in this section. The results are analyzed using the mechanical back-up configuration.

6.3.1 Lift

The lift coefficient results have been plotted in Figure 6.5.

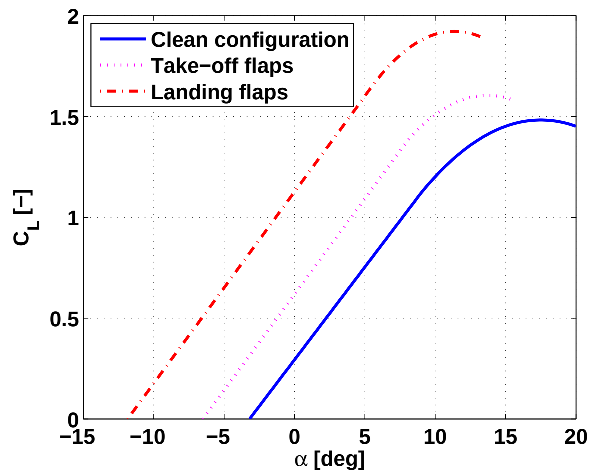

Figure 6.5: C_L vs α

Clean, take-off and landing conditions are considered. As can be seen, the maximum lift coefficient, needed in landing condition has been reached. This has been accomplished by using a simple flap, covering the wingspan from 10 to 71% and covering the wing chord from 75% to the trailing edge.

The flap deflections needed for take-off lift and landing lift are respectively 7 and 27 degrees. This is rather low for a simple flap. As usually, the landing flap deflection of a simple flap is about 40 degrees.

6.3.2 Drag

The results of the drag analysis are presented in Figure 6.6.

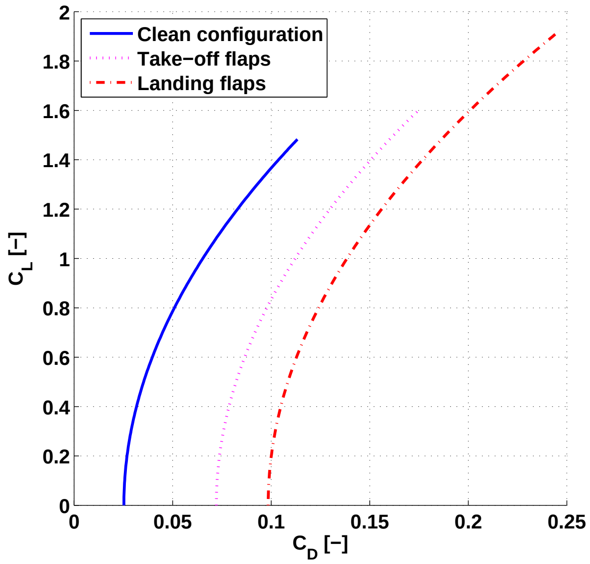

Figure 6.6: C_L vs C_D

As can be seen, the drag increases with lift (induced drag). The drag also increases heavily due to flap deflection. However, the difference between landing and take-off configuration is not as big as between clean and take-off configuration, although the flap deflection increases more between take-off and landing configuration. This is due to the altitude and speed difference between clean (cruise) and the landing and take-off.

6.3.3 Pitching Moment

The results for the pitching moment can be found in Figure 6.7.

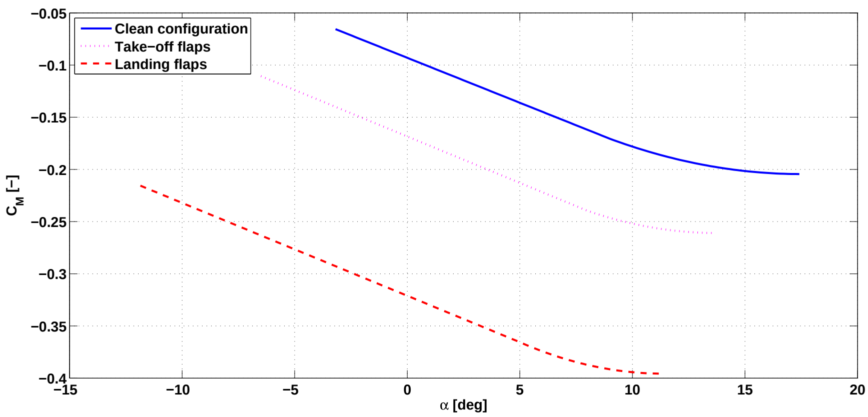

Figure 6.7: C_M vs α

As can be seen, the pitching moment is highly influenced by flap deflection. In Chapter 7, these results are further used in trim calculations and elevator sizing.

6.3.4 Recommendations

As the flap deflections turned out to be a little low, it is recommended to resize the flaps (make them smaller along the wingspan). This will also give more space for the ailerons.

For further optimization, a custom airfoil can be designed, in order to minimize the drag of the aircraft.

As the Roskam method is mainly based on statistics, a more refined method should be used in further design stages. Computational fluid dynamics software can be used to get a more realistic estimation of the aerodynamic characteristics of the aircraft.

The influence of the fuselage geometry on the drag coefficient should be analyzed. After that, the fuselage shape should be optimized for minimum drag.

7
Stability and Control

In this chapter, the stability and control of the aircraft is analyzed. First the horizontal and vertical tails are sized according to methods from Roskam. Next the dynamic stability is analyzed using the program CEASIOM, which presents results on the five different eigenmodes. Finally the hinge moments on the control surfaces are determined, which includes the performance of these surfaces.

7.1 Static Stability

This section will focus on the static stability of the aircraft. First of all, a design choice is presented between inherently and de-facto stable. Next the horizontal and vertical tail are sized, along with the control surfaces.

7.1.1 Inherently Stable vs. De-Facto Stable

The first decision that needs to be made while analyzing the stability and control of the aircraft, is whether the aircraft is inherently stable or de-facto stable. For an aircraft to be inherently stable, it should not rely on a feedback augmentation system for their stability. De-facto stability is when the aircraft is only stable with a feedback augmentation system [53]. With the FBW system incorporated in this design, de-facto stability is something that could be achieved. However, it was chosen that in this preliminary design the aircraft needs to be inherently stable. In more detailed design, options could be explored where de-facto stability is an option. This will lead to smaller tail sizes and thus leading to weight and drag reductions.

7.1.2 Horizontal Tail Sizing

The horizontal tail surface has been sized in order to comply with a certain static stability margin. Roskam [53] states that this should be 0.1 for single engine propeller driven aircraft. However with the FBW system in the aircraft, this stability margin could be decreased. Using a mechanical back-up system, it was chosen to select a stability margin of 0.1. For the full FBW system the stability margin is chosen to be less, which results in lower surface area. The stability margin is further defined using Equation (7.1).

$$SM = \overline{x_{ac}} - \overline{x_{cg}} \tag{7.1}$$

To size the horizontal tail, the location of the center of gravity and aerodynamic center are plotted against the tail size in a so-called x-plot, as shown in Figure 7.1. This x-plot shows how the locations vary with the surface area of the horizontal tail, and allow for a quick selection of a stability margin. Table 7.1 shows the results from the horizontal tail sizing, where the aspect ratio was fixed at the start. In order to increase aerodynamic performance, the aspect ratio has to be as high as possible. This optimization is based on reference aircraft only.

Further investigation can be done on th influence of the AR on the aerodynamics, this was outside of the scope.

Table 7.1: Results of the horizontal tail sizing

Dimension	Value	Unit
η_{e_i}	0.1	[-]
η_{e_o}	0.9	[-]
Λ_{c4}	0.175	[rad]
λ_h	0.5	[-]
AR	4.3	[-]
b_e	2.31	[m]
b_h	2.90	[m]
c_e	0.24	[m]
c_h	0.67	[m]
S_e	0.63	[m^2]
S_h	1.96	[m^2]

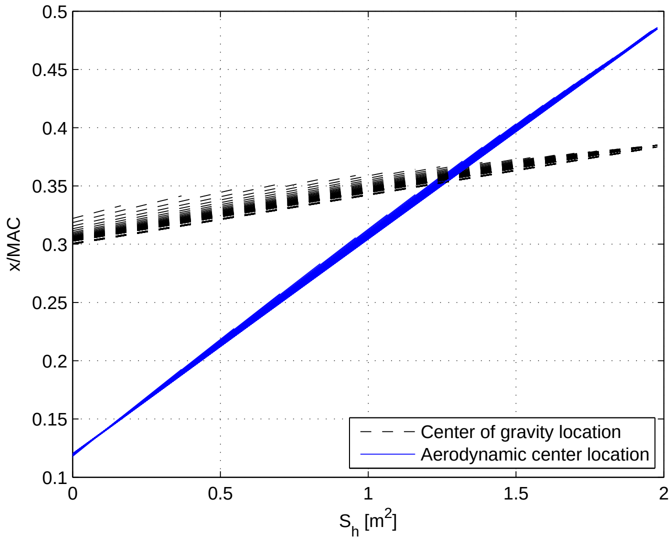

Figure 7.1: The x-plot used in sizing the horizontal tail

Trim Angle Horizontal Tail

For this preliminary design of the aircraft it is decided to have the lowest possible (negative) trim angle, while satisfying the requirements for the most critical flight situations. The most critical flying situation for elevators is landing as at this condition you have the highest flap angle, which induces the highest hinge-moment to be counteracted. Nevertheless, there is a limit on the max./min deflection angle in order to avoid a tail stall. The negative(up) limit is defined at -20 deg, the positive(down) limit is defined at 25 deg.[6] In the further calculations, the trim angle of the horizontal stabilizer i_h is be determined applying longitudinal moment equilibrium. Firstly, the required Tail C_{L_h} and Wing Lift Coefficient C_{L_w} are computed with the equations for vertical equilibrium and for moment equilibrium in Matrixform 7.2. η_h is estimated from Roskam.

$$\begin{bmatrix} \frac{x_{cg}-x_{ac}}{c_w} & \frac{S_h}{S_w}\eta_h\frac{x_{cg}-x_{ac}}{c_w} \\ 1 & \frac{S_h}{S_w}\eta_h \end{bmatrix}\begin{bmatrix} C_{L_w} \\ C_{L_h} \end{bmatrix} = \begin{bmatrix} -C_{m_{ac}} \\ \frac{MTOW}{\frac{1}{2}\rho V^2} \end{bmatrix} \tag{7.2}$$

The incidence angle for longitudinal trim at cruise($\delta_{e,cruise} = 0$ rad) is computed with Equation (7.3).

$$i_h = C_{L,h}/C_{L,h_\alpha} - \alpha_h = -4.4\text{deg} \tag{7.3}$$

The Lift coeffient derative with angle-of attack of the horizontal tail C_{L,h_α} is estimated from Roskam methods. [56]

Acceptable Elevator Deflection Range

Now it has to be made sure, that in the most critical flight condition, the elevator deflection lies inside the acceptable elevator deflection range.

From [80], it is know that the most critical condition is the landing configuration right above stall speed with fully extended flaps.

From the first line of the Matrix equation, assuming a wing lift coefficient of $C_{L_w} = 1.3$, the required horizontal tail lift coefficient C_{L_h} for equilibrium is determined. Now the elevator deflection is computed with

$$\delta_e = \frac{C_{L_h} - C_{L_{h_\alpha}}(\alpha_h + i_h)}{C_{L_{h_{\delta_e}}}} \tag{7.4}$$

,where the derivatives $C_{L_{h_{\delta_e}}}$ and $C_{L_{h_\alpha}}$ are estimated with Roskams Method [56].

Trimming for cruise implies an elevator deflection outside the elevator range; therefore, in the landing configuration, the stabilizer incidence angle has to be increased more negatively, resulting in a corrected Tail incidence angle of $i_h = -5.5$ deg. Comparing this incidence angle seems with reference aircraft this angle seems to be relatively high. For the future work, it is therefore recommended to perform an alternative analysis of the lift surfaces with a CFD method in order to evaluate the reliability of the results.

7.1.3 Vertical Tail Sizing

The vertical tail has been sized using a requirement for the lateral stability derivative C_{n_β}, taken from Roskam and equal to 0.0573 rad^{-1}. First the contribution of the fuselage to C_{n_β} is calculated using Equation (7.5). Next the contribution of a vertical tail is added using Equation (7.6) and this relation is used to plot the surface of the vertical tail versus C_{n_β}. Using the requirement for C_{n_β} from Roskam, a vertical tail surface can be acquired. Of course when using a FBW system, this requirement can relaxed and the C_{n_β} could be decreased in order to get smaller tail sizes.

$$C_{n_{\beta_f}} = -K_n K_{R_1} (\frac{S_{B_S} l_f}{Sb}) \tag{7.5}$$

$$C_{n_\beta} = C_{n_{\beta_f}} + C_{L_{\alpha_V}} \left(\frac{S_V x_v}{Sb} \right) \tag{7.6}$$

Using this procedure, several iterations were done in order to get a final result. Figure 7.2 shows the resulting plot for the sizing of the vertical tail. As can be seen, the iterations do not really change the result significantly as the input from Class I results is already fairly accurate. Table 7.2 shows the results of the vertical tail sizing and include all of the relevant dimensions of the vertical tail.

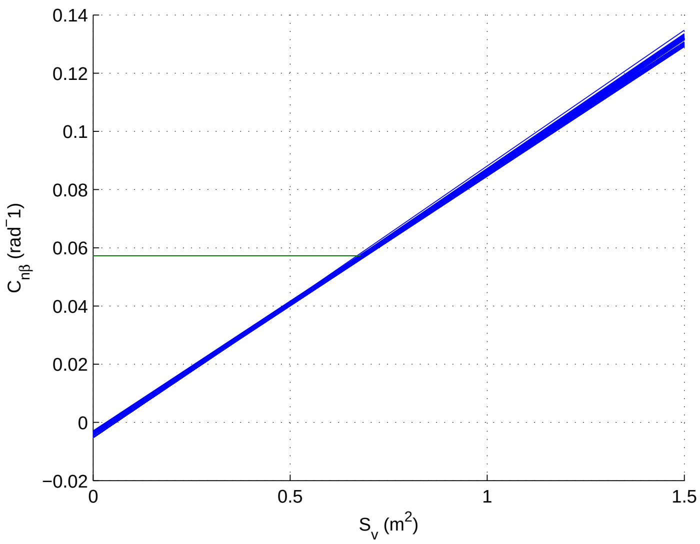

Figure 7.2: Lateral x-plot for sizing the vertical tail

Table 7.2: Results of the vertical tail sizing

Dimension	Value	Unit
η_{rudder_i}	0	[-]
η_{rudder_o}	1	[-]
Λ_{c4}	0.4	[rad]
λ_v	0.5	[-]
AR	2	[-]
b_r	1.17	[m]
b_v	1.17	[m]
c_r	0.19	[m]
c_v	0.58	[m]
S_r	0.27	$[m^2]$
S_v	0.68	$[m^2]$

RUDDER DESIGN REQUIREMENTS

FAR-P23-section 233: aircraft muse be able to carry out 90 degrees crosswinds landing up to a wind velocity of 25 knots.[6]
MFT-PROJECT-06:The aircraft shall have a minimum demonstrated crosswind of 15 kts.

CROSSWIND LANDING

The most critical speed is the max. allowable crosswind $V_{cross} = 25\text{kts} = 12.86\text{m/s}$ at minimum flight speed ($1.1 V_{stall} = 23.837\text{m/s}$) (see Fig Figure 7.3). Now it has to be made sure, that in this flight condition, the rudder deflection lies inside the elevator deflection range in order to avoid stall. From reference literature it is assumed a rudder deflection range of $-25\,\text{deg} < \delta_r < 25\,\text{deg}$. [6]

CROSSWIND CALCULATIONS

This equation is used to determine the side force on the aircraft.

$$F_w = \frac{1}{2}\rho V_{cross}^2 S_S C_{D_y} = \frac{1}{2}\rho V_{cross}^2 S_S C_{D_y} = 344.4N \tag{7.7}$$

Table 7.3: Input for crosswind calculations

Variable	Value	Unit
V_{cross}	12.86	[m s^{-1}]
V_{stall}	21.67	[m s^{-1}]
$V_{approach}$	23.84	[m s^{-1}]
S_S	5	[m^2]
C_{D_y}	0.65	[-]
d_c	0	[m]
C_{n_0}	0	[-]
C_{y_0}	0	[-]
C_{n_β}	0.057	[-]
$C_{n_{\delta_r}}$	-0.21	[-]
C_{y_β}	-0.3	[-]
$C_{y_{\delta_r}}$	0.187	[-]

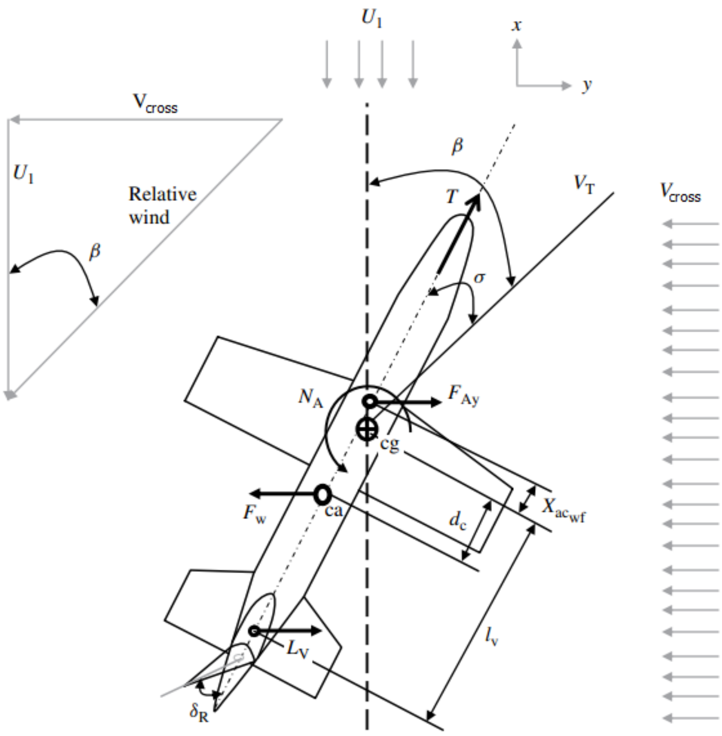

Figure 7.3: Drawing corresponding to the crosswind calculations[6]

Now the corresponding sideslip-angle β is determined.

$$\beta = \tan^{-1}\left(\frac{V_{cross}}{V_{approach}}\right) = 0.4947 rad \approx 28.34\,\text{deg} \tag{7.8}$$

Now, assuming $C_{D_y} = 0.65$ and assuming the center of side area lying at the same distance from the nose as the center of gravity, this results in two equations with two unknowns, the rudder deflection δ_r and the crab angle σ :

$$\frac{1}{2}\rho V_T^2 Sb(C_{n_0} + C_{n_\beta}(\beta - \sigma) + C_{n_{\delta_r}}\delta_r) = 0 \tag{7.9}$$

$$\frac{1}{2}\rho V_{cross}^2 S_S C_{D_y} = \frac{1}{2}\rho V_T^2 S(C_{y_0} + C_{y_\beta}(\beta - \sigma) + C_{y_{\delta_r}}\delta_r) \tag{7.10}$$

Solving these equations a crab angle and a rudder deflection angle is obtained. As the rudder deflection lies far below the maximum, it is approved that the aircraft is designed such that it is able to land with the crosswind specified in the regulations.

7.2 Aileron Sizing

For designing the aileron, four parameters need to be determined. The aileron platform area S_a, the aileron chord c_a, the maximal aileron inward and outward position η_{i_e} and η_{o_e}. The maximum up and down aileron deflections are taken from[6]. Following the recommendations to size first the flaps and then the elevator[6], the location of inner edge of the aileron along the wing span (η_{i_a}, η_{o_a}) is limited by the flap design up to 70 percent of the wingspan. The final design is affected by the required hinge moment, the aileron effectiveness, aerodynamic and mass balancing, flap geometry, aircraft structure, and cost.

Table 7.4: Main Wing Parameters

Parameter	Value	Unit
b	10.69	$[m]$
η_{i_a}	0.72	[-]
η_{o_a}	1	[-]
c_a	0.21	[m]
c_w	1.07	[m]
S_a	0.6735	[m^2]

A chord length of 20 percent of the wing chord was utilized based on reference aircraft.

7.2.1 Requirements on Roll Rate

From FAR 23.157 there is the requirement, that the aircraft should be able to reach a bank angle of 60 deg in 4 sec. Furthermore from [6] it is desired that a bank angle of 45 deg can be reached in 2.5 sec for Level 2 Pilot comfort. The recommended max deflection lies usually at +- 25 deg, as at higher deflections usually flow separation occurs.[6]

7.2.2 Roll Rate: Calculations

The Aileron roll control derivative is estimated with the following equation.[6]

$$C_{l_{\delta_\alpha}} = \frac{2C_{L_{\alpha_W}}\tau C_r}{SB}\left[\frac{y^2}{2}+\frac{2}{3}\left(\frac{\lambda-1}{b}\right)y^3\right]_{y_i}^{y_o} \tag{7.11}$$

$$t_{ss} = \sqrt{\frac{2\phi_1}{\dot{P}}} \tag{7.12}$$

With this the aileron lift a the induced moment can be determined. Now the steady state roll rate and the bank angle, at which this is achieved, are determined. From this, the roll rate acceleration is calculated, which is used in Crefeq:tss to calculate the time to reach the required bank angle.

$$P_{ss} = \sqrt{\frac{2L_A}{\rho(S_w+S_h+S_v)C_{D_R}y_D^3}} \tag{7.13}$$

$$\dot{P} = \frac{P_{ss}}{2\phi_1} \tag{7.14}$$

A settling time of 2 seconds is needed with which a Level 2 pilot comfort is achieved, which is suitable for this application.

7.3 Hinge Moments

In order to size the actuators the hinge moments are required. Using the following two equations for the horizontal tail as an example, the hinge moments for the rudder (Figure 7.9, Figure 7.10), aileron (Figure 7.7,Figure 7.8) and elevator (Figure 7.5, Figure 7.6) are estimated. Eq. 7.15 calculates the control surface hinge coefficient, with the hinge moment using the hinge moment derivatives C_{h_α}, $C_{h_{\delta_e}}$ and the zero angle of attack hinge moment as an input. These values are computed and validated with the methods and data of reference aircraft provided in Roskam's Method [56], which were digitized with MATLAB. The program schematic is presented in Figure 7.4.

$$C_h = C_{h0} + C_{h_\alpha}\alpha_h + C_{h_\delta}\delta \tag{7.15}$$

$$HM = C_h\bar{q}S_c c_c \tag{7.16}$$

7.3.1 Elevator

The elevator hinge moment shows a linear behavior with respect to deflection angle. Furthermore you can see in Figure 7.5, that at $\alpha = 0$ deg the $\delta_e = 0$ corresponds to $Mh = 0$ Nm, as one would expect. With increasing angle of attack α, a negative (upwards) deflection δ_e is needed in order to have $Mh = 0$ Nm. When the control surface area is increased, the absolute value of the hinge moment increases linearly and a steeper hinge moment line appears.

Figure 7.4: Schematic of hinge moment calculation procedure using Roskam

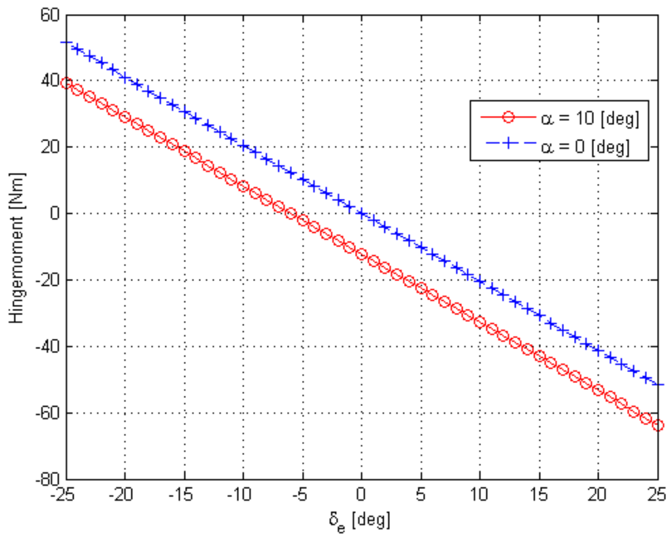

Figure 7.5: Variation of hinge moment for the elevator with angle of attack, with $c_e = 0.4 * c_h$ and hinge line at $0.2 * c_e$

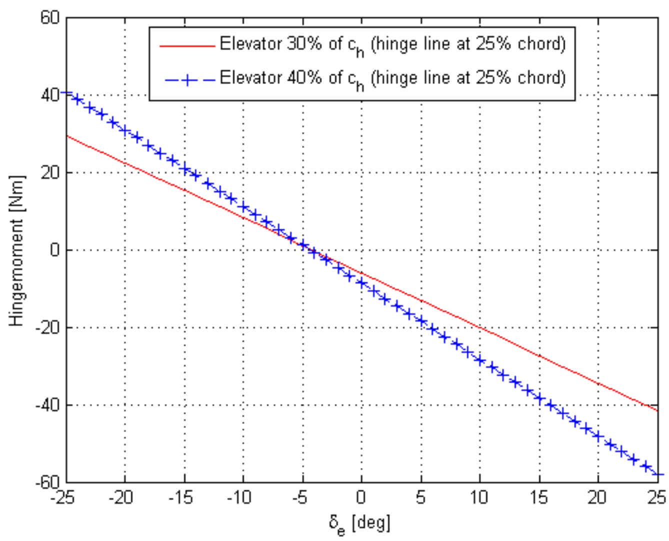

Figure 7.6: Variation of hinge moment for the elevator with elevator chord, hinge line at $0.25 * c_e$ and $\alpha = 10$ deg

7.3.2 AILERON

When the angle of attack $\alpha = 0$ deg, the hinge moment is $Mh = 0$ at a deflection of $\delta_a = 0$ deg and increases linearly with a negative slope. Now when the angle of attack α is increased, the curve shifts to the left and a negative(upwards) deflection of the aileron is needed in order to have $Mh = 0$ Nm, as expected. Now, when the area of the aileron is increased, the (negative) slope is increased, as the hinge moments Mh increase.

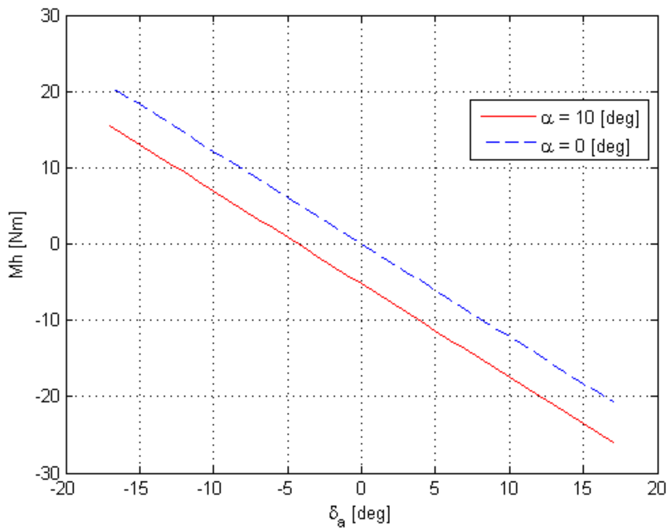

Figure 7.7: Variation of hinge moment for one aileron with angle of attack, with hinge line at $0.3 * c_a$ and $c_a = 0.2 * c_w$

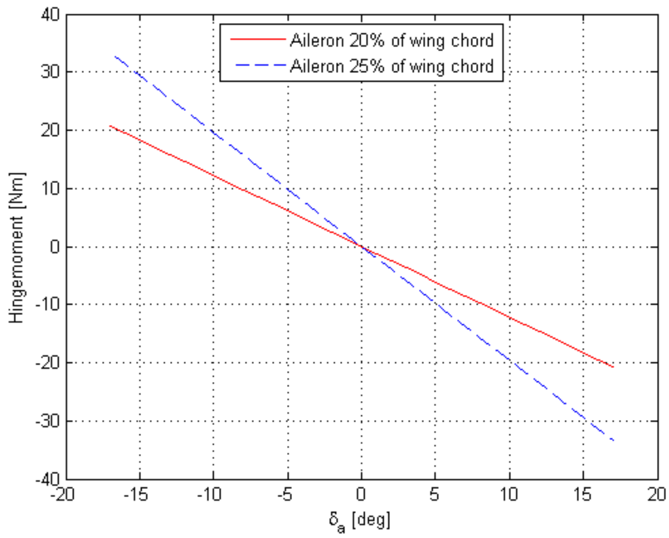

Figure 7.8: Variation of hinge moment for one aileron with aileron size, with hingeline at $0.3 * c_a$ and $\alpha = 0$ deg

7.3.3 RUDDER

The rudder hinge moment shows also a negative slope and a leftwards shift of the curve with increased angle of sideslip β. Again, increasing the control area yields a steeper(more negative) slope, as the hinge moments Mh increase for a certain rudder deflection δ_r.

7.3.4 RECOMMENDATIONS

From [81], there is the rule of thumb, that the relation between the control forces for aileron to elevator to rudder, should be approximately 1 to 2 to 6, respectively. Nevertheless, a relation of 1:10:0.1 was determined with this design, as the rudder Hinge moments are relatively low. Furthermore, the incidence angle appears to be higher than the reference aircraft of similar configuration. It is therefore recommended to recalculate the derivatives using other design books or even CFD methods, if possible.

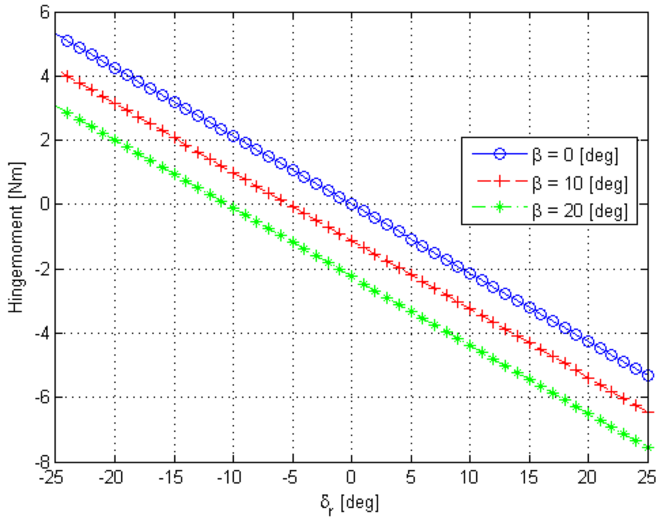

Figure 7.9: Variation of Hinge moment for the rudder with sideslip angle, with hinge line at $0.1 * c_v$ and rudder chord $c_r = 0.4 * c_v$

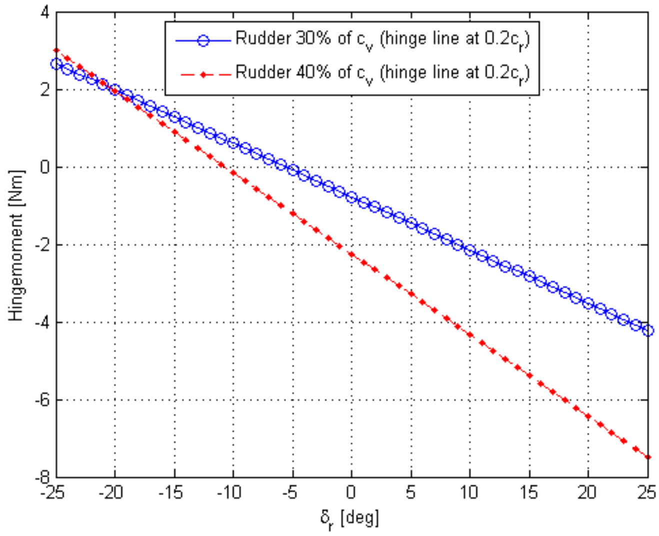

Figure 7.10: Variation of Hinge moment for the rudder with control surface size, with hinge line at $0.2 * c_r$ and $\beta = 20$ deg

7.4 Dynamic Stability

For analyzing the dynamic stability of the aircraft, use has been made of the program CEASIOM. In this program, the aircraft can be fully modeled. This includes the dimensions of the structure, but also the center of gravity locations including payload and fuel. Using this information, the program analyzes the response of the aircraft during the different eigenmodes. Both longitudinal (phugoid and short period) and the lateral (Dutch roll, roll and spiral) eigenmodes will be analyzed using this program.

The eigenmodes will be analyzed at cruise speed at different altitudes ranging from 0 to 2500 m. For each eigenmode there is a figure about the stability of the motion, a table containing some characteristics and finally some response plots. As the CS-23 requirements do not provide specific requirements on the frequency and damping characteristics, the military requirements will be taken as a guideline. There are three different levels for these requirements, expressing the handling quality of the aircraft [57]:

- Level 1: Flying qualities which are clearly adequate for any given mission phase
- Level 2: Flying qualities which are adequate to complete the mission flight phase but some increase in pilot workload or degradation in mission effectiveness, or both, exists.
- Level 3: Flying qualities such that the aircraft can be controlled safely, but pilot workload is excessive or mission effectiveness is inadequate, or both. However, the aircraft can be safely landed.

Of course the goal is to reach Level 1 flying qualities, however it is not a big problem to be below that due to the available FBW system. Furthermore there are different categories of aircraft, where single engine propeller aircraft fall under Class I aircraft.

7.4.1 PHUGOID

Looking at Figure 7.11, the stability of the phugoid can be seen to be below satisfactory. It is in the acceptable region, but that is usually only for emergency conditions. Table 7.5 shows the characteristics for the phugoid at cruise speed at 2500 m. The reason that the phugoid is not in the satisfactory region is the damping coefficient, as the military regulations state that it should be at least 0.04.

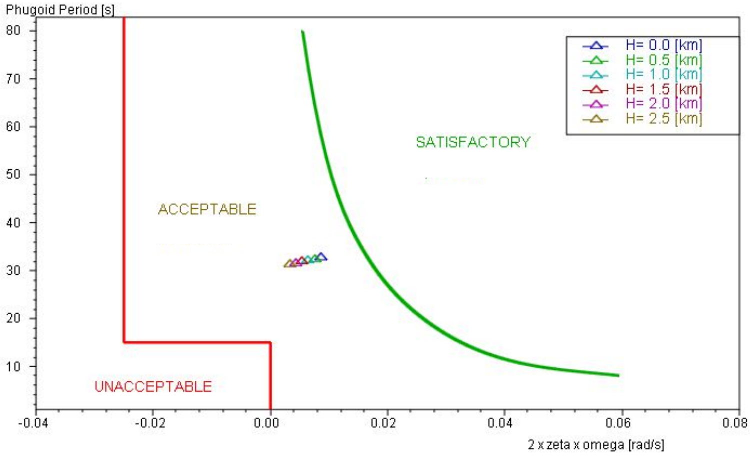

Figure 7.11: Phugoid analysis

Table 7.5: Phugoid characteristics at cruise speed at 2500 m.

Phugoid		
Eigenvalue	$-0.0019 \pm j \cdot 0.1920$	[-]
Undamped natural frequency	0.1920	[rad/s]
Damping ratio	0.0099	[-]
Period	32.7	[s]
Time to half amplitude	363.8	[s]

7.4.2 SHORT PERIOD

The short period analysis is shown in Figure 7.12, where at all of the altitudes the short period falls in the satisfactory region. The most important contributor to the short period is the derivative C_{m_α}, so it was important to get the center of gravity model right in CEASIOM. Also the damping ratio is most dependent on the derivative C_{m_q}, the pitching moment due to pitch rate which is largely influenced by the horizontal tail. Table 7.6 show the values of these derivatives of the aircraft from CEASIOM compared to the Cessna 172 derivatives [82].

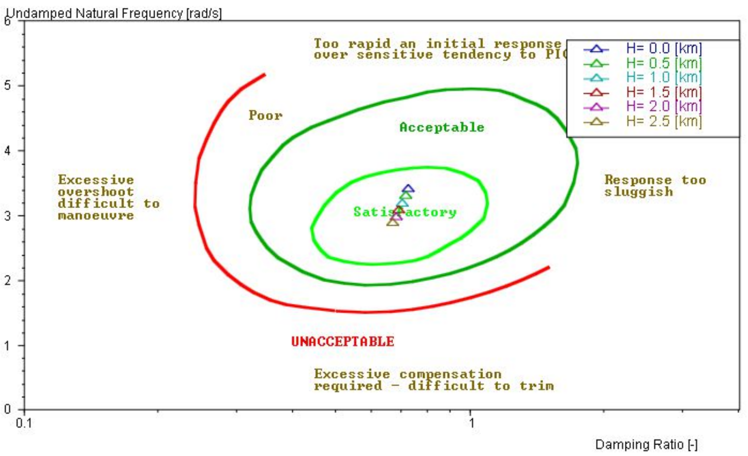

Figure 7.12: Short period analysis

Table 7.7 show the results from CEASIOM regarding the short period characteristics. The military requirements state that the damping ratio should be between 0.3 and 2 and that the undamped natural frequency should be between 0.9 and 6 for a load case similar to the cruise phase. Both of these requirement are clearly met, underlining the results shown in Figure 7.12.

Table 7.6: Short period derivatives at cruise speed at 2500 m.

Derivative	Value [-]	Cessna 172
C_{m_α}	-0.66	-0.89
C_{m_q}	-13.63	-6.2

Table 7.7: Short period characteristics at cruise speed at 2500 m.

Short period		
Eigenvalue	$-1.9836 \pm j \cdot 1.9264$	[-]
Undamped natural frequency	2.7651	[rad/s]
Damping ratio	0.7174	[-]
Period	3.2617	[s]
Time to half amplitude	0.3494	[s]

7.4.3 DUTCH ROLL

The Dutch roll requirements are taken from military requirements again, but there is also a requirement from CS23 on this. It was mentioned in the Baseline report as requirement MFT-CS23-FP-29. It stated: 'Any combined lateral-directional oscillations (occurring between the stalling speed and the maximum allowable speed appropriate to the configuration)("Dutch-roll") shall be damped to 1/10 amplitude in 7 periods with the primary controls free and in a fixed position (except when compliance with CS 23.672 is shown).'

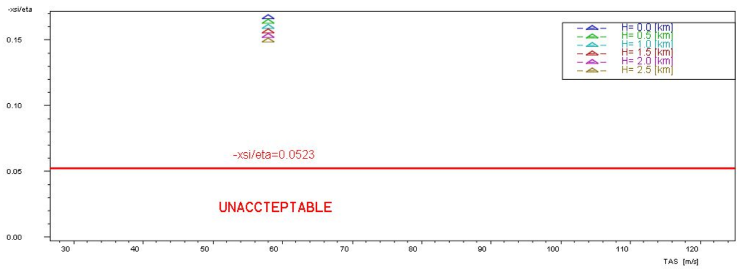

Figure 7.13: Dutch roll analysis

The results from CEASIOM in Figure 7.13 show that the Dutch roll characteristics easily meet the Level 1 requirements. The military requirements state that the damping ratio for the Dutch roll should be at least 0.08 and the undamped natural frequency at least 0.4. Looking at Table 7.8 both of these are met giving the aircraft Level 1 flying qualities for the Dutch roll. Also the requirement MFT-CS23-FP-29 is met, looking at the period and time to half amplitude. To get to 1/10 amplitude about 3.5 times the time to half amplitude is needed. This means that within three periods the Dutch roll has damped to 1/10 amplitude, well below the required seven periods.

Table 7.8: Dutch roll at cruise speed at 2500 m.

Dutch roll		
Eigenvalue	$-0.2058 \pm j \cdot 1.4152$	[-]
Undamped natural frequency	1.4301	[rad/s]
Damping ratio	0.1439	[-]
Period	4.4399	[s]
Time to half amplitude	3.3676	[s]

7.4.4 ROLL

Next the roll-mode characteristics were analyzed, the results from CEASIOM are presented in Figure 7.14. These results are not the most favorable, as the handling quality is not very good. They are analyzed using a subjective rating method, the Cooper-Harper Pilot assessment rating, but the most important conclusion from this graph is that the achievable roll acceleration is around 45 deg/s. This will increase the workload greatly because the pilot will need to closely monitor this during all turns, but can of course be reduced using the FBW system. Table 7.9 shows the roll-mode characteristics, where the first conclusion is quickly made that this is not an oscillatory eigenmode due to the real eigenvalue.

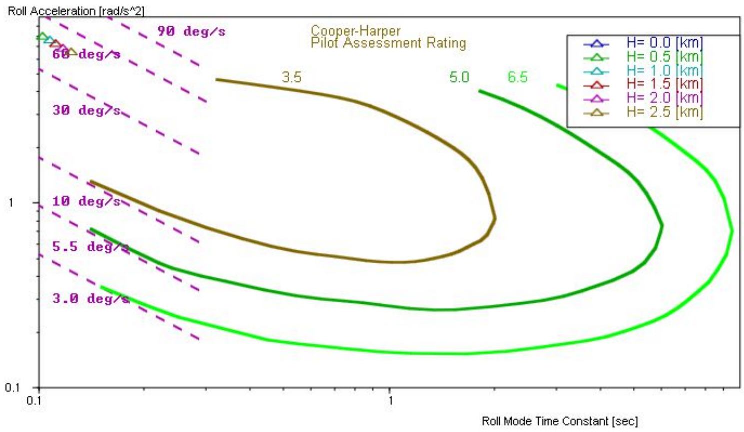

Figure 7.14: Roll analysis

Table 7.9: Roll at cruise speed at 2500 m.

Roll		
Eigenvalue	$-8.5581 \pm j \cdot 0$	[-]
Undamped natural frequency	8.5581	[rad/s]
Damping ratio	1.00	[-]
Period	0	[s]
Time to half amplitude	0.0810	[s]

7.4.5 Spiral

The last eigenmode to be analyzed is the spiral and the results are presented in Figure 7.15. This eigenmode is also very stable and clearly provides Level 1 flying qualities. To achieve this, the military requirements state that the time to double amplitude is to be at least 20 seconds. Table 7.10 shows the spiral characteristics of the aircraft and the time to double amplitude clearly meets the requirements.

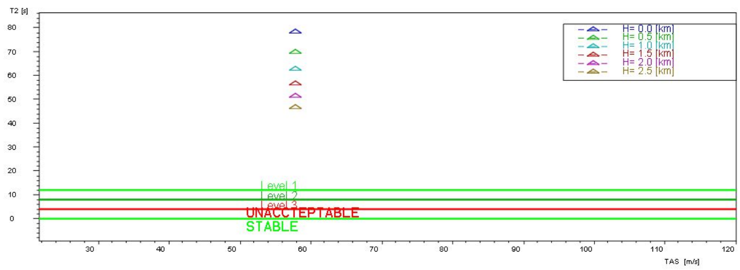

Figure 7.15: Spiral analysis

Table 7.10: Spiral characteristics at cruise speed at 2500 m.

Spiral		
Eigenvalue	$0.0130 \pm i \cdot 0$	[-]
Undamped natural frequency	0.0130	[rad/s]
Damping ratio	-1.00	[-]
Period	0	[s]
Time to double amplitude	53.1862	[s]

8
FLY-BY-WIRE

This chapter will first describe the Fly-By-Wire (FBW) layout. Furthermore the Flight Envelope Protection (FEP) and the Autoland will be discussed. At the end of this chapter the actuators is discussed.

8.1 FLY-BY-WIRE LAYOUT

One of the main features of the trainer aircraft is the FBW system. The main reason to use FBW is to have an easier integration of Flight Envelope Protection (FEP). For the trainer aircraft, several options for the FBW have been considered. First of all, the most safe option in terms of certification risk, is FBW with a mechanical back-up. The other two options considered are aircraft with full FBW. One of those options considers graceful degradation, which will be discussed in detail later. One option that will not be discussed in this chapter is the FBW with a partial mechanical back-up. This has been done in Airbus, where the trim and rudder pedals are mechanically backed up [83]. It is however rather difficult to fly with only partial control and therefore this is considered to be unsuitable for a trainer aircraft.

8.1.1 FBW WITH MECHANICAL BACK-UP

One of the safest options in terms of development risk is the FBW with a mechanical back-up. With this option, the pilot can fly with FBW but when it fails the FBW can be disengaged and the aircraft can be flown with a conventional mechanical system.

The advantage of a mechanical back-up system is that it would be easier to certify than a full FBW system. According to the ARP4761 [1], all failure that could lead to a catastrophic consequence should have a maximum probability of occurrence of 10^{-9} per flight hour. With a mechanical (back-up) system, the FBW could be designed using limited authority. A limited authority system is only allowed to apply a limited control surface deflection on top of the mechanical output. The other option is a full authority system. A full authority system is allowed to apply the full range of control surface deflections. Having a limited authority system is easier to certify than a full authority, because the pilot can still overrule the FBW. If chosen for full authority FBW with mechanical back-up, a certain clutch has to be designed to disconnect the FBW in case of failure.

Furthermore, with a mechanical system a FBW system without redundancy could be used. This will decrease the cost of the flight control systems compared to FBW with redundancy. With a mechanical system, 8.3% of the market share is needed to meet the cost requirement. This is relatively low compared to the market share of the other options, as can be found in Section 14.2.3. Another benefit of having a mechanical back-up is that it requires less power than a full FBW system. This is because there is no redundancy in the FBW system and thus also no redundancy in the actuators, flight computers and other electronics.

There are however also some disadvantages to the option of FBW with mechanical back-up. When a hard limit FEP would be used in a FBW with mechanical back-up, the actuators that are used should be able to override the pilot's input. When the pilot, for example, gives a full negative elevator deflection the FEP should be able to give a full positive elevator deflection. Therefore the actuators need to overcome the force exerted due to the pilot plus the force needed for a full deflection.

Another disadvantage of a mechanical system is that the handling characteristics should be designed for mechanical flight controls. This means that; for example, a reduced stability margin is not possible when using a mechanical back-up system. The third disadvantage of using a mechanical back-up system is that it has less value as a safety system. The idea is that the FBW system is used to increase safety, however when the FBW system fails the increased safety will also be gone. Thus the pilot, in case of FBW failure, cannot rely anymore on the safety of the FBW.

The last disadvantage of having a mechanical back-up system is that a mechanical system needs more maintenance, such as lubrication and adjustments due to cable stretch over time. The increase in maintenance can potentially increase the direct operating cost of the aircraft.

8.1.2 FULL FBW

The second option that is being considered is a full FBW system. With a full FBW system there is no mechanical back-up, however the requirement to have a safety critical system still remains. To comply with this requirement, a full FBW system needs either triple or quadruple redundancy [84]. In Section 14.2.3, it can be found that in a bad market

[1] Guidelines and Methods for Conducting the Safety Assessment Process on Civil Airborne Systems and Equipment

approximately 12.5 % and 16% market share is needed for triple and quadruple redundancy, respectively. This means that it will be impractical to build a full FBW aircraft with at least quadruple redundancy, since the probability of reaching such a market share is quite marginal. It must be noted that technology also advances, including the mean time between failure (MTBF) of FBW components, such as actuators. Therefore the FBW system could potentially be made using triple or even dual redundancy, which will decrease the cost and weight of a full FBW system.

Another disadvantage of having a full FBW system is the difficulty of certification. Although FBW systems are already widely used in commercial airliners and fighter jets, in general aviation FBW systems are merely investigated. Since FBW systems are not widely used in general aviation aircraft, there are no regulations for it at the moment in CS23. Therefore at this moment the FBW system needs to be certified according to CS25. Furthermore, people in general, are skeptical about the reliability of software. This also makes it more difficult to certify than having a mechanical system.

The third disadvantage of full FBW is that it needs more power than a FBW system with mechanical back-up. The main reason for this is the redundancy of the FBW, which includes extra actuators, flight computers and other electronics. But also artificial force feedback has to be installed, because the pilot must get feedback according to CS23. Such a force feedback system also increases the power consumption.

The major advantage of FBW however is that FEP is relatively easily integrated. Furthermore it also has more value as a safety system than FBW with a mechanical back-up. This is because full the whole FBW system will have the safety critical level of 10^{-9} per flight hour. This means that there is no need to switch to a back-up system and therefore the FBW could be used even if one of the components fails.

Another advantage of having a full FBW system is that the maintenance of the mechanical back-up system is not needed anymore, which potentially decreases the direct operating cost.

Finally, the advantage of a relaxed stability margin can be explored with a full FBW system. Having relaxed stability, the control surface areas can be reduced. Having smaller control surfaces the drag and the imposed stresses are reduced.

8.1.3 Full FBW with Graceful Degradation

The last option which is considered is having a full FBW with graceful degradation. With graceful degradation the control surfaces are split up into several sections. Each section will then get its own actuator, which is smaller than an actuator needed for a full control surface. If one actuator then fails, the other actuators can still actuate the other control surfaces. This way the aircraft is still controllable.

The main advantage of a system using graceful degradation is that there is no need for clutches in the FBW system. This could lead to a less complex actuation system, and thus could reduce the weight. Reducing the overall weight of the aircraft, could reduce control surfaces. This would then lead to a lower drag, which is investigated in Section 6.2.3. Lowering the drag will lower the fuel consumption and could thus lower the DOC.

Another advantage is that a moving part is removed from the FBW system. Fewer moving parts can increase the reliability, since fixed parts normally need less service and last longer than moving parts. On the other hand a disadvantage of graceful degradation however is that, when a actuator is stuck, the aircraft will be less maneuverable. Therefore the development cost and certification risk of full FBW with graceful degradation potentially increases, since the aircraft must be controllable at all times, even when one of the actuators has failed.

The use of graceful degradation could also lead to a lower cost, however just as for the weight, these statements should be made carefully. Although the cost and weight could decrease for the actuators, it is unknown at this moment what will happen to the weight and cost of the control surfaces. These effects have not been investigated up until this point and it is interesting to research this in future work.

8.1.4 Conclusion and Recommendation

Both full FBW and FBW with mechanical back-up have their own advantages and disadvantages. These advantages and disadvantages are summarized in Table 8.1.

Table 8.1: Advantages and Disadvantages of different FBW systems

	FBW with Mechanical Back-up	Full FBW	Full FBW with GD
Certification Risk	+	-	- -
Development Risk	+	-	-
Development Cost	+	-	- -
Direct Operating Cost	-	+	+ +
Value as Safety System	-	+	+
Maintenance	-	+	+
Power Consumption	+	-	-

The aircraft design at this moment is based on FBW with a mechanical back-up due to the sensitivity of the design w.r.t the FBW systemm, although there is no quantitative data regarding development and certification risk.

Switching from a FBW system with mechanical back-up to a full FBW system, will increase development risk and certification risk a lot. However for the aircraft design it is easier to switch from a FBW system with mechanical back-up to a full FBW. For example, at this moment a certain stability margin has been taken into account. Using a full FBW the aircraft could be designed to have relaxed stability, which basically is a lower stability margin. This can lead to a decrease in control surface area and thus decrease the weight. This way the aircraft can enter a so-called reversed snowball effect (i.e. reducing the weight more and more).

It must be noted though, that for a full FBW with quadruple redundancy 16% of the the market share is needed in a bad market in order to reach the break even point in 5 years, as can be read in Chapter 14. At this moment this is considered to be not feasible. Depending on the investor and the risk that investor is willing to take, one should choose for either full FBW or FBW with a mechanical back-up. If the investor wants a lower development risk he/she should chose for a FBW system with mechanical back-up. If the investor decides to take the risk, he/she could decide to go for a full FBW.

8.2 Flight Envelope Protection

One of the main goals of this project is to reduce the amount of catastrophic failures in general aviation. To reduce these failures, the use of Flight Envelope Protection (FEP) in general aviation is investigated. There are two main methods, in which FEP can be incorporated. One being hard limits, meaning that the pilot can never override the FEP unless it is disconnected. The second being soft limits in which the pilot can still override the flight envelope with excessive force. Both of these FEP philosophies have their own advantages and disadvantages, which will be discussed here.

8.2.1 Hard Limits

The main advantage of a hard limit system is that it is always within a safe flight regime. Especially for less experienced student pilots, it would be useful to have a hard limit FEP system. Student pilots are more likely to get confused about the aircraft state in a stressed situation. If the pilot does not know the aircraft state, he or she could still bring the aircraft in unsafe conditions.

Although the main advantage of having a hard limit FEP system is quite significant, it also has some disadvantages. One of them is that a hard limit system is hard to integrate into an aircraft which utilizes FBW with a mechanical back-up system since a hard limit system should be able to override the forces introduced by the pilot.

Another disadvantage is that the pilot cannot fly the aircraft at its full capability, which can have catastrophic consequences. For example, when flying directly into a mountain, the pilot might want to overrule the flight envelope protection in order to save his life. Although the FEP could be disengaged, it must be noted during what state the aircraft autopilot hands over control to the pilot. In an accident with a China Airlines Boeing 747 [85], the autopilot disconnected when the rudder could not compensate the asymmetrical loading due to an engine failure, in a dive. However, the pilots were unaware that full rudder to one side was applied and they only recovered the aircraft at about 10,000 feet from approximately 40,000 feet.

8.2.2 Soft Limits

In a soft limit system the pilot will always be able to override the FEP. The main advantage is that the pilot is always able to operate the aircraft to its full capabilities, so in case of a dangerous situation the pilot can override the FEP. This could also be useful in stall and spin training, because the FEP does not necessarily have to be disengaged to get into a spin or stall. The only thing that has to be done is using excessive force on the control stick. The other advantage is that a soft limit system can be used in a setup with FBW and a mechanical back-up. However as explained earlier, with soft limit the pilot can unintentionally bring the aircraft in unsafe conditions. For less experienced pilots (i.e. student pilots) this can cause a problem.

8.2.3 Auto Throttle

There are also possibilities to have an auto throttle build in. Although one might think this is necessary for FEP, this is not entirely true. There are several ways to keep the airspeed up, one is by giving more thrust. Airspeed may also be increased by lowering the nose. Most general aviation accidents, however, happen at low altitudes [86], where it might not be a good idea to put the nose down to regain airspeed. Therefore it is recommended to build in an auto throttle function.

8.2.4 Controlled Flight into Terrain

One option for the FEP system is Controlled Flight into Terrain (CFIT) protection. This could prevent the aircraft from flying into the terrain, which increases the overall safety of the aircraft. The disadvantage of having CFIT protection, is that it increases the complexity the FEP. This will probably also lead to higher cost. During this study, CFIT protection has not been investigated in detail. Therefore in further study CFIT protection can be investigated.

8.2.5 Conclusion and Recommendation

The way FEP is handled in aircraft is just a matter of philosophy. Where Boeing uses a soft limit FEP, Airbus aircraft use a hard limit FEP. When using a mechanical system, full authority is not recommended, due to the large forces the actuators should be able to give. When using a full FBW system however, it is a matter of preference which FEP system to use. Therefore, if full FBW is considered for the final design, one might propose to make it something that can be chosen by the customer. Just as in a car, where the customer could choose to have air conditioning or not.

8.3 AUTOLAND

One of the requirements is to have a solo training mode with flight envelope protection and autoland. Several options, such as: Instrument Landing System (ILS), Microwave Landing System (MLS), Ground-Based Augmentation System (GBAS), Satellite-Based Augmentation System (SBAS), Visually-Guided Landing System (VSGL) and the Parachute Landing System were considered in the mid-term report [64]. The most feasible option was the SBAS system. The SBAS system is an enhanced global navigation satellite system (GNSS), which uses cross-continental ground stations. These ground stations ensure that differential corrections can be made for the GNSS, improving the accuracy of the whole system. The main advantages of SBAS are:

- Relatively low cost compared to other autoland system.
- Large grow, SBAS is expected to grab 50 to 60% of the market in 2020-2030 [87].
- Major advantages for small and medium sized airport, which are mainly used by general aviation, since no local ground system needs to be used.

However with every advantage comes a disadvantage. The main disadvantages of SBAS are:

- Currently only available in Northern-America, Europe, India and Japan [88].
- Ground personnel is not yet trained for SBAS operations.
- Only certified for CAT I approaches up until now, which does not cover full autoland.

In the Mid-Term Report estimates have been made for the weight, cost and power of the SBAS [64]. These estimates can be found in Tables 8.2 to 8.4 respectively. These estimates however, only contain double redundancy. The autoland system should be designed for safety critical levels though. The reason for this is that the autoland operations are relatively close to ground. This means that when the autoland fails, there might be no time for the pilot to recover from the failure, which can lead to catastrophic consequences. Therefore atleast triple or quadruple redundancy should be expected to get the system certified. This means that the total cost is more than €100,000 . It might be considered though, to sell two types of aircraft: one with autoland and one without. In such a way an flight school could decide to buy; for example, one aircraft with autoland for every six aircraft without autoland. This can be done, since in dual training mode the aircraft is not required to have an autoland option.

Table 8.2: Autoland Mass

Mass			Based on
Radio altimeter	1.8	[kg]	Free Flight Systems TRA-3500
SBAS/INS/Computer	1.0	[kg]	Rockwell Collins Athena 411
Total subsystems	2.8	[kg]	
Redundancy factor	2.0	[-]	
Installation/cables correction	1.4	[-]	Educated guess
Total system	7.85	[kg]	

Table 8.3: Autoland Cost

Cost			
Radio altimeter	7,000	[$]	King KRA-10A
SBAS/INS/Computer	15,000 (*)	[$]	Athena 411
Total subsystems	22,000	[$]	
Redundancy factor	2.0	[-]	
Installation/cables correction	1.2	[-]	Educated guess
Total system	52,800	[$]	

** Guestimate: based on other avionics*

However, not only are the cost for an autoland system high, it is also not allowed to do a full autoland yet. Diamond and Beechcraft have demonstrated autonomous landings with their Diamond DA-42 and Beechcraft Bonanza [89] respectively and both aircraft used the Athena 411 and probably also a radar altimeter [90]. Although the Athena 411 can autonomously land an aircraft, it is not yet certified for private and commercial aircraft. Although it seems possible to certify the Athena 411 for private and commercial aircraft, due to the collapse of the general market Beechcraft has paused the program for autolanding at this moment [89]. Therefore at this moment, autoland is considered to be not feasible yet for general aviation aircraft. Continuing with the autoland induces a high risk for the development of the trainer aircraft, since it relies on the work on the certification by external companies.

Table 8.4: Autoland Power

Power			
Radio altimeter	25	[W]	Free Flight Systems TRA-3500
SBAS/INS/Computer	18	[W]	Rockwell Collins Athena 411
Total subsystems	43	[W]	
Loss/margin correction	1.2	[-]	Educated guess
Total system	51.6	[W]	

The idea of autoland however is to land the pilot safely when he panicks, because; for example he got in bad weather and cannot find the airport anymore, it could already help to just point the aircraft to the nearest airfield. Therefore instead of autoland an auto approach could be investigated, putting the aircraft in front of the runway. Such an auto-approach could be performed by cheaper system, such as the Garmin GTN 625 GPS [91]. The GARMIN GTN 625 GPS weights 2.48 kg and costs $8473.00, the power is approximated to not be higher than Rockwell Collins Athena 411, which is 18 W. Since a failure in auto-approach does not necessarily have to lead to a catastrophic failure, the system does not necessarily have to be safety critical. Furthermore the Garmin GTN 625 GPS is already certified for private and commercial use. Therefore the auto-approach is considered to be more feasible than an autoland system.

In conclusion, for now it is recommended to start with an auto-approach, which already helps the pilot finding and/or lining up with the runway. In the future, when autoland in general aviation is certified, it might be considered to upgrade from auto-approach to autoland. Based on the Beechcraft Bonanza [89], it seems that the autoland could be installed externally relatively easily. So when the aircraft will later be upgraded with an autoland system, not a lot of changes in the design have to be made.

8.4 ACTUATORS

A elaborate discussion of the actuator technology was performed in the mid-term report [64]. Outcome of this discussion was the recommendation of the usage of either EHA or EMA actuators. After consultation with the company Rosner-TDL, the conclusion was made that the EMA actuation technology would be the most suitable one. This is due to the better maintainability of these systems [92]. Reducing the downtime of the trainer aircraft and therefore decreasing the cost for inspections is a major point of consideration in this design. Disadvantage of EHA actuators is their still present hydraulic circuit which requires special maintenance.

Reference indicate that the MTBF of off the shelf EMA actuators is at the present time in the order of 5000 hours [93]. By considering Chapter 17 the conclusion can be made that a triple redundant actuation system can easily meet the safety critical reliability. The power requirements of the actuators were derived in Section 10.6.2. Based on the chosen FBW layout the hinge moments can reduced by a significant value and therefore the cost, weight and power of the actuators can be reduced as well. A more elaborate discussion can be found in Section 10.6.2.

Weight estimation of the actuators was done by combining the Cessna weight estimation method for mechanical control systems with Moog 915 actuator data [94]. The Moog 915 actuator offers a stall-torque of 34 Nm, a no-load speed of 250 deg/s and a weight of 3.18 kg. Further it includes a clutch which can be used for disengagement. The Cessna class II weight estimation method for flight control includes the weight for cables, pulleys, push-pull rods and cockpit controls. The contribution of the flight controls and the actuators were added. Further a 5% contingency was included on top. It was assumed that every level of redundancy for the actuators is a factor of three. That means three actuators are needed to control aileron, elevator and rudder. Both ailerons are controlled by one actuators, this is done by some kind of cable and pulley system where the actuators is attached to.

Weight estimation FBW with mechanical back-up is given by

$$W_{\text{control}} = 1.05(0.0168 W_{\text{MTOW}} + 3 W_{\text{actuator}}) \tag{8.1}$$

For full FBW it was assumed that 2/3 of the mechanical control system weight is still present

$$W_{\text{control}} = 1.05\left(\frac{2}{3} 0.0168 W_{\text{MTOW}} + 3 n_{\text{redundancy}} W_{\text{actuator}}\right) \tag{8.2}$$

For the graceful degradation it was assumed that it has the same weight as the full FBW with single redundancy. It is likely that the GD concept needs a more elaborate mechanical system but this is accounted for in the actuator weight because the Moog 915 includes a clutch which can be estimated to be approximately half of the weight. This clutch is not needed anymore in the GD FBW layout since the control surfaces are split. Therefore the clutch weight is used to account for the higher mechanism weight.

9
Performance

In this chapter the flight performance of the aircraft is analyzed. The methods for doing so are described step-by-step in Chapter 5 of Ref. [57]. The purpose of analyzing the flight performance of the aircraft is to check whether the current proposed design meets requirements from both mission specifications and regulations. If discrepancies are discovered between what is required from the aircraft and what it will be able to deliver it shall be argued whether or not to make changes to the design and reiterate. Note that both the aircraft lacking the required performance and the aircraft being able to perform better than required are discrepancies, and both shall be addressed. Staying closer to the set requirements may reduce the weight and cost of the design.

The first five sections of this chapter describe the analysis of stall, takeoff, climb, landing, and max. speed respectively (Sections 9.1 to 9.5). The flight performance module is executed outside of the main iteration loop of the second preliminary design sequence and it only checks compliance with the requirements. In Section 9.6 the results of the module after the final design iteration are presented.

Figure 9.1 shows the block diagram, which gives a rough overview of how the analysis tool is built up. It shows the different modules and how they are connected to each other.

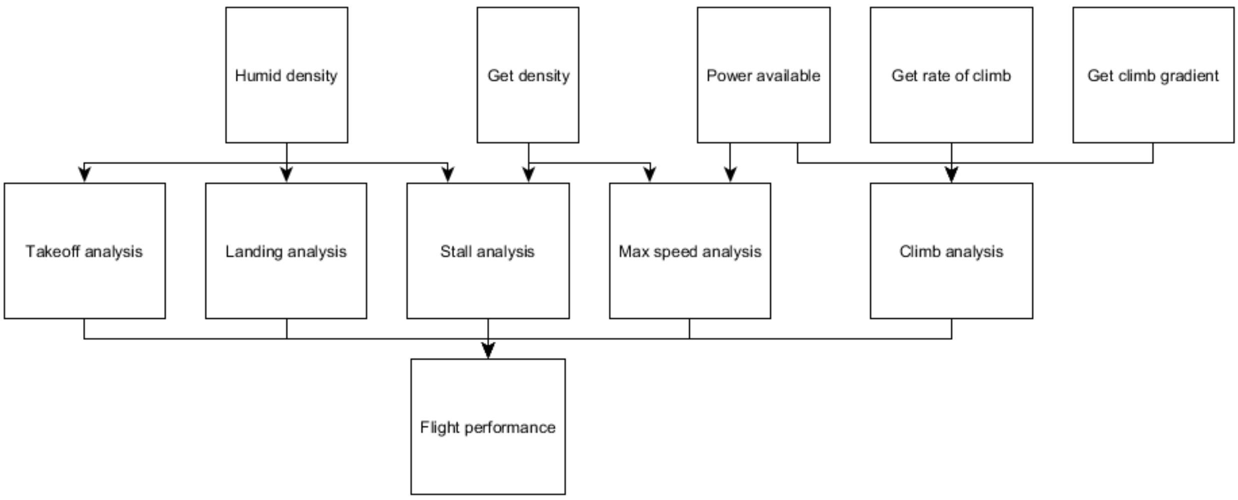

Figure 9.1: Block diagram of the flight performance analysis tool

9.1 Stall

From CS 23.45 and 23.49 it follows that the stall characteristics shall be analyzed for the following conditions:

1. still air and a standard atmosphere (23.45.a);
2. a relative humidity of 80 percent (23.45.d);
3. propellers in takeoff position (23.49.a.1);
4. landing gear extended (23.49.a.2);
5. wing flaps in the landing position (23.49.a.3);
6. center of gravity in the most unfavorable position within the allowable landing range (23.49.a.6); and
7. engines at idle (23.49.e.1).

To analyze the most critical condition aircraft weight is assumed equal to the maximum take off weight.

Condition 1 calls for $T = 288$ K, $P = 101\,325$ Pa, and $\rho_0 = 1.225$ kg/m^3.

Condition 2 calls for a change in air density. The density of humid air at otherwise standard ISA sea level conditions was calculated as follows.

Relative humidity is defined as $\phi = \dfrac{\rho_w}{\rho_w^*}$, where ϕ is the relative humidity expressed as a fraction, ρ_w is the actual water vapor density and ρ_w^* is the saturated water vapor density [95]. ρ_w^* is a function of the temperature, and can be approximated by $\rho_w^*(T) = 5.018 + 0.32321T + 8.1847 \cdot 10^{-3}T^2 + 3.1243 \cdot 10^{-4}T^3$, which is an empirical fit that is valid for $T \in [0,40]$°C. The actual water vapor density can then be expressed as $\rho_w = \phi\rho_w^*(T)$.

For dry air the amount of molecules per cubic meter can be calculated with $n_{tot} = \dfrac{\rho_0}{M_{air}}$, where n_{tot} is the amount of air molecules in mol, ρ_0 is the ISA sea level density, and M_{air} is the molar mass of air in kg/mol. For wet air the amount of water molecules per cubic meter can be calculated similarly with $n_w = \dfrac{\rho_w}{M_w}$, where n_w is the amount of water molecules in mol, ρ_w is the actual water vapor density in kg/m^3, and M_w is the molar mass of water in kg/mol. Because there can be no more than n_{tot} molecules per cubic meter, the presence of the water molecules reduces the amount of air molecules in the same volume. The amount of air molecules present in a cubic meter of wet air can then be calculated with $n_{air} = n_{tot} - n_w$.

The combined density of humid air can be calculated with $\rho_h = n_w M_w + n_{air} M_{air}$, which can be rewritten by substituting the previously defined equations for the molar contents and the definition of the relative humidity. This yields the equation of the density of humid air:

$$\rho_h = \rho_0 + \phi\rho_w^*(T)\left[1 - \frac{M_{air}}{M_w}\right] \tag{9.1}$$

For ISA sea level conditions it follows that $\rho_w^* = 12.762$ g/m^3. For the given relative humidity of 80% and using $M_w = 18.02$ g/mol and $M_{air} = 28.57$ g/mol it then follows that $\rho_h = 1.219$ kg/m^3.

Condition 5 calls for using $C_{L_{max,flap}}$, which is an output of Step 25.

Condition 7 calls for $T = 0$ N. The other conditions do not have influence on the equations for stall. The stall speed is then a function of $C_{L_{max,flap}}$ and can be written as follows, Equation (9.2).

$$V_S = \sqrt{\frac{2W_{TO}}{\rho_h C_{L_{max,flap}} S}} \tag{9.2}$$

The variation of the Mach number at stall with altitude was derived as follows. The speed of sound can be written as $a = \sqrt{\gamma RT}$, yielding the variation of the speed of sound, Equation (9.3).

$$\left(\frac{a}{a_0}\right) = \left(\frac{T}{T_0}\right)^{0.5} \tag{9.3}$$

The stall speed can be written as Equation (9.2), yielding the variation of the stall speed, Equation (9.4).

$$\left(\frac{V_S}{V_{S_0}}\right) = \left(\frac{\rho}{\rho_0}\right)^{-0.5} \tag{9.4}$$

The variation of pressure can be written as in Equation (9.5),

$$\left(\frac{p}{p_0}\right) = \left(\frac{T}{T_0}\right)^{\left[-\frac{g_0}{LR}\right]} \tag{9.5}$$

, yielding the variation of density using $p = \rho RT$, Equation (9.6).

$$\left(\frac{\rho}{\rho_0}\right) = \left(\frac{T}{T_0}\right)^{\left[-\frac{g_0}{LR}-1\right]} \tag{9.6}$$

Substituting Equation (9.6) in Equation (9.4) yields Equation (9.7).

$$\left(\frac{V_S}{V_{S_0}}\right) = \left(\frac{T}{T_0}\right)^{\frac{1}{2}\left[\frac{g_0}{LR}+1\right]} \tag{9.7}$$

The Mach number at stall can be written as follows, Equation (9.8).

$$M_S = \frac{V_S}{a} \tag{9.8}$$

, yielding the variation of the Mach number, Equation (9.9).

$$\left(\frac{M_S}{M_{S_0}}\right) = \left(\frac{V_S}{V_{S_0}}\right)\left(\frac{a}{a_0}\right)^{-1} \tag{9.9}$$

Substituting Equation (9.7) and Equation (9.3) into Equation (9.9) yields Equation (9.10).

$$\left(\frac{M_S}{M_{S_0}}\right) = \left(\frac{T}{T_0}\right)^{\left[\frac{g_0}{2LR}\right]} \tag{9.10}$$

The temperature can be written as a function of the altitude: $T(h) = T_0 + Lh$, where $L = -0.0065$ J/kg/K is the lapse rate; and substituting the function of the temperature in the variation of Mach number finally yields Equation (9.11).

$$M_S(h) = M_{S_0}\left(\frac{T_0 + Lh}{T_0}\right)^{\left[\frac{g_0}{2LR}\right]} \tag{9.11}$$

9.2 TAKEOFF

All conditions from CS 23.45 apply. These were already listed in Section 9.1. For analyzing the takeoff characteristic the conditions from CS 23.51 also apply. These require the following:

1. engines operating within approved operating limitations (23.51.a.1); and
2. at an altitude of 50 ft the aircraft's speed must be higher than $1.3V_{S_1}$.

To analyze to most critical situation MTOW is again used. Furthermore the requirements listed in Chapter 3 of Ref. [50] add the condition that the aircraft shall have a maximum takeoff distance over a 50 ft obstacle of 500 m, so $s_{TO} \leq 500$ m.

Given these conditions and requirements Table 5.1, p. 119, Ref. [57] gives $V_3/V_{s_{TO}} = 1.3$, $f_{P_{TO}} = 1.0$. According to Equation 5.8, p. 119, Ref. [57] thrust of single engine, fixed blade propeller aircraft can be related to its takeoff power by Equation (9.12).

$$T = 4.60\left(D_p P_{TO}\right)^{2/3} \tag{9.12}$$

, where T is the thrust in lbs, D_p is the propeller diameter in ft, and P_{TO} is the takeoff power in hp. The friction coefficient, μ', can be calculated with Equation (9.13).

$$\mu' = \mu_g + 0.72\left(\frac{C_{D_0}}{C_{L_{max_{TO}}}}\right) \tag{9.13}$$

, Equation 5.9, p. 121, Ref. [57], where μ_g is the wheel-ground rolling friction coefficient, C_{D_0} is the zero-lift drag coefficient, and $C_{L_{max_{TO}}}$ is the maximum lift coefficient at takeoff. The value of $\mu_g = 0.30$ was obtained from page 40 or Ref. [57], using the highest value to be most conservative. All other parameters needed to analyze the takeoff characteristics of the aircraft are inputs from previous steps. Note that this formula is written in imperial units. The inputs to this formula were therefore first converted from SI to imperial units.

The analysis was conducted as follows.

$$s_{TO} = \mathrm{f}_{TO} h_{TO}\left[\frac{1}{\gamma_{LOF}} + \frac{\left(\frac{V_3}{V_{s_{TO}}}\right)^2\left(\frac{W}{S}\right)_{TO}\left\{\left[\left(\frac{T}{W}\right)_{TO} - \mu'\right]^{-1} + \sqrt{2}\right\}}{\left(h_{TO}\rho g C_{L_{max_{TO}}}\right)\left(1+\sqrt{2}\gamma_{LOF}\right)}\right] \tag{9.14}$$

Using equation 5.6, p. 117, Ref. [57], Equation (9.14), the takeoff distance of the aircraft as it has been defined up to this point is calculated. The result is compared to the takeoff distance as dictated by the requirements. If the two deviate by more than 5%, design iterations are in order, Ref. [57], p. 123. Roskam notes that the parameters of most influence on the takeoff distance are $\left(\frac{T}{W}\right)_{TO}$, $\left(\frac{W}{S}\right)_{TO}$, and $C_{L_{max_{TO}}}$, which is of importance for the design iterations.

The equation calls for $\left(\frac{T}{W}\right)_{TO}$, so it was necessary to rewrite the equation for the thrust as previously described to find the thrust-to-weight ratio as a function of the weight-to-power ratio. This was done as follows. The thrust can be written as, Equation (9.15),

$$T = \left(\frac{T}{W}\right) W_{TO} \tag{9.15}$$

and the power can be written as, Equation (9.16),

$$P_{TO} = \left(\frac{W}{P}\right)_{TO}^{-1} W_{TO} \tag{9.16}$$

Substituting that in the equation that relates thrust to power yields Equation (9.17).

$$\left(\frac{T}{W}\right) W_{TO} = k_{TP}\left[D_p\left(\frac{W}{P}\right)_{TO}^{-1} W_{TO}\right]^{2/3} \tag{9.17}$$

Dividing both sides by W_{TO} and simplifying finally yields Equation (9.18).

$$\left(\frac{T}{W}\right) = \frac{k_{TP}}{W_{TO}^{1/3}}\left[D_p\left(\frac{W}{P}\right)_{TO}^{-1}\right]^{2/3} \tag{9.18}$$

9.3 CLIMB

All conditions from CS 23.45 apply. These were already listed in Section 9.1. For analyzing the takeoff characteristic the conditions from CS 23.65, 23.66, and 23.77 also apply. CS 23.66, however, only applies for multi-engine aircraft, hence it does not call for any requirements here. The conditions following from CS 23.65 and 23.77 are:

1. having a minimum steady rate of climb of at least 300 feet per minute (23.65.a);

2. having a minimum steady angle of climb of at least 1:12 (23.65.a);
3. at sea level (23.65.a);
4. maximum continuous power (23.65.a.1);
5. landing gear retracted (23.65.a.2);
6. wing flaps in takeoff position (23.65.a.3); and
7. have a minimum steady angle of climb of 1:30 for balked landings (23.77.a).

To analyze to most critical situation MTOW is used. Furthermore the requirements listed in chapter 3 of Ref. [50] add the condition that the aircraft shall have a minimum rate of climb of 800 feet per minute. This requirement overrules the CS 23.65.a requirement of having a minimum steady rate of climb of 300 feet per minute. Also the CS 23.65.a requirement of having a minimum steady angle of climb of at least 1:12 is more critical than the 1:30 requirement for balked landings from (23.77.a). Furthermore it is assumed that the rated maximum continuous power is equal to the takeoff power.

$$RC = 33000\left[\eta_p\left(\frac{W}{P}\right)^{-1} - \frac{\left(\frac{W}{S}\right)^{1/2}}{19\left(\frac{C_L^{3/2}}{C_D}\right)\sigma^{1/2}}\right] \tag{9.19}$$

To analyze the rate of climb performance, Equation 5.21 (p. 126, Ref. [57]) is used, where RC is the rate of climb in ft/min, η_p is the propeller efficiency, $\left(\frac{W}{P}\right)$ is the power loading in lbs/hp, $\left(\frac{W}{S}\right)$ is the wing loading in lbs/ft^2, C_L and C_D are the lift and drag coefficients, respectively and σ is the density ratio defined by $\sigma = \frac{\rho}{\rho_0}$, where ρ is the density at a given flight condition and ρ_0 is the ISA sea level density. Note that this equation is written for imperial units. Since the inputs to this formula are known in SI units they were converted for the purpose of using this equation.

$$CGR = -\left(\frac{L}{D}\right)^{-1} + \frac{C_L^{1/2}18.97\eta_p\sigma^{1/2}}{\left(\frac{W}{P}\right)\left(\frac{W}{S}\right)^{1/2}} \tag{9.20}$$

To analyze the angle of climb performance Equation 5.22 (p. 126, Ref. [57]), is used where CGR is the climb gradient, defined as $CGR = \frac{U}{W}$, where U is the velocity in x_B direction and W is the velocity in the z_B direction, and $\left(\frac{L}{D}\right)$ is the aerodynamic efficiency.

The analysis of the climb performance is threefold. First the steady rate of climb of the aircraft is calculated with Equation 5.21 from Roskam and the result was compared to the requirement of the minimum of 300 ft/min. Then the steady angle of climb, or climb gradient, is calculated using Equation 5.22 from Roskam and the result was compared to the minimum of 1:12. Finally the absolute ceiling of the aircraft is calculated by solving Equation 5.21 from Roskam for $RC = 0$ ft/min. The latter determines the upper line of the flight envelope. For the determination of the absolute ceiling it was assumed the aircraft is flown at conditions that maximize the rate of climb. It can be shown that this requires $\left(\frac{C_L^3}{C_D^2}\right)$ to be at a maximum, which leads to $C_L = \sqrt{\frac{3C_{D_0}}{k}}$ and $C_D = C_{D_0} + k\left(\sqrt{3C_{D_0}k^{-1}}\right)^2 = 4C_{D_0}$, with $k = \frac{1}{\pi Ae}$.

9.4 Landing

All conditions from CS 23.45 apply. These are listed in Section 9.1. For analyzing the landing characteristic the conditions from CS 23.75 also apply. CS 23.75, however just contains the definition of the landing distance. The landing distance is constrained by the mission requirements, listed in Chapter 3 of Ref. [50]. It has to be smaller than or equal to 400 m. To analyze the most critical situation MTOW is used. Usually the maximum landing weight is used to analyze the landing distance. However, in this case it is justifiable to use the maximum takeoff weight. This is because one of the major missions of the aircraft will be to fly circuits, which involves flying a short distance, performing a touch and go and repeating. The most critical case is when the aircraft takes off with maximum takeoff weight and lands after a single circuit. In this case its landing weight will be close to the maximum takeoff weight, thus justifying the use of the MTOW.

The landing distance was calculated using the equations from section 5.9 of Ref. [57]. Using that method the landing distance is split up into two parts, the air segment, denoted by s_{air}, and the ground run, denoted by s_{LG}.

$$s_{air} = \left(\frac{1}{\bar{\gamma}}\right)\left[\frac{V_A^2 - T_{TD}^2}{2g} + h_L\right] \tag{9.21}$$

The air part can be calculated using Equation 5.81 (p. 162, Ref. [57]), where $\bar{\gamma}$ is the average access thrust over the weight, taken as 0.10 as described by Roskam in the same page, V_A is the approach speed, defined as $V_A = 1.3V_{S_L}$, where V_{S_L} is the landing stall speed, V_{TD} is the touchdown speed, which can be calculated using Equation 5.87 (p. 164, Ref. [57]), $V_{TD} = V_A\sqrt{1-\frac{\bar{\gamma}^2}{\Delta n}}$, where $\Delta n = 0.10$ was taken as described by Roskam, g is the gravitational acceleration, and h_L is the obstacle height, which is required to be 50ft.

$$s_{LG} = \frac{V_{TD}^2}{2\bar{a}} \tag{9.22}$$

The ground part was calculated using Equation 5.88 (p. 164, Ref. [57]), where $\bar{a}$ is the average deceleration, which was taken as $\bar{a}/g = 0.30$ as described by Roskam on the same page.

9.5 Maximum Speed

The final performance characteristic that was analyzed is the maximum speed. The maximum speed as a function of altitude closes the flight envelope on the right side. CS 23.335 constrains the minimum design cruising speed as function of the wing loading, $V_C \geq 33\sqrt{\left(\frac{W}{S}\right)}$. To satisfy this requirement the maximum speed shall be higher than this speed.

The maximum speed of the aircraft was calculated as follows. When the aircraft flies at the maximum speed the power available equals the power required, $P_a = P_r$. The power available drops with altitude, hence it is a function of h, $P_a = f(h)$. The relation was obtained from manufacturer data, as described in Section 10.6. The power required can be written as:

$$P_r = DV = C_D\frac{1}{2}\rho V^3 S = \left(C_{D_0} + kC_L^2\right)\frac{1}{2}\rho V^3 S \tag{9.23}$$

, where P_r is the power required in Watt, D is the drag in Newton, V is the velocity in m/s, C_D is the drag coefficient, ρ is the density of air at the altitude for which the maximum speed is to be determined in kg/m^3, S is the wing surface area in m^2, C_{D_0} is the zero lift drag coefficient, k is defined as $k = \frac{1}{\pi Ae}$, and C_L is the lift coefficient. This equation can be solved for V to get the maximum speed:

$$V_{max} = \sqrt[3]{\frac{P_a}{S}\frac{2}{\rho}\frac{1}{C_{D_0} + kC_L^2}} \tag{9.24}$$

Furthermore horizontal, straight, symmetrical flight is assumed, yielding $L = W$. This allows the lift coefficient to be written as a function of airspeed:

$$C_L = \frac{W}{S}\frac{2}{\rho}\frac{1}{V^2} \tag{9.25}$$

The maximum speed can be obtained iteratively by updating the speed between the equation for V_{max} and C_L repeatedly.

9.6 Results

In this section the results from the performance calculations are presented. Table 9.1 shows the resulting performance of the aircraft along with the requirements set at the start of the design. Clearly, all of the requirements are easily met.

Table 9.1: Performance characteristics

Performance	Aircraft value	Unit	Requirement	Unit
Take-off distance	340	[m]	500	[m]
Landing distance	317	[m]	400	[m]
Rate of climb	1605	[fpm]	800	[fpm]
Climb gradient	0.3459	[-]	0.0833	[-]

9.6.1 Payload-range diagram

Using Breguet's equation for range a payload-range diagram can be created, presented in Figure 9.2. The required minimum range is 800km. From Figure 9.2 this point is highlighted and the maximum allowable payload to reach this range is about 160kg. This means that with two average sized people, the minimum range is reached. The useful load (payload + fuel weight) is equal to 213kg, where the maximum amount of fuel that can be carried is 84.3kg (120 liters). The payload-range diagram shows that the impact the payload has on the range is very large, as it varies between 400km and 2000km.

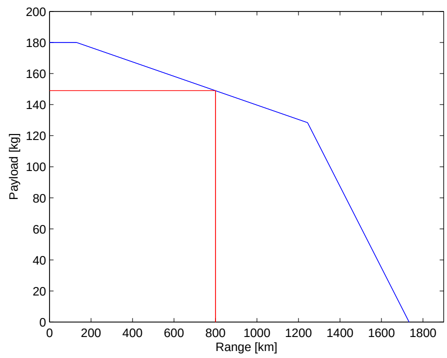

Figure 9.2: Payload-range diagram

9.6.2 Flight envelope

The flight envelope of the aircraft is shown in Figure 9.3. The stall speeds, ceilings and maximum speeds form the boundaries of this flight envelope. The absolute ceiling of the aircraft is much higher than the service ceiling, due to the fact that oxygen is required if the pilot wants to fly longer than 30 minutes above 10,000 feet [40].

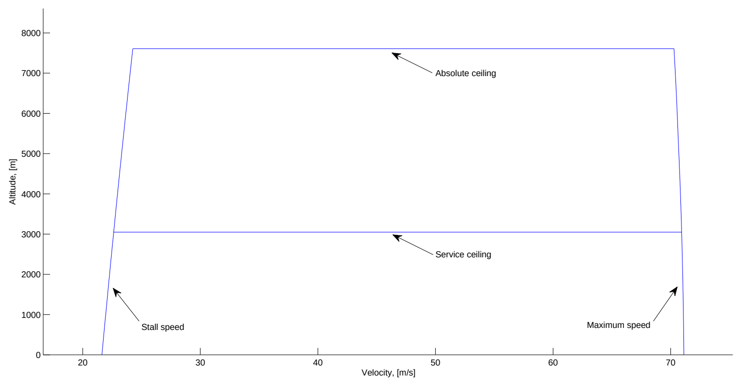

Figure 9.3: Flight envelope

10
AIRCRAFT SYSTEMS

This chapter will provide an overview of the aircraft subsystems and components. The Fly-By-Wire system is featured in a separate chapter because of the emphasis on that element during design.

This chapter will start with a complete description of the systems and their connection. This is followed by a description of the fuel system, the cockpit instrumentation, the avionics components, the propulsion subsystem and finally electrical power supply and actuation.

10.1 SYSTEMS OVERVIEW

The entire aircraft system is complicated and consists of many inter-related subsystems. The block diagram in Figure 10.1 illustrates the hardware connections between these various aircraft subsystems.

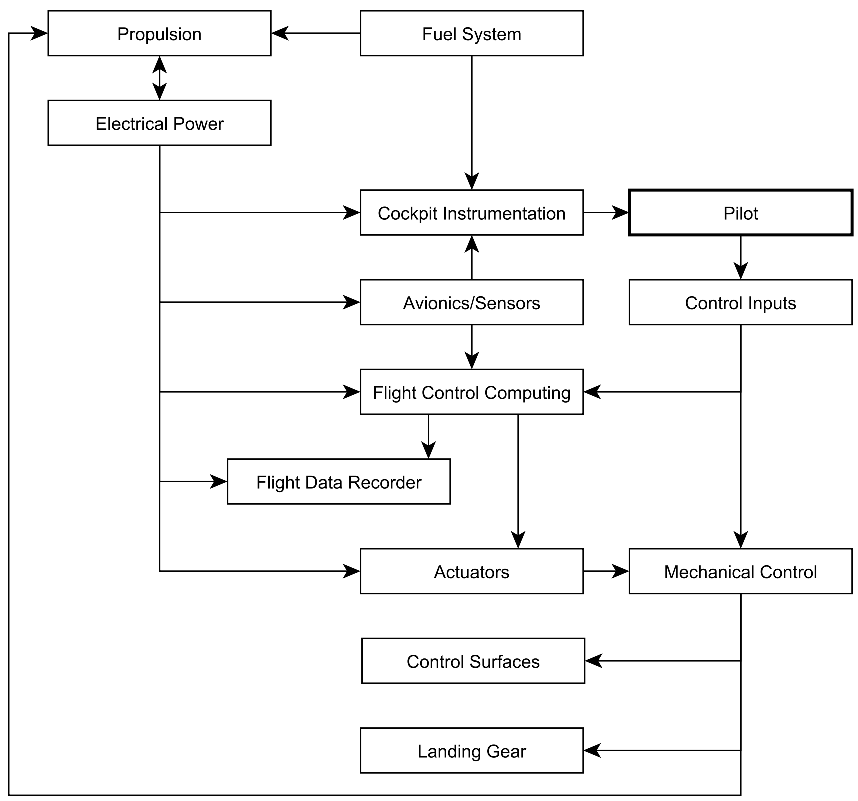

Figure 10.1: Complete aircraft hardware block diagram of connected systems

Numerous flows of data exist within the complete aircraft system. Figure 10.2 describes the communication network within the aircraft, showing the various flows of information and the relations between elements.

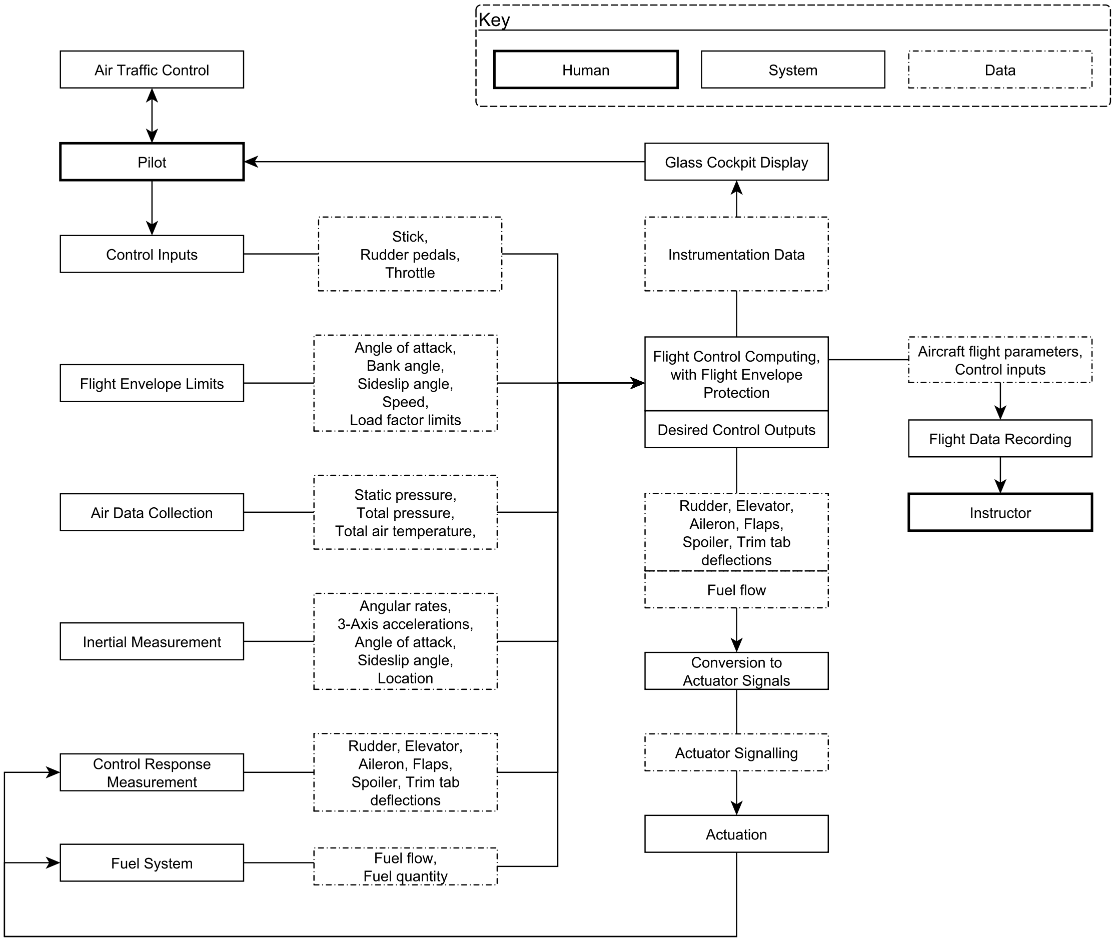

Figure 10.2: Block diagram illustrating flows of information and communication between systems.

10.2 Fuel System

The fuel system of the aircraft provides the engine with a steady supply of fuel. It should store sufficient fuel for the entire flight duration and ensure proper fuel feed during even the most limiting flight conditions that might be encountered.

The fuel tanks of the aircraft should be able to hold sufficient fuel for the aircraft to be able to fly its design range. [39] This aircraft will be fitted with two bladder tanks, one in each wing to make use of the otherwise unused space in the wingbox. These bladder tanks have the advantage over discrete metal or integral fuel tanks because of lower maintenance costs and the possibility of insertion into the wing through a small opening.[96] Vents are fitted to prevent excessive build-up of pressure, for example due to heat, and to maintain positive pressure in the tanks as they run empty. [39]

The fuel will be transferred from the tanks to the engine via fuel lines. The system will be based on the gravity-feed principle because the aircraft is designed with a high wing configuration. [96, 97]

Indication of fuel quantity remaining is important for the pilot. It should be indicated separately for each tank, to monitor balance and fuel use. A fuel flow gauge also provides useful information. The pilot is able to select the left, right or both fuel tanks using a selector valve. As such, the lateral balance of the aircraft can be controlled by managing fuel quantities in each fuel tank. [96, 98]

A block diagram illustrating the basic fuel system lay-out is provided in Figure 10.3.

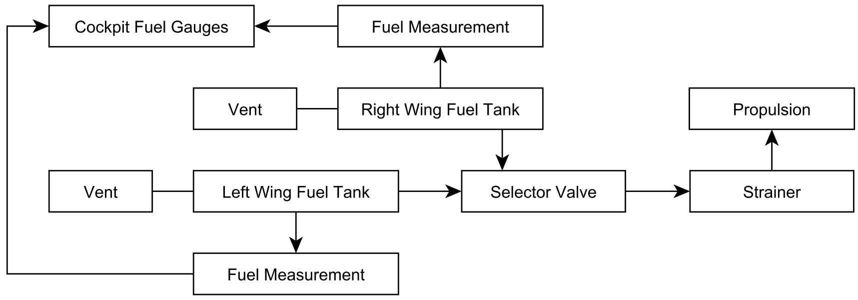

Figure 10.3: Hardware block diagram of the aircraft fuel system

10.3 Cockpit Instrumentation

The minimum required instruments required for VFR are documented in CS23.1303 [40]. Two types of instruments should be present. Flight and navigation instruments and powerplant instruments. Since the pilot navigates on visual cues during VFR conditions, the required flight and navigation instruments are pretty limited. However, some basic instruments are needed. Each aircraft should at least have the following:

- Airspeed indicator;
- Altimeter;
- Non-stabilized magnetic direction indicator;
- Free air temperature indicator;
- Fuel quantity indicator for each fuel tank installed;
- Oil pressure indicator for each engine;
- Oil temperature indicator for each engine;
- Fire warning means;
- A tachometer indicator for each engine;

During VFR conditions, the pilot mainly navigates on visual reference. In IFR conditions, the pilot relies solely on the cockpit instruments for navigation. Therefore, more instruments are needed for flight and navigation purposes in order to certify the aircraft for IFR flights. However, IFR capabilities greatly increase the market value of the aircraft, since it can then be used for a greater range of PPL ratings. In addition to the instruments needed for VFR, an aircraft certified for flight under IFR conditions needs the following instruments [99] :

- Two-way radio communication and navigation equipment suitable for the route to be flown;
- Gyroscopic rate-of-turn indicator, except if a third attitude instrument system, usable through flight attitudes of 360 degrees of pitch and roll is present;
- Slip-skid indicator;
- Sensitive altimeter adjustable for barometric pressure;
- A clock displaying hours, minutes and seconds with a sweep-second pointer or digital presentation;
- Generator or alternator of adequate capacity;
- Gyroscopic pitch and bank indicator (artificial horizon);
- Gyroscopic direction indicator (directional gyro or equivalent;

This aircraft design, as for most modern aircraft, uses a glass cockpit configuration for displaying the instrumentation. In a glass cockpit, information can be shown selectively. Not all information that the pilot can perceive from his/her instruments is relevant during every stage of flight. Therefore, in a glass cockpit, the pilot can choose which information should be displayed. This is an advantage over analog cockpits, since information can be visualized more clearly.

It is recommended to look at off the shelf flight decks for the FBW trainer. These flight decks already contain all required instrumentation display capabilities for VFR and IFR. The flight decks have to be connected to the appropriate sensors to display all information. Two example manufacturers offering off-the-shelf flight decks are Garmin and Avidyne.

10.4 Avionics

This section discusses the avionics elements of the aircraft, starting with the sensors, followed by a discussion of the flight control computer and the recording of flight data.

10.4.1 Sensors
The Fly-By-Wire operation of the aircraft requires airdata, location, attitude and angular rate data as input to the feedback loop.

Airdata is provided with basic pitot tube setup and temperature measurement. The angle of attack may be measured using a system based on differential pressure measurement. It is simple, there is experience with this kind of system and it is used in small aircraft and even in fighter aircraft. [100–102]

In order to avoid one-wing stalls, a sideslip sensor is most likely required for the FBW system. It is assumed that a sensor similar to the angle of attack sensor can be used for the sideslip angle, as no specific information on such sensors could be found. There might be a way around implementation of this sensor using software analysis of other measurements.

An Attitude and Heading Reference System (AHRS) could provide 3-axis information on orientation and roll rates of the aircraft. This attitude information is required for regular flight as well as being necessary for the Flight Envelope Protection system. A possible AHRS system such as the Athena 411, which is an integrated system developed by Rockwell Collins, provides heading, location and 3-axis attitude information. [103]

10.4.2 Flight Control Computer
Computations for the FBW system are performed in the Flight Control Computers (FCC). The FCC take input from the various sensors located throughout the aircraft and uses flight control law algorithms to decide on an aircraft response. It is an essential element of the FBW and FEP systems.

Autopilot systems are already incorporated in existing GA aircraft, example systems are the Avidyne DFC90 [104] or the Garmin GFC700 [105]. The systems use servos to actuate the mechanical control system already in place. Both the Avidyne and Garmin systems already employ flight envelope protection.

A FBW system that is safety-critical and the main control system of the aircraft will have to be certified according to much stricter standards than a separate autopilot.

10.4.3 Flight Data Recorder
A valuable addition for training flight is a Flight Data Recorder for recording the control inputs and associated aircraft response. The flight instructor is then able to obtain this information from the aircraft after flight for student debrief. It opens up options of detailed examining of student actions, explaining situations and the associated appropriate response whilst on the ground.

10.5 Propulsion
The propulsion subsystem is one of the main subsystems of the aircraft. It provides ground maneuverability as well as thrust to take flight and stay airborne. The FBW trainer will be a single-engine aircraft.

A hybrid or even full electric solution has been considered. In terms of sustainability, an electric aircraft has the advantage since the aircraft has much lower carbon emissions during operations. Also, an electric aircraft is much cheaper to maintain, causing the DOC to drop considerably. Airbus, for example, is developing a light electric aircraft [106].

However, the maximum flight time of such a two-seated, electrical aircraft is less than one hour at the moment, due to the limitations of electric batteries. This makes such a solution unsuitable for cross-country flights required in PPL training. Furthermore, the development risk associated with an electric solution is considered too high when combined with the risk already taken in developing a FBW system for the trainer. Therefore, hybrid or electrical solutions are discarded. It must be noted that future trainers might exploit hybrid or full electrical solutions, however.

The aircraft will be powered by a piston engine. Piston engines are relatively cheap and usually the engine-of-choice for small aircraft. Some piston engines used in aviation run on automotive fuel, decreasing the DOC of such an engine with a considerable amount.

With the MATLAB tool created it was possible to determine the minimum required power to fulfill the performance requirements. It was found that at least 96 metric horse power are needed. There are a lot of different engine manufacturers that sell engines in the range of 100 horse power. However most of these engines are not certified according to FAR 33. In Table 10.1 all found certified engines in the required power range are listed.

Table 10.1: FAR33 certified engines considered for the aircraft [12, 18, 24, 46–49]

Manufacturer	Model	Power (kW)	SFC (g/kwh)	Weight (kg)	TBO (hr)	Price (Eur)	Fuel
Rotax	912S	73.5	285	63.70	2000	21000	MoGas
Rotax	914F	84.5	276	75.50	2000	?	MoGas
Continental	O-200	73.5	321	90.26	2000	20000	AvGas
Lycoming	O-235	84.5	286	111.13	2400	29700	AvGas
Centurion	Centurion 2.0	99.0	214	134.00	1500	?	Diesel/Jet A

By examining the values it becomes clear that the best engine is the Rotax 912S. It is by far the lightest engine, has a good SFC and a low price. Further it operates on MoGas which is a lot cheaper than AvGas. DOC are discussed in more detail in Chapter 14. The Centurion engine is interesting because it uses Diesel fuel which has a higher energy density. This is also the reason for the low SFC. For this aircraft however the engine is overpowered and almost double the weight of the Rotax 912S.

10.6 Electrical Power

In this chapter the electrical power system is discussed. First, some general information is given on the electrical power that is extracted from the engine. After that some specific attention is given to the power required for the FCS actuators. Finally, the sizing of the battery system is performed resulting in a new weight and volume estimation for the battery system.

10.6.1 Extracted power

Power is extracted from the engine to feed subsystems that are crucial to the proper operation of the aircraft. Power can be extracted either mechanically or electrically, most commonly using a generator. This section shortly discusses the amount of power being extracted from the engine.

Mechanical power is taken from the engine mainly to feed the fuel pumps and pumps for hydraulic systems. In this aircraft, hydraulics are used only for the braking system in the landing gear, which is a closed system that does not require pumps. Furthermore, the fuel feed system may also be powered by an electrical pump. Extracting mechanical power from the engine is therefore not necessary.

Electrical power is extracted from the engine through the use of a generator, connected to the engine. For this particular aircraft, electrical power is extracted for the following systems:

- Exterior and interior lighting;
- Avionics (including FCS sensors, cockpit instruments & communication equipment);
- Fuel pump;
- FCS actuators;

For avionics, a continuous power requirement of 120W is assumed [64]. As an educated guess, a continuous power of 200W for the exterior and interior lighting is assumed. For the fuel pump a continuous power of 60W is assumed.

The power consumption of the FCS actuators is quite crucial for this design and will therefore be treated in more detail in the following section.

10.6.2 Power Requirement Actuators

In this section, the required power of the FCS actuators is determined. In the first subsection, some requirements will be discussed. Then, the used method will be described. A distinction is made between the actuation sizing of the FBW with mechanical backup and the full FBW systems. In the third subsection the results will be presented and discussed. In the final subsection a conclusion will be presented, which also includes suggestions for further research.

Requirements

In order to properly size the actuation system, some CS23 requirements should be taken into account. First of all, requirements exist on the maximum force the pilot is allowed to experience in the FCS. These requirements are important to take into account when a mechanical system with added servo motors is being used. Furthermore, the stick force per g requirements should be taken into account. These requirements exist so as not to let the pilot overstress the aircraft too easily. The most relevant requirements for the actuation sizing are summarized in Table 10.2.

Requirement CONS-LEG-CS23-FP-21 is relevant for a system with a mechanical linkage. For a full FBW system, this force feedback must be added artificially and thus this requirement becomes obsolete.

Method

This section discusses the method used to determine the required electrical power for the flight control actuation. Two different methods are described, for a control system with mechanical backup and for a full FBW control system. The dimensions and mass of the actuation system are related to the required output power and will therefore be determined based on the results presented in this section.

FBW with mechanical backup

In this system, a mechanical system will be augmented with servo motors in order to provide FEP capabilities. The servos will be connected to the standard mechanical system. To give the servo motors the capability to help the pilot in dangerous situations, they must be sized such that forces applied by the pilot may be overcome. Therefore the requirements on maximum control forces experienced by the pilots, found in Table 10.2 become relevant. Also, the stick force per g requirement for the elevator in requirement CONS-LEG-CS23-FP-32 must be met.

For the sizing of the actuators, the assumption is made that the maximum force exerted by the pilot is equal to the maximum allowed forces dictated by CS23 regulations. The actuators will be sized assuming this maximum force is applied by the pilot, assuming a stick length of 0.5m.

Table 10.2: Requirements for the flight control system [40, 50].

Requirement ID	Requirement
CONS-LEG-CS23-FP-08	The stick force shall, under no circumstance (not even for temporary application), be higher than 267N for pitch.
CONS-LEG-CS23-FP-09	The stick force shall, under no circumstance (not even for temporary application), be higher than 133N for roll.
CONS-LEG-CS23-FP-13	The rudder pedal force shall, under no circumstance (not even for temporary application), be higher than 667N for yaw.
CONS-LEG-CS23-FP-14	The pitch control force for prolonged application shall not exceed 44.5N.
CONS-LEG-CS23-FP-15	The roll control force for prolonged application shall not exceed 22N.
CONS-LEG-CS23-FP-16	The yaw control force for prolonged application shall not exceed 89N.
CONS-LEG-CS23-FP-21	The stick force shall vary with speed so that any substantial speed change results in a stick force clearly perceptible to the pilot.
CONS-LEG-CS23-FP-32	The elevator control force needed to achieve the positive limit maneuvering load factor may not be less than $W/14N$ (where W is the maximum weight in kg), or 66.8N, whichever is greater, except that it need not be greater than 156N, for stick controls.

FULL FBW SYSTEM

In order to compute the required output power of the actuators the first step is to compute the aerodynamic hinge moments on the control surfaces. The calculation of the hinge moments is performed in Section 7.3.

$$P_{req} = M_h \omega \tag{10.1}$$

The computation of the required power using the hinge moments is given in Equation (10.1), where ω is the deflection rate of the respective control surface in rad/s. The deflection rates are dictated by CS-23 requirements and are given in Table 10.3, with representative maximum deflections of the control surfaces and the corresponding rotation speeds.

Table 10.3: Reference control surface deflections of a general aviation aircraft with the recommended deflection rates according to CS-23 [40].

Control Surface	Time [s]	Max. Deflection [deg]	Speed [deg/s]
Ailerons	0.2	± 17	85
Rudder	0.3	± 25	83.3
Elevator	0.2	± 25	125
Flaps	4	-40	10

In order to reach maximum deflection of each control surface within the times specified in Table 10.3, two different methods can be used. The first is to assume constant output power, with a varying rotational speed. The second method is to assume constant rotational speed, which leads to a varying output power.

When assuming constant power, the rotational speed varies as a function of the hinge moment acting on the control surface. The minimum required power should be computed bearing the deflection times documented in Table 10.3 in mind. The time to rotate the control surface over a certain deflection is given by Equation (10.2) (example with elevator deflection, also applicable to ailerons and rudder).

$$t_{rot_{\Delta\delta_e}} = \omega \cdot \Delta\delta_e \tag{10.2}$$

$$t_{rot_{\Delta\delta_e}} = \frac{P}{M_h}\Delta\delta_e \tag{10.3}$$

Finding ω from Equation (10.1) and rewriting yields Equation (10.3). When applying Equation (10.3) for the full range of motion of the control surface and summing all rotation times, the total time to rotate the control surface from neutral to full deflection is computed.

$$t_{rot} = \sum_{\delta_e=0}^{\delta_e=25} t_{rot_{\Delta\delta_e}} \tag{10.4}$$

In order to find the minimum required power to reach the specified rotation time, an initial value for the actuator output power is chosen. The total time to deflect over the full range of deflection angles for each specific control surface is computed according to Equation (10.4), using the initial value for the power. This process is iterated, decreasing the power as needed in order to meet the deflection time requirement using minimum actuator power.

When assuming constant rotational speed, the speeds documented in the last column of Table 10.3 should be used. In this method, the required output power is a function of the hinge moment. Since the hinge moment varies with control surface deflection, a plot can be made showing the required actuator power at a certain control surface deflection.

In both methods, a check is implemented to see if the hinge moments in certain flight conditions are too excessive for the pilot to handle. In case of a FBW system with a mechanical back up this can impose regulatory problems, since regulations pose limits on the control forces that a pilot is allowed to experience [40].

Using the above-mentioned methods, the required actuator power is computed for the full range of deflections of the respective control surface (see Table 10.3), in varying flight attitudes. The air speed used in computation is the design maneuvering speed, V_A. For the elevator and the ailerons, the required power is computed for a range of AoA of 0 – 10 degrees, which is the expected range of AoA during flight. The required power for the rudder is computed for a sideslip angle range of 0 – 20 degrees, in order to meet requirements on demonstrated crosswind [50].

Results & Discussion

This section discusses the results obtained from the above mentioned method. The power required for the control surfaces will be computed as a function of control surface deflection and compared under different circumstances.

Elevator

Using the hinge moments computed in Section 7.3 for the elevator and a rotation speed of 125 [deg/s] (see Table 10.3 yields the following results. Figure 10.4 shows how the power required for the elevator actuator changes when the aircraft is flown at a different angle of attack. At $\alpha = 0[deg]$ the power required shows a symmetrical trend over the range of elevator deflections, as is expected since a symmetrical airfoil is used. When the aircraft is flown at $\alpha = 10$ [deg] the power distribution shifts. It is observed from Figure 10.4 that the maximum required power occurs at $\alpha = 10$ [deg] with maximum positive elevator deflection. Therefore, further comparisons are made using the most demanding case at an angle of attack of 10 [deg].

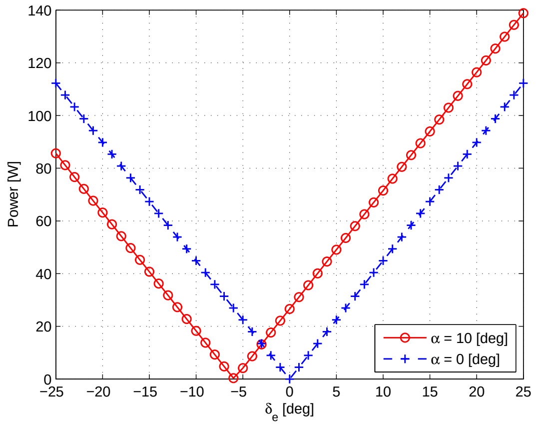

Figure 10.4: Power required for elevator actuator as a function of elevator deflection, variation with AoA

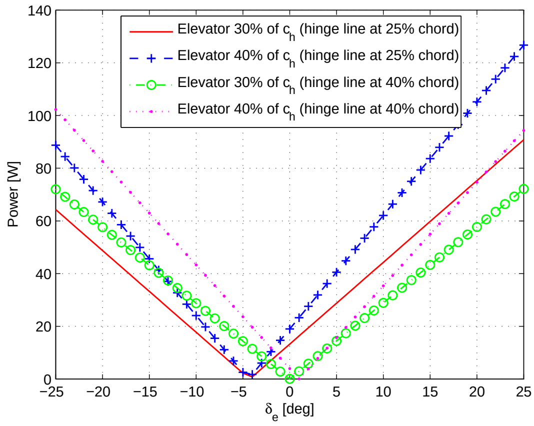

Figure 10.5: Power required for elevator actuator as a function of elevator deflection, variation with elevator size

A control surface must be sized such that the aircraft is controllable. However, the size of the surface also influences the hinge moments and therefore the required actuator power. Figure 10.5 shows this comparison. As is observed, reducing the control surface area reduces the required power most significantly at high elevator deflections.

Changing the location of the hinge line also influences the required actuator power. This is illustrated in Figure 10.6. It is observed that the required maximum power at positive deflections decreases when the elevator hinge line is moved further aft.

It is interesting to look at the average power required for the elevator when operating it with a constant rotation speed. The average and maximum power required for the elevator in different configurations is documented in Table 10.4. The first column specifies the location of the hinge line as a function of the elevator chord. The second column specifies the chord-wise size of the elevator as a fraction of the total horizontal stabilizer chord.

Aileron

The ailerons provide roll control for the aircraft. Required power for the actuators of one aileron is computed in the same fashion as for the elevator. The results are presented here. Again, the power required for the ailerons is computed with different configurations, changing the Aoa, the hinge line location and the control surface area. It is found that the behavior of the required power for the ailerons is analogous to that of the elevator.

As for the elevator, it is observed from Figure 10.7 that the required power shifts, and maximum required power increases, as the AoA increases. Comparisons for aileron size and hinge line location are therefore performed with $\alpha = 10$deg. From Figure 10.8 it is observed that required power decreases with a decreased control surface size. This is in line with expectations. From computations performed in Section 7.2.1, an aileron size of 20% of the wing chord is sufficient in terms of controllability of the aircraft.

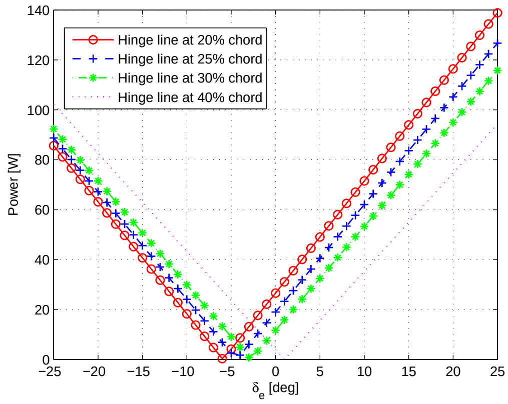

Figure 10.6: Power required for elevator actuator as a function of elevator deflection, variation with hinge line location

Table 10.4: Average and maximum power requirement for the elevator; rotation over the full range of motion with a constant speed of [125 deg s^{-1}] ($\alpha = 10$[deg])

Location hinge line $\left[\frac{1}{c_e}\right]$	$\frac{c_e}{c_h}$ [-]	P_{avg} [W]	P_{max} [W]
0.20	0.40	60.3	138.9
0.25	0.30	40.7	90.8
0.25	0.40	56.6	126.7
0.30	0.40	53.7	115.8
0.40	0.30	36.8	72.1
0.40	0.40	50.2	102.3

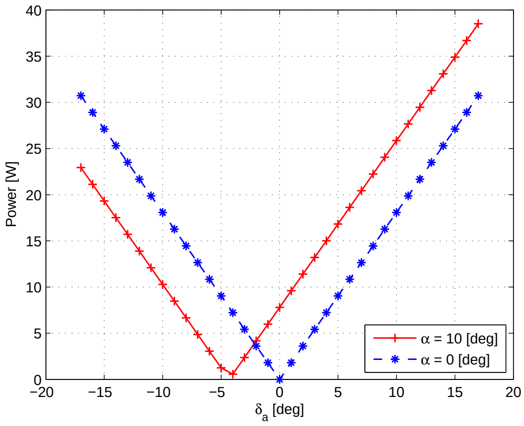

Figure 10.7: Power required for one aileron actuator as a function of aileron deflection, variation with AoA

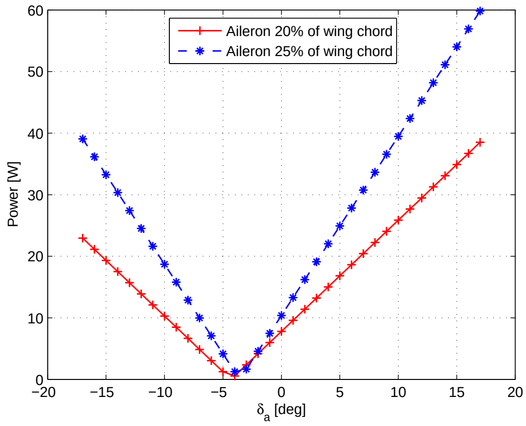

Figure 10.8: Power required for one aileron actuator as a function of aileron deflection, variation with aileron size

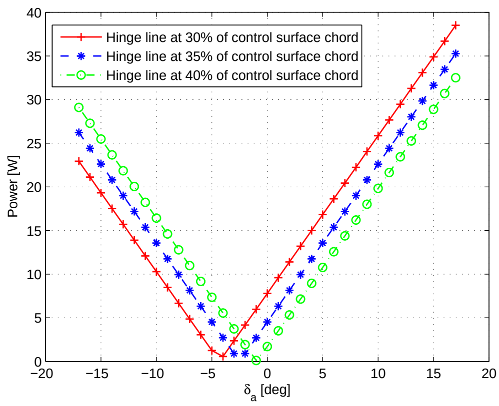

Figure 10.9: Power required for one aileron actuator as a function of aileron deflection, variation with hinge line location

From Figure 10.9 it is clear that required maximum power decreases when the location of the hinge line is shifted further aft of the control surface chord.

The average and maximum power requirements for each aileron configuration considered are tabulated in Table 10.5.

Table 10.5: Average and maximum power requirement for one aileron; rotation over the full range of motion with a constant speed of [85 deg s^{-1}] ($\alpha = 10$[deg])

Location hinge line $\left[\frac{1}{c_a}\right]$	$\frac{c_a}{c_w}$ [-]	P_{avg} [W]	P_{max} [W]
0.30	0.20	16.8	38.5
0.30	0.25	26.5	59.8
0.35	0.20	16.1	35.3
0.40	0.20	15.9	32.5

It is observed that one aileron requires significantly less power on average than the elevator. The two aileron actuators together will have a rough average power consumption of 32W when taking $0.2c_w$ as the aileron chord. This is roughly half of the average power consumption of the elevator actuator, which is in line with FAR rules of thumb for the ratio between control surface forces [81].

Rudder

Finally, the results are presented for the required power of the rudder actuator. The results are, as expected, similar to those of the elevator and aileron controls.

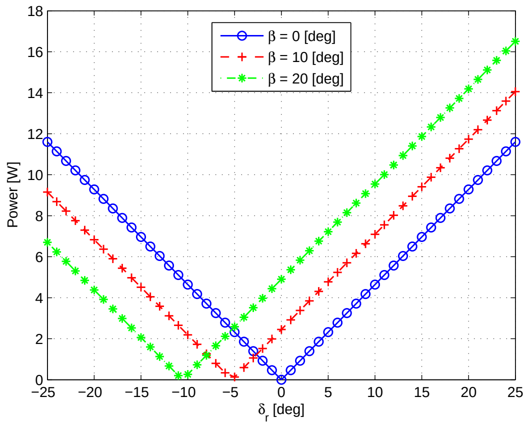

Figure 10.10: Power required for the rudder actuator as a function of rudder deflection, variation with side-slip angle

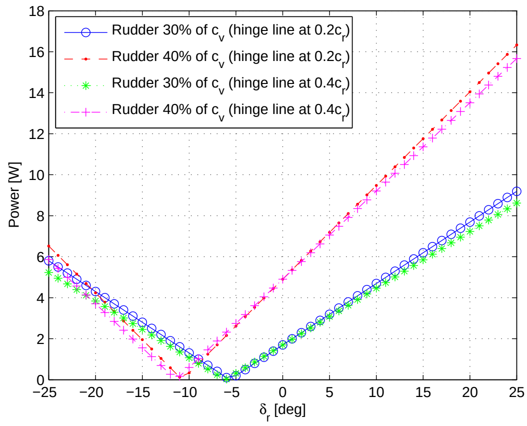

Figure 10.11: Power required for the rudder actuator as a function of rudder deflection, variation with rudder size

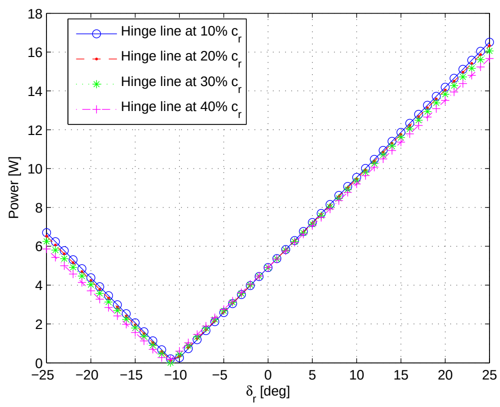

Figure 10.12: Power required for the rudder actuator as a function of rudder deflection, variation with hinge line location

Figure 10.10 shows that the power required for the rudder actuator varies with the side-slip angle as that for the elevator and aileron changes with angle of attack. Also, the required power decreases significantly when the rudder is decreased in size. This is observed from Figure 10.11. From Figure 10.12 it appears that the power required for the rudder is not significantly influenced by the location of the hinge line.

Again, the average and maximum power required during operation of the rudder is considered. The results are documented in Table 10.6.

Table 10.6: Average and maximum power requirement for the rudder; rotation over the full range of motion with a constant speed of 83.3 [deg s^{-1}] ($\beta = 20$ [deg])

Location hinge line $\left[\frac{1}{c_r}\right]$	$\frac{c_r}{c_v}$ [-]	P_{avg} [W]	P_{max} [W]
0.10	0.40	6.9	16.5
0.20	0.30	4.0	9.2
0.20	0.40	6.9	16.3
0.30	0.40	6.7	16.1
0.40	0.30	3.7	8.6
0.40	0.40	6.6	15.7

It must be noted that the results for the rudder actuator are considered to be very low, and are not in line with the rule of thumb in [81], which states that the rudder usually experiences the highest control force. The reason for the low computed power for the rudder actuator is unclear at the moment of writing and should be investigated in future studies. The results for the power required for the rudder actuator are not considered completely valid.

CONCLUSION & RECOMMENDATION

In this final section, the total power required for the flight control actuation system is computed, which is used to determine the required battery size in Section 10.6.3. Also, some recommendations for further studies are given.

The powers in this section are computed considering the configuration with a mechanical back up. The power is determined such that the actuators are able to cope with the aerodynamic loads (hinge moments) experienced during flight. In a mechanical back-up system, the actuators may be required to overrule pilot input as well. This will require stronger actuators. However, in order to compute the total power required for the actuators, this is not taken into account. The reason for this is the uncertainty in required FBW authority in order to provide sufficient control input to restore the aircraft from dangerous attitudes and prevent accidents. The amount of required authority in a system with mechanical back-up is dependent on the dynamic behavior of the aircraft, which is yet to be determined.

Table 10.7: Power required for the FCS actuation system

Control surface	P_{avg} [W]	P_{max} [W]
Elevator	60.3	138.9
Aileron	16.8	38.5
Aileron	16.8	38.5
Rudder	6.9	16.5
Total	100.8	232.4

The total power required for the flight control actuation system is documented in Table 10.7. As can be seen the total average power required is $100.8W$ and the peak power required is $232.4W$. It must be noted that this is the output power of the actuators and not the required electrical power. No actuator efficiencies have been taken into account in these computations. The values in Table 10.7 are considered to be the highest required values for the actuator power. In a full FBW system the required power, and thus actuator size, may be reduced by reducing the hinge moments on the control surfaces. The option of splitting control surfaces is also considered to lower the required power for the actuators. Even though this graceful degradation principle requires a higher number of actuators, they each operate a smaller surface with a smaller hinge moment. Therefore the continuous amount of power required for actuation of the conrol surfaces in a graceful degradation configuration is expected to be smaller than the values presented in Table 10.7.

In order to reduce required actuator power in a full FBW system, the hinge moments may be reduced. To achieve reduced hinge moments, the control surfaces can be balanced. Another option is to vary the location of the hinge line of a control surface. One way of balancing a control surface is by adding a horn balance. A horn balance is a small area of the control surface in front of the hinge line. Figure 10.13 is an example of such a horn balance. This part of the control surface will reduce the hinge moment by producing an additional force, counteracting aerodynamic forces. The price of a decreased hinge moment is added weight and an increase in drag. However, the required power will be less which results in smaller actuators and a decrease in actuator weight.

Using control surface balancing can reduce the hinge moments acting on the control surface with 20% [92]. This would allow the actuators to be scaled down. However, adding such balance horns will increase the drag and the weight of the control surface. Further reduction of the hinge moments may be realized by optimizing surface area of the control surface and location of the hinge lines.

It is suggested to further investigate the aerodynamic and mass penalties caused by reducing the hinge moments. Potentially, reducing the hinge moments can lead to a significant reduction in the actuator mass and volume. This

Figure 10.13: Example of a horn balanced rudder on a Beech E-18S Super 18 [7]

would allow for easier incorporation of higher levels of redundancy, which might expedite certification procedures. However, if reducing the hinge moments comes at a too high price in terms of aerodynamics, it might negatively influence the design to an unacceptable level. Also, further study is recommended in the area of optimizing the control surfaces for adequate control with a minimum control surface area and to find the optimum hinge line location in order to reach minimum hinge moments.

10.6.3 Battery sizing

The aircraft will contain batteries for two main reasons. To cope with peak loads during demanding use of the electronic FCS and in order to provide the aircraft with electrical power in case of an engine out situation. The batteries will be fed continuously from the generator incorporated in the engine. For more information on the engine selection and the generator, the reader is referred to Section 10.5. To determine the required energy from the batteries, the engine out situation is considered leading. The batteries must be able to provide the aircraft with enough electrical power to allow the pilot to safely land the aircraft. This is especially demanding in the full FBW configuration, since loss of electrical power in this case would mean total loss of control.

In a full FBW system, double redundancy in the batteries is used in order to decrease the probability of losing control of the aircraft. In order to compute the electrical power that is required to be stored, an actuator efficiency of 80% is assumed [39]. In case of an engine out situation at cruise altitude, a time of 30 minutes is assumed for the battery sizing. Equation (10.5) is used to compute the required battery energy to safely operate the aircraft in an engine out situation.

$$E_{req} = P_{req} t_{glide} \tag{10.5}$$

Using the values from Section 10.6.1 for the avionics, lighting and fuel pumps and the values from Section 10.6.2 for the flight control actuation, the total required electrical power can be computed.

From Section 10.6.2 the output power of the actuators is known. To find the required electrical power, the efficiency of the actuators should be taken into account. The efficiency is assumed to be 80% [39]. The required continuous power is assumed to be equal to the average required power of the actuators. The peak load is assumed equal to the maximum power required for the actuators. Taking the before mentioned efficiency into account, the continuous power requirement for the actuators is assumed to be 126W, and the maximum power requirement is 290.5W.

It must be noted that the required power for the actuators is computed over the full range of deflection of the control surfaces, and therefore the continuous power assumed is quite conservative. More detailed analysis of the aircraft dynamic behavior to control input is required in order to determine a more suitable range of control surface deflections. This will give a better estimation of the continuous power requirement for the flight control actuation.

Table 10.8: Required electrical power for the aircraft

Control surface	P_{cont} [W]	P_{peak} [W]
FCS actuation	126.0	290.5
Lighting	200.0	200.0
Avionics	120.0	120.0
Fuel pump	60.0	60.0
Total	566.0	670.5

The total electrical power extracted from the engine is now documented in Table 10.8. It is assumed that during normal operations, the generator incorporated in the Rotax 912 engine can cope with the electrical power demand of the aircraft. In case of an engine-out situation, the battery packs must provide the electrical power in order to reach the ground in a safe manner. The value of continuous power from Table 10.8 will be used to size the battery pack (e.g. P_{req} in Equation (10.5) is equal to the total P_{cont} in Table 10.8).

Table 10.9: Estimated battery mass and volume for Li-Ion and Ni-Cd batteries with a safety factor of 1.5, assuming 283Wh required energy and dual redundancy

Battery type	Energy specific weight [Wh/kg]	Energy specific volume [Wh/L]	Estimated mass [kg]	Estimated volume [L]
Li-Ion	240	600	3.54	1.42
Ni-Cd	90	150	9.43	5.66

Assuming $t_{glide} = 30min = 0.5$hr, the total required energy from the batteries is 566.0(0.5) = 283Wh. A comparison between different battery types was performed in [64]. Two types of batteries are considered here. Li-Ion batteries and Ni-Cd batteries. The battery weight and volume estimated are tabulated in Table 10.9. A safety factor of 1.5 has been taken into account, and the estimated mass and volume already include a duel redundant battery system.

As can be seen, a Li-Ion battery system is superior in terms of weight and volume. However, as is observed from operations of the Boeing 787, Li-Ion batteries can give large problems during operation [107]. Also, the purchase cost of Li-Ion batteries is higher than that of Ni-Cd batteries and the life cycle of Li-Ion batteries is lower.

In order to reach a conclusion about which type of battery to use, it is important to research the exact effect of the additional weight of Ni-Cd batteries as compared to the additional cost of Li-Ion batteries. By conducting this research a conclusion can be drawn if the additional DOC leading from a higher aircraft weight are worth the decrease in purchase cost of the Ni-Cd batteries as opposed to the Li-Ion batteries. This conclusion should be drawn in future work.

11
Design Integration

The purpose of this chapter is to give a short and concise overview of the aircraft design. In the first section a general overview of the aircraft parameters is given. In the second section the total mass breakdown is presented, including center of gravity locations. Also, the loading diagram is presented in this section.

11.1 Aircraft parameters

This section summarizes some of the most important aircraft parameters. The overview is given in Table 11.1.

Table 11.1: Overview of the

Aircraft parameters					
Wing			**Horizontal tail surface**		
AR_w	10	[-]	AR_h	4.30	[-]
S_w	11.43	[m^2]	S_h	1.96	[-]
b_w	10.69	[m]	b_h	2.90	[m]
c_w	1.07	[m]	c_h	0.67	[m]
λ_w	0.90	[-]	λ_h	0.50	[-]
Λ_w	2	[deg]	Λ_h	5	[deg]
$\left(\frac{t}{c}\right)_w$	0.16	[-]	$\left(\frac{t}{c}\right)_h$	0.12	[-]
Vertical tail surface			**Aerodynamic properties**		
AR_v	2	[-]	$C_{L_{cruise}}$	0.34	[-]
S_v	0.68	[m^2]	$C_{L_{max_{clean}}}$	1.6	[-]
b_v	1.17	[m]	$C_{L_{max_{takeoff}}}$	1.6	[-]
c_v	0.58	[m]	$C_{L_{max_{landing}}}$	1.9	[-]
λ_v	0.50	[-]	$\frac{L}{D}_e$	13.6	[-]
Λ_v	22.9	[deg]	$\frac{L}{D}_r$	11.4	[-]
$\left(\frac{t}{c}\right)_v$	0.12	[-]			
Design speeds					
V_a	57.5	[m s^{-1}]			
V_c	58.0	[m s^{-1}]			
V_d	86.0	[m s^{-1}]			
$V_{s_{clean}}$	23.6	[m s^{-1}]			
$V_{s_{landing}}$	21.7	[m s^{-1}]			

11.2 Mass Budget

To determine the mass budget, the Class II weight estimation from Roskam has been used for the majority of the components. Where more detailed design was done, better estimates were used from those areas. This was the case for all of the fixed equipment items and the landing gear. For the fuselage- and wingstructure, a detailed analysis was done, giving more detailed component masses. All of the locations of center gravity were also determined, either using definitions from Roskam or making a reasonable estimation. All of these results are presented in Table 11.3. One thing to note is that there is still a contingency weight available of 10 kg, for which no center of gravity location is defined. The presented results apply for the FBW system with mechanical back-up; the weight of the flight control system increases for full FBW systems with increasing redundancy(See Table 11.2). As an estimation, two-thirds of the mechanical flight control system are kept, as there will still be flight controls throughout the aircraft, and extra actuators are added. This affects all of the different components and leads to a higher MTOW.

For some components a distribution was assumed, used in further structural analysis. The weight of the flight control system was assumed to be equally distributed between the main wing and the horizontal tail. For the dis-

Table 11.2: MTOW for different configurations

FBW with Mechanical backup	FBW and 4x Redundancy	FBW and graceful degradation
636.8 kg	681 kg	628.8 kg

tributed load of the payload, DINED (anthropometric database) was used. There it was found that, for Dutch males between 20 and 30 years old, using the 82^{th} percentile, in 2004, the buttock-popliteal depth is 550 mm.

Table 11.3: Mass Distribution

	m		C.G. Location (x-direction)	
Engine Mass	101.0	[kg]	0.100 - 0.700	[m]
Nose Landing Gear Mass	6.6	[kg]	0.700	[m]
Rear Landing Gear Mass	24.6	[kg]	2.900	[m]
Fuselage Mass	92.1	[kg]	0.000 - 7.000	[m]
Horizontal Tail Mass	8	[kg]	6.100 - 7.000	[m]
Vertical Tail Mass	2.7	[kg]	6.216 - 7.000	[m]
Wing Mass	67.4	[kg]	2.100 - 3.100	[m]
Auxiliary Power Unit Mass	12.8	[kg]	3.000	[m]
Auxiliary Items Mass	4.3	[kg]	2.000	[m]
Flight Control System Mass	21.2	[kg]	3.100 - 6.500	[m]
Furnishing Mass	25.4	[kg]	2.000	[m]
Hydraulics, Pneumatics and Electrical System Mass	13.0	[kg]	2.100	[m]
Instrument and Avionics Mass	29.9	[kg]	2.000	[m]
Contingency Mass	10	[kg]	-	[-]
Fuel Mass	73.7	[kg]	2.100 - 2.389	[m]
Payload Mass	145	[kg]	1.725 - 2.275	[m]
Complete Aircraft	637.7	[kg]	2.079	[m]

Table 11.4 shows the effect of having different FBW systems with different redundancies. Of course, with increasing redundancy the weight also increases. However, using the graceful degradation the MTOW will actually decrease due to the smaller actuators. All of these options are still viable, but clearly the choice does have a big effect on final MTOW.

Table 11.4: MTOW for different FBW systems

FBW system	MTOW [kg]
FBW system with mechanical back-up	637.7
Dual redundant full FBW system	646.2
Triple redundant full FBW system	663.4
Quadruple redundant full FBW system	681.0
Dual redundant full FBW system with graceful degradation	628.8
Triple redundant full FBW system with graceful degradation	628.8

Figure 11.1 shows a pie chart with all of the different components of the aircraft. It contains both the absolute value of each component, but also the percentage of the MTOW it takes up.

Figure 11.2 illustrates the loading diagram of loading the payload and the fuel to the empty weight of the aircraft. Three different wing positions are shown: the original wing position, a 10% shift forward and a 10% shift towards the back. The original wing position is the middle one and this graph implies that the payload and fuel locations are roughly the same. The center of gravity shift in the entire mission will stay between 38 - 43 % of the chord length behind the leading edge of the MAC.

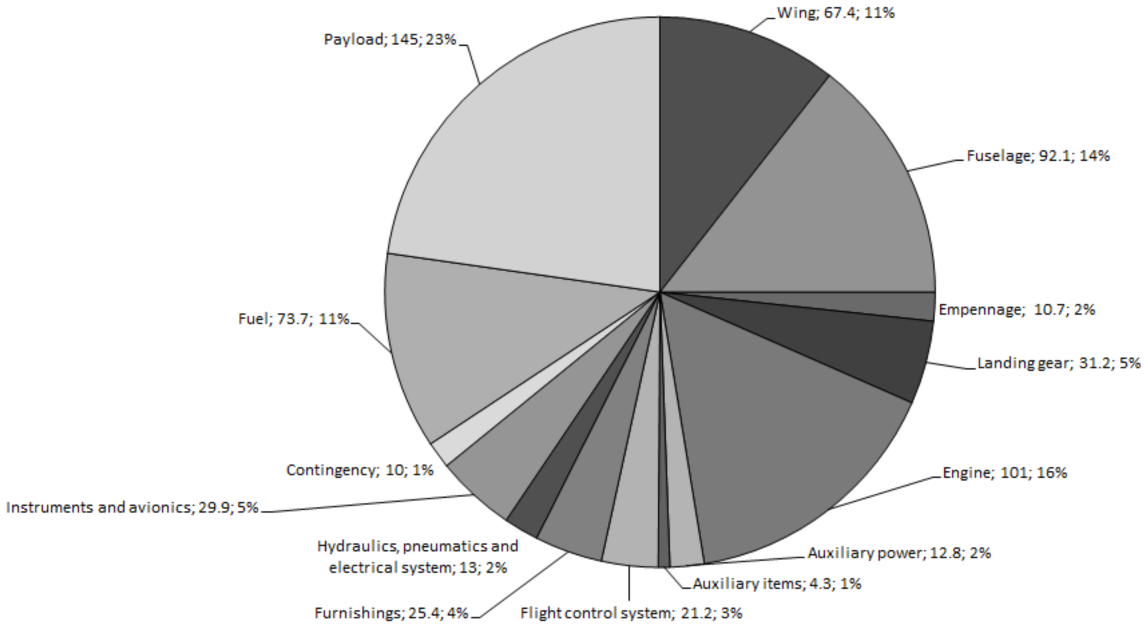

Figure 11.1: Weight distribution [kg, percent MTOW]

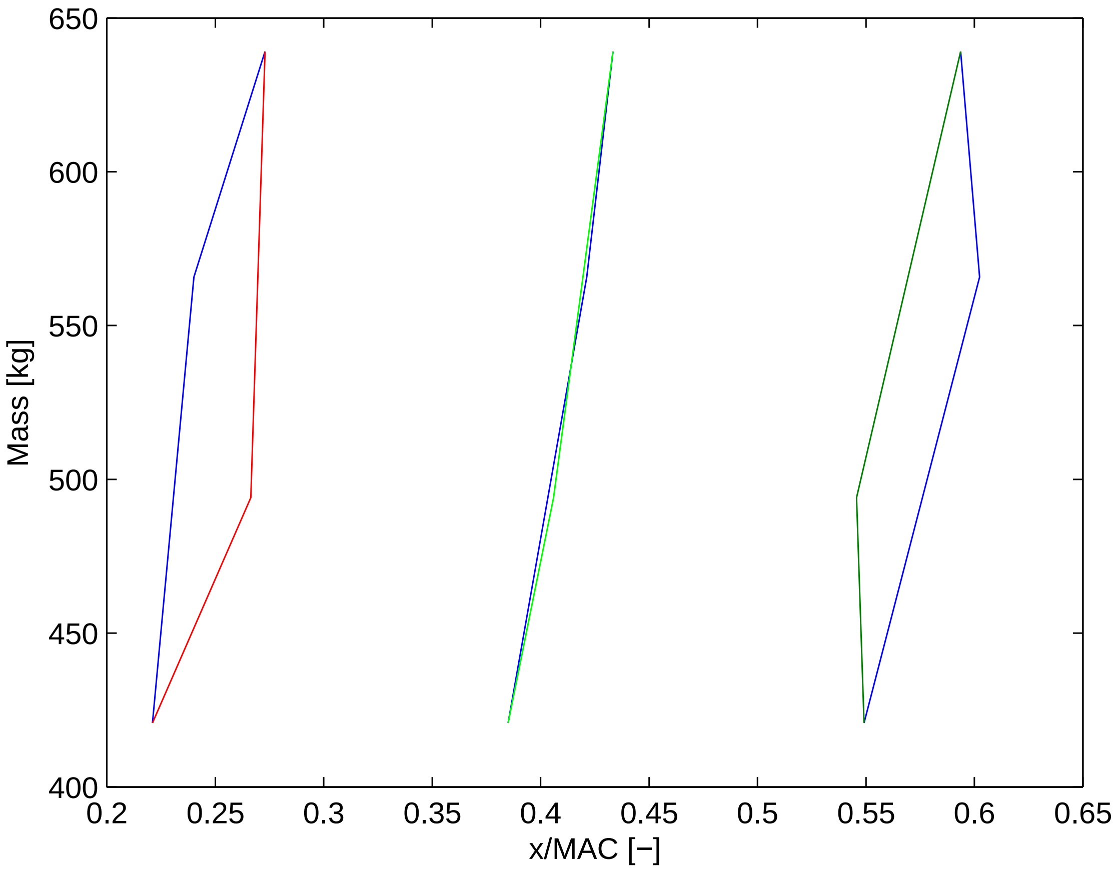

Figure 11.2: Loading diagrams

12
Operations and Logistics

The operations and logistics of the aircraft mainly consists out of maintenance related operations (inspections and repairs). Next to that, the operations which are needed after use of the digital parachute will briefly be explained.

12.1 Proposed System

Hangar: The aircraft can be parked outside, but it is recommended to store it in a protected place in order to increase its lifetime.
Runway: A runway for take-off and landing, either paved or a dirt road with a lenght of min. 400m. is needed.
Fuel station: A Fuel station is needed in order to refuel the aircraft at the home airport EURO95 or Avgas, depending on the chosen configuration.

12.2 Inspections

The first part of maintenance are the inspections of the aircraft. Several inspections have to be performed in order to ensure airworthiness of the aircraft. These inspections are explained in this section. Alternative inspection programs are not discussed in this section, as they mostly apply to commercial aviation.

12.2.1 Preflight Inspection

The preflight inspection is performed before every flight. The pilots checks everything in the cockpit, including the documentation of the aircraft. Next to that, the pilot has to check control surfaces, engine, landing gear and the structural integrity of the aircraft.

12.2.2 100 Hours Inspection and Annual Inspection

As the name already suggests, the 100 hours inspection has to be performed after every 100 flight hours. This inspection is only applicable when the aircraft is used to carry any person for hire or when it is provided by the flight instructor during flight instruction.

Next to that an annual inspection has to be performed. This inspection can only be performed by a mechanic with an inspection authorization.

The annual and 100 hours are similar in scope and detail. The specification of the inspections can be found in *14 CFR part 43* [108].

12.3 Repairs

Repairs are conducted after inspections have indicated failure of aircraft parts.

12.3.1 Preventive Maintenance

Preventive maintenance consist of the uncomplicated repairs and procedures, defined in 14 CFR [108]. All preventive maintenance may be performed by a certified pilot (this excludes student pilots and recreational pilots).

12.3.2 Minor & Major Repairs

Repairs have to be classified minor or major. Repairs which are considered major can be found in 14 CFR part 43, appendix A [108]. Major repairs can only be performed by a mechanic with inspection authorization at a certificated repair station with an appropriate rating.

Minor repairs can be performed by a certificated mechanic at a repair station with appropriated certification.

12.4 Digital Parachute

The deployment of the digital parachute indicates an emergency situation. In general, the emergency procedure of the airport where the autoland will be performed will have to be followed. When the aircraft has landed, the pilot's state has to be checked. When the digital parachute has been used because of the medical state of the pilot, a medical team has to take care of him/her.

After that, the aircraft can taxi to the hangar if the pilot is in healthy state or the aircraft has to be towed towards the hangar when the pilot is not uncooperative.

Researching and introducing such a system, including Hardware development is not feasible for a single company (see Section 8.3), as it involves high risks. Therefore a detailed study of this system is not included in this report now.

13
Project Design and Development Logic

This chapters gives an overview of the main steps that have to be performed in the post-DSE phase. The steps are visualized with block-diagrams and briefly described. In Figure 13.1 the main milestones are shown. For every main milestone a separate flow chart is made. It has to noted that some overlap exists between these steps as described in [60].

First the preliminary design has to be concluded, this requires the selection of a FBW system concept. Common choices and the influences on the design are discussed in Chapter 8. Thereafter the detailed design phase can start, this includes the refinement of the preliminary design down to smallest detail. This phase is followed by a testing phase which eventually leads to the issue of the type certification. Results of the testing phase might lead to changes in the design of the aircraft. After the type certification is issued the mass production phase can start. The major milestone of this phase is the start of the delivery phase. The product support has to start with the beginning of the deliveries of the aircraft.

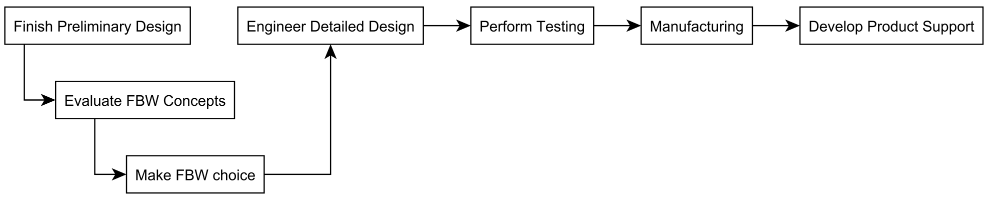

Figure 13.1: Flow chart of main steps to be complete until market introduction.

Block diagram for the detailed design phase is shown in Figure 13.2. In the detailed design phase more advanced tools are used like CFD and FEM programs. Further testing on the subsystems is done as well. Special attention has to be paid on the realization of the FBW system. Since certification is a major difficulty design iterations which may include changes in the preliminary design. Another major factor of this phase is the consultation with external companies for subsystems. This may include development of complicated components like hardware for the FBW system or just a supply contract for off the shelf components like rims.

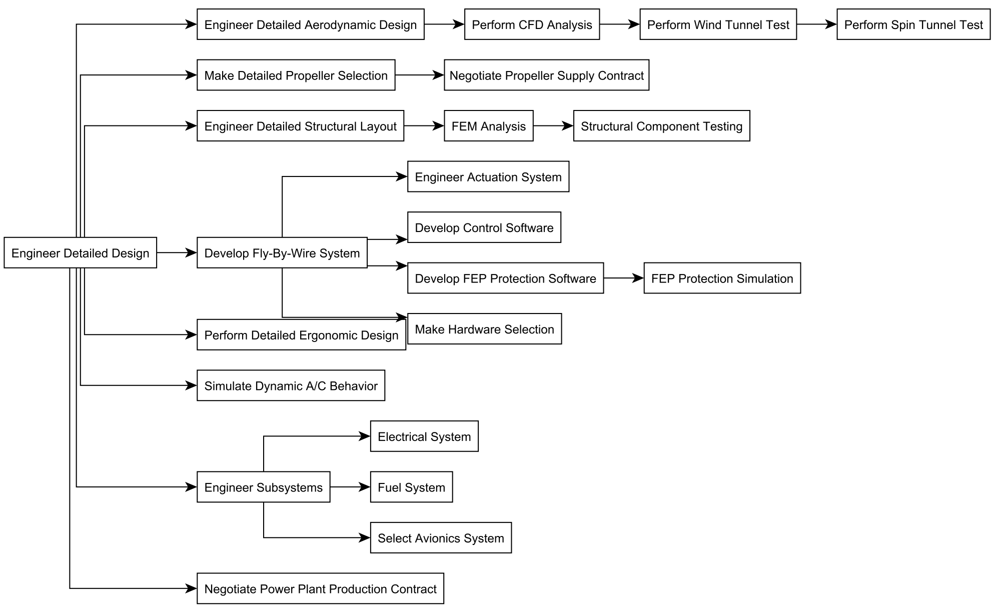

Figure 13.2: Block diagram of steps that have to be performed in the detailed design stage.

A flow diagram of the testing phase is given in Figure 13.3. Purpose of testing is to validate the design models used and verify that the technical requirements are met. The testing phase consists mainly of two parts. First the internal testing within the company and second the external testing with the flight authorities for receiving the type certification.

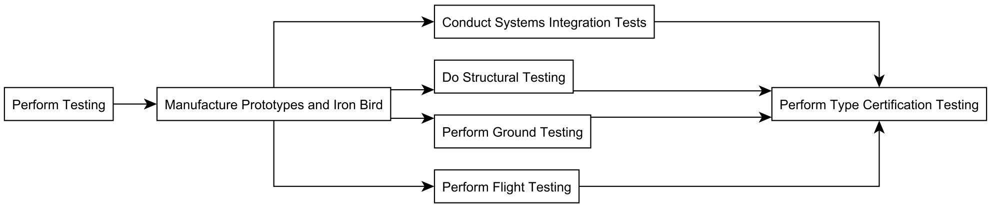

Figure 13.3: Block diagram for required testing procedure.

Close to the end of the testing phase the manufacturing phase can start. This phase is shown in Figure 13.4. At the beginning of the production phase organizational steps have to be taken. This might include the planning of the production processes, in other words how to assemble the aircraft the most efficient way. Another important factor is supply chain management to assure that the continuous supply of all materials and products is assured all the time during production and that eventual problems can be early detected and resolved. Other aspects of the supply chain management would the development of set of criteria the suppliers have to fulfill. Such a criteria could be an ISO 9001 certification. Introduction of lean manufacturing methods like six-sigma represent another important part of this initial phase. After planning is done the assembly of the aircraft can start. This is the point where eventually all previously performed parts come together. The final stage is the delivery of the aircraft. It has to be noted that this phase repeats and iterates itself during the whole length of production. For example advances made in the design require other part supplier or changes in the assembly line management might lead to reduce cost.

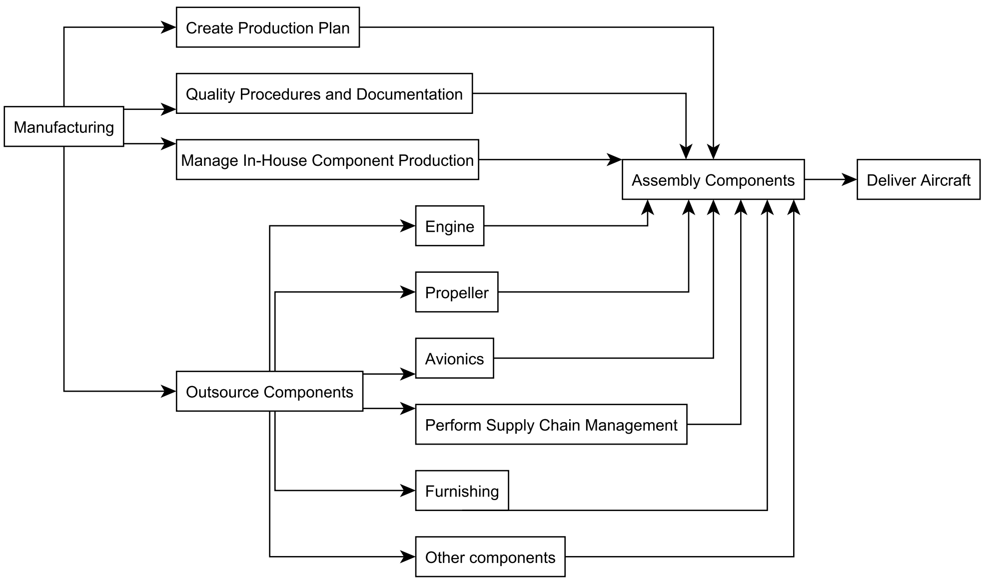

Figure 13.4: Flow chart for actions during manufacturing.

After the delivery of the aircraft has started the product support phase has to start. A flow diagram is given in Figure 13.5. Purpose of this phase is to help customers maintain their product and to invoke design changes in the current aircraft fleet. Often the support of the delivered aircraft is not directly done by the producer but by certified maintenance companies. They have to be controlled and their supply with spare parts has to be satisfied. Another part of the product support is to receive customer feedback which may include feedback on small design flaws, customer needs or safety critical design changes. This feedback is evaluated and finally a updated product is produced.

In this section the steps were presented that have to be performed in the post DSE-phase. It was shown that five major steps have to be executed until product market introduction can be reached. Refinement and a more in depth analysis of the above presented steps is needed to make an accurate planning.

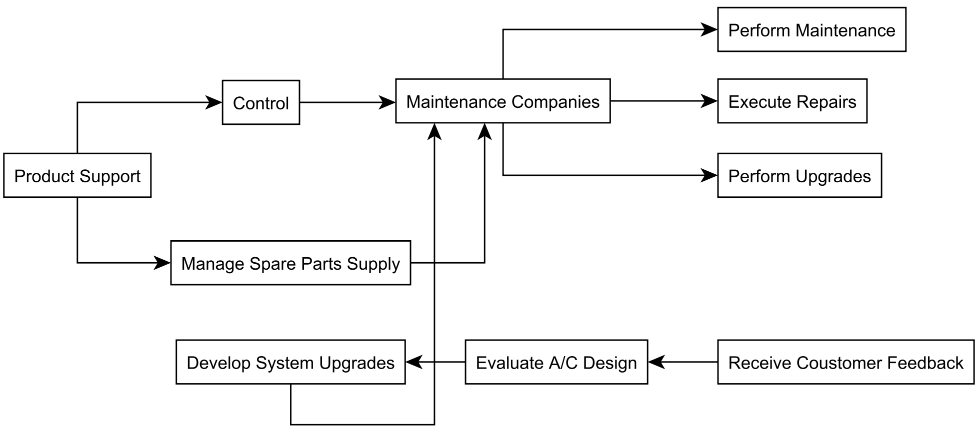

Figure 13.5: Support flow chart for actions after market introduction.

14
COST

14.1 PROJECT DEVELOPMENT COST

In order to estimate the selling price of the aircraft, project development cost has to be estimated. This will be done in Section 14.1.1. Next to that, the direct operation cost has to be estimated (and optimized), which will be discussed in Section 14.2.

14.1.1 EASTLAKE MODEL

The (base) model used is the Eastlake model [60]. This model has been adapted to incorporate FBW and has been build into a MATLAB script.

ENGINEERING

Engineering cost accounts for man-hours needed to design and perform the necessary research and development. Engineering cost is dependent on engineering hours (H_{ENG}), rate of engineering labor (R_{ENG}) and the consumer price index relative to 2012 (CPI_{2012}). When these parameters are known, the engineering cost can be calculated with Equation (14.1).

$$C_{ENG} = 2.0969 \cdot H_{ENG} \cdot R_{ENG} \cdot CPI_{2012} \tag{14.1}$$

The engineering hours are dependent on the weight of the airframe ($W_{airframe}$), maximum level speed (V_H), planned number of aircraft produced over a 5-year period (N) and composite compensation factor (f_{comp}). When these parameters are known, the engineering hours can be estimated with Equation (14.2).

$$H_{ENG} = 0.0396 \cdot W_{airframe}^{0.791} \cdot V_H^{1.526} \cdot N^{0.183} \cdot (1 + f_{comp}) \tag{14.2}$$

The composite compensation f_{comp} is a value between 0 and 1 corresponding to the fraction of the aircraft that is made out of composites. Airframe weight ($W_{airframe}$) can be estimated by subtracting avionics, engine and other fixed equipment weight from the empty weight.

Note: the factor 2.0969 in Equation (14.1) *is to compensate for changes since 1984.*

TOOLING

Tooling cost accounts for designing, manufacturing and maintaining all tools (such as jigs, fixtures and molds). Tooling cost depends on tooling hours (H_{TOOL}), rate of engineering labor (R_{TOOL}) and the consumer price index relative to 2012 (CPI_{2012}). When these parameters are known, the tooling cost can be calculated with Equation (14.3).

$$C_{TOOL} = 2.0969 \cdot H_{TOOL} \cdot R_{TOOL} \cdot CPI_{2012} \tag{14.3}$$

Where tooling hours are dependent on airframe weight ($W_{airframe}$), maximum level speed (V_H), planned number of aircraft produced over a 5-year period (N) and composite compensation factor (f_{comp}). When these parameters are known, the tooling hours can be estimated with Equation (14.4).

$$H_{ENG} = 1.0032 \cdot W_{airframe}^{0.764} \cdot V_H^{0.899} \cdot N^{0.178} \cdot \left(\frac{N}{60}\right)^{0.066} \cdot (1 + f_{comp}) \tag{14.4}$$

MANUFACTURING

Manufacturing cost accounts for all the labor cost needed to manufacture the aircraft. Manufacturing cost depends on manufacturing hours (H_{MFG}), rate of manufacturing labor (R_{MFG}) and the consumer price index relative to 2012 (CPI_{2012}). When these parameters are known, the manufacturing cost can be calculated with Equation (14.5).

$$C_{MFG} = 2.0969 \cdot H_{MFG} \cdot R_{MFG} \cdot CPI_{2012} \tag{14.5}$$

Where tooling hours are dependent on airframe weight ($W_{airframe}$), maximum level speed (V_H), planned number of aircraft produced over a 5-year period (N) and composite compensation factor (f_{comp}). When these parameters are known, the tooling hours can be estimated with Equation (14.6).

$$H_{MFG} = 9.6613 \cdot W_{airframe}^{0.74} \cdot V_H^{0.543} \cdot N^{0.524} \cdot (1 + 0.25 f_{comp}) \tag{14.6}$$

QUALITY CONTROL

The cost which is related to quality control accounts for technicians and equipment needed to demonstrate that the product is properly manufactured. The quality control cost is dependent on manufacturing cost (C_{MFG}) and a composites compensation factor (f_{comp}). The quality control cost can be calculated with Equation (14.7).

$$C_{QC} = 0.13 \cdot C_{MFG} \cdot (1 + 0.5 f_{comp}) \tag{14.7}$$

DEVELOPMENT SUPPORT

Another part in cost estimation, is introduced by the development support. This part accounts for all process supporting factors (such as overheads, administration and logistics). Development support cost is dependent on airframe weight ($W_{airframe}$), maximum level speed (V_H), number of prototypes (N_P), consumer price index relative to 2012 (CPI_{2012}) and a composite compensation factor (f_{comp}). When all these parameters are known, the development support cost can be estimated with Equation (14.8).

$$C_{DEV} = 0.06458 \cdot W_{airframe}^{0.873} \cdot V_H^{1.89} \cdot N_P^{0.346} \cdot CPI_{2012} \cdot (1 + 0.5 f_{comp}) \tag{14.8}$$

FLIGHT TEST OPERATIONS

In order to get the aircraft certified, flight tests have to be performed. These flight tests are inducing a significant cost. The flight test operations cost depends on airframe weight ($W_{airframe}$), maximum level speed (V_H), number of prototypes (N_P) and consumer price index relative to 2012 (CPI_{2012}). The flight test operations cost can be calculated with Equation (14.9).

$$C_{FT} = 0.009646 \cdot W_{airframe}^{1.16} \cdot V_H^{1.3718} \cdot N_P^{1.281} \cdot CPI_{2012} \tag{14.9}$$

MATERIALS

The materials cost accounts for the cost of raw materials (such as aluminum sheets or pre-impregnated composites). The materials cost is dependent on the weight of the airframe ($W_{airframe}$), maximum level speed (V_H) and planned number of aircraft produced over a 5-year period (N). Materials related cost can be calculated with Equation (14.10)

$$C_{MAT} = 24.896 \cdot W_{airframe}^{0.689} \cdot V_H^{0.624} \cdot N^{0.792} \cdot CPI_{2012} \tag{14.10}$$

ADDITIONAL COST

Additional parts Additional costs and discounts have to be considered. These can be accounted for per aircraft. For these loose components, a quantity discount factor can be calculated, which accounts for the lower production-price per unit in case of batch-production. The quantity discount factor can be calculated with Equation (14.11). As can be concluded from this equation, the quantity discount depends on experience effectiveness (F_{EXP}) and the amount of produced aircraft (N).

$$QD = (F_{EXP}^{1.4427 \cdot ln(N)}) \tag{14.11}$$

The loose components account for cost of avionics, power plant (engine), landing gear and the propeller. The landing gear will give a "negative price" because it is fixed. All the component prices (before discount) are summarized in Table 14.1. The quantity discount factor will be multiplied with these costs.

Table 14.1: Add caption

Component	Price (before discount) [€]
Avionics	3285
Landing Gear	-5475
Power plant	15330
Propeller	2294

Reliability Cost Aircraft manufacturers need a reliability insurance. Usually, the reliability insurance cost is dependent on the number of aircraft sold and the accident rate, but because the accident rate is not available between 12-17% is added to the total project development price.

FBW ADJUSTMENTS

In order to incorporate the cost of the FBW system, the model has to be adjusted. This is done by adding the cost of sensors, actuators and flight computers.

Although this incorporates the hardware cost of the FBW system, it still leaves uncertainties in the cost estimation; for example, it is not known how the engineering time is influenced by the development of a FBW system. A contingency of €50000 per aircraft will be considered in order to account for this.

14.1.2 RESULTS

For all the discussed configurations, the amount of aircraft which have to be sold in order to reduce the selling price to slightly below or equal to €400K can be estimated. Next to the normal redundancy, another form of redundancy is considered: graceful degradation (GD). This is done with the model, discussed before. The number of aircraft sold is computed to compare with the market analysis. When not enough aircraft can be sold, the concept is not feasible.

The price of an actuator is estimated by assuming the prices are comparable to the actuators of the autopilot of the Cessna Citation II. This would be about €2623,62 per actuator [109]. To avoid underestimation of the cost of actuators, the price per actuator have been rounded to €3000. The sensors are assumed to cost the same as the ones used in the Diamond DA42. This would be an average of €11500 . The flight computer has a cost of about €7300 [64].

Table 14.2: Cost Results

Parameter	Mech. Back-up	Dual redundancy	Triple redundancy
Input			
V_h [kts]	138	140	136
$W_{airframe}$ [lbs]	443.29	443.29	464.5
Actuators [#]	3	6	9
Sensors [#]	3	6	9
Output			
Aircraft sold per year	12	14	18

Parameter	Quadruple redundancy	Dual redundant GD	Triple redundant GD
Input			
V_h [kts]	136	144	144
$W_{airframe}$[lbs]	465.18	432	432
Actuators [#]	12	6	9
Sensors [#]	12	6	9
Output			
Aircraft sold per year	23	14	18

The input and output of the model has been specified in Table 14.2. As can been seen from this table, the least redundant FBW system also has the lowest amount of units which have to be sold in order to comply with the maximum selling price (Mech. Back-up). In contrast, the most redundant needs the highest sales. A more detailed breakdown of the cost per configuration can be found in.

The results of the GD configurations are the same as of the non-GD configurations with the same redundancy. However, this is caused by using the same actuator price. The price of the smaller actuators needed for the GD configuration, might actually be lower. Unfortunately manufacturers of actuators are not really eager to give away data about their products, so a prediction of the cost of using GD can not be made at the moment.

When the results of the market of the trainer aircraft, at this moment, are compared, the minimum market share needed to break even can be calculated. This has been done using a trainer aircraft market which is minimal 144 shipments per year and maximal 192 shipments per year. The result can be found Table 14.3.

Table 14.3: Needed Share

Configuration	Good market	Bad market
Mech. back-up	6.30%	8.30%
Dual redundancy	7.30%	9.70%
Triple redundancy	9.40%	12.50%
Quadruple redundancy	12%	16%
Dual redundant GD	7.30%	9.70%
Triple Redundant GD	9.40%	12.50%

As new manufacturer in this market, with a expensive product, one should not expect a very high share. However, 10% is feasible, 10%-15% is questionable and higher than 15% seems rather impossible. Therefore, a quadruple redundant system seems rather impossible from cost view in a bad market. A complete overview of the cost per sub part can be found in Table 14.4

Table 14.4: Development Cost of the Trainer Aircraft per Aircraft

Cost Part	Mech. Back-up	Dual Redundancy	Triple Redundancy	Quadruple Redundancy	Dual Redundant GD	Triple Redundant GD
Engineering	47770 €	40720 €	33510 €	27550 €	41620 €	35180 €
Tooling	30400 €	26130 €	22090 €	18430 €	26160 €	22390 €
Manufacturing and Labor	147520 €	134090 €	122180 €	109040 €	133190 €	120750 €
Development Support	2490 €	2050 €	1600 €	1260 €	2110 €	1720€
Flight Test Operations	320 €	260 €	210 €	160 €	260 €	210 €
Quality Control	19180 €	17430 €	15880 €	14180 €	17310 €	15700 €
Materials	11650 €	11200 €	10850 €	10330 €	11220 €	10750 €
Avionics	13550 €	13340 €	13100 €	12870 €	13330 €	13130 €
Powerplant and Propeller	13131 €	12930 €	12700 €	12470 €	13620 €	12730 €
Landing Gear	-4065 €	-4002.59 €	-3931 €	-3861.4 €	-3998 €	-3937.6 €
Fly-By-Wire	32294 €	63598 €	93695 €	122720 €	63530 €	93855 €
Contigency FBW Development	50000 €	50000 €	50000 €	50000 €	50000 €	50000 €
Reliability	33833.5 €	30497.7 €	27382.7 €	24291.4 €	30578.6 €	27434.7 €
Total	398073.5 €	398243.1 €	399266.7 €	399440.0 €	398930.6 €	399912.1 €
Number of Aircraft that Need to be Sold	56	69	88	112	70	86

14.2 Direct Operating Cost

14.2.1 Model & Assumptions

The model, used for direct operating cost is described in [60]. This model incorporates maintenance, storage, fuel, insurance, inspection, engine overhaul and loan costs.

Costs like insurance and loans are dependent on decisions of the owner of the aircraft. Therefore it is assumed that the customer does not have a loan on the aircraft and that the owner insures the aircraft for the full buying price.

In the next sections, the calculations of all the different parts of the direct operating cost per year will be discussed.

Maintenance

Maintenance cost is a significant cost due to operation of the aircraft. Maintenance cost is dependent on maintenance to flight hour ratio (F_{MF}), hourly rate of a certified A&P mechanic (R_{AP}) and flight hours per year (Q_{FLGT}). Maintenance cost can be estimated by using Equation (14.12). The maintenance to flight hour ratio (F_{MF}) is estimated as 0.35 [60].

$$C_{AP} = F_{MF} \cdot R_{AP} \cdot Q_{FLGT} \tag{14.12}$$

Storage

As a lot of pilots do not own their own hangar, cost for storage has to be considered. The cost of storage is approximated as $250 per month (equal to €182.50). Therefore the yearly cost of storage will be C_{STOR} =€2190

Fuel

One of the most significant costs in (general) aviation is the fuel cost. The fuel cost is dependent on fuel flow during cruise (FF_{cruise}), flight hours per year (Q_{FLGT}) and the price of fuel (R_{FUEL}). The yearly cost of fuel can be calculated with Equation (14.13).

$$C_{FUEL} = FF_{cruise} \cdot Q_{FLGT} \cdot R_{FUEL} \tag{14.13}$$

Insurance

Insurance is one of the aircraft owner dependent costs. Assuming (initially) that an aircraft-owner insures for the whole aircraft selling-price, the yearly insurance cost can be calculated with Equation (14.14).

$$C_{INS} = 365 + 0.015 \cdot C_{AC} \tag{14.14}$$

ANNUAL INSPECTION
Annual inspection costs can be estimated. According to [60] this is approximately €365.

The hundred-hours-inspection is not considered model from [60]. The level of detail in the hundred-hour-inspection is the same as the annual inspection. However, the mechanic does not need the same ratings and is therefore assumed to be 20% less expensive. The hundred-hour-inspection cost can be calculated with Equation (14.15).

$$C_{HHI} = \frac{Q_{FLGT} \cdot 365}{120} \tag{14.15}$$

ENGINE OVERHAUL
In order to be able to pay for an engine overhaul, the owner has to save money for it. The engine overhaul fund cost is dependent on overhaul cost ($C_{OVERHAUL}$), flight hours till overhaul (Q_{OVER}) and flight hours per year (Q_{FLGT}). Engine overhaul cost per year can be estimated with Equation (14.16)

$$C_{OVER} = \frac{Q_{FLGT}}{Q_{OVER}} \cdot C_{OVERHAUL} \tag{14.16}$$

14.2.2 OPTIMIZATION OPTIONS
Since direct operating cost is a parameter for which has to be optimized in this project, a good understanding on what can be optimized and how to do this has to be obtained. This has been done by generating pie charts of the relative magnitude of the different aspects which are used to calculate the direct operating cost. Two different situations are considered; private use and flight school use. As the final configuration/specification of the aircraft is not known yet, the following assumptions on input have been made.

- Private use is 300 hours per year [60];
- Flight school use is 1000 hours per year [60];
- Aircraft cruises on 75% power, implying a fuel flow of 5.3 gallons per hour [110];
- Fuel cost is €3.57/gallon, based on Euro 95 gas [111];
- Aircraft is bought with own money;
- Aircraft is insured for a value of €400000.

OVERVIEW
The results for calculating the direct operating cost, with the assumed input can be found in Figure 14.1.

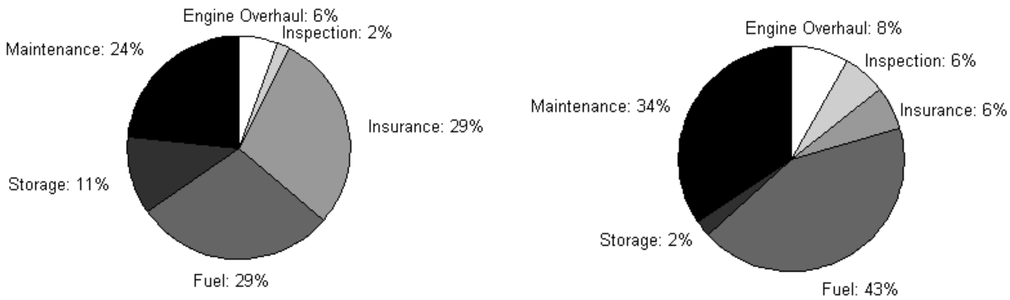

(a) DOC Division Private Use

(b) DOC Division Flight-school Use

Figure 14.1: DOC In Two Situations

Figure 14.1a implies that for private use, insurance, fuel and maintenance cost are the biggest parts. When looking at Figure 14.1b, the insurance cost becomes less significant when the aircraft is used in a flight school. Optimization of direct operating cost is therefore assumed to be the most efficient when focusing on fuel, maintenance and insurance.

FUEL
Optimizing the cost of fuel basically means that the optimum combination of fuel flow per hour (FF_{fuel}) and fuel cost (R_{fuel}).

The two options for different types of fuel basically are Avgas and Euro 95. These fuels can respectively be used with the Continental IO-240-B3B and the Rotax 912s engine. However, the Continental engine has 25 hp more than the Rotax engine.

The relative difference between the fuel cost of using the Continental engine and the Rotax engine can be calculated. Although the continental engine delivers more power, in the following calculations, it will be assumed that with both engines, cruise will be performed on 75% power. The extra power that the Continental engine can deliver, would be needed when weight and drag run out of bounds.

The Continental engine has a fuel flow of $FF_{continental}$ = 5.5 [gallons/hr] where the Rotax engine has FF_{fuel} = 5.3 [gallons/hr]. Next to that, the price of Avgas is equal to $R_{Avgas} = e5.72$ [1/gallons] and the price of Euro 95 is equal to R_{euro95} =€3.57 [1/gallons]. Now, the relative difference can be calculated with Equation (14.17).

$$Diff = \left(\frac{R_{Avgas} \cdot FF_{continental}}{R_{euro95} \cdot FF_{Rotax}} - 1\right) \cdot 100 \tag{14.17}$$

From this calculation can be found that using the Continental engine can increase the cost of fuel with 66%. As fuel cost was already concerned a big part of the direct operating cost, ideally an Euro 95 using engine has to be used.

Next to that the fuel flow has to be minimized. As fuel flow is directly proportional to power setting and therefore power required, from Equation (14.18) can be found that the drag should be minimized.

$$P_R = DV \tag{14.18}$$

MAINTENANCE

Maintenance also is big part of the direct operating cost. The maintenance cost parameter which has to be optimized (or at least not made worse) is the maintenance to flight hour ratio (F_{MF}). The following relevant influences are discussed in [60].

- Maintenance performed by owner or mechanic;
- Engine accessibility;
- Type of landing gear;
- Radios installed;
- Type of fuel tanks;
- Complexity of flaps.

If the influence of the choice of the aircraft owner is not taken into account, the maintenance cost can be optimized by certain design choices. Maintenance to flight hour ratio usually is driven up by bad engine accessibility, retractable landing gear, IFR radios, integral tanks and complex flap systems

Due to the "conventional" type of design, chosen for this trainer, good engine accessibility is a matter placing the "hood" conveniently. Next to that, it has not been decided yet which kind of radios are to be installed. However, when the aircraft is not used for IFR operations, installing IFR radios should be avoided as it drives up the cost. The last influence for which has been optimized is the complexity of the flap system. Simple flaps have been chosen (as more complex flaps are not usual for general aviation) which will not increase the maintenance to flight hour ratio.

INSURANCE

Insurance cost usually dependents on the insured price of the aircraft and the experience of the pilot (in the model only on insure price). The flight envelope protection can reduce the difference in insurance price due to experience. The reduced probability of a unexperienced pilot crashing the aircraft will make the insurance less expensive for unexperienced pilots, which highly affects the insurance cost of a flight school. Nevertheless, the insurance cost of a flight school was not a very significant part.

Next to that, a great opportunity will be available for owners of the aircraft. Since it is not likely to lose the full aircraft anymore, the owner can safe a lot of money on insurance cost. If there is reduced probability of a crash, one can choose to insure for a lower value than the purchase price.

14.2.3 RESULTS

For all the different configurations the direct operating cost has been analyzed. The only direct operating cost parameter that is different between the configurations is the fuel flow during cruise. The results for the direct operating cost can be found in Table 14.5. A more detailed breakdown of the direct operating cost of all FBW configurations can be found in Tables 14.6 and 14.7.

Table 14.5: DOC in euro per hour (€/hr)

Configuration	Fuel-flow	DOC private use	DOC flight-school
Mech. back-up	4.817	65.94	47.68
Dual redundancy	4.791	65.85	47.59
Triple redundancy	5.1445	67.11	48.85
Quadruple redundancy	5.15	67.13	48.87
Dual redundant GD	4.583	65.11	46.85
Triple Redundant GD	4.583	65.11	46.85

When looking at the results, the graceful degradation configurations are ideal from the view of direct operating cost.

Table 14.6: Direct Operating Cost 300 hour Inspection

Cost Part	Mech. Back-up	Dual Redundancy	Triple Redundancy	Quadruple Redundancy	Dual Redundant GD	Triple Redundant GD
Maintenance	15.33 €/hr	15.33 €/hr	15.33 €/hr	15.33 €/hr	15.33 €/hr	15.33 €/hr
Storage	7.30 €/hr	7.30 €/hr	7.30 €/hr	7.30 €/hr	7.30 €/hr	7.30 €/hr
Fuel	17.22 €/hr	17.13 €/hr	18.39 €/hr	18.41 €/hr	16.39 €/hr	16.39 €/hr
Insurance	21.22 €/hr	21.22 €/hr	21.22 €/hr	21.22 €/hr	21.22 €/hr	21.22 €/hr
Inspection	1.22 €/hr	1.22 €/hr	1.22 €/hr	1.22 €/hr	1.22 €/hr	1.22 €/hr
Engine Overhaul	3.65 €/hr	3.65 €/hr	3.65 €/hr	3.65 €/hr	3.65 €/hr	3.65 €/hr
Total	65.94 €/hr	65.85 €/hr	67.11 €/hr	67.13 €/hr	65.11 €/hr	65.11 €/hr

Table 14.7: Direct Operating Cost 1000 hour Inspection

Cost Part	Mech. Back-up	Dual Redundancy	Triple Redundancy	Quadruple Redundancy	Dual Redundant GD	Triple Redundant GD
Maintenance	15.33 €/hr	15.33 €/hr	15.33 €/hr	15.33 €/hr	15.33 €/hr	15.33 €/hr
Storage	2.19 €/hr	2.19 €/hr	2.19 €/hr	2.19 €/hr	2.19 €/hr	2.19 €/hr
Fuel	17.22 €/hr	17.13 €/hr	18.39 €/hr	18.41 €/hr	16.39 €/hr	16.39 €/hr
Insurance	6.37 €/hr	6.37 €/hr	6.37 €/hr	6.37 €/hr	6.37 €/hr	6.37 €/hr
Inspection	2.92 €/hr	2.92 €/hr	2.92 €/hr	2.92 €/hr	2.92 €/hr	2.92 €/hr
Engine Overhaul	3.65 €/hr	3.65 €/hr	3.65 €/hr	3.65 €/hr	3.65 €/hr	3.65 €/hr
Total	47.68 €/hr	47.59 €/hr	48.85 €/hr	48.87 €/hr	46.85 €/hr	46.85 €/hr

15
RISK ASSESSMENT

This chapter will describe the risks that might occur in development of a FBW trainer aircraft and during flight of such an aircraft. After analyzing the risks and mitigation methods, they are mapped according to probability and consequence on a risk map.

15.1 RISK DESCRIPTIONS

This section discusses the descriptions of the risk associated with the Minimum Fly-By-Wire Trainer Aircraft.

15.1.1 GENERAL RISKS

These are the general risks for the development of a small trainer aircraft.

GR.1 **Market acceptance:** Due to political or economical reasons, the market could be too small/could shrink during the development of the aircraft. Therefore, it is essential to base the market predictions on reliable sources. The market analysis performed in the Baseline Report [50] indicates an overall small market for trainer aircraft, but a market growth is expected in the following 10 years. This analysis is supported by the fact that Airbus plans to put 2017 80 hybrid trainer-aircraft [112] on the market and actual market development.

GR.2 **Market development/competitors:** Both before and after market introduction, competitors may appear who could take part of the market. The aircraft has the distinctive advantage of increased safety through a FEP, auto-land and digital flight data measurement. This gives a head-start in the development of the system, therefore mitigating the risk by appearing competitors. There are currently no two-seated FBW trainer aircraft on the market and to this information, the only company developing small FBW aircraft is Diamond-Aircraft.

GR.3 **Weight/cost growth iterations:** The design of an aircraft is an iterative process and small unexpected changes in the later design stages might lead to large changes in the overall design, which would lead to delays and cost increases. This risk is mitigated by including safety factors in the estimations. As the design progresses, further levels of detail improve the accuracy of the design iterations. The sensitivity analysis provides an indication of the effects of changing different parameters on the aircraft weight. An important factor that should be considered is the choice of engine. If weight growth leads the weight up to high, a different engine is required, which would have a major impact upon the entire design of the aircraft and its structure.

GR.4 **Changing/New Governmental Trade laws:** In the detailed market analysis an analysis of the actual situation and a prognosis on the trade laws developments for the different markets need to be performed. The risk exists that trade laws change and create difficulties in exports and imports.

GR.5 **Data loss:** The possibility exists, that data without back-up gets permanently lost due to an inconvenient event. Therefore all digital data should be stored with some back-up system.

GR.6 **Product Risk:** This is the risk, that the product may not be delivered to market within resources (time, money) available. If delivered within resources, the risk exists, that the product may not work as envisioned.

15.1.2 FLY-BY-WIRE DEVELOPMENT RISKS

The development of a FBW system for small aircraft comes with a number of associated risks, they are listed below.

FR.1 **Certification:** A major risk associated with the development of this fly-by-wire trainer lies in certification, as there are no specifically fixed requirements on a fly-by-wire aircraft. Inability to get the aircraft certified would be catastrophic to the project. The odds of getting the aircraft certified depends on the way in which the fly-by-wire system is implemented.

The aircraft is likely to be certifiable if the system is fitted with a mechanical back-up, such that in-flight failure can be resolved by disconnecting the FBW actuation systems.

Completely FBW systems pose differing risks depending on the level of redundancy. Triple and Quadruple redundancy systems have been shown to be certifiable for larger aircraft, but these come at a cost of weight. Double redundancy would save weight, might be certifiable, but no such system has been certified for now. The required redundancy level also depends on the reliability of the actuators and other subsystems.

A dual or triple redundancy system designed with a graceful degradation philosophy, could lower weight whilst improving the odds of certification.

FR.1.a Mechanical back-up
FR.1.b Full double redundancy
FR.1.c Full triple redundancy
FR.1.d Full quadruple redundancy
FR.1.e Graceful degradation

FR.2 **Development of Certification Standards for Small Aircraft:** Due to the accumulation of experience with fly-by-wire systems, it is very probable that certification of fly-by-wire systems will become easier in the future, especially for small, single-engined machines. Nevertheless, as the certification rules are in a development stage the risk exists that they change during the development of the aircraft, which would have implications on the system requirements, and could trouble the development of the aircraft in all aspects.

FR.3 **Software Development:** The main risks linked to software development appear at two points in time, either at a late design stage before certification or after market introduction. If delays or errors appear before certification, they will cause certification delays and will increase the costs significantly. Generally it must be said that, as in most complex projects, the estimated total required development time and cost will rise with the elaboration of the fly-by-wire software in more details. On the other hand, if errors appear after market introduction, they can change the public perception of fly-by-wire systems and might decrease the market significantly or even cause a change of certification procedures. This event has the power to stop the project entirely. This risk will be mitigated by following the software development standards DO 178-B and by having staff experienced in software design for safety-critical systems.

FR.4 **Hardware Development/Availability:** Some hardware (actuators, computers, connection buses, sensors, etc.) will need to be designed especially for the specific fly-by-wire layout utilized, although this should carefully be traded off and avoided, whenever possible. Hardware, which is newly designed, creates the possibility of development of delays and cost increase. This risk will be mitigated by starting development early and by working together with avionics manufacturers from early on.

FR.5 **PPL Regulations:** At the current point it would be possible to perform PPL-training with an aircraft fitted with fly-by-wire systems. Nevertheless, for the future the possibility exists that this might be prohibited due to several reasons, one of them the increased knowledge required from the students, as they need to understand and operate the complex flight control system. To mitigate this risk, this trainer will contain a simple FBW system with just a direct law-mode and a FEP (which can be turned off). This decision ensures that flying on this aircraft will represent the handling of a mechanically controlled aircraft, and that PPL training will remain possible with this aircraft.

FR.6 **Reduced Redundancy:** In the design of the fly-by-wire system, a certain security level is achieved by adding redundancy, which for example means using several computers with different hardware and software performing the same tasks. The risk exists, that a influence from outside affects all computers in the same fashion (e.g electromagnetic attack), and the calculated redundancy is therefore futile. This risk could be mitigated by using hardware from different manufacturers in the redundant components.

15.1.3 Operational Risks

This section lists and describes the risks that occur in operation of the aircraft, as well as the measures that are taken to mitigate probability and consequence of these risks.

OR.1 **Engine failure:** The engine is a complicated aircraft subsystem, consisting of a lot of moving parts and thus subject to wear. The loss of propulsion does not need to have catastrophic consequences because the aircraft can be put down through gliding flight.

The risk of engine failure occurring is minimal if the engine is subjected to the specified maintenance, inspection and timely overhauls.

OR.2 **Structural disintegration:** Structural breakage can occur in numerous parts of the aircraft, with varying severity of the consequences.

OR.2.a wing
OR.2.b control surfaces
OR.2.c landing gear
OR.2.d fuselage

OR.3 **Communication loss:** It might happen during flight that the communication systems fail. This would leave the pilot unable to communicate with Air Traffic Control or with other pilots, potentially causing dangerous situations.

OR.4 **Sensor errors:** Erroneous readings on sensors could provide the FBW system with faulty information on aircraft attitude, which could lead to dangerous corrections from the Flight Envelope Protection system. This could result in the airplane crashing.

The aircraft will be fitted with redundant sensors for the FEP system. The combination of various sensor readings will introduce a minimal delay in the system, but it will prevent malfunctioning sensors from causing dangerous situations. When a mechanical back-up is used, the whole FBW is disengage in case of error and therefore erroneous sensor readings cannot cause dangerous situations anymore.

OR.5 **Loss of electrical power:** A partial loss of electrical power can be resolved using back-up power supplies. A complete electrical black-out would lead to a complete loss of control in the case of a FBW system without mechanical back-up.

OR.5.a Partial failure

OR.5.b Complete failure

The electrical power supply system will be designed such that no single failure will be catastrophic. There will be back-up batteries to provide power in case one battery, the alternator, or the engine fails. In case of dual battery failure, the engine-driven alternator will be able to provide power. In this manner, a complete power failure will become extremely improbable.

OR.6 **Partial loss of control:** A partial loss of control could occur for various reasons, but for most cases is not very catastrophic because malfunction on one of the control surfaces can be resolved using the other controls. Especially using the FBW system, a partial loss of control may be resolved using the Flight Control Computers to maintain controllability and minimize the consequence.

OR.6.a **Stall:** An airplane in stall conditions could cause a partial loss of control, which could prove dangerous at the hands of an inexperienced pilot. Most stall conditions can be resolved using the control surfaces. Furthermore, the FEP system will prevent the pilot from entering a stall situation.

OR.6.b **Hail:** Impact from large hailstones could break some of the aircraft control surfaces.

OR.6.c **Blockage:** Part of the controls could become blocked due to ice or other reasons. The aircraft will most likely not be certified for flight into known icing conditions.

OR.6.d **Actuator Failure:** Failure of the actuators that move the control surfaces would limit control of the aircraft. However, the primary control surfaces will be fitted with reliable actuators and redundant actuation, such as to make failure extremely improbable.

OR.7 **Complete loss of control:** All controls of the aircraft could get lost due to an error coming from a central source, such as the electrical power system. The probability of a complete loss of control is next to none. For example, a complete loss of electrical power would only occur if the engine/alternator and both battery systems fail.

OR.8 **On board fire:** An onboard fire will have catastrophic consequences. Therefore all the possible sources of fire must be sufficiently isolated from critical components of the aircraft.

OR.9 **Pilot unable to fly:** Due to medical reasons (unconsciousness,...), the pilot could become unable to fly, with the risk of the aircraft getting out of control and crashing. The risk of pilot inability to fly is hard to reduce, but might be possible through medical check-ups. The consequence can be reduced with a back-up auto-land system.

OR.10 **Brake failure:** If the braking system were to break, the aircraft can not be stopped within the required runway length.

OR.11 **Exhaust leakage:** The heating system for the aircraft will most likely be of the exhaust shroud type. This introduces the risk of carbon monoxide leaking from the exhaust system into the cockpit. This risk can be mitigated by regular inspection of the exhaust pipe for cracks. Furthermore, fitting a carbon monoxide indicator in the cockpit will allow the pilot to open up the ventilation and shut off the heating if leakage were to occur.

OR.12 **Fuel system:** Various risks are associated with the fuel system.

OR.12.a **Leakage:** Small leaks might occur for fuel tanks and lines. They should be found by inspection of the aircraft and should not pose a threat at an undetectable level. Threat can be minimized by having the fuel system separated from the electrical system and properly protected from engine heat.

OR.12.b **Fuel pump failure:** Failure of a fuel pump, if those are fitted, should be prevented with proper maintenance, but will also be resolved using a redundant second pump, powered using a separate power source.

15.2 Risk Map

In the risk maps, each risk is assigned an individual probability of risk and corresponding severity of the consequences. The project development risks are mapped in Table 15.1. The risk map for the risks during operation of the aircraft is provided in Table 15.2.

Table 15.1: Risk map for development risks

	Negligible	Marginal	Critical	Catastrophic
Certain				
Likely				FR.1.b
Possible		GR.2	GR.3,FR.3,FR.1.c	FR.1.e
Unlikely		GR.4	GR.6, FR.4, FR.5, GR.1	FR.1.c,FR.1.d
Rare			GR.5	FR.1.a

Table 15.2: Risk map for operational risks

	Negligible	Marginal	Critical	Catastrophic
Certain				
Likely				
Possible	OR.5.a, OR.9	OR.3		
Unlikely	OR.11	OR.1, OR.10	OR.2, OR.6.b, OR.6.c	
Rare	OR.4, OR.6.d	OR.6.a, OR.12	OR.5.b	OR.7, OR.8

16 REQUIREMENTS COMPLIANCE MATRIX

In this chapter, it is checked whether or not all of the requirements set at the start of the design are met. This is done using a requirement compliance matrix, which shows whether the requirement is met and if so where in the final report this can be found.

16.1 PERFORMANCE REQUIREMENTS

The performance requirements set at the Baseline report are list in Table 16.1. All of them are met, most of them are presented in Chapter 9 which includes all of the calculations. The requirement on emissions is not really elaborated on in this report. Comparing the emissions to the DA-20 can be done for the American version (Continental IO-240-B3B) and the European version (Rotax 912s). As the aircraft uses the same engine as the European version, it is first compared to that one. The fuel flows are thus the same and the same gasoline (Euro 95) is used. The only factor of importance is now the speed of the aircraft. The cruise speed of a Diamond DA-20 (138 kts) is much larger than the cruise speed of the aircraft (113), thus increasing the emissions per kilometer.

Now comparing it to the American version, there are several differences. The fuel flows at 75% power will be different and the type of fuel used is different (AvGas). The fuel flow of the Continental engine is 5.5 gal/hr and the Rotax has a fuel flow of 5.3 gal/hr. In one hour the Diamond has flown 256 km, while the aircraft has flow 209 km. This means that the Diamond uses 0.021 gal/km and the aircraft 0.025 gal/km. Furthermore from [113] it can be concluded that burning automotive fuel releases more CO_2 than AvGas, causing higher overall emissions than the DA-20.

Table 16.1: Performance requirements compliance matrix

Number	Description	Design	Section
MFT-PER-FP-01	Minimum cruise speed of 90 kts	113 kts	Section 9.6.2
MFT-PER-FP-02	Minimum demonstrated crosswind of 15 kts	25 kts	Section 7.1.3
MFT-PER-FP-03	Minimum rate of climb of 800 ft/min	1605 ft/min	Section 9.6
MFT-PER-FP-04	Minimum range of 800 km in solo training configuration	1500 km	Section 9.6.1
MFT-PER-FP-05	Maximum take-off distance (50 ft obstacle) of 500 meters	340 m	Section 9.6
MFT-PER-FP-06	Maximum landing distance (50 ft obstacle) of 400 meters	317 m	Section 9.6
MFT-PER-EM-01	Emissions at or below the level of a Diamond DA-20	Higher emissions	[-]

16.2 STAKEHOLDER REQUIREMENTS

Next to the performance requirements, there are also some stakeholder requirements. These are all functions that add value to the aircraft, especially for flight schools. The requirement on reconfiguration is not met, as it was decided that the auto-land system would not become removable. This was done because the final weight of the entire auto-land system was lower than expected (around 8 kg). The increase in complexity and difficulty of certification outweighs the savings of weight in this case. The only problem that is still left for the auto-land system is the difficulty of certification. This means The aircraft is operable in both the USA and Europe, as most of the regulations from CS-23 also apply in the American version FAR 23.

16.3 GENERAL SYSTEM REQUIREMENTS

The general system requirements compliance matrix is shown in Table 16.3. Most of them were pretty straight forward and were easily met. However the certification of the aircraft is going to be the most difficult to reach. Due to

Table 16.2: Stakeholder requirements compliance matrix

Number	Description	Design	Section
MFT-STH-TRA-01	Ability to record the flight state for electronic debrief	Yes	Section 10.4.3
MFT-STH-TRA-02	Ab-initio training for a single engine land license (VFR and IFR)	Yes	Section 10.3
MFT-STH-TRA-03	Aircraft shall have FEP	Yes	Section 8.2
MFT-STH-TRA-04	Autoland capability in solo training configuration	Unsure	Section 8.3
MFT-STH-TRA-05	Reconfiguration between dual and solo modes possible in max 2 hours	N.A.	[-]
MFT-STH-EASA-01	Aircraft operable in USA and Europe	Yes	[-]

the advanced technology used and no available CS-23 requirements on this FBW system, it is a critical point of this design. With the wide variety of options available, this report shows that there are enough options to get this design through certification.

Table 16.3: General systems requirements compliance matrix

Number	Description	Design	Section
MFT-SYS-COS-01	Direct purchasing costs shall be less than 400K Euro per unit	Yes	Chapter 14
MFT-SYS-RES-01	The preliminary design shall be completed within the allocated time of 10 weeks	Yes	Appendix D
MFT-SYS-RES-02	The preliminary design shall be completed by nine students	Yes	Appendix C
MFT-SYS-PPL-01	The aircraft shall be a single-engine aircraft	Yes	Section 4.2
MFT-SYS-PPL-02	The aircraft shall be fitted with duplicate primary flying controls	Yes	Section 10.3
MFT-SYS-PPL-03	The aircraft shall give students the opportunity to train for both VFR and IFR ratings	Yes	Section 10.3
MFT-SYS-COMM-01	The student pilot and instructor shall be able to communicate at all times	Yes	Section 4.2
MFT-SYS-COMM-02	The student pilot and instructor shall be able to communicate with air traffic control (ATC) via radio	Yes	Section 10.3
MFT-SYS-EASA-01	The aircraft shall be certifiable according to the EASA CS-23 for Utility Aircraft	Yes	[-]

16.4 CS-23 Requirements

The most important CS-23 requirements from the Baseline report are put into the requirements compliance matrix, shown in Table 16.4. There are a lot missing compared to the baseline report, but they turned out to be too detailed for this design stage. The ones listed here have been investigated and were met during this preliminary design.

16.5 Fly-by-wire Requirements

Finally, there were some FBW requirements set at the start of the design. The probability of failure was critical in creating the different options for the FBW system. If dual redundancy was the only viable option, it would not have provided a failure that was low enough. This report shows that triple redundancy is an option, so this requirement

Table 16.4: CS-23 requirements compliance matrix

Number	Description	Design	Section
MFT-CS23-FP-01	V_{S_0} at maximum weight shall not exceed 113 km/h	Yes	Section 9.6.2
MFT-CS23-FP-04	Steady gradient of climb at sea level shall be at least 8.3%	0.3459	Section 9.6
MFT-CS23-FP-22	The aircraft shall possess static longitudinal stability	Yes	Section 7.1.2
MFT-CS23-FP-25	The aircraft shall possess static directional stability	Yes	Section 7.1.3
MFT-CS23-FP-28	Any short period oscillation shall be heavily damped	Yes	Section 7.4.2
MFT-CS23-FP-29	'Dutch-roll' shall be damped to 1/10 amplitude in 7 periods	Yes	Section 7.4.3
MFT-CS23-ST-05	V_C (in kts) shall not be less than $33\sqrt{W/S}$	Yes	Section 5.2.1
MFT-CS23-ST-06	V_D (in kts) shall not be less than 1.50 times the minimum cruise speed	Yes	Section 5.2.1

has been met. Of course, with actuators on the rudder, aileron and elevator 3-axis control of the aircraft is possible. Furthermore, the control feel of a conventional aircraft is possible by programming some control laws in the FBW system.

Table 16.5: FBW requirements compliance matrix

Number	Description	Design	Section
MFT-FBW-01	The FBW system shall be certifiable for use in the aircraft	Yes	[-]
MFT-FBW-03	The probability of catastrophic failure of the FCS shall be no higher than 10^{-9}	Yes	Chapter 17
MFT-FBW-04	The FBW system shall allow for 3-axis control of the aircraft	Yes	[-]
MFT-FBW-06	The FBW system shall keep the aircraft attitude within the flight envelope boundaries	Yes	Section 8.2
MFT-FBW-07	The FBW system shall be able to provide the control feel of a conventional aircraft	Yes	[-]

17
RAMS Characteristics

In this chapter the RAMS characteristics are described. The purpose of the RAMS analysis is the mitigation of risks during the project.

17.1 Reliability

The required reliability for different components of the aircraft can be derived from ARP4761. This guideline assigns a maximum failure rate to a certain hazard level. Other guidelines to improve reliability of an aerospace system are [114]:

- DO-178C;
- DO-254;
- ARP4754.

The whole FBW system requires a maximum failure rate of 1E-09 failures per flight hour due its catastrophic consequence in case of a failure. This reliability can only be achieved by redundancy which is illustrated in Table 17.1. The table shows he the minimum required MTBF and failure rate for different redundancy levels to achieve a safety critical system. For the values in the table the assumption was made that failures are independent from each other.

Table 17.1: Minimum MTBF and failure rate for safety critical systems

Redundancy	MTBF (h)	failure rate (1/h)
Single	1E09	1.0E-09
Double	3.16E04	3.16E-05
Triple	1E3	1E-03
Quadruple	1.78E2	5.62E-03

Without redundancy a system (or independent subsystem) has to be able to operate around one billion hours before an error would be statistically expected. It is obvious that this cannot be achieved. Therefore some kind of redundancy is needed.

For the FBW control computer two different redundancy concepts can be used. The first centralized concept duplicates the control computers. In case of an error the other computer takes over and controls the aircraft. In the second concept a decentralized computer system, which consists of many small computers that each have a different task, yields the required redundancy. Every node of this decentralized system also processes the task of a certain amount of other nodes. A judging algorithm detects errors in nodes and outputs the most reasonable command.

17.2 Availability

In this section the expected availability is estimated. According to [60] a common flight school performs around 1000 hours of flight training a year with each of its trainers. Assuming that the aircraft is airborne at five days a week, one obtains an average of 3.85 flight hours during these days. Based on this number ten 100 hour inspections have to be performed during a year. [] gives an indication that a 100 hour inspection requires around 20 man hours of a mechanic. This translates to a downtime of around 1.5 days for every 100 hour inspection. Therefore the 100 hour inspections contribute to 15 days of downtime every year. If 19.25 flight hours are performed each week, a 100 hour inspection has to take place in a 2.5 weeks interval. In chapter 14 it was determined that the maintenance to flight ratio of the aircraft is going to be 0.35. This means that 350 hours of maintenance has to be performed every year on the aircraft. Based on the fact that 200 hours of maintenance is performed during the 100 hour inspections, 150 hours is left for other maintenance. This maintenance can include daily maintenance (like flight preparation) and maintenance performed in other intervals (e.g. 50 hours). It is assumed that maintenance, which is not part of the 100 inspection, does only produce a downtime on an hourly basis and thus no major interference with the flight schedule is expected.

For a private aircraft owner 300 flight hours were assumed in Chapter 14. This leads to 105 hours of maintenance. The breakdown leads to 60 hours for the 100/annual inspection and 45 hours for other inspections.

In Section 17.3 the tasks that have to be performed during the different inspections is discussed.

17.3 MAINTAINABILITY

Maintenance of an aircraft takes place in certain intervals. Mandatory for general aviation aircraft is the 100 hour/annual inspection. It takes place after 100 hours of flight operation or after 1 year after the last 100 hour maintenance [115]. Furthermore, dependent on the systems of the aircraft, maintenance has to be performed on a daily, 50, 200, 500 and 1000 hour interval level. In Table 17.2 and Table 17.3 certain maintenance task are tabulated vs their frequency. These values were derived from a Cessna 152 flight manual and were adjusted to incorporate the FBW system [51]. These tables give a good indication of the maintenance that has to be performed on the aircraft.

Table 17.2: Example of components needing maintenance during the 100 hour/annual inspection [51].

Propeller	• Engine controlls	**Airframe**
• Spinner	• Engine shock mounts	• Aircraft exterior
• Spinner bulkhead	• Alternator	• Aircraft structure
• Blades	• Magnetos	• Windows, doors, seals
• Bolts/Nuts	• Firewalls	• Seats
• Hub	• Central air filter	• Seat belts
Engine compartment	**Fuel system**	• Control lock
• Engine oil	• Fuel strainer	• Instruments
• Oil cooler	• Fuel tank caps/vents	• Electrical system
• Induction air filter	• Fuel tanks, sump drains, fuel line	**Control Systems**
• Induction airbox	• Fuel vent valve/line drain	• Aileron, Rudder, Elevator hinges
• Cold and hot air hoses	• Engine primer	• Rudder pedal assemblies
• Induction airbox	**Landing Gear**	• Control surface skin
• Cylinder	• Fairings	• Control surface actuators
• Crankcase	• Torque links, steering rod	• FBW hardware
• Hoses	• Bearings	• Flap motor
• Intake/Exhaust system	• Tires	• Decals and labeling
• Ignition harness	• Struts/Shimmys	• Cable and pulleys
• Sparkplug	• Brakes	• Disconnect clutch
• Vacuum system	• Steering rods	• Actuator wiring

A more detailed list can be found in FAR 43 Appendix D.

Table 17.3: Components that need inspection/maintenance during other maintenance intervals

Daily	**50 hours**	Landing gear lubrication
Fuel tank filler	Engine oil system	**1000 hour**
Fuel tank sump drains	Shimmy damper	Lubrication of control system
Pitot and static ports	**200 hours**	**1500 hour**
Fuel strainer	Vacuum relieve valve filter	TBO of propeller
AOA sensor	Vacuum system central air filter	**2000 hour/15 years**
Induction air filter	Brake master cylinders	TBO of engine
Oil dipstick	**500 hours**	**30 days**
Fuel liner drain tee	Vacuum system central air filter (replacement)	Battery

17.4 SAFETY

Safety is one of the factors during aircraft design. Since not all systems can be made safety critical, either due to technical difficulties or weight considerations, systems are classified according to the impact of their failure. Guidelines for this are given in ARP4761 [114]. Systems whose failure has a catastrophic influence, i.e. death of people, are called safety critical systems. They usually require a maximum failure rate of 1E-09 failures per hour. For the aircraft two safety critical functions were identified:

- Provide lift;
- Provide flight control.

'Provide lift' is safety critical in the sense that a failure to provide lift usually means the structure is disintegrated. Of course under the assumption that the 'failure to provide lift' was not induced by the pilot, for example by stalling the aircraft. The second safety critical function is 'flight control'. A loss of controllability of the aircraft leads almost certainly to death or serious injuries of the pilot and its passengers.

The function 'provide control' is executed by the aileron actuation, rudder actuation, elevator actuation, the flight control computer, the (optional) autoland system and its peripheral devices.

To improve safety a FMEA(Failure Mode and Effect Analysis) should be carried out for all subsystems in the future design process especially for the FBW system structure. A FMEA analysis can be used on systems engineering level, on a hardware level and on a software level.

18 CONCLUSION & RECOMMENDATIONS

In this report a study has been done for a minimum Fly-By-Wire trainer aircraft. On top of the FBW system, Flight Envelope Protection and Autoland have been investigated. The whole FBW system is integrated with the design of a general aviation aircraft. This design of the aircraft consists of Aerodynamics, Structures, Stability & Control, and Power.

This preliminary design study resulted in a two seater, single engine, high wing aircraft with a conventional tail. The aircraft has a maximum take-off weight between 628.8 kg and 681 kg, depending on the chosen layout. The layouts that were considered are: FBW with mechanical back-up, full FBW and full FBW with graceful degradation. When a mechanical back-up is used, a market share between 6.3 and 8.3% is needed. When full fly by wire is used, triple redundancy is probably required. This results in a needed market share between 9.4 and 12.5%. Both in order to achieve the maximum selling price of 400k€.

Flight Envelope Protection can be implemented in several ways, either using hard limits or soft limits. The first one denying the pilot to override the envelope limits. With soft limits the pilot can still override the envelope protection. When using a full FBW system it is just a matter of philosophy which system can be used. When using a mechanical system however, it is more logical to implement soft limits. Additionally to the FEP an auto throttle function is suggested to increase airspeed again. Another method could to increase the airspeed is to lower the nose, at low altitudes however this is not suggested. Furthermore controlled flight into terrain protection could be investigated, to increase the safety even further.

The autoland system (as a "digital parachute") seems not feasible with current hardware techniques. Certification of such a system will depend on research of other companies. Therefore, a system has been chosen which will only fly the approach till 200 and 250 ft altitude (respectively for Europa and the USA).

Concluding, a full FBW trainer aircraft technically is possible. However certification and sales are uncertain. Therefore it is up to the investor to chose whether or not he/she wants to take the risk of investing in a full FBW system. The more safe option, in terms of certification risk, is to have a mechanical back-up system. The main disadvantage of using a mechanical back-up system though are its limitations, such as: no reduced stability margin and difficult to use FEP with hard limits.

In order to actually achieve the use of FBW systems in a small trainer aircraft and improve safety in general aviation, some future research is suggested. First of all, this is only a preliminary design study. Therefore, the general aircraft design should be further refined and worked out in greater detail. An interesting field of research may be the reduction of hinge moments on the control surfaces by adding balance horns or by smartly placing the control surface hinge lines. This may potentially decrease the power consumption and of the fly-by-wire system and may also make it easier to certify.

It is recommended to do extensive research on the hardware layout of the FBW aircraft and to gather more specific information on FBW components. In this study, proper information on actuators in particular is still sparse. Manufacturers of such actuators, sensors and flight computers may be contacted in order to gain more information in terms of weight, dimensions, power consumption and reliability of these components. Especially the reliability of all FBW components is an important issue. If more is known about the reliability of the individual components, the reliability of the entire system can be properly determined. Having this information makes it easier to convince certification authorities of the validity of the design and therefore has a direct influence on the success of the FBW trainer.

Furthermore, it is suggested to do additional research on different methods of employing FEP and to investigate the potential reduction of accidents and fatalities that may be achieved. This information can help to convince flight schools and private owners of the enormous advantages a FBW trainer has to offer, and help strengthen the position on the market.

BIBLIOGRAPHY

[1] Federal Aviation Administration, *FAA Statistics,* http://www.faa.gov/data_research/aviation_data_statistics/civil_airmen_statistics/2013/Air17-2013.xls (2013), Accessed on: 23 june 2014.

[2] General Aviation Manufacturers Association, *Databook GAMA,* www.gama.aero/files/GAMA7233_AR_FINAL_LOWRES.pdf (2012), Accessed on: 23 june 2014.

[3] E. Gill, *AE3211-I Lecture Notes;Verification and Validation for the Attitude and Orbit Control System,* (2014), TU Delft.

[4] S. Houston, R. Walton, and B. Conway, *Analysis of General Aviation Instructional Loss of Control Accidents,* The Journal of Aviation/Aerospace Education & Research **22**, 35 (2012).

[5] NASA Glenn Research Center, *Aircraft Rotations: Body Axes,* https://www.grc.nasa.gov/www/k-12/airplane/rotations.html, Accessed on: 17 June 2014.

[6] Mohhamad H. Sadraey, *Aircraft Design - A Systems Engineering Approach 2012* (John Wiley & Sons, Ltd, 2013).

[7] Maj Russ Erb, *Beech E-18S Super 18 Pictorial Tour,* http://www.eaa1000.av.org/pix/beech18/beech18.htm (2014), Accessed on: 17 June 2014.

[8] Continental Motors Inc., *O-240 Series Engine Operator's Manual*, P.O. Box 90, Mobile, AL 36601, USA (2011).

[9] Continental Motors Inc., *IO-360 Series Engine Maintenance and Operatorś Manual*, P.O. Box 90, Mobile, AL 36601, USA (2011).

[10] Avco Lycoming Division, *0-360 and Associated Models*, Lycoming Engines, 652 Oliver Street, WilliamsPort, PA 17701, USA (1977).

[11] Avco Lycoming Division, *O, IO, HIO-540 Operators Manual*, Lycoming Engines, 652 Oliver Street, WilliamsPort, PA 17701, USA (1984).

[12] BRP-Powertrain GmbH & Co KG, *Betriebshandbuch für Rotax Motortype 912 Serie*, BRP-Powertrain GmbH & Co KG, Rotaxstrassße 1, A-4623 Gunskirchen, Austria (2010).

[13] Atlantic Aero, Inc, *550 Tuned Induction Conversion*, PO Box 35408, Greensboro, NC 27425, USA (2007).

[14] Hoffmann Propeller GmbH & Co.KG, Private communication (2014), Ulrich Kosney - Sales and Services.

[15] Air Alliance GmbH, Private communication (2014).

[16] IHS Jane's, *Jane's Defence & Security,* https://janes.ihs.com/Grid.aspx (2014), Accessed on: 25 April 2014.

[17] IAOPA, *Airports & Fuelprices,* http://www.iaopa.eu/airports-and-fuel-prices (2014), Accessed on: 30 April 2014.

[18] E-FEEL AERONAUTICS SARL, *Variable costs,* http://www.cessna-rotax.com/costs/costs-savings/ (2014), Accessed on: 24 June 2014.

[19] Air Alliance GmbH, *1997 DIAMOND DA20 KATANA,* http://www.air-alliance.de/index.php?article_id=518&clang=0 (2014), Accessed on: 29 April 2014.

[20] Brandstofprijzen.info, http://www.brandstofprijzen.info/ (2014), Accessed on: 29 April 2014.

[21] Continental Motors Inc., *Service Information Letter SIL98-9C*, P.O. Box 90, Mobile, AL 36601, USA (2013).

[22] Sensenich Wood Propeller Co., *Aircraft Propellers,* http://www.sensenich.com/products/browse/14 (2014), Accessed on: 28 April 2014.

[23] Avco Lycoming Division, *Service Instruction No. 1009AV*, Lycoming Engines, 652 Oliver Street, WilliamsPort, PA 17701, USA (2013).

[24] Avco Lycoming Division, *Aftermarket Engine Price List*, Lycoming Engines, 652 Oliver Street, WilliamsPort, PA 17701, USA (2012).

[25] Hartzell Propeller Inc, Private communication (2014), Kristy - Customer Service Rep.

[26] Don George Aircraft Engines & Parts, *Continental Aircraft Engines,* http://www.dongeorgeaircraft.com/ (2014), Accessed on: 24 April 2014.

[27] Flugzeugservice Willy Ader LTB, Private communication (2014).

[28] EASA, *EASA.IM.A.223*, European Aviation Safety Agency, Ottoplatz 1, 50679 Cologne, Germany (2012).

[29] EASA, *EASA.A.364*, European Aviation Safety Agency, Ottoplatz 1, 50679 Cologne, Germany (2011).

[30] EASA, *EASA.IM.A.007*, European Aviation Safety Agency, Ottoplatz 1, 50679 Cologne, Germany (2013).

[31] EASA, *EASA.IM.A.051*, European Aviation Safety Agency, Ottoplatz 1, 50679 Cologne, Germany (2013).

[32] EASA, *EASA.A.075*, European Aviation Safety Agency, Ottoplatz 1, 50679 Cologne, Germany (2013).

[33] Piper Aircraft, Inc., *Arrow - Piper,* http://www.piper.com/aircraft/trainer-class/archer/ (2014), Accessed on: 24 April 2014.

[34] Cirrus Design Corporation, *SR22 International 2014 Price List,* https://cirrusaircraft.box.com/shared/static/7si3v4o6zx33fk61kn0f.pdf (2014), Accessed on: 28 April 2014.

[35] Cirrus Design Corporation, *SR20 International 2014 Price List,* https://cirrusaircraft.box.com/shared/static/utcsnmtj7b632jm10jyo.pdf (2014).

[36] ECB, *ECB: Euro exchange rates USD 28.04.2014,* http://www.ecb.europa.eu/stats/exchange/eurofxref/html/eurofxref-graph-usd.en.html (2014), Accessed on: 28 April 2014.

[37] MatWeb, *Material Property Data,* http://www.matweb.com/ (2014), Accessed: 17 June 2014.

[38] ACP Composites, *Product Specification Reference Sheet,* http://www.acpsales.com/upload/

Mechanical-Properties-of-Carbon-Fiber-Composite-Materials.pdf (2012), Accessed: 17 June 2014.

[39] J. Roskam, *Airplane Design: Part IV: Layout of landing gear and systems* (DAR Corporation, 1986).

[40] *Certification Specifications for Normal, Utility, Aerobatic and Commuter Category Aeroplanes - CS-23*, European Aviation Safety Agency (2012).

[41] The Goodyear Tire & Rubber Co., *Aircraft Tire Data Book*, 1144 East Market Street, Akron, Ohio 44316, USA (2010).

[42] Saarstahl AG, *Werkstoff-Datenblatt Saarstahl - 60SiCrV7*, Bismarckstraße 57-59, 66333 Völklingen, Germany (2014).

[43] Grove Aircraft Landing Gear Systems Inc., *Catalog 114*, 1800 Joe Crosson Drive, El Cajon, CA 92020, USA (2014).

[44] Sandelving Aviation Supply, *LORD Shimmy Damper SE1051-2,* http://www.aircraftspruce.eu/lord-shimmy-damper-se1051-2.htm (2014), Accessed on: 23-6-2014.

[45] Cessna Aircraft Company, *Pilot's Operating Handbook And Flight Training Supplement Skycatcher*, 3 Cessna Blvd, Wichita, Kansas 67215, USA (2011).

[46] BRP-Powertrain GmbH & Co KG, *Betriebshandbuch für Rotax Motortype 914 Serie*, BRP-Powertrain GmbH & Co KG, Rotaxstrassße 1, A-4623 Gunskirchen, Austria (2010).

[47] Continental Motors Inc., *OVERHAUL MANUAL. FOR AIRCRAFT ENGINE. , MODELS. C75,C85,C90 & 0-200*, P.O. Box 90, Mobile, AL 36601, USA (1980).

[48] Technify Motors GmbH, *Centurion 2.0 - Dieselflugmotor mit 135 PS,* http://www.centurion.aero/typo3/index.php?id=101 (2014), Accessed on: 24 June 2014.

[49] Avco Lycoming Division, *0-235 and 0-290 SERIES AIRCRAFT ENGINES*, Lycoming Engines, 652 Oliver Street, WilliamsPort, PA 17701, USA (1988).

[50] N. A. Grebe, N. Barfknecht, A. van den Berg, M. van den Broek, J. van den Elshout, L. van Horssen, W. Jousma, F. Rijks, and D. de Vries, *DSE - Minimum Fly-By-Wire Trainer - Perform the Preliminary Design of a FBW light training aircraft with minimum direct operating costs*, Tech. Rep. (Delft University of Technology, 2014).

[51] Cessna Aircraft Company, *Model 152 Series 1978 thru 1985 Service Manual*, 3 Cessna Blvd, Wichita, Kansas 67215, USA (1995).

[52] J. Roskam, *Airplane Design: Part I: Preliminary Sizing of Airplanes* (DAR Corporation, 1985).

[53] J. Roskam, *Airplane Design: Part II: Preliminary Configuration Design and Integration of the Propulsion System* (DAR Corporation, 1997).

[54] J. Roskam, *Airplane Design: Part III: Layout Design of Cockpit, Fuselage, Wing and Empennage: Cutaways and Inboard Profiles* (DAR Corporation, 1989).

[55] J. Roskam, *Airplane Design: Part V: Component Weight Estimation* (DAR Corporation, 1999).

[56] J. Roskam, *Airplane Design: Part VI: Preliminary Calculation of Aerodynamic, Thrust and Power Characteristics* (DAR Corporation, 1990).

[57] J. Roskam, *Airplane Design: Part VII: Determination of Stability, Control and Performance Characteristics: FAR and Military Requirements* (DAR Corporation, 2002).

[58] S. Hulshoff, *Project Guide Design Synthesis Exercise; Minimum Fly-By-Wire Trainer,* (2014), TU Delft.

[59] T. Maxon, *Cockpit Conundrum: Shortage of Pilot Candidates Puts a Drag on Regional Carriers,* http://www.dallasnews.com/business/airline-industry/20140419-cockpit-conundrum.ece (2014), Accessed on: 29 April 2014.

[60] S. Gudmundsson, *General Aviation Aircraft Design. Applied Methods and Procedures*, 1st ed. (Butterworth-Heinemann, 2014).

[61] Bureau of Labor Statistics, *USDL-13-2393*, Tech. Rep. (United States Department of Labor, 2013).

[62] CTV London, *London's Diamond Aircraft announces massive layoffs,* http://london.ctvnews.ca/london-s-diamond-aircraft-announces-massive-layoffs-1.1171957 (2013), Accessed on: 25 April 2014.

[63] Thomson Reuters, *Flugzeugbauer Grob findet neuen Investor - 100 Jobs gerettet,* http://de.reuters.com/article/deEuroRpt/idDELS45160220090128 (2009), Accessed on: 25 April 2014.

[64] N. A. Grebe, N. Barfknecht, A. van den Berg, M. van den Broek, J. van den Elshout, L. van Horssen, W. Jousma, F. Rijks, and D. de Vries, *DSE - Minimum Fly-By-Wire Trainer - Perform the Preliminary Design of a FBW light training aircraft with minimum direct operating costs Mid-Term Report*, Tech. Rep. (Delft University of Technology, 2014).

[65] J. Pearce, *Burton's line in lead poisoning,* European neurology 57 , 118 (2007).

[66] Sandvik Coromant, *FAA press release on unleaded Avgas,* http://www.faa.gov/news/press_releases/news_story.cfm?newsId=14714 (2013), Accessed on: 23-6-2014.

[67] Australian Aluminium Council, *Recycling of Aluminium,* http://aluminium.org.au/recycling (2014), Accessed on: 23-6-2014.

[68] J. Dahn and G. M. Erlich, *Linden's Handbook of Batteries, 4th edition* (McGraw Hill, 2011).

[69] J. Roskam, *Airplane Design: Part VIII: Airplane Cost Estimation: Design, Development, Manufacturing and Operating* (DAR Corporation, 2002).

[70] T. Megson, *Aircraft Structures for Engineering Students*, 5th ed. (Elsevier, 2013).

[71] Federal Aviation Administration, *Aviation Maintenance Technician Handbook - General* (United States Department of Transportation, 2008).

[72] A. Ruina and R. Pratap, *Introduction to Statics and Dynamics*, 1st ed. (Oxford University Pressr, 2008).

[73] Aerospace Specification Metals Inc., *Aluminum 7075-T6,* http://asm.matweb.com/search/

SpecificMaterial.asp?bassnum=MA7075T61 (2014), Accessed: 22 June 2014.
[74] MatWeb, *Aluminum Weldalite 049-T8,* http://www.matweb.com/search/datasheet.aspx?matguid=af305b3ea6f14e498f846cfc852c2608&ckck=1 (2014), Accessed on: 23-6-2014.
[75] W. Timmer, *AE2100 Project Reader -Aircraft*, Tech. Rep. (Delft University of Technology, 2012).
[76] Sandvik Coromant, *From gun barrels to landing gear,* http://www.sandvik.coromant.com/en-us/knowledge/featured-articles/pages/from-gun-barrels-to-landing-gear.aspx (2014), Accessed on: 23-6-2014.
[77] D. Blom, E. Gillebaart, G. Kooij, G. Kuru, T. Noyon, A. Nundlall, F. Peters, J. Smit, C. Wijnterp, and M. Wormer, *DSE - Minimum MEDEVAC Aircraft*, Tech. Rep. (Delft University of Technology, 2010).
[78] Tomas Melin, *Tornado,* http://www.redhammer.se/tornado/, Edited by W. Jousma.
[79] D. Howe, *Aircraft Conceptual Design Synthesis* (Springer, 2000).
[80] G. La Rocca, *AE3211-I Lecture Notes; Weight estimation and iterations in AC design,* (2014), TU Delft.
[81] Peter Kaempf, *Handkraefte beim Entwurf einer Flugzeugsteuerung,* http://www.peterkaempf.de/media/e639a7e324e6db35ffff8116ac144227.pdf (1993), Accessed on: 19-5-2014.
[82] J.A. Mulder, W.H.J.J. van Staveren, J.C. van der Vaart, E. de Weerdt, C.C. de Visser, A.C. in 't Veld, E. Mooij, *Flight Dynamics* (TUDelft, 2013).
[83] Bob Sanford, *Airbus Flight Control Laws,* http://www.airbusdriver.net/airbus_fltlaws.htm (2004), Accessed: 20 June 2014.
[84] W. Falkena, *Investigation of Practical Flight Control Systems for Small Aircraft*, Ph.D. thesis, TU Delft (2012).
[85] National Transportation Safety Board Bureau of Accident Investigation, *Aircraft Accident Report China Airlines Boeing 747-SP (NTSB/AAR-86/03)*, Tech. Rep. (NTSB, 1985).
[86] University of Minnesota, *General Aviation - Accidents and Fatalities,* http://enhs.umn.edu/current/injuryprevent/aviation/magnitude.html (2001), Accessed on: 23 june 2014.
[87] L.E.K. Consulting, *EGNOS Cost Benefit Analysis in Aviation,* http://egnos-portal.gsa.europa.eu/aviation/cost-benefits-analysis (2009), Accessed on: 8-5-2014.
[88] Egnos, *What is SBAS?* http://egnos-portal.gsa.europa.eu/discover-egnos/about-egnos/what-sbas (2011), Accessed on: 8-5-2014.
[89] F. George, *Look Mom No Hands,* AVIONICS NEWS , 58 (2006).
[90] *Rockwell Collins autopilot performs successfully during Aurora Centaur's first fully autonomous takeoff and landing test flight,* https://www.rockwellcollins.com/sitecore/content/Data/News/2012_Cal_Yr/GS/FY12GSNR32-Aurora_Centuar.aspx (2012), Accessed on: 13-5-2014.
[91] Garmin, *Garmin GTN 625 GPS,* https://buy.garmin.com/en-US/US/in-the-air/avionics-safety/gps-nav-comm/gtn-625/prod67882.html (2014), Accessed: 22 June 2014.
[92] Rosner & Rosner GbR - Actuation Systems, Private communication (2014), Norbert Rosner.
[93] Moog Inc., *Model 965 Rotary Servo Actuator,* http://www.moog.com/products/actuators-servoactuators/multi-purpose/rotary-actuators/model-965/ (2014), Accessed on: 19 May 2014.
[94] Moog Inc., *Model 915 Rotary Servo Actuator,* http://www.moog.com/products/actuators-servoactuators/multi-purpose/rotary-actuators/model-915/ (2014), Accessed on: 19 May 2014.
[95] C. R. Nave, *HyperPhysics: Relative Humidity,* (2005), Accessed on: 2 June 2014.
[96] Federal Aviation Administration, *Aviation Maintenance Technician Handbook - Airframe* (United States Department of Transportation, 2012).
[97] H. Gavel, *On Aircraft Fuel Systems; Conceptual Design and Modeling*, Ph.D. thesis, Linköpings University (2007).
[98] *SKYbrary,* http://www.skybrary.aero/ (2014), Accessed on: 13-5-2014.
[99] Federal Aviation Authorities, *Federal Aviation Regulations - Part 91 - General Operating & Flight Rules,* (2014).
[100] V. P. A. Calia and F. Schettini, *Air Data Failure Management in a Full-Authority Fly-By-Wire Control System,* Proceedings of the 2006 IEEE , 3277 (2006).
[101] Aviation Week, *Business-booming, AoA avionics,* http://aviationweek.com/awin/business-booming-angle-attack-avionics (2013), Accessed on: 14-5-2014.
[102] Aviation Week, *AoA Products,* http://www.alphasystemsaoa.com/kits.html (2014), Accessed on: 14-5-2014.
[103] Rockwell Collins, *Athena 411 Integrated Flight Control System,* https://www.rockwellcollins.com/sitecore/content/Data/Products/Controls/Flight_Controls/Athena_411_Integrated_Flight_Control_System.aspx (2014), Accessed: 20 June 2014.
[104] Avidyne, *DFC90 Attitude-Based Digital Autopilot for Avidyne PFD or Aspen EFD-equipped aircraft,* http://www.ryaninternational.com/products/dfc90/index.asp (2014), Accessed on: 14-5-2014.
[105] Garmin, *GFC700 Information,* https://buy.garmin.com/en-US/US/in-the-air/flight-decks/gfc-700/prod70143.html (2014), Accessed on: 14-5-2014.
[106] Tony Osborne, *Airbus to Establish Light Electric Aircraft Family,* http://aviationweek.com/commercial-aviation/airbus-establish-light-electric-aircraft-family (2014), Accessed on: 19-5-2014.
[107] M. M. Ahlers, A. Cooper, and T. Patterson, *Another battery incident troubles Boeing's 787 Dreamliner,* (2014), Accessed on: 22 June 2014.
[108] Electronic Code of Federal Regulations, *PART 43—MAINTENANCE, PREVENTIVE MAINTENANCE, RE-*

BUILDING, AND ALTERATION, http://www.ecfr.gov/cgi-bin/text-idx?tpl=/ecfrbrowse/Title14/14cfr43_main_02.tpl, Accessed on: 21 May 2014.

[109] F. N. Postema, Private communication (2014).

[110] UltralightNews, *Rotax 912, Rotax 912 ULS, Rotax 914 aircraft engine fuel and torque specifications and data,* http://www.ultralightnews.com/rotaxinfo/rotax912-fuelconsumption.html (2014), Accessed: 18 June 2014.

[111] AFN Europe, *The Exchange Fuel Prices,* http://www.afneurope.net/GasPrices/tabid/87/Default.aspx (2014), Accessed: 18 June 2014.

[112] Aviation Week, *Airbus To Establish Light Electric Aircraft Family,* http://aviationweek.com/commercial-aviation/airbus-establish-light-electric-aircraft-family, Accessed on: 20 May 2014.

[113] US Energy Information Administration, *Voluntary Reporting of Greenhouse Gases Program,* http://www.eia.gov/oiaf/1605/coefficients.html (2011), Accessed on: June 22 2014.

[114] S. Nordhoff, *DO-178C/ED-12C,* Tech. Rep. (SQS, 2014).

[115] Southwest Texas Aviation Inc., *Cirrus Maintenance Info,* http://www.swta.net/cirrusproductinfo/cirrusmaintenanceinfo.html (2014), Accessed on: 23-6-2014.

A
FUNCTIONAL BREAKDOWN AND FLOW

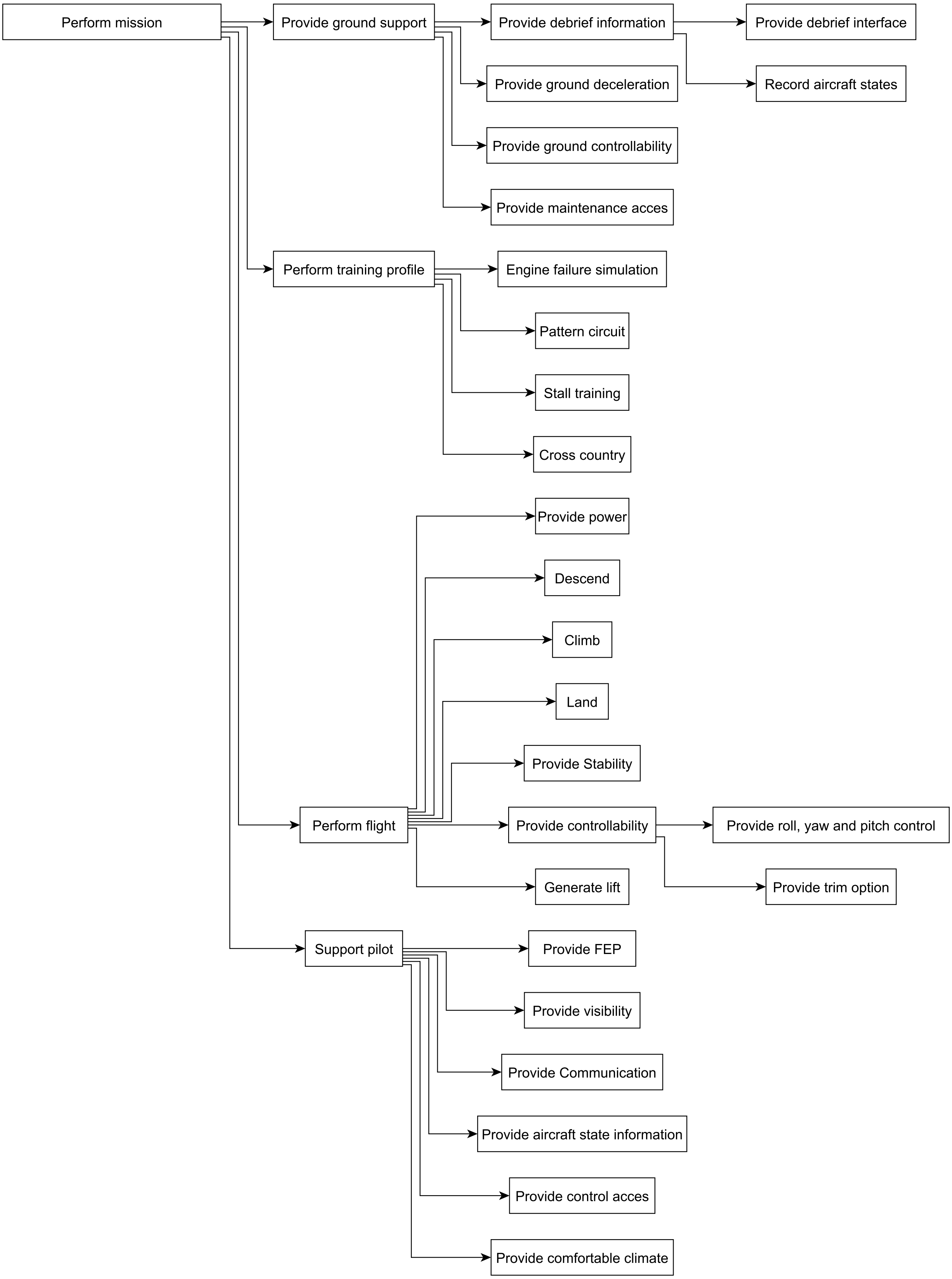

Figure A.1: Functional breakdown

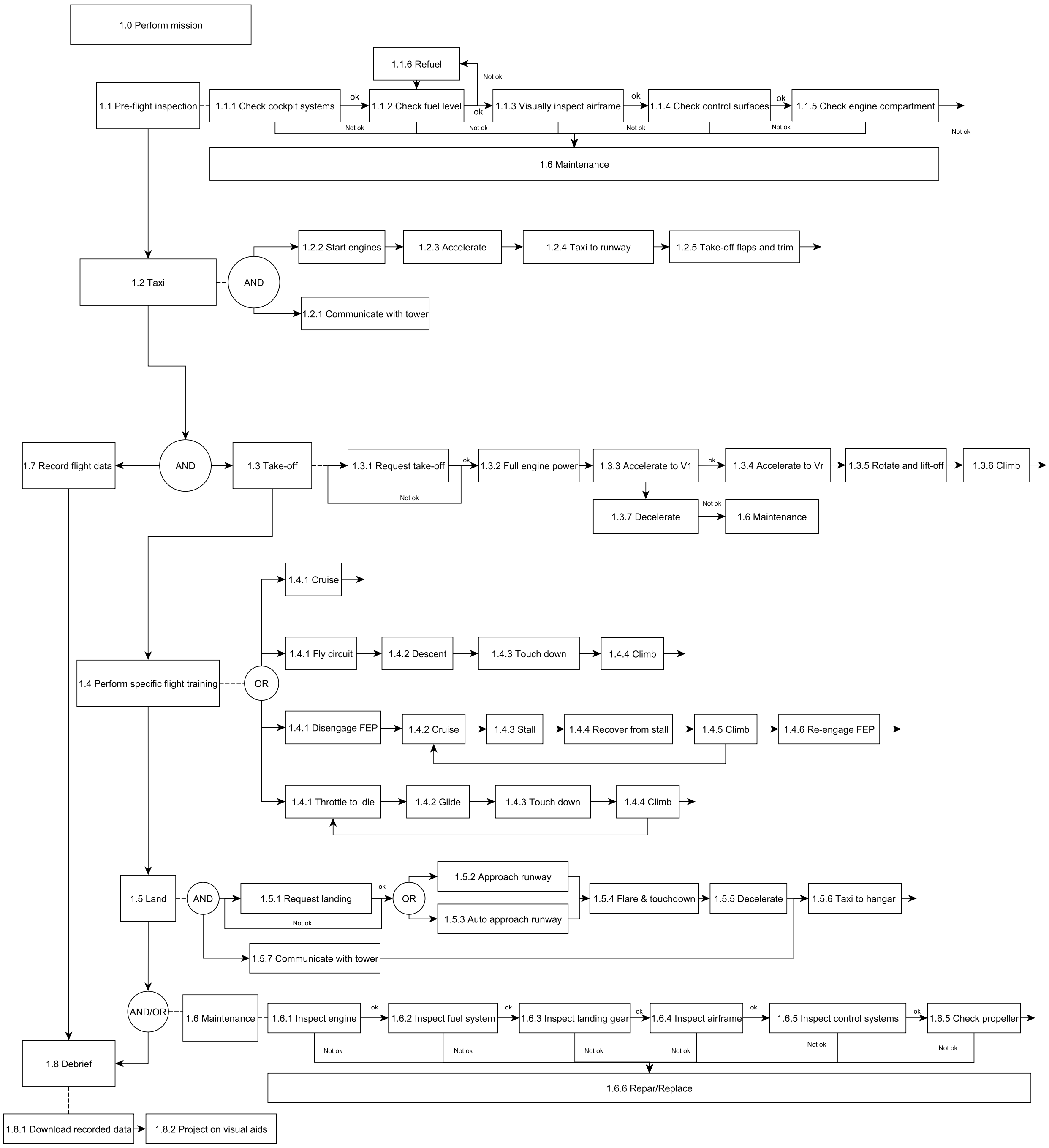

Figure A.2: Functional flow diagram

B
AIRFOIL DATA

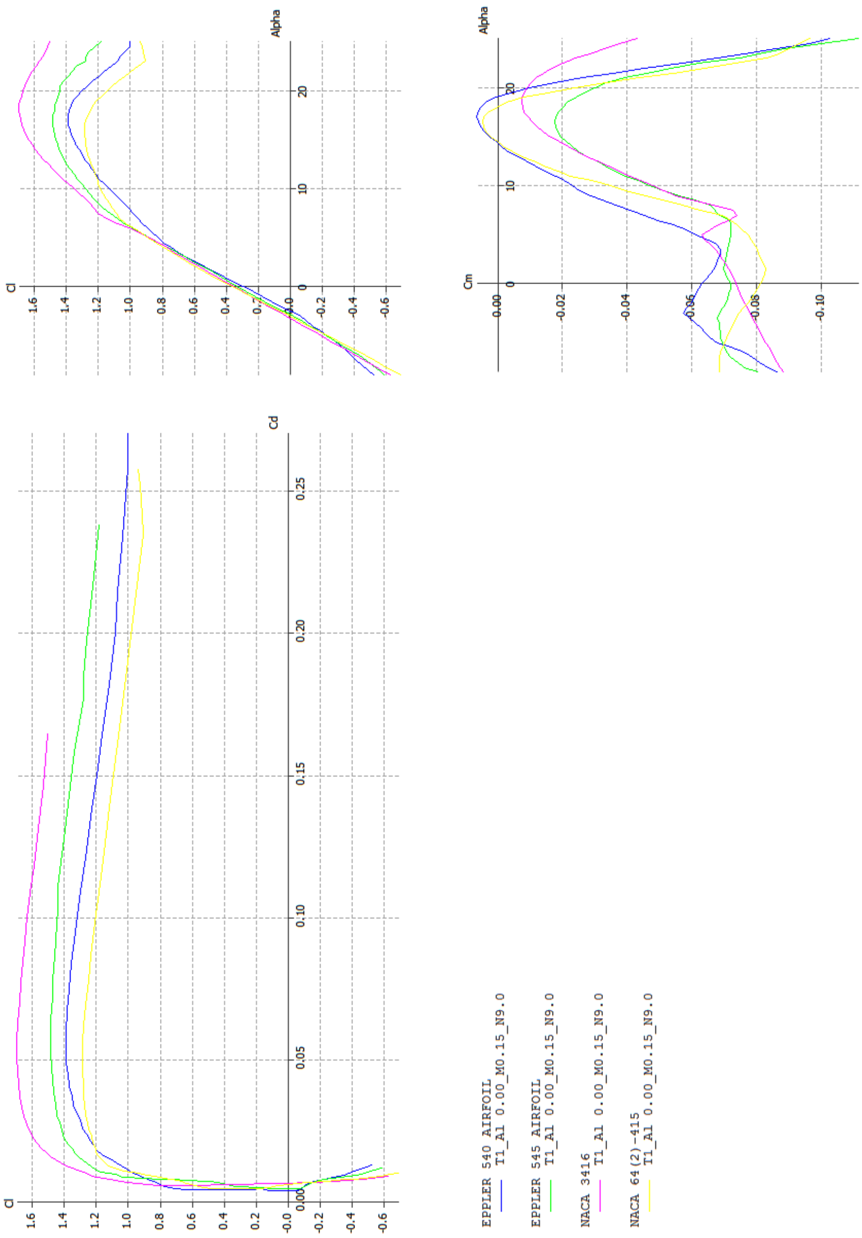

Figure B.1: Airfoil data, used in airfoil selection. Alpha in degrees.

C
WORK DISTRIBUTION

In Table C.2, the distribution of work is presented. Firstly , the authors of the chapters are presented. During the project work, some additional time intensive responsibilites were assigned, which are listed underneath. The MATLAB manager was responsible for the development of the MATLAB script and merging the new files into one working iteration. The CAD-manager was responsible for all drawings done with Catia.

Table C.1: Abbreviation of names

Person	Abbreviation
N. O. Abuter Grebe	NA
N. Barfknecht	NB
A. J. van den Berg	AB
M. J. van den Broek	MB
J. van den Elshout	JE
L. J. van Horssen	LH
W. Jousma	WJ
F. G. J. Rijks	FR
D. de Vries	DV

Table C.2: Distribution of work by group members

Section	Member
Preface	FR
Summary	JE, DV
1	MB
2.1	AB
2.2-2.3	NB
2.4	AB,NB
3.1	WJ
3.2	NA
3.3	AB
3.4, 3.5	DV
3.6	AB
3.7	AB
4.1-4.2	DV
5.1	MB
5.2-5.3	LH
5.4	MB
5.5	LH
5.6-5.7	NB
6	WJ
7.1	NA, JE
7.2, 7.3	NA
7.4	JE, DV
8	LH
9	JE, DV
10.1-10.2	MB
10.3	FR
10.4-10.5	MB
10.6	FR
11	JE
12	NA, WJ
13	NB
14	WJ
15	NA, MB
16	JE
17	NB
18	FR, WJ, LH
App. A	WJ
App. B	WJ
App. C	NA
App. D	FJ
CAD-manager	DV
MATLAB programming	NA, NB, AB, MB, JE, LH, WJ, FR, DV
MATLAB manager	AB

D
PROJECT GANTT CHART

Figure D.1: Gantt Chart Part 1

Figure D.2: Gantt Chart Part 2